Cancer vaccine strategies to improve immunotherapy: many roads lead to Rome

Tondini, E.

Cancer vaccine strategies to improve immunotherapy

Many roads lead to Rome

Elena Tondini

Cancer vaccine strategies to improve immunotherapy
Many roads lead to Rome
Elena Tondini

The research performed in this thesis was performed at the department of Immunology, formerly known as Immunohematology and Blood Transfusion, of the Leiden University Medical Center. This work was supported by the Leiden University Profiling Area Bioscience: the Science Base of Health grant.

Layout: Elena Tondini
Cover design: adapted from the illustration "Immunological Synapse" by David S. Goodsell, RCSB Protein Data Bank (doi: 10.2210/rcsb_pdb/goodsell-gallery-022). Use was granted under the CC-BY-4.0 license.
Thesis printing: Legodigit S.r.l.

ISBN 978-90-9035-041-7

Cancer vaccine strategies to improve immunotherapy

Many roads lead to Rome

Proefschrift

ter verkrijging van

de graad van doctor aan de Universiteit Leiden
op gezag van rector magnificus Prof. Dr. Ir. H. Bijl,
volgens besluit van het college voor promoties

te verdedigen op
donderdag 21 oktober 2021
klokke 11.15 uur

door
Elena Tondini
geboren te Trento, Italië in 1990

PROMOTOR:
Prof. Dr. F.A. Ossendorp

CO-PROMOTOR:
Dr. D.Filippov

LEDEN PROMOTIECOMMISSIE:
Prof. dr. A. Geluk
Prof. dr. M. Barz
Dr. S. van Kasteren
Dr. M. Verdoes (*Radboudumc*)

Table of contents

1 INTRODUCTION

Immunotherapy of cancer

Immunotherapy of cancer is a spectacularly progressing field which comprises a growing number of treatments aimed at modulating the immune system to eradicate malignancies. It is a direct result of our understanding, which developed over the past 50 years, that the immune system is an active player in cancer pathophysiology and that it can determine both regression and progression of the disease.

The primary reason for which the immune system has evolved is to recognize abnormal situations jeopardizing our health and survival, such as the invasion of unwanted pathogens, the wounding of a tissue and, in the case of cancer, the presence of abnormally growing mutated cells. The immune system can spontaneously react against cancerous cells and exert some control over the progression of the disease [1]. In fact, it has been postulated and to a certain extent demonstrated that the immune system mediates the clearance of most of premalignant cells which start to accumulate mutations. However, premalignant and malignant cells possess the ability to evolve and adapt rapidly, eventually subverting immune surveillance [2, 3]. The aim of immunotherapy is to reawake these spontaneous mechanisms as well as to mobilize other immune pathways to generate a powerful immune response, strong enough to overturn tumor suppression.

Even though several cellular targets of immunotherapeutic approaches have been described, therapeutic efficacy of many immunotherapies is dependent on the activation of one specific type of immunity, namely T cell immunity. In fact, from all immune cell subsets, T cells have the potential to directly recognize cancerous cells and mediate tumor specific eradication. T cells can, by virtue of highly specific receptors, discriminate malignant cells form healthy cells based on molecular changes as small as single point mutations [1]. Importantly, the mobilization of an optimal T cell response strongly depends on a favorable environment, both at the time when the T cell response is initiated and during the effector phase [4]. For these reasons, different immunotherapeutic strategies act by intervening at different stages of the T cell response.

There are various immunotherapeutic strategies which directly or indirectly aim at enhancing anti-tumor T cell responses, or the effects of which converge to T cells for therapeutic efficacy. Based on their mode of action, they can be grouped in distinct categories: therapeutic vaccination, T cell transfer, immune-modulatory antibodies, bispecific antibodies, cytokine-based therapies

or immune-stimulating molecules (see **Figure 1**).

To understand T cell-based immunotherapies, it is fundamental to know how T cell immunity is initiated, how it acts and how it is regulated.

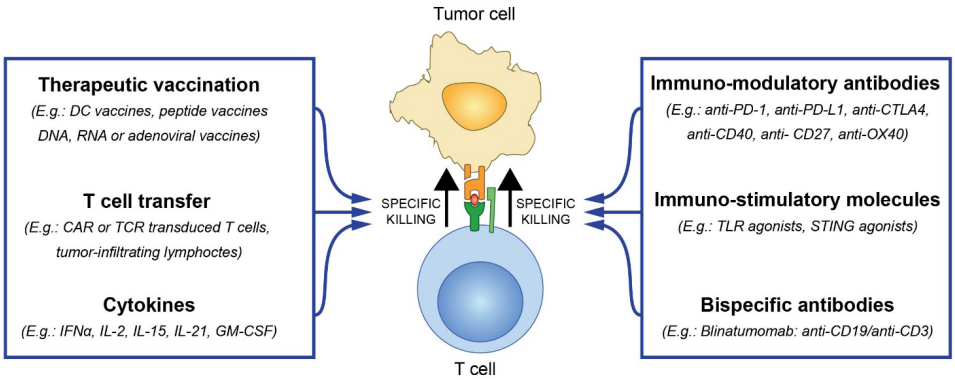

Figure 1: Immunotherapies converging to T cell immunity for therapeutic efficacy

T cell immunity

T lymphocytes derive from hematopoietic lymphoid precursors in the bone marrow and develop in the thymus. Every T cell possess a unique T cell receptor (TCR) generated by genetic recombination that can recognize antigenic peptide fragments bound to MHC molecules. During development in the thymus, self-antigen reactive clones are deleted through the central tolerance process, while clones positively selected for MHC recognition differentiate into naïve lymphocytes and start circulating in the body, ready to differentiate into effector cells at the encounter with their antigen [5].

To make sure that naïve lymphocytes properly react during danger situations but at the same time to avoid inappropriate activation, the immune system has evolved a process to control the initiation of T cell activation, called T cell priming [6]. T cell priming is a necessary step to activate T lymphocytes and to allow them to optimally differentiate into effector cells. It requires the integration of three separate signals. The first signal consists in the recognition by the TCR of an antigenic peptide presented by another cell on MHC molecules. The second signal is given through the co-stimulatory molecules that are present on the T cell surface. These receptors are proteins that are present on all naïve cells (CD27, CD28) and that can be further upregulated upon TCR triggering (OX40, ICOS, 4-1BB). When stimulated, these molecules activate an intracellular signaling cascade that promotes the expression of T cell differentiation and effector genes.

The third signal is given by cytokines. Similarly to co-stimulation, cytokine receptors stimulate critical T cell functions, such as cell division and differentiation. Cytokines known to be important during priming are IL-12, GM-CSF and type I interferons. Once these three signals are delivered to a naïve T lymphocyte, the T cell clone will start proliferating and differentiating, as well as producing proteins for the effector functions. These three signals are indispensable and irreplaceable for the generation of a functional T cell response. Sub-priming can occur when lymphocytes do not receive all three signals. Sub-primed T cells become dysfunctional or anergic, which results in tolerance for the antigen.

The key mediator for T cell priming, which uniquely ensures proper T cell activation, is a class of cells called antigen-presenting cells (APCs) [7]. Dendritic cells (DCs) are the most specialized type of APCs known for priming T cells. In fact, DCs are equipped with a series of sensing and uptake receptors [8]. The sensing receptors can recognize either PAMPs (pathogen-associated molecular patterns) or DAMPs (danger-associated molecular patterns) and are vital to alert the immune system about a possible abnormal situation. Among pattern recognition receptors (PPR) is the Toll-like receptor (TLR) family, a family of structurally related receptors that has evolved in superior organisms. Their primary function is to alert the immune system by activating innate immunity and starting an inflammatory response, which is propaedeutic for the initiation of adaptive immunity. For this reason, TLR stimulation is also exploited for vaccination. Other PRRs are the C-type lectin receptor family, the NOD-like receptors and RIG-I-like receptors. Once the ligands bind to the sensing receptors of DCs, they start a signaling cascade which induces the upregulation of co-stimulatory molecules (such as CD80, CD86 and CD70) and cytokines (i.e. IL-12, IL-15, type I interferons), a process known as DC maturation [9]. Moreover, they promote antigen uptake and proteasomal processing for loading of peptide on MHC molecules. Combined, these features create the perfect conditions for T cell priming and provide all three signals. Within the DC population, different subsets have been distinguished based on their localization and subspecialization [10]. Lymph node-resident DCs reside uniquely in lymphoid organs and participate to the initiation of the T cell responses. Within this subset, conventional DCs (cDCs) 1 and 2 and plasmocytoid DCs (pDCs) are found. cDCs1 are specialized in CD8 T cell stimulation, while cDC2 play an important role in the induction of CD4 T cell responses. pDCs are strong producers of type I interferons and are key mediators during antiviral immunity. Migratory DCs are found in tissues and peripheral organs,

and only travel to the lymph nodes upon antigen encounter. They comprise different types, which are alike to lymph-node resident cDCs and similarly show segregated abilities to stimulate either CD8 or CD4 T cells. In the skin, dermal CD103+/XCR1+ cDC1s are the responsible subset for antigen transport to the lymph nodes. During inflammation, another type of DC arises from monocytes (mo-DCs) which also participate to the promotion of an immune response.

Once primed, T cells can differentiate into effector and memory cells [11]. T lymphocytes are divided into two subsets based on the expression of the TCR co-receptor CD8 or CD4. The two co-receptors determine their affinity for peptide-bound MHC class I or class II. CD8 T cells recognize peptides form intracellular proteins presented on MHC class I molecules, while CD4 T cells recognize peptides on MHC class II, which are derived from antigens acquired extracellularly. Their ability to distinguish intracellularly- or extracellularly- derived peptides also determines their different effector functions. CD8 T cells differentiate into cytotoxic T cells (CTL) which can directly attack and kill cells that are presenting the epitope. Effector functions of CTLs consist in transferring granules containing enzymatic proteins that will damage the target cells, production of cytokines such as IFNγ or TNFα and upregulation of death-inducing ligands such as FasL or TRAIL [12].

CD4 T cells differentiate into helper cells (Th). There are distinct Th phenotypes that can develop, which are determined both by the stimuli received during priming and by the type of threat [13]. All these responses differ in cytokine production and influence the recruitment of immune cell subsets as well as their effector functions on target cells. Th1 responses support the clearance of intracellular infections by enhancing both CTL priming and function as well as promoting IgG antibody production by B cells and activating macrophages. Th2 responses are instead more skewed to resolving extracellular infections, by inducing the recruitment and activation of mast cells and eosinophils and supporting the production of IgE antibodies. Several other Th types have been discovered throughout the years. A particular type of differentiated CD4 T cells are regulatory T cells (Treg), a specialized type of immune suppressing cells functional for the induction of peripheral tolerance.

Finally, after a pathogenic invasion has been controlled, T cell necessitates of negative regulation to end the response and avoid overreactions. Mechanisms that negatively regulate T cell activation are the upregulation on APCs of CTLA4, a protein that competes with CD28 for binding of the co-stimulatory molecules

CD80 and CD86, stimulation of inhibitory receptors (PD-1, TIM-3, LAG3, NKG2A) or cytokine-driven suppression (IL-10, TGF-beta). Most effector cells will eventually die, however, a pool of memory cells can survive and readily activate upon antigen re-encounter [14].

Anti-tumor T cell immunity

The appreciation of the role of T lymphocytes in anti-tumor immunity was a gradual process that occurred between the 1970s and the 1990s, right after the discovery of CTLs, mainly through mouse studies. Starting from the late 1980s, these discoveries were also extended to humans, opening the way for additional mechanistic, therapeutic and diagnostic studies that are still advancing nowadays [15]. This early research unraveled both the nature of the antigens recognized as well as the concept of tumor immunoediting and escape.
Three main sources of tumor expressed antigens have been discovered:

1. **Viral antigens**: tumors that have been induced by oncogenic viruses (for example human papilloma virus, Epstein-Barr virus or T cell leukemia virus) can present epitopes derived from viral proteins. These epitopes can be recognized by T cells as they derive from foreign, non-self proteins.
2. **Mutation-derived antigens**: mutations that occur in expressed genes can give rise to new sequences and potential epitopes. Non-synonymous point mutations that result in one amino acid alterations give rise to so-called neoantigens. Other type of immunogenic mutations are frameshift mutations, which result in completely novel reading frames during protein translation or fusion genes. All these alterations are tumor-specific and are not present in normal cells, so no central tolerance is induced against them.
3. **Cancer germline antigens**: this class includes non-mutated genes that are found to be expressed or overexpressed by a large range of tumors. This group can be further divided into three subclasses:
    a. Some tumors can express genes that are normally expressed only during development or by germline cells. Examples of these genes are the melanoma antigen family (MAGE), the cancer/testis antigen (CTAG) and the antigen G (GAGE) families. Interestingly, many of these genes are found on the X chromosome but for many of them the function is still unknown. For these proteins no central tolerance is generally induced.
    b. Certain tumors express tissue-specific differentiation antigens such as

Melan-A or GP100, which are found on melanocytes and melanomas.

c. Lastly, yet other tumor types can overexpress certain genes compared to healthy tissue and lower the threshold for immunogenicity. Known overexpressed shared antigens are HER2, which is found in many epithelial tumors, and MUC-1 in adenocarcinomas.

Many of these antigens were identified by analyzing patients-derived T cells *ex vivo* after co-culture with autologous tumors [16-18]. However, despite the existence of detectable tumor-specific T cell responses, in many cases tumors eventually grow out, leading to the development of the disease. The reason why this occurs has also been the subject of extensive studies. Two main mechanisms were discovered. The first is the process of immunoediting [1]. This theory postulates that in the early stages of tumor growth, tumor-specific T cell responses shape the composition of the tumor by exerting an evolutionary pressure on the different tumor clones. Only tumor cells that will manage to evolve escaping strategies will survive. For example, mutations that modify the targeted antigen, or cause the loss of it, will give an evolutionary advantage to the clone, as it can be no longer recognized by the T cells. Another possible escape mechanism is the mutation of one of the components of the antigen presentation machinery that will affect the presentation of the epitope on the cell surface. The third mechanism involves the development of immune suppression mechanisms. The three main strategies of immune suppression consist in the upregulation on the tumor cells and in the tumor microenvironment of ligands of immune inhibitory receptors (PD-L1, PD-L2), inhibitory cytokines (IL-10, IL-6, TGF-b), and the recruitment of Tregs in the tumor [19].

Also on the T cell side, some factors can demote proper activity. It is not completely understood how these spontaneous responses are initiated in the first place, but it is highly likely that T cells are sub-primed and do not receive full co-stimulation, leading to low functioning T cells [20]. Because of their lower potency, T cells are subjected to chronic activation and antigen exposure, which culminates with an exhausted phenotype characterized by low killing capability, upregulation of inhibitory receptors (PD-1, LAG3, CTLA4, TIM-3) and low proliferative potential [21].

Altogether, these factors contribute to the weakening of anti-tumor T cell responses. At the time of tumor detection, patients often present dysfunctional T cell responses which may be rescued by immunotherapy.

Current status of therapeutic vaccination

Therapeutic vaccination aims to induce or re-activate T cell responses against tumor-specific antigens. The vaccine can be targeted to any of the antigen classes described above, depending on the tumor type and the antigens it expresses. Even though cancer vaccination is based on a straightforward logic, years of research have failed to bring this concept into clinical translation. The reasons for this are multiple: the challenge of properly activating T cells in an immune-suppressed environment, the different inhibitory and evading mechanisms taking place in tumor cells, and the realization that not all antigens are necessarily relevant in mediating tumor rejection [22]. However, the latest successes of other immunotherapies, together with advancements in immune profiling and neoantigen identification, provide a new rationale for improving previous attempts, since therapeutic vaccination represents a highly specific therapy against cancer cells, that could potentially leave healthy cells unharmed.

The field of cancer vaccines is currently focused on two fronts: the identification of relevant antigens and the refinement of vaccine formulations. The progress in different high throughput technologies such as DNA and RNA sequencing, has finally made it possible to identify the numerous patient-specific mutation-derived antigens [23-26]. Moreover, the advances in proteome and peptidome techniques are enriching our knowledge about the immune landscape of tumors and how frequently epitopes can be found to be presented on tumor cells [24, 27-29]. The challenge remains on how to make the best use of these potential antigens. Many studies reveal that vaccine formulation can influence the quality of the T cell response generated by the vaccine [22, 30]. The choice of the adjuvant also influences immune activation and can differentially skew the response induced.

Based on current knowledge, an optimal cancer vaccine should fulfill the following requirements:

- Preferential targeting of the vaccine to DCs, to create the optimal conditions for T cell priming
- Inclusion of an adjuvant that will skew a type 1 immunity (CTL and Th1 responses)
- Inclusion of multiple antigens to induce a broad specificity
- Flexibility of manufacture to produce not only off-the-shelf products but also personalized vaccines

Many different strategies are being investigated to tackle these challenges, among which peptide- and DNA-based vaccines.

Peptide-based vaccines

Peptide vaccines rely on delivering the selected epitopes (which is on average 9 to 20 amino acids long) within an extended amino acid sequence (usually around 25 to 35 amino acids). This approach is more effective compared to administration of the exact (minimal) epitopes because it circumvents undesired binding of the peptide epitopes on the MHC molecules of non-professional APCs, which could trigger T cells in absence of proper co-stimulation [31, 32]. At the same time, peptides are better endocytosed and processed by DCs compared to full length proteins [33, 34]. Peptide vaccines can simply be delivered as a mixture together with the adjuvants. Even though this is sufficient to induce T cell responses, it is reportedly not enough to achieve tumor control in the clinic [22, 35-38]. Possible reasons behind this lack of success are inefficient peptide delivery causing poor antigen uptake by DCs in vivo, which are a rare subset compared to other cellular types, and their sub-optimal activation due to dispersal of adjuvant and antigen after injection. These factors may determine sub-optimal T cell priming. Many approaches are currently under investigation to address these issues, which will expectedly improve optimal T cell activation by optimized cancer vaccines.

TLR-ligand conjugated vaccines

The Toll-like receptor family (TLRs) is a family of receptors that recognizes pathogen-associated structures and plays a fundamental role in early immune activation and the initiation of an immune response. Because of their sensing role, TLRs can be found on various cellular subsets, but the highest diversity of expression is found on DCs . What makes TLRs interesting in the vaccination field is that many of the ligands and chemical structures responsible for TLR activation have been identified over the years, leading the way for their use as adjuvants both in their native form or as synthetically reproduced molecules (**Table 1**).

Synthetic TLR ligands can be manipulated for conjugation to protein antigens or peptides. Conjugation of peptide and TLR ligands represents one strategy to enhance DC targeting and at the same time to co-deliver antigen and maturation signals in the same cells, thereby potentiating T cell priming [39] (**Figure 2**).

Table 1: Overview of TLR ligands and agonists

TLR	Localization	Recognized structure	Ligands and agonists	Commercialized adjuvants
1/2	Surface	Bacterial lipoproteins	Pam_3CysSK_4, FSL-1, MALP-2 Zymosan,	Amplivant™
2/6	Surface			
3	Endosomes	Viral dsRNA	Poly-I:C, Poly A:U	Poly-ICLC, Ampligen
4	Surface	Bacterial glycolipids	LPS, MPA, GLA, AGPs	MPL™, CRX-527
5	Surface	Bacterial flagellin	Flagellin	-
7	Endosome	Viral ssRNA	Imidazoquinolines, Hydroxyadenines	Aldara, Imiquimod, Resiquimod
8	Endosomes			
9	Endosomes	Unmethylated DNA	CpG-ODNs	PF-3512676 (CpG 7909)
10	Surface	Unknown	-	-

Many pre-clinical studies have described the benefit of using TLR ligand-peptide conjugates to target different TLRs such as TLR2 [40-42], TLR4 [40], TLR7 [43, 44], TLR7/8 [45, 46] and TLR9 [42, 47]. All these studies report methodologies to successfully conjugate ligands to antigen without disrupting the immunological properties of the ligand or the antigen but, most importantly, they highlight how this strategy improves vaccine potency. Conjugated vaccines to a TLR2 ligand were shown to favor enhanced uptake and antigen presentation by DCs *in vitro* and *in vivo* compared to the soluble, separate components [41, 42].

The attachment of the TLR2 agonist was also described to increase DC targeting *in vivo*, via undetermined endocytic receptors, and to affect intracellular trafficking towards antigen presentation or storage compartments [34, 42, 48]. Overall, this was associated to enhanced T cell induction by the conjugated vaccine which translated into improved tumor control [49]. These studies winded up to the clinical evaluation of a peptide conjugate vaccine bearing the TLR2 ligand UPam (Amplivant) [50] for the treatment of malignancies positive for Human Papilloma Virus (HPV) (Trial identification number: NCT02821494). This vaccine contains two peptides covering immunodominant region of the E6 protein of HPV16, which contains multiple CD8 and CD4 T cell epitopes.

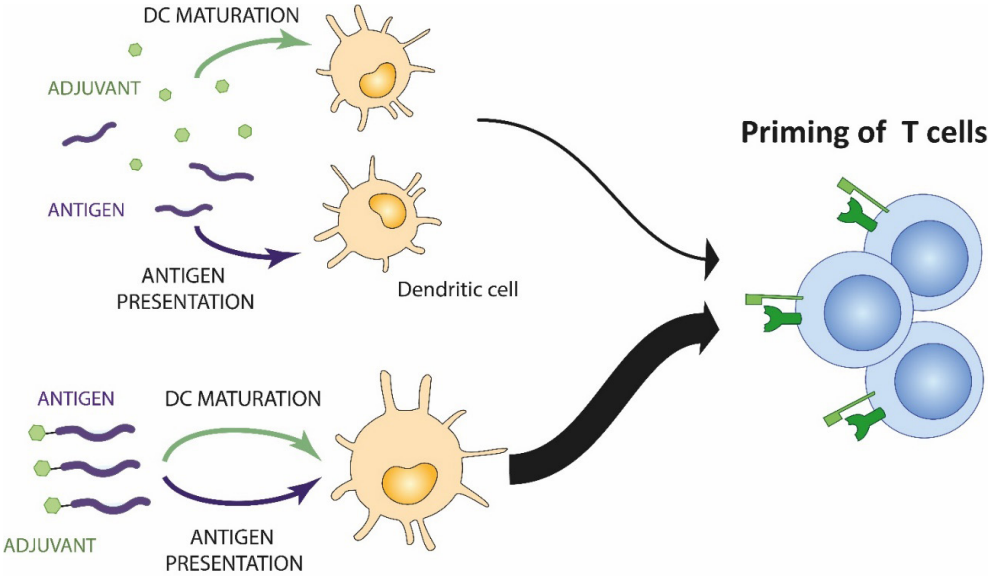

Figure 2: Covalent attachment of adjuvants to antigen results in improved immunological activation of T cells

Formulated peptide vaccines

Another approach to optimize peptide vaccines is their encapsulation in nano- or micro-sized particles. The benefits of these methods consist of increased half-life of the vaccine and reduced dispersal of the components. Different encapsulation strategies have been reported, among which liposomes, polymeric nanoparticles and nanogels. One interesting feature of these carriers is that their properties (such as size, composition, surface charge or tags) can be manipulated to maximize uptake and DCs targeting. For example, it has been shown that nano-sized particles are better internalized by DCs via pinocytosis or endocytosis compared to micro-sized particles [51, 52], which are preferentially taken up via phagocytosis by macrophages. Furthermore, positively charged particles seem to facilitate DC uptake as well as maturation [53, 54]. For example, the loading of peptide vaccines in nanoparticles or liposomes enhanced the induction of T cell responses in different pre-clinical studies. In many cases, this was also associated to enhanced control tumor rejection [55-58]. Another property that can be modulated is content release. For example, vaccine components can be conjugated to the particles via reduction sensitive linkers, which will be hydrolyzed only in highly reducing environments such as cellular lysosomes. This idea has been applied to dextran nanogels for the delivery of a full protein vaccine [59]. Covalent loading

of protein into positively charged nanogels led to the highest DC uptake in vitro, and to induction of strong specific T cell responses that could mediate rejection of tumors [60].

DNA vaccines

DNA vaccination consists in the delivery of the epitope encoded in its genetic form as linear DNA sequences, and it relies on DNA transcription followed by antigen production by host cells upon injection. The advantage of this methodology is the extreme versatility in accommodating any type of sequence, the stability of the molecule and an inherent adjuvanticity thanks to activation of PAMPs or DAMPS receptors [61, 62].

The ability of DNA vaccines to induce adaptive immunity was proven nearly 30 years ago [63-65]. Since then, many studies have investigated the possibility of gene immunization. Numerous preclinical and clinical studies have explored multiple methods for optimizing vector design, delivery and routes of administration [66]. Immune responses by DNA vaccines can be induced by intramuscular, intradermal or intravenous administration [64, 67, 68] and original administration devices such as gene gun [69], electroporation [70] and tattooing [71] have been developed to increase transfection efficiency and induction of both T cell and antibody-mediated immune responses.

Especially in light of personalized cancer vaccines, it represents a platform that can guarantee the necessary freedom to include multiple potential antigens in a rapidly manufactured vaccine encoding a string of multiple minigenes. Therefore, linear DNA vaccination is a versatile approach which has currently gained a lot of attention for specific immunotherapy of cancer.

Scope of the thesis

Cancer vaccines have the potential of raising T cell responses that can specifically eradicate tumors. However, multiple challenges are hampering clinical translation of this therapy. Next to identifying the correct antigens, it is important to rationally design vaccines to increase vaccine potency, DC targeting and, finally, the quality of the T cell response generated. In this thesis, three different approaches to improve the current vaccination strategies were explored.

In **chapter 2**, the possibility of conjugating the synthetic TLR4 ligand CRX-527 to peptide antigens was investigated. This novel adjuvant represents an attractive option to increase vaccine potency as it represents a detoxified version of

LPS, one of the most potent immune-stimulatory molecules known. A synthetic route for this conjugate and different potential linkers and positions for peptide conjugation were established. It was demonstrated that the use of a glycol linker preserves the immune-stimulatory activities of the ligand without affecting epitope processing and presentation of a model peptide. Moreover, not only it has shown effective T cell priming *in vivo*, but also increased differentiation into effector memory T cells. This study presents and validates CRX-527-peptide conjugates for their potential use in cancer immunotherapy.

After validating the molecular and immunological quality of CRX-527 peptide conjugates, three distinct conjugates bearing different antigens were synthetized, and their ability to induce specific CD8 or CD4 T cell responses and eradicate tumors was tested. In **chapter 3**, it was demonstrated that the conjugated vaccine improved T cell activation compared to a mixture of peptide and CRX-527, resulting in improved protection upon prophylactic and therapeutic vaccination. This study marks the use of CRX-527 as a potential adjuvant for cancer vaccination as well as the efficacy of conjugation as a strategy to improve vaccines in two different tumor models.

Conjugated vaccines could benefit from the integration of more than one signaling pathway. To explore this hypothesis, peptide conjugates bearing two different ligands were designed. In **chapter 4**, the TLR7 agonist derived from 2-butoxy-8-hydroxyadenine was connected to mannose-6 phosphate, a ligand that normally mediates intracellular trafficking via its endosomal receptor. This combination showed increased potency in inducing DC maturation, however antigen presentation was dampened. This study illustrates the interplay between signaling and trafficking pathways in dendritic cells. In **chapter 5**, the possibility of combining the TLR1/2 ligand Pam_3CysSK_4 with the synthetic TLR7 ligand based on the 2-butoxy-8-hydroxyadenine derivative was tested. Two dual peptide-conjugates were synthetized and validated for their ability to activate DCs and induce CD8 and CD4 T cell responses

In **chapter 6**, the formulation of antigenic peptides into reduction-sensitive cationic nanogels was explored. This vaccine formulation was shown to enhance antigen uptake and presentation by DCs more efficiently than free synthetic peptide. In addition, cationic nanogel were able to mature DCs. Injection of peptide-loaded nanogels carrying either a CD8 or a CD4 epitope increased the breadth and the quality of the T cell response generated. This study shows the potential of nanogels as a promising vaccine delivery platform for peptide antigens.

The targeting of tumor-specific neoantigens for cancer vaccination requires a platform that can easily support the production of personalized vaccines. In **chapter 7**, a DNA vaccine containing a string of multiple neoantigens was developed and tested as a potential approach for personalized vaccines. The DNA vaccine was capable to mobilize neoantigen-specific T cell responses *in vivo* and, in combination with anti-PD-1 immunotherapy, mediate tumor control. This study provided proof of concept for a feasible design of personalized vaccines targeting multiple neoantigens in a single vaccine entity. In addition, it demonstrated the complementary efficacy of distinct immunotherapies to established tumors. In **chapter 8** the findings of this thesis are summarized and discussed.

REFERENCES

1. Dunn, G.P., L.J. Old, and R.D. Schreiber, *The immunobiology of cancer immunosurveillance and immunoediting.* Immunity, 2004. **21**(2): p. 137-48.

2. Teng, M.W., et al., *From mice to humans: developments in cancer immunoediting.* J Clin Invest, 2015. **125**(9): p. 3338-46.

3. Schreiber, R.D., L.J. Old, and M.J. Smyth, *Cancer immunoediting: integrating immunity's roles in cancer suppression and promotion.* Science, 2011. **331**(6024): p. 1565-70.

4. Xia, A., et al., *T Cell Dysfunction in Cancer Immunity and Immunotherapy.* Front Immunol, 2019. **10**: p. 1719.

5. Germain, R.N., *T-cell development and the CD4-CD8 lineage decision.* Nat Rev Immunol, 2002. **2**(5): p. 309-22.

6. Smith-Garvin, J.E., G.A. Koretzky, and M.S. Jordan, *T cell activation.* Annu Rev Immunol, 2009. **27**: p. 591-619.

7. Malissen, B., et al., *Integrative biology of T cell activation.* Nat Immunol, 2014. **15**(9): p. 790-7.

8. Kaisho, T., *Pathogen sensors and chemokine receptors in dendritic cell subsets.* Vaccine, 2012. **30**(52): p. 7652-7.

9. Dalod, M., et al., *Dendritic cell maturation: functional specialization through signaling specificity and transcriptional programming.* EMBO J, 2014. **33**(10): p. 1104-16.

10.Eisenbarth, S.C., *Dendritic cell subsets in T cell programming: location dictates function.* Nat Rev Immunol, 2019. **19**(2): p. 89-103.

11. Chang, J.T., E.J. Wherry, and A.W. Goldrath, *Molecular regulation of effector and memory T cell differentiation.* Nat Immunol, 2014. **15**(12): p. 1104-15.

12. Podack, E.R. and A. Kupfer, *T-cell effector functions: mechanisms for delivery of cytotoxicity and help.* Annu Rev Cell Biol, 1991. **7**: p. 479-504.

13. Wan, Y.Y. and R.A. Flavell, *How diverse--CD4 effector T cells and their functions.* J Mol Cell Biol, 2009. **1**(1): p. 20-36.

14. Marrack, P., J. Scott-Browne, and M.K. MacLeod, *Terminating the immune response.* Immunol Rev, 2010. **236**: p. 5-10.

15. Coulie, P.G., et al., *Tumour antigens recognized by T lymphocytes: at the core of cancer immunotherapy.* Nat Rev Cancer, 2014. **14**(2): p. 135-46.

16. Vanky, F. and E. Klein, *Specificity of auto-tumor cytotoxicity exerted by fresh, activated and propagated human T lymphocytes.* Int J Cancer, 1982. **29**(5): p. 547-53.

17. Rosenberg, S.A., et al., *Use of tumor-infiltrating lymphocytes and interleukin-2 in the immunotherapy of patients with metastatic melanoma. A preliminary report.* N Engl J Med, 1988. **319**(25): p. 1676-80.

18. Van den Eynde, B., et al., *Presence on a human melanoma of multiple antigens recognized by autologous CTL.* Int J Cancer, 1989. **44**(4): p. 634-40.

19. Guerrouahen, B.S., et al., *Reverting Immune Suppression to Enhance Cancer Immunotherapy.* Front Oncol, 2019. **9**: p. 1554.

20. Vonderheide, R.H., *The Immune Revolution: A Case for Priming, Not Checkpoint.* Cancer Cell, 2018. **33**(4): p. 563-569.

21. Baitsch, L., et al., *The three main stumbling blocks for anticancer T cells.* Trends Immunol, 2012. **33**(7): p. 364-72.

22. Morse, M.A., W.R. Gwin, 3rd, and D.A. Mitchell, *Vaccine Therapies for Cancer: Then and Now.* Target Oncol, 2021. **16**(2): p. 121-152.

23. Castle, J.C., et al., *Exploiting the mutanome for tumor vaccination.* Cancer Res, 2012. **72**(5): p. 1081-91.

24. Yadav, M., et al., *Predicting immunogenic tumour mutations by combining mass spectrometry and exome sequencing.* Nature, 2014. **515**(7528): p. 572-6.

25. Diken, M., et al., *Discovery and Subtyping of Neo-Epitope Specific T-Cell Responses for Cancer Immunotherapy: Addressing the Mutanome.* Methods Mol Biol, 2017. **1499**: p. 223-236.

26. Scurr, M.J., et al., *Cancer Antigen Discovery Is Enabled by RNA Sequencing of Highly Purified Malignant and Nonmalignant Cells.* Clin Cancer Res, 2020. **26**(13): p. 3360-3370.

27. Wang, Q., et al., *Direct Detection and Quantification of Neoantigens.* Cancer Immunol Res, 2019. **7**(11): p. 1748-1754.

28. Zhang, X., et al., *Application of mass spectrometry-based MHC immunopeptidome profiling in neoantigen identification for tumor immunotherapy.* Biomed Pharmacother, 2019. **120**: p. 109542.

29. Sturm, T., et al., *Mild Acid Elution and MHC Immunoaffinity Chromatography Reveal Similar Albeit Not Identical Profiles of the HLA Class I Immunopeptidome.* J Proteome Res, 2021. **20**(1): p. 289-304.

30. Melief, C.J., et al., *Therapeutic cancer vaccines.* J Clin Invest, 2015. **125**(9): p. 3401-12.

31. Bijker, M.S., et al., *Superior induction of anti-tumor CTL immunity by extended peptide vaccines involves prolonged, DC-focused antigen presentation.* Eur J Immunol, 2008. **38**(4): p. 1033-42.

32. Faure, F., et al., *Long-lasting cross-presentation of tumor antigen in human DC.* Eur J Immunol, 2009. **39**(2): p. 380-90.

33. Zhang, H., et al., *Comparing pooled peptides with intact protein for accessing cross-presentation pathways for protective CD8+ and CD4+ T cells.* J Biol Chem, 2009. **284**(14): p. 9184-91.

34. Rosalia, R.A., et al., *Dendritic cells process synthetic long peptides better than whole protein, improving antigen presentation and T-cell activation.* Eur J Immunol, 2013. **43**(10): p. 2554-65.

35. Aranda, F., et al., *Trial Watch: Peptide vaccines in cancer therapy.* Oncoimmunology, 2013. **2**(12): p. e26621.

36. Bezu, L., et al., *Trial watch: Peptide-based vaccines in anticancer therapy.* Oncoimmunology, 2018. **7**(12): p. e1511506.

37. Pol, J., et al., *Trial Watch: Peptide-based anticancer vaccines.* Oncoimmunology, 2015. **4**(4): p. e974411.

38. Vacchelli, E., et al., *Trial watch: Peptide vaccines in cancer therapy.* Oncoimmunology, 2012. **1**(9): p. 1557-1576.

39. Kastenmuller, W., et al., *Dendritic cell-targeted vaccines--hope or hype?* Nat Rev Immunol, 2014. **14**(10): p. 705-11.

40. Belnoue, E., et al., *Targeting self and neo-epitopes with a modular self-adjuvanting cancer vaccine.* JCI Insight, 2019. **5**.

41. Zom, G.G., et al., *Novel TLR2-binding adjuvant induces enhanced T cell responses and tumor eradication.* J Immunother Cancer, 2018. **6**(1): p. 146.

42. Khan, S., et al., *Distinct uptake mechanisms but similar intracellular processing of two different toll-like receptor ligand-peptide conjugates in dendritic cells.* J Biol Chem, 2007. **282**(29): p. 21145-59.

43. Liu, Y., et al., *Synthetic MUC1 breast cancer vaccine containing a Toll-like receptor 7 agonist exerts antitumor effects.* Oncol Lett, 2020. **20**(3): p. 2369-2377.

44. Gential, G.P.P., et al., *Peptides conjugated to 2-alkoxy-8-oxo-adenine as potential synthetic vaccines triggering TLR7.* Bioorg Med Chem Lett, 2019. **29**(11): p. 1340-1344.

45. Lynn, G.M., et al., *Peptide-TLR-7/8a conjugate vaccines chemically programmed for nanoparticle self-assembly enhance CD8 T-cell immunity to tumor antigens.* Nat Biotechnol, 2020. **38**(3): p. 320-332.

46. Du, J.J., et al., *Multifunctional Protein Conjugates with Built-in Adjuvant (Adjuvant-Protein-Antigen) as Cancer Vaccines Boost Potent Immune Responses.* iScience, 2020. **23**(3): p. 100935.

47. Shirota, H. and D.M. Klinman, *TLR-9 agonist immunostimulatory sequence adjuvants linked to cancer antigens.* Methods Mol Biol, 2014. **1139**: p. 337-44.

48. van Montfoort, N., et al., *Antigen storage compartments in mature dendritic cells facilitate prolonged cytotoxic T lymphocyte cross-priming capacity.* Proc Natl Acad Sci U S A, 2009. **106**(16): p. 6730-5.

49. Zom, G.G., et al., *Efficient induction of antitumor immunity by synthetic toll-like receptor ligand-peptide conjugates.* Cancer Immunol

Res, 2014. **2**(8): p. 756-64.

50. Willems, M.M., et al., *N-tetradecylcarbamyl lipopeptides as novel agonists for Toll-like receptor 2.* J Med Chem, 2014. **57**(15): p. 6873-8.

51. Cruz, L.J., et al., *Targeted PLGA nano- but not microparticles specifically deliver antigen to human dendritic cells via DC-SIGN in vitro.* J Control Release, 2010. **144**(2): p. 118-26.

52. Fifis, T., et al., *Size-dependent immunogenicity: therapeutic and protective properties of nano-vaccines against tumors.* J Immunol, 2004. **173**(5): p. 3148-54.

53. Fromen, C.A., et al., *Nanoparticle surface charge impacts distribution, uptake and lymph node trafficking by pulmonary antigen-presenting cells.* Nanomedicine, 2016. **12**(3): p. 677-687.

54. Vangasseri, D.P., et al., *Immunostimulation of dendritic cells by cationic liposomes.* Mol Membr Biol, 2006. **23**(5): p. 385-95.

55. Varypataki, E.M., et al., *Efficient Eradication of Established Tumors in Mice with Cationic Liposome-Based Synthetic Long-Peptide Vaccines.* Cancer Immunol Res, 2017. **5**(3): p. 222-233.

56. Zamani, P., et al., *Nanoliposomal vaccine containing long multi-epitope peptide E75-AE36 pulsed PADRE-induced effective immune response in mice TUBO model of breast cancer.* Eur J Cancer, 2020. **129**: p. 80-96.

57. Xiang, S.D., et al., *Design of Peptide-Based Nanovaccines Targeting Leading Antigens From Gynecological Cancers to Induce HLA-A2.1 Restricted CD8(+) T Cell Responses.* Front Immunol, 2018. **9**: p. 2968.

58. Galliverti, G., et al., *Nanoparticle Conjugation of Human Papillomavirus 16 E7-long Peptides Enhances Therapeutic Vaccine Efficacy against Solid Tumors in Mice.* Cancer Immunol Res, 2018. **6**(11): p. 1301-1313.

59. Li, D., et al., *Reduction-Sensitive Polymer-Shell-Coated Nanogels for Intracellular Delivery of Antigens.* ACS Biomater Sci Eng, 2017. **3**(1): p. 42-48.

60. Li, D., et al., *Strong in vivo antitumor responses induced by an antigen immobilized in nanogels via reducible bonds.* Nanoscale, 2016. **8**(47): p. 19592-19604.

61. Klinman, D.M., G. Yamshchikov, and Y. Ishigatsubo, *Contribution of CpG motifs to the immunogenicity of DNA vaccines.* J Immunol, 1997. **158**(8): p. 3635-9.

62. Cho, H.J., et al., *Immunostimulatory DNA-based vaccines induce cytotoxic lymphocyte activity by a T-helper cell-independent mechanism.* Nat Biotechnol, 2000. **18**(5): p. 509-14.

63. Tang, D.C., M. DeVit, and S.A. Johnston, *Genetic immunization is a simple method for eliciting an immune response.* Nature, 1992. **356**(6365): p. 152-4.

64. Ulmer, J.B., et al., *Heterologous protection against influenza by injection of DNA encoding a viral protein.* Science, 1993. **259**(5102): p. 1745-9.

65. Wang, B., et al., *Gene inoculation generates immune responses against human immunodeficiency virus type 1.* Proc Natl Acad Sci U S A, 1993. **90**(9): p. 4156-60.

66. Fioretti, D., et al., *DNA vaccines: developing new strategies against cancer.* J Biomed Biotechnol, 2010. **2010**: p. 174378.

67. Raz, E., et al., *Intradermal gene immunization: the possible role of DNA uptake in the induction of cellular immunity to viruses.* Proc Natl Acad Sci U S A, 1994. **91**(20): p. 9519-23.

68. Williams, B.B., et al., *Induction of T cell-mediated immunity using a c-Myb DNA vaccine in a mouse model of colon cancer.* Cancer Immunol Immunother, 2008. **57**(11): p. 1635-45.

69. Porgador, A., et al., *Predominant role for directly transfected dendritic cells in antigen presentation to CD8+ T cells after gene gun immunization.* J Exp Med, 1998. **188**(6): p. 1075-82.

70. Luxembourg, A., et al., *Enhancement of immune responses to an HBV DNA vaccine by electroporation.* Vaccine, 2006. **24**(21): p. 4490-3.

71. Bins, A.D., et al., *A rapid and potent DNA vaccination strategy defined by in vivo monitoring of antigen expression.* Nat Med, 2005. **11**(8): p. 899-904.

2

SELF-ADJUVANTING CANCER VACCINES FROM CONJUGATION-READY LIPID A ANALOGUES AND SYNTHETIC LONG PEPTIDES

Reintjens NRM*, Tondini E*, de Jong AR, Meeuwenoord NJ, Chiodo F, Peterse E, Overkleeft HS, Filippov DV, van der Marel GA, Ossendorp F, Codée JDC

J Med Chem. 2020; 63(20):11691-11706

*equal contribution

ABSTRACT

Self-adjuvanting vaccines, wherein an antigenic peptide is covalently bound to an immunostimulating agent, have been shown to be promising tools for immunotherapy. Synthetic Toll-like receptor (TLR) ligands are ideal adjuvants for covalent linking to peptides or proteins. We here introduce a conjugation-ready TLR4-ligand, CRX-527, a potent powerful lipid A analogue, in the generation of novel conjugate-vaccine modalities. Effective chemistry has been developed for the synthesis of the conjugation-ready ligand as well as the connection vaccine modality that proved to be potent in activation of dendritic cells, in facilitating antigen presentation and in initiating specific CD8+ T cell-mediated killing of antigen-loaded target cells in vivo. Synthetic TLR4-ligands thus show great promise in potentiating the conjugate vaccine platform for application in cancer vaccination.

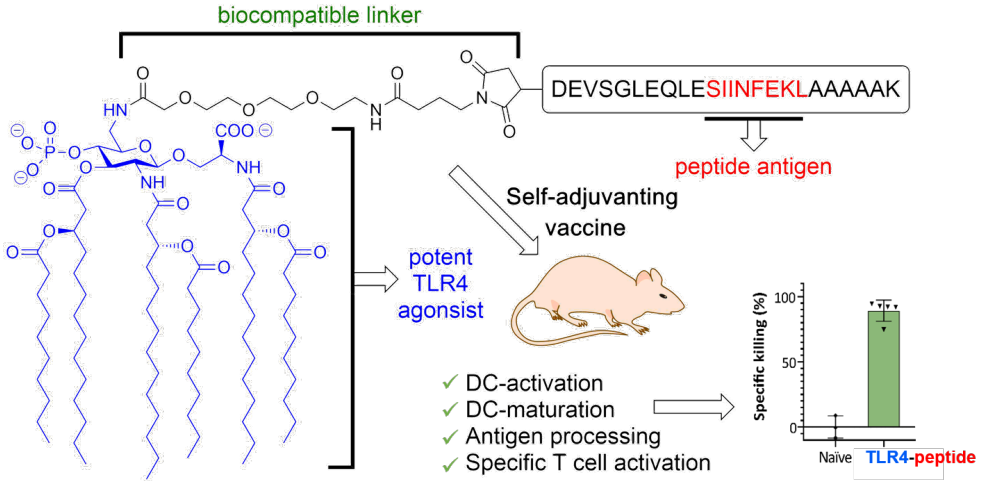

INTRODUCTION

Immunotherapy has become a powerful strategy to combat cancer. Significant advances have been made in the activa tion of anti-tumor T cell immunity, including the development of immune checkpoint blockade antibodies[1], chimeric antigen receptor T cells (CAR T cells)[2] and vaccination strategies, in which the immune system is trained to recognize cancer neoantigens.[3,4] To optimally direct an immune reaction against cancer via vaccination, adjuvants are used to activate antigen-presenting cells, such as dendritic cells (DCs) and macrophages. DCs express pathogen recognition receptors (PRRs)[5], through which they recognize invading pathogens and initiate an immune response, which eventually leads to the priming of T cells.[6]

Pathogen associated molecular patterns (PAMPs) are ligands for these PRRs and can be used as molecular-adjuvants. Molecular-adjuvants are well-defined single molecule immunostimulants that act directly on the innate immune system to enhance the adaptive immune response against antigens. Many well-defined PAMPs have been explored over the years, and the most extensively targeted PRR-families are the Toll-like receptors (TLRs)[7], C-type lectins[8], and Nucleotide-binding Oligomerization Domain (NOD)-like receptors[9,10]. To further improve vaccine activity, the antigen and adjuvants have been combined in covalent constructs, delivering "self-adjuvanting" vaccine candidates.[11,12] In the immune system, the stimulation of different TLRs can activate distinct signaling cascades and thereby support the generation of polarized types of immune reactions. Hence, targeting of distinct TLRs in vaccination influences the nature of the adaptive immune response induced.[13,14].

Several TLR agonists[11,15,16] have been conjugated to antigenic peptides (often synthetic long peptides, SLPs), including ligands for TLR2,[17–22] TLR7,[23,24] and TLR9,[20,2 5,26] yielding vaccine modalities with improved activity with respect to their non-conjugated counterparts. Lipid A (**Figure 1A**), a conserved component of the bacterial cell wall, is one of the most potent immune-stimulating agents known to date and it activates the innate immune system through binding with TLR4. The high toxicity of lipid A makes it unsuitable for safe use in humans, but monophosphoryl lipid A (MPLA, **Figure 1A**), a lipid A derivative in which the anomeric phosphate has been removed, has proven its effectiveness as an adjuvant in various approved vaccines.[27–29] It has also been used recently in conjugates in which it was covalently attached to a tumor-associated carbohydrate antigen (TACA) or a synthetic bacterial glycan.[30–34] The latter conjugate was able to elicit

a robust IgG antibody response in mice, critical for effective anti-bacterial vaccination.[34] MPLA thus represents a very attractive PAMP to be explored in SLP conjugates, targeting cancer epitopes. The physical properties and challenging synthesis of lipid A derivatives, however, limit its accessibility.[35–37] Because of its potent immunostimulating activity, many mimics of MPLA have been developed and the class of aminoalkyl glucosamine 4-phosphates (AGPs) has been especially promising.[38–41] AGPs have been shown to be efficacious adjuvants and to be clinically safe, resulting in their use in a Hepatitis B vaccine.[42] CRX-527 (**Figure 1A**) has been established as one of the most potent AGPs.[38]

We here introduce conjugation-ready derivatives of CRX-527 for application in the development of adjuvant-SLP vaccines conjugates. We have established a robust synthetic route to generate linker-equipped CRX-527 analogues and used these in the assembly of SLP conjugates. The self-adjuvanting SLPs carrying this TLR4-ligand are capable of mobilizing a strong T cell immune response against the incorporated antigen and are capable of promoting effective and specific killing of target cells expressing the antigen *in vivo*.

RESULTS AND DISCUSSION

Synthesis of the ligands and conjugates.

In the development of the conjugation-ready CRX-527-derivates we set out to probe both the influence of the nature of the linker and the mode of connectivity of the linker to the TLR4-ligand, CRX-527 (See **Figure 1B**). In lipopolysaccharides bacterial *O*-antigens are connected to a lipid A anchor through the C6-position of the glucosamine-C4-phosphate residue and from the crystal structure of lipid A in complex to the TLR4-MD2 complex, it is apparent that this position is exposed from the complex.[43] The C6-position of the glucosamine-C4-phosphate can thus be used for conjugation purposes. Indeed, previous work on anti-bacterial MPLA conjugate vaccines has shown that the adjuvant can be modified at this position without compromising adjuvant activity.[34] We explored two types of linkers at the C6-position of CRX-527: a hydrophobic alkyl linker (**A**) and a hydrophilic triethylene glycol (TEG) linker (**B**). These linkers were connected to CRX-527 through an ester bond,[34] or *via* a more stable amide bond. To connect the ligands to the SLPs, the linkers were equipped with a maleimide, to allow for a thiol-ene conjugation to the sulfhydryl functionalized SLP. We used the ovalbumin derived SLP, DEVSGLEQLESIINFEKLAAAAAK ($DEVA_5K$) as a model antigen.[20] Herein, the MHC-I epitope SIINFEKL is embedded in a longer peptide motif to

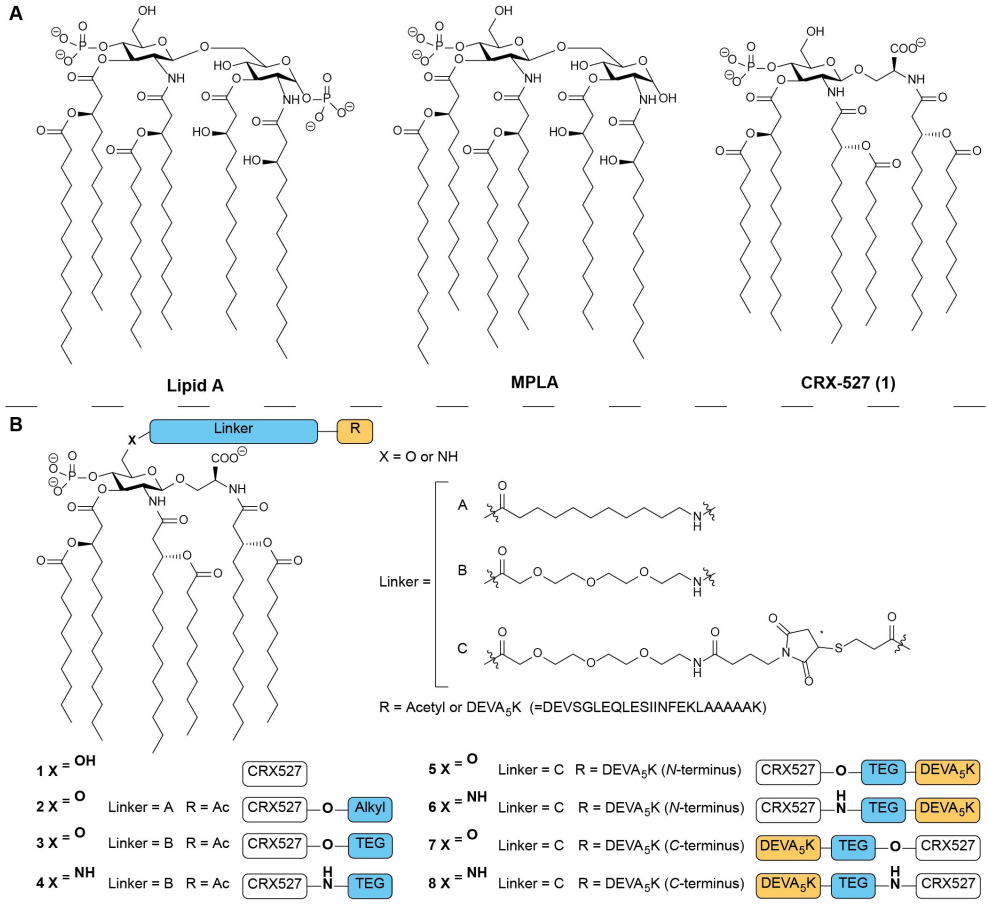

Figure 1. (A) Representative structures of lipid A of *E. coli* and MPLA of *Salmonella enterica* serotype minnesota Re 595; Structure of CRX-527 (1). (B) Structures of CRX-527 derivatives 2-4 and CRX-527 conjugates 5-8. The $DEVA_5K$ peptide in the conjugates carries the SIINFEKL epitope in its sequence.

ensure that the peptide will have to undergo proteasomal processing to produce the minimal epitope. The target compounds generated for thy are depicted in **Figure 1** and include CRX-527 (**1**), ester-linker CRX-527 **2** and **3**, amide-linker CRX-527 **4** as well as the conjugates **5** and **6** having the CRX-527 ligand at the *N*-terminus of the peptide and conjugates **7** and **8**, with the ligand at the *C*-terminus of the SLP. To obtain CRX-527 derivatives **1**-**4**, building blocks **16a/b** were required and the assembly of these key intermediates was accomplished as depicted in **Figure 2A**. Based on the synthesis route to CRX-527 developed by Johnson and co-workers[41], we assembled glucosaminyl serine building block **11** from glucosamine donor **9** and serine **10**. Condensation of **9** and **10** under the

influence of boron trifluoride etherate proceeded in a completely β-selective manner to give a mixture of the desired product and unreacted donor **9**. The mixture could be separated after hydrogenolysis of the benzyl ester giving acid **11** in 63% yield on 170 mmol scale. Next, all acetyls were removed, before the benzyl ester was re-installed using phase transfer conditions to deliver triol **12**. To enable the introduction of the chiral lipid tail we masked the C4- and C6-hydroxyl groups in **12** with a silylidene ketal. This protecting group strategy proved to be crucial as the use of a C6-O-*tert*-butyldimethylsilyl (TBDMS) group as previously reported,[41] led to an intractable mixture when the lipid tails were attached. As lipid A analogues bearing fewer lipid tails may have a different immunological response[44], the purity of the ligand is of utmost importance. Next, the Troc-protecting groups were removed from both amine groups, after which an *N*,*N*,*O*-triacetylation event using fatty acid **14** (Supporting information Scheme 1) and EDC·MeI and catalytic DMAP (0.03 eq.) delivered compound **15**. On a 9.5 mmol scale this intermediate was obtained in 57% over two steps. The silylidene ketal was removed, and then the primary alcohol was selectively protected with a TBDMS group, and the phosphate triester was installed at the C4-OH. Desilylation provided key building block **16a** on a multi-gram scale. The alcohol in **16a** was transformed into the corresponding primary azide using Mitsunobu conditions delivering **16b**.

With building blocks **16a/b** available in sufficient amounts, attention was directed to the assembly of ligands **1**-**4,** having either an alkyl or triethylene glycol (TEG) linker (**Figure 2B**). Debenzylation of **16a** using Pd/C gave the original CRX-527 (**1**). Elongation of **16a** with the *N*-acetylated linkers **17** or **18**, under the influence of EDC·MeI and DMAP, furnished the fully protected linker-CRX-527 compounds that were subjected to a hydrogenation reaction to obtain ligands **2** and **3**. In contrast to the findings of Guo and coworkers, in their synthesis of linker functionalized MPLA derivatives, where the C6-ester bond was found unstable,[34] no hydrolysis of esters **2** and **3** was observed. Ligand **4** was obtained from azide **16b** by zinc mediated reduction, condensation with linker **18** and subsequent hydrogenation.

Next, the synthesis of the CRX-527-peptide conjugates **5**-**8** was undertaken (**Figure 2C**). Based on the immunological evaluation of the ligands **1**-**4** (*vide infra*, **Figure 3**) the TEG linker was used for the assembly of the peptide antigen conjugates. First, **16a** and azido linker **19** were conjugated under the agency of EDC.

Reduction of the azide and benzyl esters was then followed by the introduction

of the maleimide functionality using sulfo-*N*-succinimidyl 4-maleimidobutyrate to give conjugation-ready CRX-527 **20a**. The amide congener of this compound was assembled from **16b** in an analogous manner. The $DEVA_5K$-peptides with a thiol function at the *N*-terminus (**21**) or the *C*-terminus (**22**) were assembled using a semi-automated solid phase peptide synthesis protocol and purified to homogeneity by RP-HPLC (See Supporting information for full synthetic details). The conjugation of the ligand and the peptide-antigen required significant optimization because of the physical properties of the ligand and the peptides. We found that the thiol-maleimide coupling could be achieved by dissolving **21** or **22** in DMF/H_2O (4/1 v/v) followed by the addition of a solution of maleimide **20a** or **20b** in $CHCl_3$. After shaking for two days, LC-MS analysis confirmed the full conversion of the maleimide and the conjugates were purified by C18 column chromatography (See Supporting information for details). **Figure 2D** shows the analysis of the conjugation of maleimide **20a** with an excess of thiol **22**, providing conjugate **7** (**Figure 2D**, left panel), which was purified by HPLC to provide the pure conjugate (**Figure 2D**, middle panel). The integrity and purity of the synthesized *N*-terminus conjugates **5** and **6**, and *C*-terminus conjugates **7** and **8** were ascertained by LC-MS analysis and MALDI-TOF MS (See **Figure 2D**, right panel for the MALDI-TOF MS spectrum of **7**).

In vitro activity.

Immunological evaluation of TLR4-ligands **1**-**4** and conjugates **5**-**8** was performed by first assessing their ability to induce maturation of dendritic cells and to present antigen to T cells *in vitro*. Binding of the lipid A to the TLR4/MD-2 complex triggers the production of inflammatory cytokines and maturation of the DCs. Production of the subunit IL-12p40 of the pro-inflammatory cytokine IL-12 is a marker of this activation. We first analyzed if the addition of the peptide would affect the interaction with TLR4 and impede the activity of the ligand. To probe activation of the DCs by the CRX-527-ligands and conjugates, murine DCs were stimulated for 24h with the different compounds and the amount of IL-12p40 in the supernatant was measured. First, the effect of the different linkers (compounds **2**-**4**) on the activity of the CRX-527 ligand was evaluated. As can be seen in **Figure 3A**, stimulation of the DCs with the CRX-527 ligand **1** induces strong IL-12p40 secretion and its activity is higher than the commercially available TLR4-ligand MPLA. The addition of an ester-alkyl linker (**2**) significantly decreased the ability of the ligand to induce DC-activation.

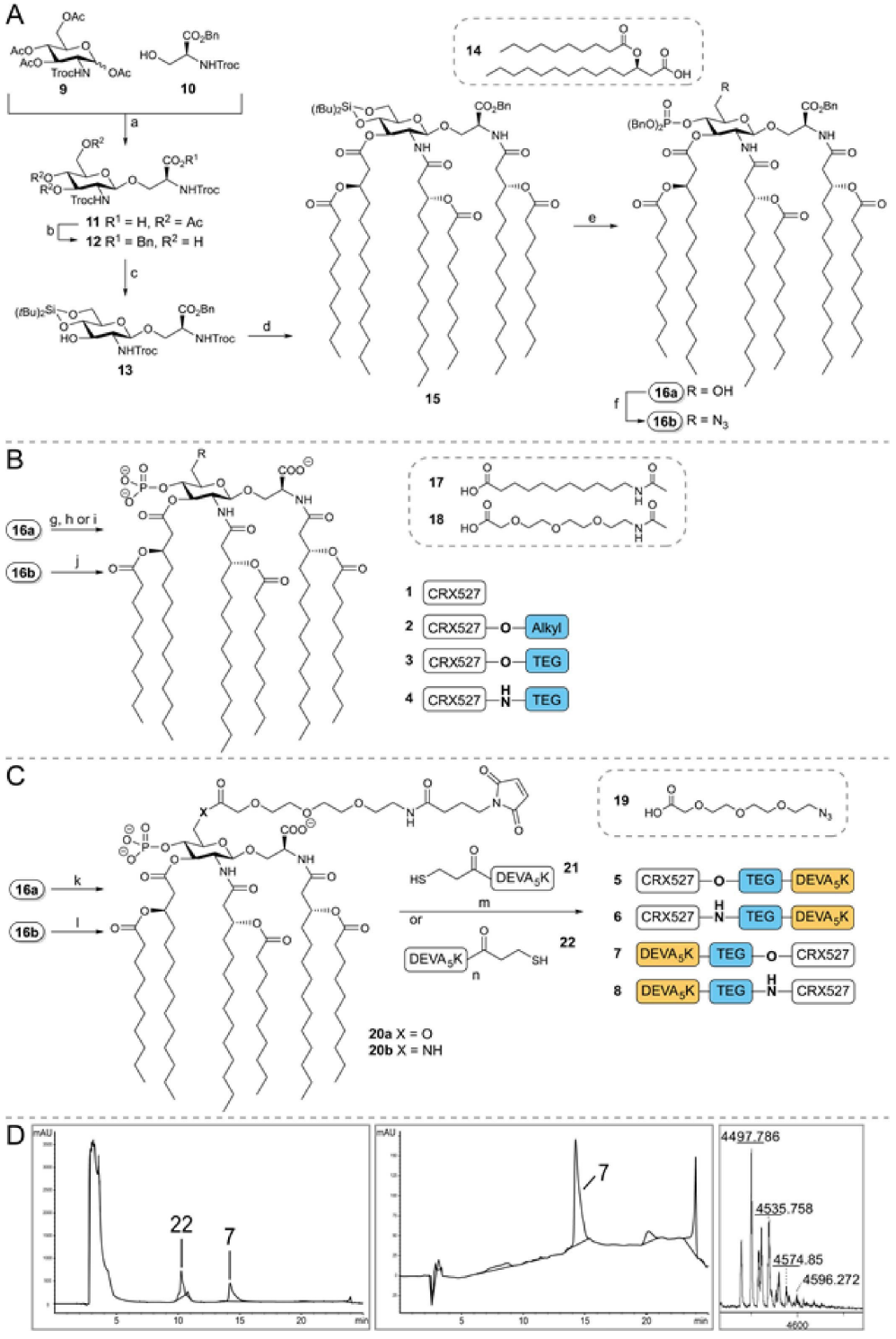
A
9
10
14
11 R1 = H, R2 = Ac
12 R1 = Bn, R2 = H
13
15
16a R = OH
16b R = N3
B
16a
16b
17
18
1 CRX527
2 CRX527 O Alkyl
3 CRX527 O TEG
4 CRX527 H N TEG
C
16a
16b
19
21
22
or
20a X = O
20b X = NH
5 CRX527 O TEG DEVA5K
6 CRX527 H N TEG DEVA5K
7 DEVA5K TEG O CRX527
8 DEVA5K TEG H N CRX527
D
mAU
22
7
min
4497.786
4535.758
4574.85
4596.272
4600

Figure 2. (A) Synthesis of building blocks **16a/b**. *Reagents and conditions*: a) *i.* $BF_3{\cdot}OEt_2$, DCM, 0°C to rt; *ii.* H_2, Pd/C, THF, 63% over two steps; b) *i.* NH_4OH, MeOH; *ii.* BnBr, TBAB, DCM/$NaHCO_3$ (aq. sat.), 79% over two steps; c) $(t\text{Bu})_2Si(OTf)_2$, DMF, -40°C, 94%; d) *i.* Zn dust, AcOH; *ii.*) **14**, EDC·MeI, DMAP, DCM, 57% over two steps. e) *i.* $HF{\cdot}Et_3N$. THF, 0°C, 92%; *ii.* TBDMSCl, pyridine, 88%; *iii.* dibenzyl *N*,*N*-diisopropylphosphoramidite, tetrazole, DCM, 0°, 1h; *iv.* 3-chloroperbenzoic acid, quant. over two steps; *v.* TFA, DCM, 84%. f) PPh_3, DEAD, DPPA, THF, 67%; (B) Synthesis of TLR4-ligands **1**-**4**. *Reagents and conditions*: g) H_2, Pd/C, THF, **1**: 89%; h) *i.* **17**, EDC·MeI, DMAP, DCE, 88%; *ii.* H_2, Pd/C, THF, **2**: 56%; i) *i.* **18**, EDC·MeI, DMAP, DCE, 74%; *ii.* H_2, Pd/C, THF, **3**: 66%; j) *i.* Zn, NH_4Cl, DCM/MeOH/H_2O; *ii.* **18**, EDC·MeI, DMAP, DCE, 40% over two steps; *iii.* H_2, Pd/C, THF, **4**: 61%; (C) Assembly of conjugates **5**-**8**. *Reagents and conditions*: k) *i.* **19**, EDC·MeI, DMAP, DCE, 80%; *ii.* H_2, Pd/C, THF, 77%; *iii.* sulfo-*N*-succinimidyl 4-maleimidobutyrate sodium salt, Et_3N, DCM, **20a**: 84%. l) *i.* Zn, NH_4Cl, DCM/MeOH/H_2O; *ii.* **19**, EDC·MeI, DMAP, DCE, 56% over two steps; *iii.* sulfo-*N*-succinimidyl 4-maleimidobutyrate sodium salt, Et_3N, DCE, **20b**: 81%; m) **21**, DMF/$CHCl_3$/H_2O, 48h, **5**: 52%, **6**: 54%; n) **22**, DMF/$CHCl_3$/H_2O, 48h, **7**: 57%, **8**: 42%. (D) LC-MS trace of crude and purified *C*-terminus conjugate **7**, and MALDI analysis of **7**.

However, the ester- or amide-TEG linker functionalized ligands mostly preserve the induction of IL-12p40, as shown for compounds **3** and **4**. For these two ligands, the activity was comparable to the unmodified ligand **1** up to 1.56 nM, and slightly reduced at the lowest concentrations. However, substantial levels of IL-12p40 could still be detected at these concentrations. Possibly, the hydrophobic nature of the alkyl linker of compound **2** induces a different configuration of the ligand that affects binding to the MD-2/TLR4 pocket, preventing activation of the signaling cascade[43]. The DC-activating capacity of compounds **1**, **3** and **4** indicates that functionalization at the C6-position with a hydrophilic linker does not inhibit binding of the ligand to the receptor.

Next, the $DEVA_5K$ peptide conjugates **5**-**8** were evaluated for their ability to induce IL-12p40 in DCs (**Figure 3B**). We analyzed whether conjugation of the peptide via the ester- (compounds **5** and **7**) or the amide-TEG linker (compounds **6** and **8**) could differently modulate the activity of the conjugates. Moreover, we investigated whether conjugation of the ligand to the *N*- or *C*-terminus of the peptide could also influence activity. Interestingly, we found that even if ligands **3** and **4** do not display any differences in activity (**Figures 3A** and **3B**), their respective peptide conjugates show differential potencies (**Figure 3B**). Specifically, the ester conjugates **5** and **7** induce high levels of IL-12p40, similarly to the ligands **3** and **4**, while the amide conjugates **6** and **8**, display overall lower levels of IL-12p40 production. No difference in activity was observed between the *N*- or *C*-terminal $DEVA_5K$ conjugates. The activity of the ester conjugates **5** and**7** titrates faster than the free ligands, **3** and **4**, as can be observed at the lowest concentrations.

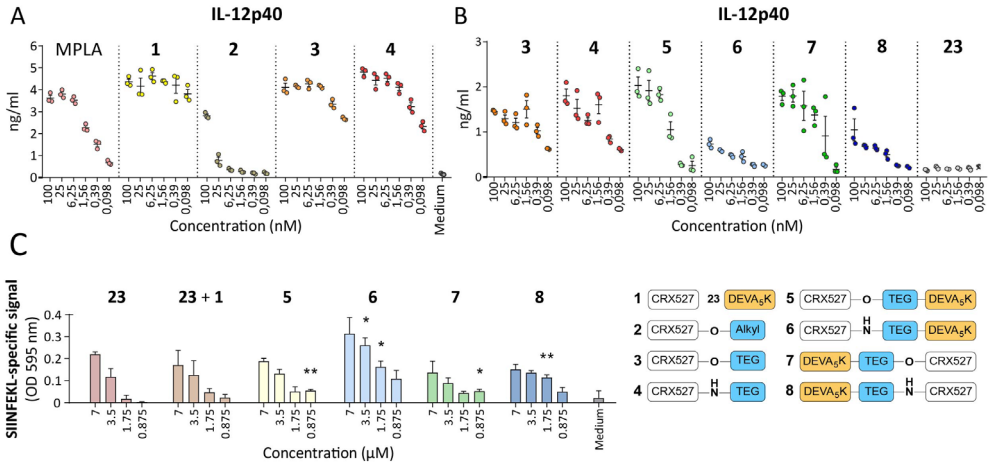

Figure 3. The TLR4-ligands and the cognate conjugates induce IL-12 production and T cell activation in vitro. (A) The D1 dendritic cell line was stimulated for 24 hours with the synthetic compounds 1-4 and the induction of DC maturation was analyzed by measuring IL-12p40 production. MPLA was included as a control for TLR4 stimulation (B) The activity of the conjugates 5-8 together with their reference ligands 3 and 4 was analyzed by measuring IL-12p40 production. Unconjugated peptide was included as negative control. (C) Antigen uptake and presentation was measured by incubation of compound-pulsed D1 with the SIINFEKL-specific hybridoma T cell line B3Z. B3Z activation was determined by colorimetric reaction of the CPRG reporter enzyme and measurement of absorbance.

These data show that conjugation of CRX-527 to a long peptide via different linkers results in immunologically active compounds and has therefore potential for vaccination. Importantly, the efficacy of peptide vaccines relies on the ability of DCs to take up the peptide and process it to enable surface presentation of the epitope on MHC molecules. Recognition of the antigen-MHC complex by the T cell receptor and simultaneous co-stimulation by mature DCs then results in the initiation of a T cell response.[45] The uptake and processing of the conjugates **5**-**8** was evaluated in an antigen presentation assay using the T cell hybridoma reporter line B3Z, which is specific for the SIINFEKL epitope contained in the $DEVA_5K$ peptide. The B3Z cell line possesses a T cell receptor, specific for the SIINFEKL epitope, which controls the expression of the beta-galactosidase reporter gene. Recognition of the SIINFEKL epitope induces the expression of the enzyme, which can subsequently be detected through a colorimetric reaction caused by the conversion of a substrate. The efficiency in antigen presentation of the conjugates was compared to free peptide **23** and to a mixture of peptide **23** and CRX-527 ligand **1**. **Figure 3C** shows that incubation of DCs with the

ester conjugates **5** and **7**, leads to similar levels of T cell activation as the free peptide and the mixture of the peptide and CRX-527 **1**. Therefore, conjugation of the peptide to the CRX-527 ligand does not affect its uptake and processing, both after *N*-terminus and *C*-terminus conjugation. Notably, incubation with the amide conjugates **6** and **8** resulted in slightly enhanced antigen presentation. In this case, the *N*-terminus conjugate **6** displayed higher antigen presentation and consequent T cell activation than its *C*-terminal counterpart. It is possible that hydrolysis takes place for the ester conjugates **5** and **7** prior to uptake in the DCs, leading to diminished uptake of the peptide moiety (as compared to their amide counterparts) and resulting in lower antigen presentation. Importantly, this read-out system is not influenced by the co-stimulatory signals provided by mature DCs, and only reports whether uptake and processing occur in DCs.

To summarize, in vitro evaluation of the conjugates revealed that the ester conjugates display higher potency in inducing DC maturation, while the amide conjugates are presented more efficiently. Therefore, the combined action of co-stimulation, induced by the triggering of the TLR4 and antigen presentation to CD8+ T cells was evaluated in an *in vivo* immunization study.

In vivo activity.

Having established that the conjugates maintained the capacity to activate DCs and to induce antigen presentation, the conjugated vaccines were compared for their ability to induce *de novo* T cell responses *in vivo*. Mice were injected intradermally with 5 nmol each of conjugates **5**-**8**, or a mixture of peptide **23** and TLR4-ligand **1**, and the presence of SIINFEKL-specific T cell responses was monitored in blood via SIINFEKL-Kb tetramer staining. Analysis of blood after the first vaccine injection demonstrated the successful induction of SIINFEKL-specific T cell responses in all groups vaccinated with the CRX-527 conjugates. No significant differences could be distinguished between the groups (Supporting information Figure 1A). Two weeks after the first injection, mice were boosted with the same formulations and the SIINFEKL-specific responses were measured in blood 7 days later. As shown in **Figure 4A** and **B**, the strongest induction of SIINFEKL-specific $CD8^+$ T cells was detected in the group that received the *N*-terminal ester conjugate **5**. Overall, the two *N*-terminal conjugates **5** and **6** displayed higher T cell induction than their *C*-terminal counterpart conjugates **7** and **8**. T cell responses were detectable also in mice vaccinated with a mixture of CRX-527 and peptide, however, these responses displayed a higher spread than all conjugate groups. One day later, the spleens and lymph nodes draining

the vaccination site were harvested to analyze the presence and the phenotype of the SIINFEKL-specific responses in these organs. Analysis of T cell responses in the spleen displayed a similar trend to that observed in blood (Supporting information Figure 1B). However, in the inguinal lymph nodes (**Figure 4C**) a higher percentage of SIINFEKL-specific T cell responses was detected for the *N*-terminal conjugates **5** and **6**. In this organ, mice vaccinated with the *C*-terminus conjugates **7** and **8** or the mixture display low T cell responses. Next, we investigated whether the phenotype of the SIINFEKL-specific T cells induced by the *N*-terminal conjugates **5** and **6** was different compared to the group that was vaccinated with the mixture of TLR4-ligand **1** and peptide **23**. The induction of differentiation into memory $CD127^{+}/KLRG1^{low}$ responses is a marker for T cell quality, which is associated with improved functions and tumor clearance.[46] This phenotype was pronounced in the groups vaccinated with the conjugates **5** and **6** and was clearly less present in the group that was vaccinated with the mixture (**Figure 4D**). Within the T cell memory population, two further subsets can be distinguished based on the expression of CD62L, a surface protein that, when present, determines homing at lymphoid tissues, rather than circulation in the blood vessels and tissues. High expression of CD62L defines central memory T cells, while lower expression of this surface protein determines effector memory T cells. This last subset recirculates in tissues and can exert immediate effector functions upon antigen reencounter. We observed significantly higher differentiation into effector memory T cells when mice were immunized with the conjugated vaccines **5** and **6** rather than the mixture (**Figure 4E**). It has been shown that the promotion of differentiation into effector memory T cells rather than short-lived effector cells is dependent on optimal priming conditions, such as the presence of helper T cells[46–48] and proper co-stimulatory signals[49,50]. These data indicate that conjugation of the TLR4-adjuvant and peptide represents an effective strategy to achieve an increased effector memory T cell phenotype, which is an important hallmark for effective vaccination.[51–53]

Finally, we investigated the functionality of the induced T cell responses upon vaccination with conjugate **6** in an *in vivo* cytotoxicity assay. Mice were immunized with the *N*-terminus conjugate **6**, and the kinetics of the T cell response was followed in blood by SIINFEKL-Kb tetramer staining (**Figure 5A**). After 14 days a boost was administered, and one week later animals were intravenously injected with cells loaded with either SIINFEKL peptide or an irrelevant peptide, to measure the ability of the induced T cells to specifically kill SIINFEKL-loaded

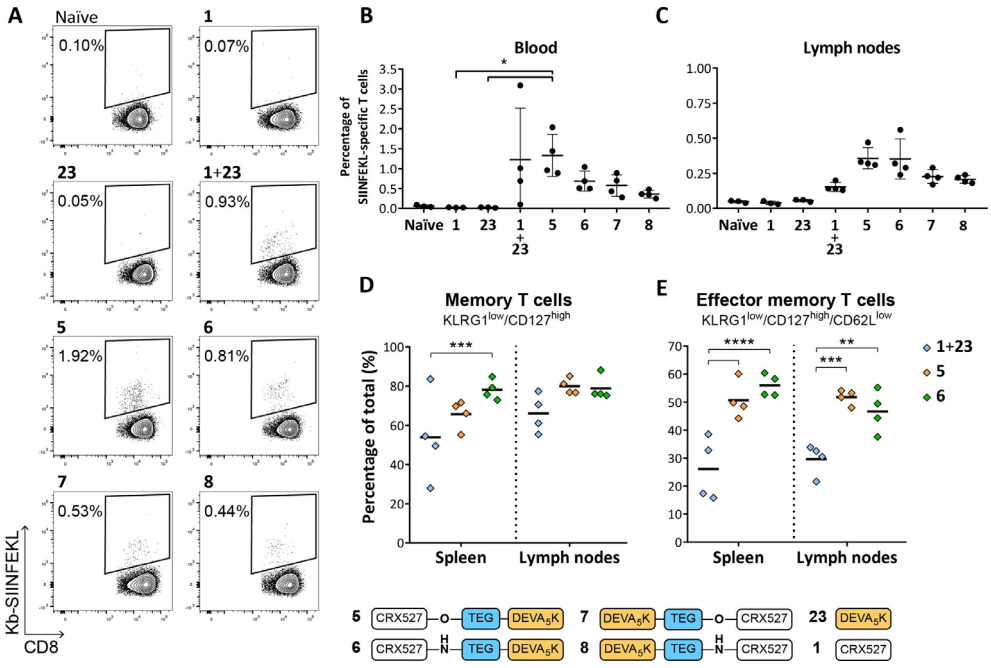

Figure 4. The conjugates induce SIINFEKL-specific T cell responses with an effector memory phenotype *in vivo*. (A) Representative plots of SIINFEKL-Kb tetramer positive T cells in blood of vaccinated mice. (B) Percentage of SIINFEKL-specific T cell responses measured by tetramer staining in blood at day 21 after booster vaccination. Every dot represents a single animal. (C) At day 22, inguinal lymph nodes were harvested and the presence of SIINFEKL-specific T cells was measured by tetramer staining in all groups. Statistical significance was determined by Kruskal-Wallis test followed by multiple comparison rank test and Dunn's correction, * $p < 0.05$. (D and E) The phenotype of SIINFEKL-specific T cells was characterized in the higher-responding groups in spleen and lymph nodes by analyzing the expression of the surface markers KLRG1, CD127 (D) and CD62L (E) by flow cytometry. Statistical significance was determined by two-way ANOVA followed by multiple comparison and Tukey correction, ** $p < 0.01$ *** $p < 0.001$, **** $p < 0.0001$.

cells. Prior to injection, the two groups of target cells were differentially labelled with the fluorescent dye CFSE, to be able to distinguish the two populations during later analysis by flow cytometry. After 18 hours, the spleens were harvested and the killing of the two peptide-loaded populations was determined in naïve and vaccinated mice via flow cytometric analysis. (**Figure 5A** and **B**). As expected, naïve mice displayed similar relative frequencies of the two CFSE-labelled populations. On the contrary, specific killing of the SIINFEKL-loaded target cells was observed in the vaccinated mice. Notably, four out of five mice that were vaccinated with conjugate **6** displayed > 90% killing. The killing degree

reflected the levels of specific $CD8^+$ T cells present, as detected in the inguinal lymph nodes by tetramer staining (**Figure 5C**).

To conclude, *in vivo* evaluation of the CRX-527-peptide conjugates shows that conjugates **5**-**8** are effective in initiating antigen-specific T cell responses. In particular, the *N*-terminus conjugates could raise higher responses than their C-terminal counterparts. Phenotypic and functional analysis of these responses revealed that CRX-527 conjugate **6** was capable of raising an adequate protective immune response, effectively killing cells presenting the antigen against which the vaccination was directed and underscoring the potential of these new conjugates for anti-cancer immunotherapy.

CONCLUSIONS

Adjuvant-antigen conjugates are promising agents for cancer immunotherapy. Well-defined molecular adjuvants are essential to stimulate relevant immune subsets and generate the most appropriate type of immunity against distinct tumor types. MPLA is one of the most potent innate immune-stimulating agents, which is currently used as an adjuvant in vaccines, but the application of this TLR4-ligand in adjuvant-antigen constructs is hampered by its challenging synthesis. CRX-527 is a potent MPLA analogue and we have here disclosed an expeditious synthesis of conjugation ready derivatives of this immune-stimulating agent and demonstrated the preparation of TLR4-ligand-peptide antigen conjugates for the first time. The assembly of the conjugation-ready ligand critically depended on the protecting group strategy and the use of a silylidene ketal in the glucosaminyl serine proved crucial for the efficient introduction of the lipid tails. The developed route of synthesis is high-yielding and could be executed on a multigram scale to allow the generation of several peptide conjugates. Different linker systems and connection modes were probed to conjugate the TLR4-ligand to a synthetic long peptide antigen. *In vitro* evaluation of the conjugates showed that the attachment of a lipophilic linker at the C6 of CRX-527 abrogates the activity of the ligand. The use of a hydrophilic glycol-based linker provided conjugates which could induce strong DC maturation, and allowed effective antigen processing and presentation. *In vivo* evaluation of the conjugates demonstrated the efficacy of the vaccine modalities in priming *de novo* $CD8^+$ T cell responses. Conjugation of the TLR4-ligand at the *N*-terminus of the peptide stimulated the best induction of T cell responses, promoting differentiation into effector memory T cell responses. Finally, it was shown that the CRX-527-pep

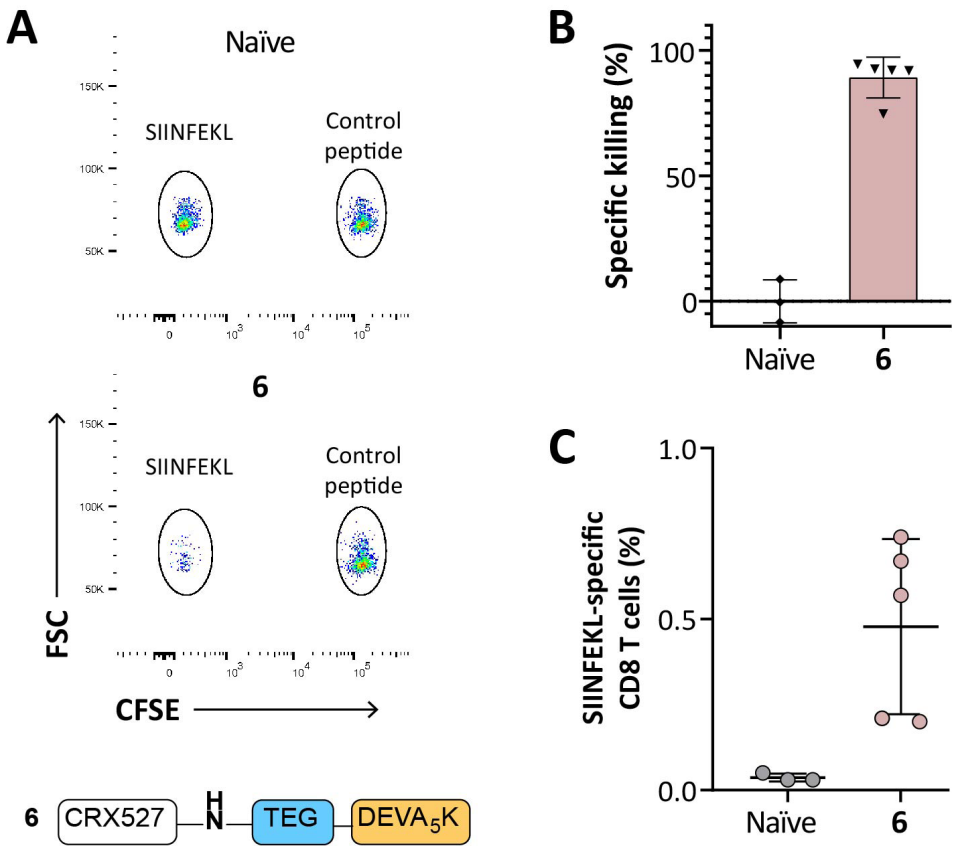

Figure 5. Immunization with CRX-527 conjugate **6** results in efficient specific killing of peptide-loaded target cells. Naïve C57BL/6 mice (n=5) were injected intradermally with 5 nmol of CRX-527 conjugate. (A**)** After booster vaccination, mice were injected with differentially CFSE-labelled target cells. 18 hours after injection, spleens were analyzed for the presence of the two CFSE-labelled target populations. (B**)** Calculated specific-killing of SIINFEKL-loaded cells. (C**)** The amount of SIINFEKL-specific T cells was determined in the lymph nodes by tetramer staining.

tide, in which the TLR4-ligand was conjugated to the *N*-terminus of the SLP through an amide linked spacer, was a potent inducer of antigen-specific effector $CD8^+$ T cell responses *in vivo*. Overall, we have developed a platform to potentiate synthetic peptide vaccines with a potent and well-defined TLR4-ligand, a powerful addition to the toolbox available to generate self-adjuvanting vaccines. CRX-527 conjugates hold great promise for the development of anti-cancer SLP-vaccines and the availability of the conjugation-ready ligand and chemistry to fuse the ligand to peptide antigens will enable the generation of conjugates bearing other peptide epitopes, such as defined oncoviral antigens or cancer

neoantigens. The generated conjugation-ready CRX-527 may also find application in the generation of well-defined anti-bacterial, viral or fungal vaccines.

EXPERIMENTAL SECTION

Materials and Methods. All reagents were of commercial grade and used as received unless stated otherwise. Reaction solvents were of analytical grade and when used under anhydrous conditions stored over flame-dried 3Å molecular sieves. All moisture and oxygen sensitive reactions were performed under an argon atmosphere. Column chromatography was performed on silica gel (Screening Devices BV, 40-63 µm, 60 Å). For TLC analysis, pre-coated silica gel aluminum sheets (Merck, silica gel 60, F254) were used with detection by UV-absorption (254/366 nm) where applicable. Compounds were visualized on TLC by UV absorption (245 nm), or by staining with one of the following TLC stain solutions: $(NH_4)_6Mo_7O_{24}{\cdot}H_2O$ (25 g/L), $(NH_4)_4Ce(SO_4)_4{\cdot}2H_2O$ (10 g/L) and 10% H_2SO_4 in H_2O; bromocresol (0.4 g/L) in EtOH; $KMnO_4$ (7.5 g/L), K_2CO_3 (50 g/L) in H_2O. Staining was followed by charring at ~150°C. ^{1}H, ^{13}C and ^{31}P NMR spectra were recorded on a Bruker AV-300 (300/75 MHz), AV-400 (400/100 MHz) spectrometer, a Bruker AV-500 Ultrashield (500/126 MHz) spectrometer, a Bruker AV-600 (600/151 MHz) or a Bruker AV-850 (850/214 MHz) and all individual signals were assigned using 2D-NMR spectroscopy. Chemical shifts are given in ppm (δ) relative to TMS (0 ppm) in $CDCl_3$ or via the solvent residual peak. Coupling constants (*J*) are given in Hz. LC-MS analysis were done on an Agilent Technologies 1260 Infinity system with a C18 Gemini 3 µm, C18, 110 Å, 50 x 4.6 mm column or a Vydac 219TP 5 µm Diphenyl, 150 x 4.6 mm column with a flow of 1, 0.8 or 0.7 ml/min. Absorbance was measured at 214 nm and 256 nm and an Agilent Technologies 6120 Quadrupole mass spectrometer was used as detector. Peptides, TLR2-ligand and conjugate were purified with a Gilson GX-281 preparative HPLC with a Gemini-NX 5u, C18, 110 Å, 250 x 10.0 mm column or a Vydac 219TP 5 µm Diphenyl, 250 x 10 mm column. Peptide fragments were synthesized with automated solid phase peptide synthesis on an Applied Biosystems 433A Peptide Synthesizer. Optical rotations were measured on an Anton Paar Modular Circular Polarimeter MCP 100/150. High resolution mass spectra were recorded on a Synapt G2-Si or a Q Exactive HF Orbitrap equipped with an electron spray ion source positive mode. Mass analysis of the TLR4-ligands and TLR4-ligand conjugates was performed on an Ultraflextreme MALDI-TOF or a 15T MALDI-FT-ICR MS system. Infrared spectra were recorded on a Perkin Elmer Spectrum 2 FT-IR. Unprotected lipid A derivatives were dissolved in a mixture of $CDCl_3$/MeOD 5/1 v/v for NMR analysis. DC activation and B3Z assay results were analysed with GraphPad Prism version

7.00 for Windows, GraphPad Software. Purity of all compounds is > 95% as determined by NMR or LC-MS analysis. FA = fatty acid.

Automated solid phase synthesis general experimental information. The automated solid-phase peptide synthesis was performed on a 250 µmol scale on a Protein Technologies Tribute-UV IR Peptide Synthesizer applying Fmoc based protocol starting from Tentagel S RAM resin (loading 0.22 mmol/g). The synthesis was continued with Fmoc-amino acids specific for each peptide. The consecutive steps performed in each cycle for HCTU chemistry on 250 µmol scale: 1) Deprotection of the Fmoc-group with 20% piperidine in DMF for 10 min; 2) DMF wash; 3) Coupling of the appropriate amino acid using a four-fold excess. Generally, the Fmoc amino acid (1.0 mmol) was dissolved in 0.2 M HCTU in DMF (5 mL), the resulting solution was transferred to the reaction vessel followed by 2 mL of 1.0 M DIPEA in DMF to initiate the coupling. The reaction vessel was then shaken for 30 min at 50°C; 4) DMF wash; 5) capping with 10% Ac_2O in 0.1 M DIPEA in DMF; 6) DMF wash; 7) DCM wash. Aliquots of resin of the obtained sequences were checked on an analytical Agilent Technologies 1260 Infinity system with a Gemini 3 µm, C18, 110 Å, 50 x 4.6 mm column or a Vydac 219TP 5 µm Diphenyl, 150 x 4.6 mm column with a 1 ml/min flow. The Fmoc amino acids applied in the synthesis were: Fmoc-Ala-OH, Fmoc-Asn(Trt)-OH, Fmoc-Asp(O*t*Bu)-OH, Fmoc-Gln(Trt)-OH, Fmoc-Glu(O*t*Bu)-OH, Fmoc-Gly-OH, Fmoc-Ile-OH, Fmoc-Leu-OH, Fmoc-Lys(Boc)-OH, Fmoc-Lys(MMT)-OH, Fmoc-Phe-OH, Fmoc-Ser(O*t*Bu)-OH Fmoc-Val-OH.

General procedure for cleavage from the resin, deprotection and purification. 30 µmol resin was washed with DMF, DCM and dried after the last synthesis step followed by a treatment for 180 minutes with 0.6 mL cleavage cocktail of 95% TFA, 2.5% TIS and 2.5% H_2O. The suspension was filtered, the resin was washed with 0.6 mL of the cleavage cocktail, and the combined TFA solutions were added dropwise to cold Et_2O and stored at -20°C overnight. The obtained suspension of the product in Et_2O was centrifuged, Et_2O was removed and the precipitant was dissolved in $CH_3CN/H_2O/$*t*BuOH (1/1/1 v/v/v) or DMSO/$CH_3CN/H_2O/$*t*BuOH (3/1/1/1 v/v/v/v). Purification was performed on a Gilson GX-281 preparative RP-HPLC with a Gemini-NX 5u, C18, 110 Å, 250 x 10.0 mm column or a Vydac 219TP 5 µm Diphenyl, 250 x 10 mm column.

General purification method for CRX-527-*O*-conjugates. A C18 column was washed subsequently with CH_3CN, MeOH, DCM/MeOH (1/1 v/v), MeOH, CH_3CN, CH_3CN/H_2O, H_2O. The reaction mixture was added on the column and the Eppendorf was rinsed with a mixture of $CH_3CN/$*t*BuOH/MilliQ H_2O (1/1/1 v/v/v, 0.50 mL), which was also added on the C18 column. The column was subsequent-

ly flushed with 6 mL of the follow solvent systems: H_2O, CH_3CN/H_2O (1/1 v/v), CH_3CN, DMSO, CH_3CN/*t*BuOH/MilliQ H_2O (1/1/1 v/v/v) and collected in Eppendorfs containing 1.0 mL of each solvent system. The column was then flush with MeOH (6.0 mL), followed by DCM/MeOH (1/1 v/v, 6.0 mL), which were collected in separate flasks, concentrated *in vacuo* at 35°C and lyophilized by dissolving in CH_3CN/*t*BuOH/MilliQ H_2O (1/1/1 v/v/v), yielding the conjugate as a white solid. *For the amide conjugates, H_2O + 0.1% TFA was used instead of H_2O.

MALDI-TOF measurements. MALDI-TOF measurements: 1 **µ**L of a DMSO solution of the compound was spotted on a 384-MTP target plate (Bruker Daltonics, Bremen, Germany) and air-dried. Subsequently 1 **µ**L of 2,5-dihydroxybenzoic acid (2,5-DHB; Bruker Daltonics) matrix (20 mg/mL in ACN/water; 50:50 (v/v)) was applied on the plate and the spots were left to dry prior MALDI-TOF analysis. An Ultraflextreme MALDI-TOF (Bruker Daltonics), equipped with Smartbeam-II laser was used to measure the samples in reflectron positive ion mode. The MALDI-TOF was calibrated using a peptide calibration standard prior to measurement.

Synthesis and Characterizations. The synthesis and characterizations for compounds **9, 10, 11, 12, 13, 15, 16a, 16b, 1, 2, 3, 4, 20a, 20b, 21, 22, 5, 6, 7, 8, 23, 14**, **17**, **18**, and **18**, can be found in the online version of the publication and in the online supplementary information.

Immunological evaluation procedures.

Cell culture. The D1 cell line is a growth factor-dependent immature spleen-derived DC cell line from C57BL/6 (H-2^b) mice. D1 and B3Z cells were cultured as described elsewhere.[55] The B3Z cell line was cultured in IMDM medium (Lonza, Basel, Switzerland) supplemented with 8% FCS (Greiner, Kremsmünster, Austria), penicillin and streptomycin, glutamine (Gibco, Carlsbad, CA, USA), β-mercaptoethanol (Merck, Kenilworth, NJ USA), and hygromycin B (AG Scientific Inc, San Diego, CA, USA) to maintain expression of the beta-galactosidase reporter gene.

In vitro DC maturation assay. The test compounds were dissolved in DMSO at a concentration of 500 µM and sonicated in water bath for 15 minutes. 50.000 D1 cell were seeded in 96-well round bottom plates (Corning, Amsterdam, The Netherlands) in 100 µl of R1 supplemented IMDM medium and 100 µl of 2 times concentrated test compounds in medium were added. After 24 hours of incubation at 37°C, supernatant was taken from the wells for ELISA analysis (BioLegend, San Diego, USA) to measure the amount of produced IL-12p40.

In vitro antigen presentation assay. The test compounds were dissolved in DMSO at a concentration of 500 µM and sonicated in water bath for 15 minutes. 50.000

D1 cells were seeded in 96-well flat bottom plates and pulsed for 2 hours with 200 µl of the test compounds in medium at the indicated concentrations. After 2 hours, cells were washed once with 200 µl of fresh medium and 50.000 B3Z were added per well in 200 µl of medium and incubated with the pulsed D1 cells overnight. The following day TCR activation was detected by measurement of absorbance at 595 nm upon color conversion of chlorophenol red-β-D-galacto-pyranoside (Calbiochem®, Merck, Bullington MA, USA) by the beta-galactosidase enzyme, followed by measurement of absorbance at 595 nm.[56,57]

Mice. Female C57BL/6 mice were purchased from Charles River Laboratories. Congenic CD45.1$^+$ C57BL/6 mice were bred at the Leiden University medical Centre animal facility. All animal experiments were in accordance with the Dutch national regulations and received ethical and technical approval by the local Animal Welfare Body.

Immunization of mice. 6-8 weeks old C57BL/6 female mice were injected intradermally at the tail base with 5 nmol of each conjugate or an equimolar mix of Lipid A and $DEVA_5K$ peptide. To prepare the vaccine, the different compounds were dissolved in DMSO at a concentration of 500 µM and sonicated in water bath for 15 minutes. The required amounts for vaccination was added to saline solution and 30 µl per mouse were injected. Fourteen days later, the animals were boosted with the same vaccine formulations. At different time points during the experiments, 20 µl of blood were collected from the tail vein for detection of SIINFEKL-specific T cell responses via SIINFEKL-H2-Kb tetramer staining. At the end of the experiments, spleens and lymph nodes were removed and processed in single cell suspensions for *ex vivo* analysis.

In vivo specific killing.Splenocytes were harvested from CD45.1$^+$ C57BL/6 naïve mice, processed into single cell suspension and labelled with either 5 or 0.005 µM CFSE for 10 min at 37°C. Cells that were labelled with 0.005 µM CFSE (CFSE low) were loaded for 1 hour at 37°C with 1µM SIINFEKL peptide, while cells that were labelled with 5 µM CFSE (CFSE high) were loaded in the same conditions with an irrelevant epitope derived from the E6 protein of Human Papilloma Virus (sequence: RAHYNIVTF). 4'000'000 splenocytes per peptide-loaded group were injected intravenously in vaccinated or naïve mice. One day after transfer, mice were sacrificed and the spleens were harvested and processed into single cell suspensions. Splenocytes were subsequently stained with eFluor®450 anti-CD45.1 antibody (eBioscience, San Diego, USA) and analyzed by flow cytometry to detect CD45.1$^+$/CFSE$^+$ target cells. Specific killing was calculated according to the following equation: Specific killing = 100 - [100*((CFSE target peptide)/(CFSE irrelevant) immunized mice)/((CFSE target peptide)/(CFSE irrelevant) naïve mice)]

REFERENCES

(1) Wei, S. C.; Duffy, C. R.; Allison, J. P. Fundamental Mechanisms of Immune Checkpoint Blockade Therapy. *Cancer Discovery*. **2018**, *8*, 1069–1086.

(2) Mchayleh, W.; Bedi, P.; Sehgal, R.; Solh, M. Chimeric Antigen Receptor T-Cells: The Future Is Now. *J. Clin. Med.* **2019**, *8*, 207.

(3) Schumacher, T. N.; Schreiber, R. D. Neoantigens in Cancer Immunotherapy. *Science*. **2015**, *348*, 69–74.

(4) Heimburg-Molinaro, J.; Lum, M.; Vijay, G.; Jain, M.; Almogren, A.; Rittenhouse-Olson, K. Cancer Vaccines and Carbohydrate Epitopes. *Vaccine* **2011**, *29*, 8802–8826.

(5) Brubaker, S. W.; Bonham, K. S.; Zanoni, I.; Kagan, J. C. Innate Immune Pattern Recognition: A Cell Biological Perspective. *Annu. Rev. Immunol.* **2015**, *33*, 257–290.

(6) Iwasaki, A.; Medzhitov, R. Toll-like Receptor Control of the Adaptive Immune Responses. *Nat. Immunol.* **2004**, *5*, 987–995.

(7) Kawai, T.; Akira, S. The Role of Pattern-Recognition Receptors in Innate Immunity: Update on Toll-like Receptors. *Nat. Immunol.* **2010**, *11*, 373–384.

(8) van Dinther, D.; Stolk, D. A.; van de Ven, R.; van Kooyk, Y.; de Gruijl, T. D.; den Haan, J. M. M. Targeting C-Type Lectin Receptors: A High-Carbohydrate Diet for Dendritic Cells to Improve Cancer Vaccines. *J. Leukoc. Biol.* **2017**, *102*, 1017–1034.

(9) Garaude, J.; Kent, A.; van Rooijen, N.; Blander, J. M. Simultaneous Targeting of Toll- and Nod-Like Receptors Induces Effective Tumor-Specific Immune Responses. *Sci. Transl. Med.* **2012**, *4*, 120ra16.

(10) Zom, G. G.; Willems, M. M. J. H. P.; Meeuwenoord, N. J.; Reintjens, N. R. M.; Tondini, E.; Khan, S.; Overkleeft, H. S.; van der Marel, G. A.; Codee, J. D. C.; Ossendorp, F.; Filippov, D. V. Dual Synthetic Peptide Conjugate Vaccine Simultaneously Triggers TLR2 and NOD2 and Activates Human Dendritic Cells. *Bioconjug. Chem.* **2019**, *30*, 1150–1161.

(11) Zom, G. G. P.; Khan, S.; Filippov, D. V.; Ossendorp, F. TLR Ligand–Peptide Conjugate Vaccines. In *Advances in Immunology*; **2012**, *114*, 177–201.

(12) Liu, H.; Irvine, D. J. Guiding Principles in the Design of Molecular Bioconjugates for Vaccine Applications. *Bioconjug. Chem.* **2015**, *26*, 791–801.

(13) Steinhagen, F.; Kinjo, T.; Bode, C.; Klinman, D. M. TLR-Based Immune Adjuvants. *Vaccine*. **2011**, *29*, 3341–3355.

(14) Dowling, J. K.; Mansell, A. Toll-like Receptors: The Swiss Army Knife of Immunity and Vaccine Development. *Clinical and Translational Immunology*. **2016**, 5:e85. https://doi.org/10.1038/cti.2016.22.

(15) Moyle, P. M.; Toth, I. Modern Subunit Vaccines: Development, Components, and Research Opportunities. *ChemMedChem* **2013**, *8*, 360–376.

(16) Ignacio, B. J.; Albin, T. J.; Esser-Kahn, A. P.; Verdoes, M. Toll-like Receptor Agonist Conjugation: A Chemical Perspective. *Bioconjug. Chem.* **2018**, *29*, 587–603.

(17) Ingale, S.; Wolfert, M. A.; Gaekwad, J.; Buskas, T.; Boons, G.-J. Robust Immune Responses Elicited by a Fully Synthetic Three-Component Vaccine. *Nat. Chem. Biol.* **2007**, *3*, 663–667.

(18) Khan, S.; Weterings, J. J.; Britten, C. M.; de Jong, A. R.; Graafland, D.; Melief, C. J. M.; van

der Burg, S. H.; van der Marel, G.; Overkleeft, H. S.; Filippov, D. V.; Ossendorp, F. Chirality of TLR-2 Ligand Pam3CysSK4 in Fully Synthetic Peptide Conjugates Critically Influences the Induction of Specific CD8+ T-Cells. *Mol. Immunol.* **2009**, *46*, 1084–1091.

(19) Abdel-Aal, A.-B. M.; Zaman, M.; Fujita, Y.; Batzloff, M. R.; Good, M. F.; Toth, I. Design of Three-Component Vaccines against Group A Streptococcal Infections: Importance of Spatial Arrangement of Vaccine Components. *J. Med. Chem.* **2010**, *53*, 8041–8046.

(20) Khan, S.; Bijker, M. S.; Weterings, J. J.; Tanke, H. J.; Adema, G. J.; van Hall, T.; Drijfhout, J. W.; Melief, C. J. M.; Overkleeft, H. S.; van der Marel, G. A.; Filippov, D. V.; van der Burg, S. H.; Ossendorp, F. Distinct Uptake Mechanisms but Similar Intracellular Processing of Two Different Toll-like Receptor Ligand-Peptide Conjugates in Dendritic Cells. *J. Biol. Chem.* **2007**, *282*, 21145–21159.

(21) Zom, G. G.; Willems, M. M. J. H. P.; Khan, S.; Van Der Sluis, T. C.; Kleinovink, J. W.; Camps, M. G. M.; Van Der Marel, G. A.; Filippov, D. V.; Melief, C. J. M.; Ossendorp, F. Novel TLR2-Binding Adjuvant Induces Enhanced T Cell Responses and Tumor Eradication. *J. Immunother. Cancer* **2018**, *6*, 146.

(22) Willems, M. M. J. H. P.; Zom, G. G.; Khan, S.; Meeuwenoord, N.; Melief, C. J. M.; van der Stelt, M.; Overkleeft, H. S.; Codée, J. D. C.; van der Marel, G. A.; Ossendorp, F.; Filippov, D. V. N -Tetradecylcarbamyl Lipopeptides as Novel Agonists for Toll-like Receptor 2. *J. Med. Chem.* **2014**, *57*, 6873–6878.

(23) Weterings, J. J.; Khan, S.; van der Heden, G. J.; Drijfhout, J. W.; Melief, C. J. M.; Overkleeft, H. S.; van der Burg, S. H.; Ossendorp, F.; van der Marel, G. A.; Filippov, D. V. Synthesis of 2-Alkoxy-8-Hydroxyadenylpeptides: Towards Synthetic Epitope-Based Vaccines. *Bioorg. Med. Chem. Lett.* **2006**, *16*, 3258–3261.

(24) Fujita, Y.; Hirai, K.; Nishida, K.; Taguchi, H. 6-(4-Amino-2-Butyl-Imidazoquinolyl)-Norleucine: Toll-like Receptor 7 and 8 Agonist Amino Acid for Self-Adjuvanting Peptide Vaccine. *Amino Acids* **2016**, *48*, 1319–1329.

(25) Kramer, K.; Young, S. L.; Walker, G. F. Comparative Study of 5′- and 3′-Linked CpG–Antigen Conjugates for the Induction of Cellular Immune Responses. *ACS Omega* **2017**, *2*, 227–235

(26) Daftarian, P.; Sharan, R.; Haq, W.; Ali, S.; Longmate, J.; Termini, J.; Diamond, D. J. Novel Conjugates of Epitope Fusion Peptides with CpG-ODN Display Enhanced Immunogenicity and HIV Recognition. *Vaccine* **2005**, *23*, 3453–3468.

(27) Alving, C. R.; Peachman, K. K.; Rao, M.; Reed, S. G. Adjuvants for Human Vaccines. *Curr. Opin. Immunol.* **2012**, *24*, 310–315.

(28) Casella, C. R.; Mitchell, T. C. Putting Endotoxin to Work for Us: Monophosphoryl Lipid A as a Safe and Effective Vaccine Adjuvant. *Cell. Mol. Life Sci.* **2008**, *65*, 3231–3240.

(29) Garçon, N.; Di Pasquale, A. From Discovery to Licensure, the Adjuvant System Story. *Hum. Vaccin. Immunother.* **2017**, *13*, 19–33.

(30) Wang, Q.; Zhou, Z.; Tang, S.; Guo, Z. Carbohydrate-Monophosphoryl Lipid A Conjugates Are Fully Synthetic Self-Adjuvanting Cancer Vaccines Eliciting Robust Immune Responses in the Mouse. *ACS Chem. Biol.* **2012**, *7*, 235–240.

(31) Zhou, Z.; Mondal, M.; Liao, G.; Guo, Z. Synthesis and Evaluation of Monophosphoryl Lipid A Derivatives as Fully Synthetic Self-Adjuvanting Glycoconjugate Cancer Vaccine Carriers. *Org. Biomol. Chem.* **2014**, *12*, 3238–

3245.

(32) Zhou, Z.; Liao, G.; Mandal, S. S.; Suryawanshi, S.; Guo, Z. A Fully Synthetic Self-Adjuvanting Globo H-Based Vaccine Elicited Strong T Cell-Mediated Antitumor Immunity. *Chem. Sci.* **2015**, *6*, 7112–7121.

(33) Liao, G.; Zhou, Z.; Suryawanshi, S.; Mondal, M. A.; Guo, Z. Fully Synthetic Self-Adjuvanting α-2,9-Oligosialic Acid Based Conjugate Vaccines against Group C Meningitis. *ACS Cent. Sci.* **2016**, *2*, 210–218.

(34) Wang, L.; Feng, S.; Wang, S.; Li, H.; Guo, Z.; Gu, G. Synthesis and Immunological Comparison of Differently Linked Lipoarabinomannan Oligosaccharide–Monophosphoryl Lipid A Conjugates as Antituberculosis Vaccines. *J. Org. Chem.* **2017**, *82*, 12085–12096.

(35) Zamyatina, A. Aminosugar-Based Immunomodulator Lipid A: Synthetic Approaches. *Beilstein J. Org. Chem.* **2018**, *14*, 25–53.

(36) Fujimoto, Y.; Shimoyama, A.; Saeki, A.; Kitayama, N.; Kasamatsu, C.; Tsutsui, H.; Fukase, K. Innate Immunomodulation by Lipophilic Termini of Lipopolysaccharide; Synthesis of Lipid As from Porphyromonas Gingivalis and Other Bacteria and Their Immunomodulative Responses. *Mol. Biosyst.* **2013**, *9*, 987.

(37) Li, Q.; Guo, Z. Recent Advances in Toll Like Receptor-Targeting Glycoconjugate Vaccines. *Molecules* **2018**, *23*, 1583.

(38) Stöver, A. G.; Da Silva Correia, J.; Evans, J. T.; Cluff, C. W.; Elliott, M. W.; Jeffery, E. W.; Johnson, D. A.; Lacy, M. J.; Baldridge, J. R.; Probst, P.; Ulevitch, R. J.; Persing, D. H.; Hershberg, R. M. Structure-Activity Relationship of Synthetic Toll-like Receptor 4 Agonists. *J. Biol. Chem.* **2004**, *279*, 4440–4449.

(39) Cluff, C. W.; Baldridge, J. R.; Stover, A. G.; Evans, J. T.; Johnson, D. A.; Lacy, M. J.; Clawson, V. G.; Yorgensen, V. M.; Johnson, C. L.; Livesay, M. T.; Hershberg, R. M.; Persing, D. H. Synthetic Toll-Like Receptor 4 Agonists Stimulate Innate Resistance to Infectious Challenge. *Infect. Immun.* **2005**, *73*, 3044–3052.

(40) Bazin, H. G.; Bess, L. S.; Livesay, M. T.; Ryter, K. T.; Johnson, C. L.; Arnold, J. S.; Johnson, D. A. New Synthesis of Glycolipid Immunostimulants RC-529 and CRX-524. *Tetrahedron Lett.* **2006**, *47*, 2087–2092.

(41) Bazin, H. G.; Murray, T. J.; Bowen, W. S.; Mozaffarian, A.; Fling, S. P.; Bess, L. S.; Livesay, M. T.; Arnold, J. S.; Johnson, C. L.; Ryter, K. T.; Cluff, C. W.; Evans, J. T., Johnson, D. A. The 'Ethereal' Nature of TLR4 Agonism and Antagonism in the AGP Class of Lipid A Mimetics. *Bioorg. Med. Chem. Lett.* **2008**, *18*, 5350–5354.

(42) Dupont, J.; Altclas, J.; Lepetic, A.; Lombardo, M.; Vázquez, V.; Salgueira, C.; Seigelchifer, M.; Arndtz, N.; Antunez, E.; von Eschen, K.; Janowicz, Z. A Controlled Clinical Trial Comparing the Safety and Immunogenicity of a New Adjuvanted Hepatitis B Vaccine with a Standard Hepatitis B Vaccine. *Vaccine* **2006**, *24*, 7167–7174.

(43) Park, B. S.; Lee, J.-O. Recognition of Lipopolysaccharide Pattern by TLR4 Complexes. *Exp. Mol. Med.* **2013**, *45*, e66.

(44) DeMarco, M. L.; Woods, R. J. From Agonist to Antagonist: Structure and Dynamics of Innate Immune Glycoprotein MD-2 upon Recognition of Variably Acylated Bacterial Endotoxins. *Mol. Immunol.* **2011**, *49* , 124–133.

(45) Trinchieri, G. Interleukin-12 and the Regulation of Innate Resistance and Adaptive Immunity. *Nat. Rev. Immunol.* **2003**, *3*, 133–146.

(46) van Duikeren, S.; Fransen, M. F.; Redeker, A.; Wieles, B.; Platenburg, G.; Krebber,

W.-J.; Ossendorp, F.; Melief, C. J. M.; Arens, R. Vaccine-Induced Effector-Memory CD8 + T Cell Responses Predict Therapeutic Efficacy against Tumors. *J. Immunol.* **2012**, *189*, 3397–3403.

(47) Butler, N. S.; Nolz, J. C.; Harty, J. T. Immunologic Considerations for Generating Memory CD8 T Cells through Vaccination. *Cellular Microbiology*. **2011**, *13*, 925–933.

(48) Seaman, M. S.; Peyerl, F. W.; Jackson, S. S.; Lifton, M. A.; Gorgone, D. A.; Schmitz, J. E.; Letvin, N. L. Subsets of Memory Cytotoxic T Lymphocytes Elicited by Vaccination Influence the Efficiency of Secondary Expansion In Vivo. *J. Virol.* **2004**, *78*, 206–215.

(49) Borowski, A. B.; Boesteanu, A. C.; Mueller, Y. M.; Carafides, C.; Topham, D. J.; Altman, J. D.; Jennings, S. R.; Katsikis, P. D. Memory CD8 + T Cells Require CD28 Costimulation . *J. Immunol.* **2007**, *179*, 6494–6503.

(50) Mousavi, S. F.; Soroosh, P.; Takahashi, T.; Yoshikai, Y.; Shen, H.; Lefrançois, L.; Borst, J.; Sugamura, K.; Ishii, N. OX40 Costimulatory Signals Potentiate the Memory Commitment of Effector CD8 + T Cells . *J. Immunol.* **2008**, *181*, 5990–6001.

(51) Shedlock, D. J.; Shen, H. Requirement for CD4 T Cell Help in Generating Functional CD8 T Cell Memory. *Science*. **2003**, *300*, 337–339.

(52) Janssen, E. M.; Lemmens, E. E.; Wolfe, T.; Christen, U.; Von Herrath, M. G.; Schoenberger, S. P. CD4+ T Cells Are Required for Secondary Expansion and Memory in CD8+ T Lymphocytes. *Nature* **2003**, *421*, 852–856.

(53) Ahrends, T.; Busselaar, J.; Severson, T. M.; Bąbała, N.; de Vries, E.; Bovens, A.; Wessels, L.; van Leeuwen, F.; Borst, J. CD4+ T Cell Help Creates Memory CD8+ T Cells with Innate and Help-Independent Recall Capacities. *Nat. Commun.* **2019**, *10*, 5531.

(54) Paquet, A. Introduction of 9-Fluorenylmethyloxycarbonyl, Trichloroethoxycarbonyl, and Benzyloxycarbonyl Amine Protecting Groups into O-Unprotected Hydroxyamino Acids Using Succinimidyl Carbonates. *Can. J. Chem.* **1982**, *60*, 976–980.

(55) Winzler, C.; Rovere, P.; Zimmermann, V. S.; Davoust, J.; Rescigno, M.; Citterio, S.; Ricciardi-Castagnoli, P. Checkpoints and Functional Stages in DC Maturation. *Adv. Exp. Med. Biol.* **1997**, *417*, 59–64.

(56) Sanderson, S.; Shastri, N. LacZ Inducible, Antigen/MHC-Specific T Cell Hybrids. *Int. Immunol.* **1994**, *6*, 369–376.

(57) Schuurhuis, D. H.; Ioan-Facsinay, A.; Nagelkerken, B.; van Schip, J. J.; Sedlik, C.; Melief, C. J. M.; Verbeek, J. S.; Ossendorp, F. Antigen-Antibody Immune Complexes Empower Dendritic Cells to Efficiently Prime Specific CD8 + CTL Responses In Vivo. *J. Immunol.* **2002**, *168*, 2240–2246.

3

SYNTHETIC PEPTIDE CONJUGATED TO THE LIPID A ANALOGUE CRX-527 ENHANCES VACCINE EFFICACY AND T CELL MEDIATED-TUMOR CONTROL

Tondini E*, Reintjens NR*, Arakelian T, Vree J, Camps MGM, Overkleeft HS, Filippov DV, van der Marel GA, Codée JDC, Ossendorp F,

Submitted for publication

*equal contribution

ABSTRACT

Adjuvants play a determinant role in cancer vaccination by optimally activating APCs and shaping the T cell response. Bacterial-derived lipid A is one of the most potent immune-stimulators known and is recognized via Toll-like receptor 4 (TLR4). In this study, we explore the use of the synthetic, non-toxic, lipid A analogue CRX-527 as an adjuvant for peptide cancer vaccines. This well-defined adjuvant was covalently conjugated to antigenic peptides as a strategy to improve vaccine efficacy. We show that coupling of this TLR4 agonist to peptide antigens improves vaccine uptake by dendritic cells (DCs), maturation of DCs and T cell activation *in vitro,* and stimulates DC migration and functional T cell priming *in vivo*. This translates into strong tumor protection upon prophylactic and therapeutic vaccination via intradermal injection against B16-OVA melanoma and HPV-related TC1 tumors. These results highlight the potential of CRX-527 as an adjuvant for molecularly-defined cancer vaccines and support the design of adjuvant-peptide conjugates as a strategy to optimize vaccine formulation.

INTRODUCTION

The success of immunotherapy in the treatment of cancer is largely dependent on the recruitment of tumor-specific T cells. T cells have the potential to recognize tumor exclusive antigens that are present on cancer cells and absent on healthy cells, such as overexpressed, viral or mutated proteins. Many pre-clinical and clinical studies have reported the potential of vaccination as a strategy to eradicate tumors, both by inducing *de novo* tumor-specific T cell responses or by reinforcing pre-existing ones (1). However, it has also become apparent that vaccinating in the context of cancer is not trivial (2). Tumors can develop several different evading mechanisms, such as the upregulation of inhibitory molecules, the recruitment of suppressor cells, and the induction of regulatory T cells (3), causing T cell dysfunction and thereby hampering full therapeutic activity. To counteract these mechanisms, it is crucial to provide T cells with the appropriate signals during priming, in order to equip them with strong effector functions.

T cell priming and activation rely on vaccine uptake by properly activated dendritic cells (DCs), and research on enhancing vaccine efficacy has greatly been focused on optimizing the delivery of vaccine content to these cells. For example, delivery of nano-sized encapsulated vaccines, such as liposomes or nanoparticles, reduces the dispersal vaccine components and promotes enhanced uptake by DCs, resulting in enhanced T cell responses and anti-tumor activity (4, 5). Alternatively, antigen and adjuvant are delivered to DCs via antibodies targeting DC molecules, such as DEC205 or DC-SIGN (6). We and others have shown that the physical coupling of antigens and adjuvants, such as a Toll-like receptor (TLR) ligands, enables the delivery of maturation signals and antigens to the same dendritic cells, improving not only the numbers but also the quality of the generated T cell response (7-10). Covalent attachment of Pam_3CysSK_4, a TLR2 ligand, to a peptide antigen greatly enhanced T cell induction as well as tumor control compared to the mixture of the two (11, 12). Peptide-based conjugates with an optimized Pam_3CysSK_4 analogue are currently tested in the clinic for the treatment of HPV-associated malignancies (13). Enhanced uptake, DC maturation and antigen presentation were also shown for conjugates bearing TLR7 (14), TLR9 (15) and NOD2 ligands (16, 17). We have recently disclosed the synthesis of a novel conjugate bearing a synthetic analogue of the TLR4 ligand lipid A, CRX-527 (18). CRX-527 mimics lipid A (19), the lipidic portion of bacterial lipopolysaccharides (LPS), maintaining its exceptional immune-stimulating activity but bypassing its toxicity, which had limited the use of lipid A as adjuvant in the

clinic. *In vivo* priming of CD8 T cells by the CRX-527 conjugate induced differentiation of superior quality T cells compared to the mixture of the adjuvant and the peptide, reflecting the potential of this conjugate for cancer vaccination (18).

We now show that peptide formulation as a lipid A conjugate improves antigen uptake and presentation by DCs *in vitro*, resulting in higher CD8 and CD4 T cell activation and cytokine production, and that prophylactic and therapeutic vaccination with CRX-527 conjugates containing tumor-specific cytotoxic T lymphocytes (CTL) or T-helper epitopes strongly promote T cell activation, resulting in effective tumor control *in vivo*.

RESULTS

CRX-527 conjugates containing CTL or T-helper epitopes are immunologically active.

We previously reported a procedure to synthesize peptide conjugates bearing the lipid A analogue CRX-527 (18). The ligand was equipped at the C6-position via an amide bond with a lin ker containing a maleimide and was conjugated to the N-terminus of a synthetic long peptide containing the model CTL epitope SIINFEKL via a thiol-ene coupling. This allowed proper internalization and class I presentation of the SIINFEKL epitope by DCs. Peptide loading of MHC class I and II molecules is dependent on different uptake and processing routes, therefore we tested whether conjugation of CRX-527 to a T-helper epitope would still allow for proper processing and epitope presentation in the MHC class II pathway. Two different long peptides containing either the CTL epitope or the T-helper epitopes derived from chicken ovalbumin were conjugated to the CRX-527 (**Fig. 1a**) and tested for their ability to induce DC maturation and antigen presentation in mouse dendritic cells. Both conjugates induced similar levels of DC maturation, as detected by IL-12 production (**Fig. 1b**), showing that the immune-stimulating properties of the lipid A analogue are not affected by the conjugation to a long peptide. To evaluate antigen presentation, the conjugates were tested with the two hybridoma reporter T cell lines B3Z and OTIIZ, which possess TCR specificity for the CTL and the T-helper ovalbumin epitopes, respectively. These reporter T cell lines are not dependent on co-stimulation and their activation is therefore indicative of the actual levels of antigen presentation of the two epitopes. DCs were pulsed with the peptides, the conjugates, or an equimolar mixture of CRX-527 and the peptides, and incubated overnight with B3Z or OTIIZ cells. As shown in **Fig. 1c** and **1d**, both CTL and T-helper conjugates strongly induce activation

of the two hybridoma cell lines compared to free peptides. The mixture of CRX-527 and peptides only induced low T cell activation, indicating that conjugation improved antigen presentation.

We next investigated the combined effect of antigen presentation and co-stimulation *in vitro* by incubating compound-pulsed DCs with purified naïve OT-I or OT-II T cells. After 48 hours, T cells were analyzed for their proliferation, activation status and cytokine production. Although OT-I cells responded to DCs pulsed with the lipid A analogue, antigen-specific proliferation was most efficient to the CRX-527 conjugate (**Fig. S1a**). This was associated with upregulation of the early activation marker CD69 and the activation marker and IL-2 receptor CD25 (**Fig. S1a**). In addition, conjugate-activated OT-I cells produced high levels of IFNγ and IL-2 as detected in culture supernatants (**Fig. S1b**). Cells were analyzed for polyfunctionality of cytokine responses and a significantly higher number of $IFN\gamma^+/TNF\alpha^+$ double producing OT-I cells were induced by the conjugate-pulsed DCs. (**Fig. 1e**).

In contrast to OT-I, OT-II cells displayed antigen-specific proliferation irrespective of CRX-527 conjugation (**Fig. S1c**). Antigen-dependent stimulation induced expression of CD25 and CD69 activation markers (**Fig. S1c**), as well as IFNγ and IL-2 production (**Fig. S1d**). IFNγ production was significantly higher in the presence of CRX-527, both in the conjugate and in the mixture. Analysis of cytokine polyfunctionality revealed that also OT-II cells primed with the CRX-527 conjugated peptide displayed a significant increase in $IFN\gamma^+/TNF\alpha^+$ double producing OT-II cells (**Fig. 1f**).

To summarize, we demonstrated for two different peptides that conjugation of the lipid A analogue CRX-527 retained the immunological properties of the two components, preserving both ligand activity as well as epitope presentation on MHC class I and II molecules. In addition, conjugation improved antigen uptake and processing by DCs as well as CD8 and CD4 T cell activation of naïve T cells *in vitro*, as indicated by enhanced polyfunctional cytokine profile.

CRX-527 conjugated to CTL or T-helper peptides impact dendritic cell activation and T cell priming in vivo

The effect on T cell activation of the conjugated vaccines was subsequently assessed *in vivo* (**Fig. 2a**). The two formulations were injected intradermally in mice which were previously adoptively transferred with CFSE-labelled OT-I or OT-II T cells. Two days after vaccination, T cells were analyzed in the inguinal lymph nodes (LNs) draining the vaccination site. In the LNs of vaccinated mice,

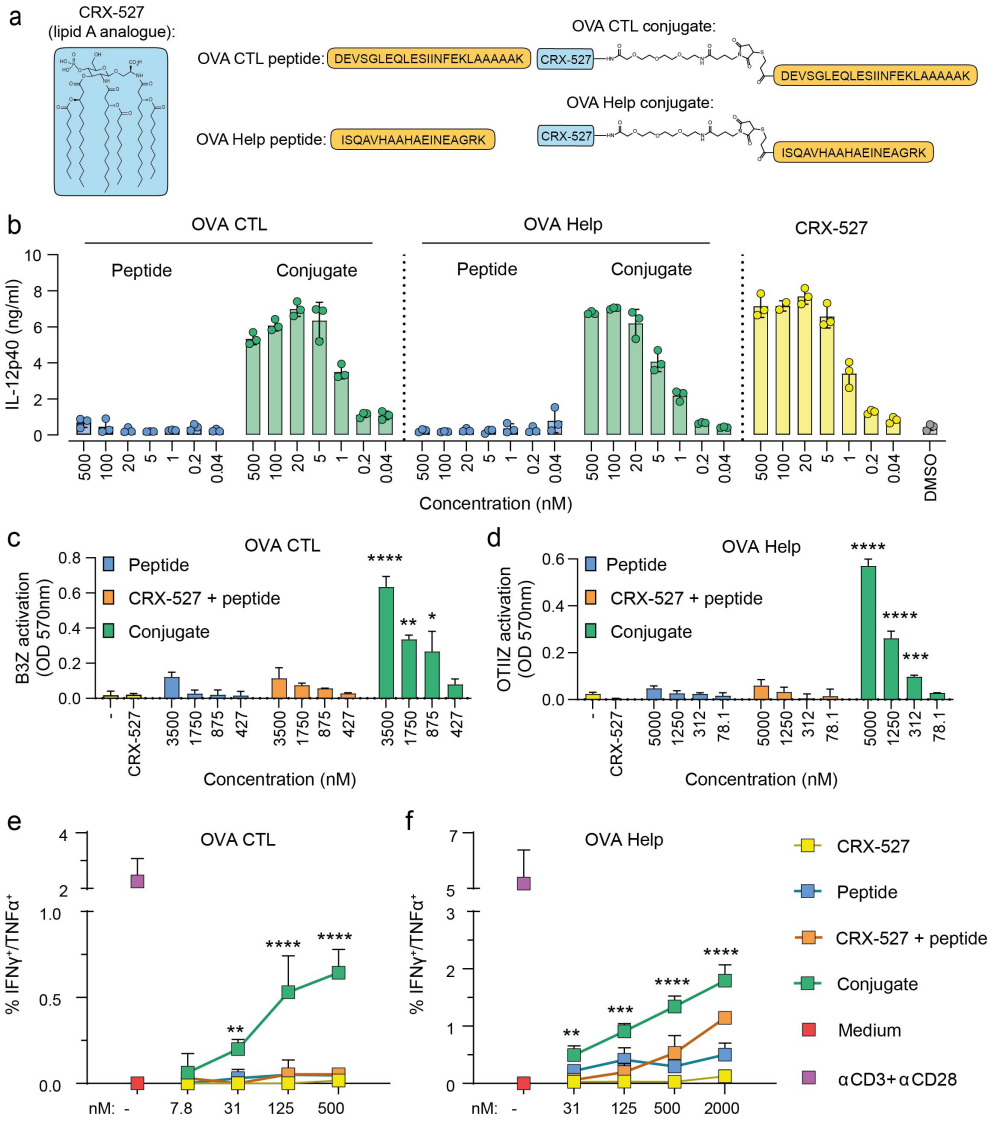

the total cell number significantly increased compared to naïve mice (**Fig. S2a** and **S2b**). This coincided with high numbers of CD11c⁺/MHC-II⁺ antigen presenting cells (**Fig. S2c**) in the same lymph nodes, indicating that the CRX-527 conjugates are immunologically active and capable of mobilizing innate immune cells. We detected a significant increase of monocyte-derived dendritic cells (Mo-DCs, **Fig. 2b** and **2c**), which are known to be strongly induced upon TLR4 stimulation (20). Moreover, albeit in lower numbers, we observed a strong influx of XCR1⁺/CD103⁺ migratory dermal DCs, the key DC subset involved in the transport and

Figure 1: CRX-527-peptide conjugates are immunologically active and can be presented both on MHC class I and II complexes. (**a**) Schematic representation of the structures of the Lipid A analogue CRX-527 and the OVA CTL and T-helper (OVA Help) peptide conjugates. (**b**) Concentration of IL-12p40 in the supernatant of D1 dendritic cells after overnight incubation with the indicated concentrations of peptides, conjugates, or CRX-527. (**C** and **D**) Peptide or conjugate uptake and presentation were evaluated by pulsing D1 DCs for 2 hours with the indicated concentration of compounds followed by overnight incubation with reporter hybridoma T cell lines. MHC class I presentation of the OVA CTL epitope was detected with the B3Z cell line (**c**); MHC class II presentation of the OVA Helper epitope was detected with the OTIIZ hybridoma (**d**) via colorimetric reaction. (**e** and **f**) D1 DCs were pulsed for 2 hours with the indicated compounds at different concentrations and incubated for 48 hours with purified naïve OT-I (**E**) or OT-II (**F**) TCR transgenic T cells. In the last 5 hours cells were incubated with Brefeldin A followed by staining for activation markers and cytokines. IFNγ/TNFα double producing OT-I (**e**) or OT-II (**f**) cells were detected by flow cytometry. Medium and stimulation with αCD3 + αCD28 antibodies were used as negative and positive controls, respectively. Statistical significance in all plots of conjugates versus mix was determined by two-way ANOVA followed by Dunnett's multiple comparison test; * p< 0.05, ** p< 0.01, *** p< 0.001, ***** p< 0.0001. Experiments were performed in triplicates and are representative of two or three independent experiments with similar results.

presentation of peripheral antigens and T cell priming (21). In addition, both DC subsets showed expression of the co-stimulatory molecule CD86 (**Fig. 2d** and **2e**). Correlating with the intradermal site of injection of the lipid A analogue, the migratory dermal DCs displayed significantly higher CD86 expression than Mo-DCs (**Fig. 2e**).

OT-I and OT-II T cell numbers in the LNs were also strongly increased in vaccinated mice. All OT-I cells underwent complete proliferation in both vaccination groups, while a portion of OT-II cells still remained undivided (**Fig. 3b**). The total numbers of OT-I and OT-II in the LNs were higher than in unvaccinated mice (**Fig. 3c**). Analysis of activation markers in OT-I CD8 T cells revealed increased expression of all markers analyzed (CD69, CD25, ICOS) in mice receiving the conjugated CTL vaccine in comparison to the mixture of CRX-527 and peptide (**Fig. 3d** upper panel and **Fig. S2d**). Increased CD69 upregulation was also observed in proliferated OT-II CD4 T cells in the T-helper conjugate group (**Fig. 3d,** lower panel), while there was no detectable difference between T-helper conjugate or mixture groups in the other analyzed markers (**Fig. 3d** lower panel and **S2d**). Analysis of of IFNγ/TNFα double producing T cells (**Fig. 3f**). IFNγ production was also detected in proliferating OT-II cells, and similar levels were induced by conjugated T-helper vaccine or mixed vaccine (**Fig. 3e,** lower panel). No detectable TNFα production was observed in OT-II (data not reported).

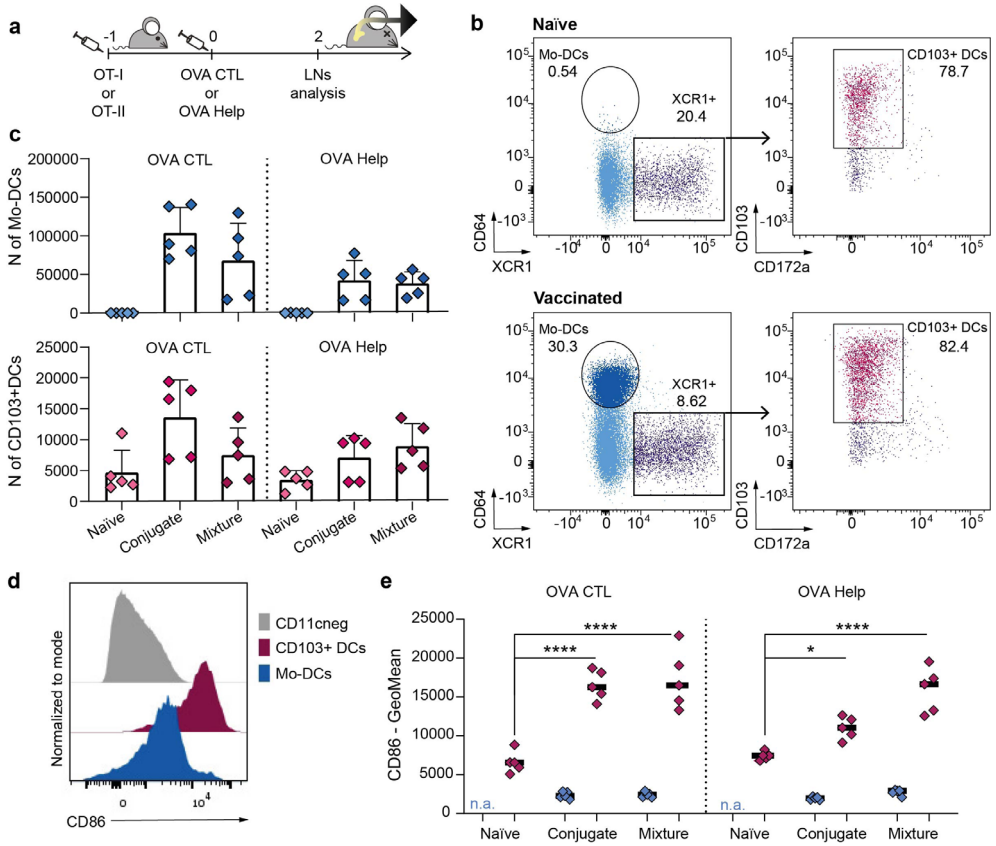

Figure 2: OVA CTL and Help peptide conjugated to CRX-527 promote DCs influx in the draining lymph node upon *in vivo* injection. (**a**) Mice (n=5 per group) were adoptively transferred with CFSE labelled OT-I or OT-II cells 24 hours before receiving 2 nmol of OVA CTL or Help CRX-527 conjugates, or an equimolar mix of peptide and CRX-527. 48 hours later the inguinal lymph nodes were harvested for analysis. (**b**) Representative dot plots for the gating of Mo-DCs and CD103+ dermal DCs in naïve versus vaccinated mice. Cells were pre-gated to exclude dead/CD19^{neg}/CD11c^{neg}/MHC class II^{neg} cells (**c**). Absolute count of Mo-DCs and XCR1+/CD103+ DCs in the inguinal lymph nodes (**d**) Representative histograms of CD86 expression in non APCs (CD11c^{neg}), Mo-DCs or XCR1+/CD103+ DCs. (**e**) Fluorescence intensity of CD86 signal (GeoMean) in Mo-DCs and XCR1+/CD103+ DCs subsets upon vaccination. Statistical significance was determined by one-way ANOVA followed by Tukey's multiple comparison test; * p< 0.05, ***** p< 0.0001

In summary, these data show that conjugated CTL and T-helper peptide vaccines induced enhanced T cell activation and potent expansion upon priming *in vivo*. Similar to what observed *in vitro*, this effect was more pronounced in CD8 T cells than in CD4 T cells.

Prophylactic vaccination with CRX-527 conjugates improves tumor control against B16OVA melanoma

We next evaluated whether vaccination efficacy of conjugate vaccines translated into improved endogenous T cell effector responses against a lethal challenge with B16OVA melanoma cells (**Fig. 4a**). Mice were primed and boosted in an interval of two weeks with the conjugates or, as control groups, a mixture of the lipid A analogue and the OVA CTL and T-helper peptides, separately or in combination. The induction of SIINFEKL-specific responses in the groups that received CTL peptide was measured in blood 7 days after each vaccine injection by H2-K^b-SIINFEKL tetramer staining (**Fig. S3a**). The levels of SIINFEKL-specific responses were similar for conjugates and mixture in the groups that received the CTL peptide only. In the groups in which the T-helper epitope was included, the levels of the OVA-specific CD8 responses were significantly increased, underlining the critical role that CD4 T cell help plays during the priming of CTL responses. After boost, a significantly higher frequency of SIINFEKL-specific CD8 T cells was observed in mice vaccinated with both CTL and T-helper CRX-527 conjugates (**Fig. S3a**).

The level of SIINFEKL-specific T cells in response to B16OVA challenge was measured in all vaccinated groups on the day of tumor inoculation and 7 days later. Naïve and T-helper vaccinated mice did not display any SIINFEKL-specific responses on the day of tumor challenge; however, some CD8 responses appeared one week later in some of the mice that were vaccinated with the T-helper conjugate or the mixture (**Fig. 4b**, left panels). These responses were not detected in unvaccinated mice and can be attributed to the presence of tumor-specific T-helper responses, which facilitated tumor-induced priming of SIINFEKL-specific responses. In the groups that were vaccinated with the CTL epitope, the levels of SIINFEKL-specific responses were detectable on the day of tumor challenge and one week after. The groups that received only CTL peptide intracellular IFNγ and TNFα cytokine production showed that significantly higher levels of IFNγ was produced by OT-I T cells in mice vaccinated with the conjugate (**Fig. 3e** upper panel). This group also displayed a significantly higher percentage did not show any tumor-specific expansion or decrease of the SIINFEKL-specific response (**Fig. 4b**, middle panel). In contrast, the groups vaccinated with the combination of the CTL and T-helper peptides displayed a significant expansion of SIINFEKL responses after tumor injection. Notably, the mice that received the conjugated vaccine displayed the highest frequencies (up to 5 %) of CD8 T cells

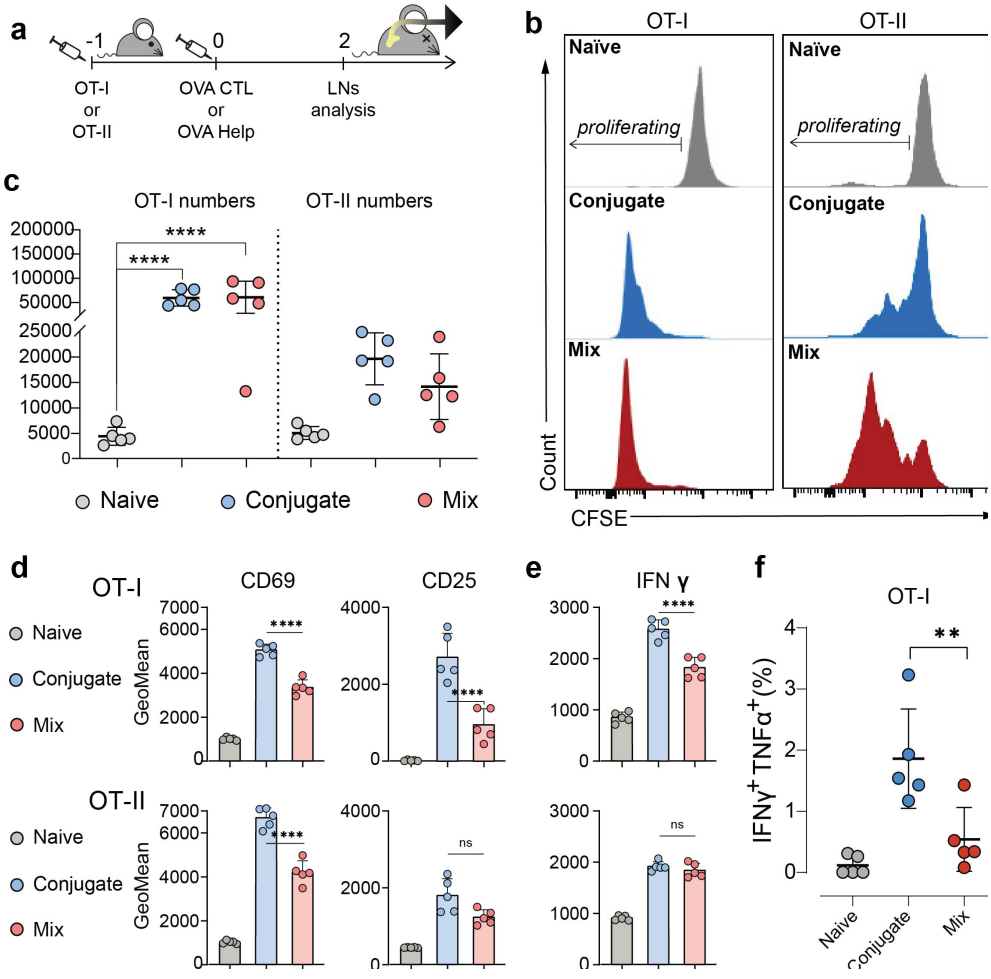

Figure 3: OVA CTL and Help Lipid A-peptide conjugates promote enhanced activation of T cells upon *in vivo* injection. (**a**) Mice (n=5 per group) were adoptively transferred with CFSE labelled OT-I or OT-II cells 24 hours before receiving 2 nmol of OVA CTL or Help CRX-527conjugates, or an equimolar mix of peptide and CRX-527. 48 hours later, the inguinal lymph nodes were harvested for analysis of OT-I or OT-II T cell proliferation and activation. (**b**) Representative histograms of CFSE signal in labelled OT-I or OT-II cells. (**c**) Absolute count of total OT-I and OT-II cells in pooled inguinal lymph nodes. (**d**) Mean fluorescence intensity (GeoMean) of CD69 and CD25 T cell activation markers in OT-I (upper) or OT-II (lower) cells as detected by flow cytometry. (**e**) Mean fluorescence intensity of IFNγ cytokine in OT-I (upper) or OT-II (lower) as detected by flow cytometry. Statistical significance of the conjugates compared to the mix in both (**d**) and (**e**) was determined by one-way ANOVA followed by Sidak's multiple comparison test; ***** p< 0.0001. (**f**) Percentage of IFNγ/TNFα double producing OT-I cells. Statistical significance was determined by one-way ANOVA followed by Tukey's multiple comparison test; ** p<0.01.

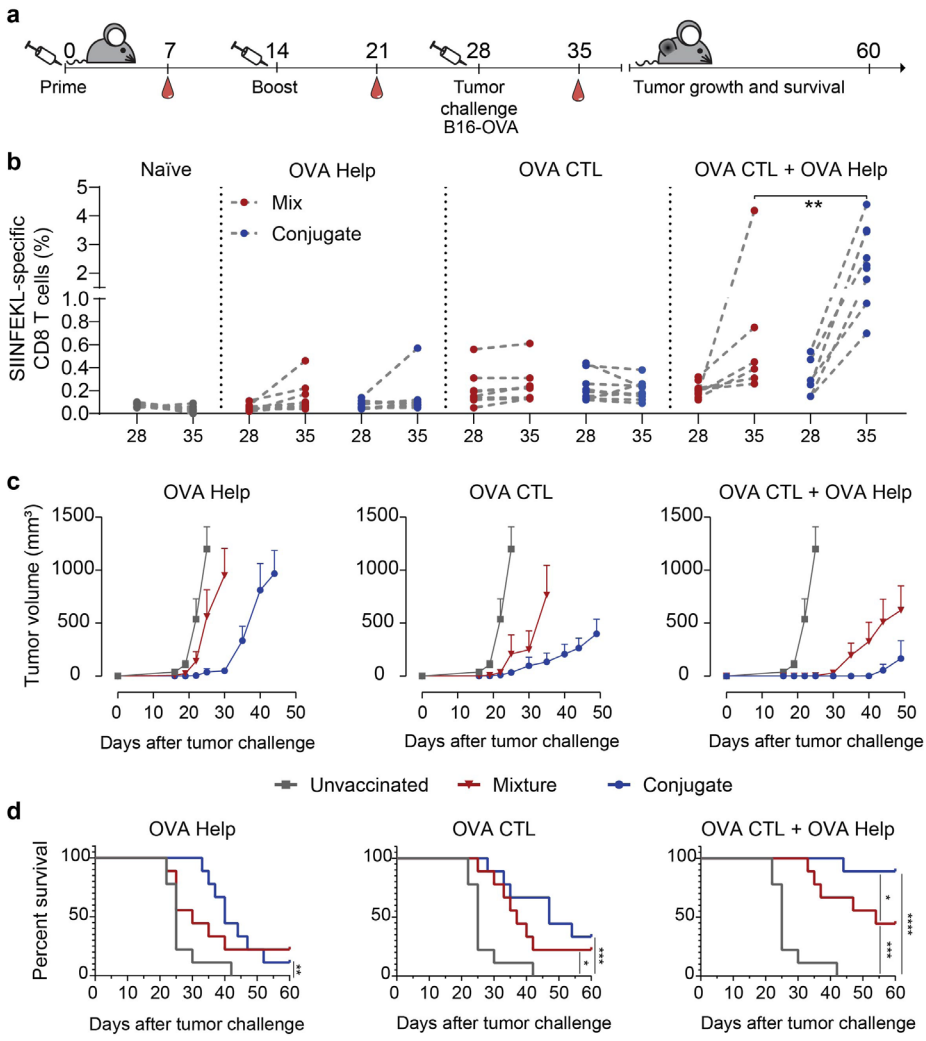

Figure 4: Prophylactic vaccination with CRX-527-peptide conjugates potentiates tumor protection compared to unconjugated vaccines (**a**) Schematic overview of the experiment. Mice (n=9) were primed and boosted at an interval of two weeks and later challenged with 100.000 B16OVA tumor cells. At the indicted time points, blood was withdrawn to analyse SIINFEKL-specific CD8 responses by specific tetramer staining. (**b**) Frequencies of SIINFEKL-specific CD8 T cell responses in all vaccinated and unvaccinated groups on the day of B16-OVA challenge and seven days after. (**c**) Average B16-OVA tumor growth in groups that were unvaccinated (grey line) or vaccinated with either CRX-527 conjugate (blue line) or a mixture of CRX-527 and peptide (red line) containing OVA CTL or Helper epitopes. (**d**) Overall survival of prophylactically vaccinated mice with the indicated epitopes in form of CRX-527 conjugates or mixture. Statistical significance was determined by Log-rank Mantel-Cox test; *p<0.05, ** p< 0.01, *** p< 0.001, ***** p< 0.0001.

of all groups (**Fig. 4b**, right panel). The ability of these responses to immunologically protect mice from tumor growth was evaluated by following tumor sizes over 60 days (**Fig. 4c**). All unvaccinated mice developed a tumor within 20 days.

Mice vaccinated with the CRX-527-T-helper conjugated or unconjugated vaccine experienced a short delay in tumor growth (**Fig. 4c**, left panel) which was more pronounced in the mice that received the conjugate vaccine and resulted in a significant increase of survival (**Fig. 4d**). The groups that were vaccinated with the CTL epitope displayed a more accentuated delay in tumor growth, which was stronger in the mice vaccinated with the CRX-527 conjugate compared to the mixture (**Fig. 4c**, middle panel). Finally, the groups that were vaccinated with both peptides showed the most effective protection from tumor growth (**Fig. 4c**, right panel). The mixture of the lipid A analogue and peptides protected less efficiently than the conjugated peptides, which resulted in long term overall survival of about 90% of animals (**Fig. 4d**).

These results highlight superior quality of the T cells induced by the CRX-527 conjugates, which translates into superior control of aggressive tumor growth, and underline the importance of combining CD4 and CD8 conjugate vaccines for optimal induction of functional T cell responses.

Therapeutic efficacy of OVA CTL and T-helper conjugates against B16OVA and TC1 tumors

Therapeutic efficacy of the CRX-527 conjugated vaccines was evaluated in mice with established B16OVA melanoma tumors that were intradermally injected with a combination of the OVA CTL and T-helper peptides ten days after tumor inoculation. The conjugate vaccine was compared to free CRX-527 and an equimolar mix of the OVA peptides with lipid A analogue. Tumor growth was significantly delayed by the therapeutic vaccinations (**Fig. 5a**) but not by CRX-527 alone. In particular, the conjugated vaccine exhibited the highest therapeutic effect and overall survival rate (**Fig. 5b** and **5c**). The frequency in blood of the induced SIINFEKL-CD8 T cell responses did not detectably differ between groups (**Fig. S3b**), however tumor immune control by the conjugated vaccine was significantly more efficient.

Finally, we analyzed whether the conjugation of the lipid A analogue could be applied to another antigenic peptide cancer model. CRX-527 was conjugated to a synthetic long peptide containing the CTL epitope, derived from the E7 protein of the Human Papilloma Virus (HPV) type 16. Mice were vaccinated either prophylactically or therapeutically against TC-1 tumors expressing the HPV E7

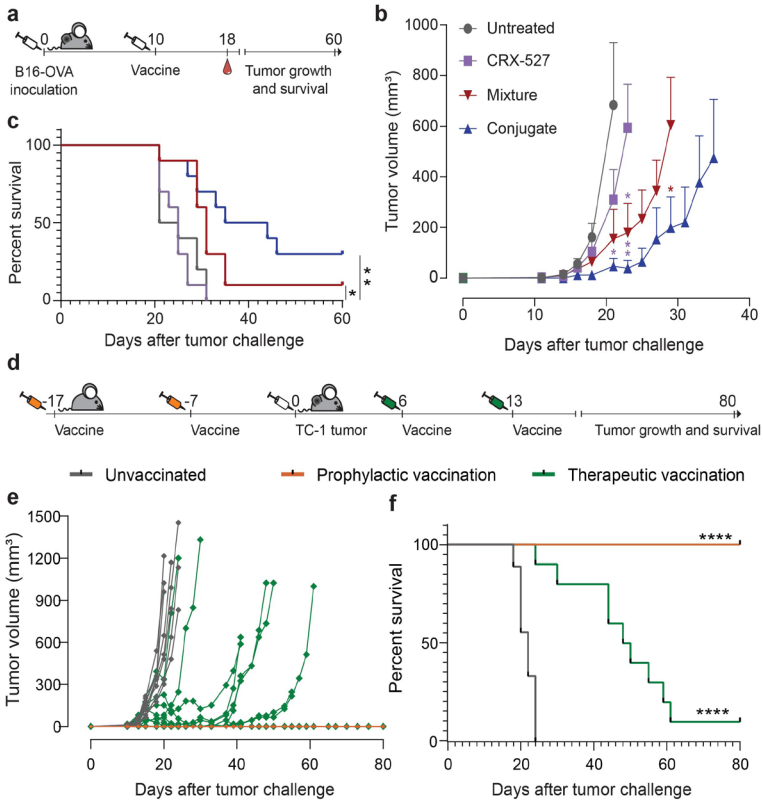

Figure 5: Therapeutic vaccination with CRX-527 conjugates results in effective therapeutic activity. (**a**) Schematic overview of the experiment. Mice (n=10 per group) were injected with 100.000 B16OVA tumor cells. Once tumors were palpable, mice were vaccinated with 1 nmol of CRX-527, a mixture of CRX-527and OVA CTL and Help peptides or the two OVA CTL and Help conjugates. Blood was withdrawn at day 18 to monitor the induction of SIINFEKL-specific CD8 responses by tetramer staining. (**b**) Average B16OVA tumor growth in the different therapeutic vaccination groups. Statistical significance between Lipid A, mix and conjugates at different time points was calculated by one-way ANOVA and Tukey's multiple comparison. The color of the stars indicates to which group the statistical significance is referred to. *p<0.05, ** p< 0.01 (**c**) Overall survival of mice therapeutically vaccinated with CRX-527or OVA CTL and Help peptides in form of mix with CRX-527 or conjugates. Statistical significance was determined by Log-rank Mantel-Cox test; *p<0.05, ** p< 0.01. (**d**) Schematic representation of prophylactic or therapeutic vaccination experiment with HPV E7 specific CRX-527 conjugates against TC-1 tumor. Mice (n=10 per group) were vaccinated either before (orange syringes) or after (green syringes) TC-1 tumor inoculation and tumor growth and survival were monitored for 80 days. (**e**) Individual tumor growth of unvaccinated (grey), prophylactically vaccinated (orange) and therapeutically vaccinated (green) mice and (**f**) their corresponding survival plot. Statistical significance was determined by Log-rank Mantel-Cox test; **** p< 0.0001.

protein. Prophylactic vaccination protected all animals long term from tumor challenge, while therapeutic vaccination could cure 10% of the animals, and delay tumor growth in 80% of mice (**Fig. 5e**), resulting in significantly increased overall survival rate (**Fig. 5f**). Overall, these data demonstrate the potential of CRX-527-peptide conjugates in improving tumor antigen-specific T cell responses for effective cancer vaccination.

DISCUSSION

In this study, we report the efficacy of self-adjuvanting peptide vaccines containing the potent TLR4 ligand lipid A analogue CRX-527 in mediating tumor control. Therapeutic cancer vaccination is a promising specific immunotherapeutic approach but presents itself with the challenge of inducing functional T cells in the context of a suppressed immune environment. For this reason, it is crucial to design vaccines that maximize T cell priming conditions. T cell priming is a multifactorial process that can be modulated at different levels. To start, vaccine efficacy strongly depends on its ability to reach dendritic cells. We show that conjugation of peptide antigen to CRX-527 enhances vaccine uptake and antigen presentation by DCs to T cells *in vitro*. Direct conjugation of antigen to pathogen-associated molecular patterns (PAMPs) as a strategy to improve DC targeting and uptake has been described for multiple ligands, including TLR ligands (15, 22, 23). TLRs are not necessarily involved in the antigen uptake process (15), however DCs express multiple scavenger and uptake receptors that mediate constant antigen uptake and that can also present affinity for PAMPs (24). Notably, TLR signaling from the endosomes plays a role in phagosome maturation and in directing the cargo towards antigen processing and MHC-loading routes, rather than the degradation compartments. This has also been described for TLR4 and it has been reported that engagement of TLR4 within the antigen-containing endosomes causes delay in antigen degradation and enhanced MHC-I cross-presentation (25-27) as well as MHC-II presentation (28, 29).

In vivo, antigen uptake and presentation can be mediated by different DCs subsets. Upon intradermal injection, the vaccine needs to reach and mobilize dermal DCs, which will migrate to the LNs to induce T cell priming. We observed an influx of $XCR1^{+}/CD103^{+}$ DCs. Among the different DC types, this subset of migratory dermal DCs plays a critical role in antigen transport from the periphery (21, 30) and is involved in antigen presentation and T cell priming. Moreover, migratory dermal DCs have a recognized role in antigen transport from the tumor

site (31) and affect therapeutic efficacy of checkpoint immunotherapies (32, 33). We observed increased influx of these DCs and upregulation of CD86. In addition, we detected a strong influx of $CD64^+$ Mo-DCs. TLR4 stimulation has been described to strongly induce recruitment of monocytes and differentiation into Mo-DCs (20, 34). This cell subset supports inflammation and immune activation as well as antigen presentation (35, 36). It remains to be determined however, how these two subsets contribute to immune activation and antigen presentation in our system.

The nature of the adjuvants influences the shaping of the response during T cell priming. LPS toxicity has long prevented the clinical exploitation of the TLR4 pathway. However, the emergence of novel detoxified ligands has recently made targeting of TLR4 a successful strategy with various applications. Monophosphoryl lipid A (MPL), a member of the LPS family isolated from *Salmonella*, is a component of commercially available prophylactic vaccines against Human Papilloma Virus and Hepatitis B. This adjuvant enabled skewing of T cell responses towards Th1 immunity (37). More recently GLA-SE, a similar lipid A analogue in a stable emulsion, has entered clinical evaluation as vaccine adjuvants for H5N1 influenza (38) as well as tuberculosis (39). This adjuvant also displays noticeable activity for cancer immunotherapy. In a pre-clinical setting, intra-tumoral injection of GLA-SE was described to synergize with vaccination or adoptive T cell transfer to mediate complete tumor regression (40). This adjuvant is currently being tested in the clinic in booster vaccination against the NY-ESO cancer testis antigen after prime with an adenoviral vector (41), in melanoma (42) and as intra-tumoral monotherapy (43). Here, we report the first-time employment of CRX-527 as adjuvant in defined self-adjuvanting cancer vaccine. This molecularly well-defined adjuvant retains strong TLR4 activating properties, is more potent than MPL (18), and was well tolerated upon injection. Most importantly, it shows strong efficacy at nanomolar doses, induction of Th1 skewed immunity and excellent pre-clinical activity in tumor control.

Finally, priming efficacy is also influenced by the presence of CD4 T-helper T cells. By analyzing self-adjuvanting vaccines containing either a CTL or a T-helper epitope separately or together, we observe maximal tumor protection when these two epitopes are combined. CTLs primed in concomitance with CD4 T cell help provided by the T-helper epitope display increased expansion potential and the highest ability of protecting from tumor growth. Helper T cells influence the breadth of the response induced and determine CTL functions (44), and absence

of T cell help during priming can result in sub-optimally primed CTL responses with phenotype similar to exhausted T cells (45). Tumors are particularly effective at inducing exhausted T cells and it is therefore essential to include CD4 T cell epitopes within the design of a cancer vaccine.

In conclusion, we have developed a versatile, molecularly well-defined, peptide-based vaccine system which incorporates the potent TLR4 ligand, CRX-527, in peptide-adjuvant conjugates for cancer vaccination. Physical conjugation of this adjuvant to different peptides potentiates dendritic cell functions, effector T cell activation and expansion, which translates into effective anti-tumor immunity *in vivo*, representing a promising platform for specific immunotherapy in the clinic.

METHODS

Cell culture. The D1 cell line is a growth factor-dependent spleen-derived immature DC cell line from C57BL/6 (H-2^b) mice. D1 cells were cultured as previously described (46). The B3Z and OTIIZ hybridoma cell lines were cultured in IMDM medium (Lonza, Basel, Switzerland) supplemented with 8% FCS (Greiner, Kremsmünster, Austria), penicillin and streptomycin, glutamine (Gibco, Carlsbad, CA, USA), β-mercaptoethanol (Merck, Kenilworth, NJ USA), and hygromycin B (AG Scientific Inc, San Diego, CA, USA) to maintain expression of the beta-galactosidase reporter gene. The B16OVA and TC-1 tumor cell lines were cultured in IMDM medium (Lonza, Basel, Switzerland) supplemented with 8% FCS (Greiner, Kremsmünster, Austria), non-essential amino acids, sodium pyruvate, glutamine, penicillin and streptomycin, (all from Gibco, Carlsbad, CA, USA), β-mercaptoethanol (Merck, Kenilworth, NJ USA). G418 (Life Technologies, Carlsbad, CA, USA) was used to maintain OVA expression in B16OVA cells and E6 and E7 expression in TC-1.

Synthesis of peptides and CRX-527 peptide conjugates. Three peptides were used in this study: the ovalbumin peptides DEVSGLEQLESIINFEKLAAAAAK and ISQAVHAAHAEINEAGRK, and the peptide GQAEDRAHYNIVTFBBKBDSTLRLBVK containing the CTL epitope from the E7 protein of the Human Papilloma Virus type 16. All three peptides were synthesized using automated peptide synthesis and purified via reversed-phase high-performance liquid chromatography (RP-HPLC). For conjugation with CRX-527, the peptides were assembled with 3-(tritylthio)propionic acid at the N-terminus prior cleaving from the resin. The CRX-527 peptide conjugates were generated and purified using the described

methods as described previously (18). The CRX-527 HPV-conjugate was purified via HPLC chromatography. More detailed experimental procedures for conjugate synthesis and LCMS and MALDI spectra can be found in Supplementary Information.

Animals. For vaccination and tumor experiments, 6-8 weeks old female C57BL/6 were purchased from Charles River Laboratories. The TCR transgenic OT-I and OT-II mouse strains were obtained from Jackson Laboratory and maintained on CD45.1^{+} C57BL/6 background. Mice were housed in specific pathogen-free (SPF) conditions at the LUMC animal facility. All animal experimentations were approved by and according to guidelines of the Dutch Animal Ethical Committee.

***In vitro* DC maturation assay.** The test compounds were dissolved in DMSO at a concentration of 500 µM and sonicated in water bath for 15 minutes. 50.000 D1 cells were seeded in 96-well round bottom plates (Corning, Amsterdam, The Netherlands) in 100 µl medium. Two times concentrated compounds were titrated in medium and 100 µl were added on top of D1. After 24 hours of incubation at 37°C, supernatant was taken from the wells to measure the amount of produced IL-12p40 by ELISA assay (BioLegend, San Diego, CA, USA) according to manufacturer instructions.

***In vitro* antigen presentation assay**. The test compounds were dissolved in DMSO at a concentration of 500 µM and sonicated in water bath for 15 minutes. 50.000 D1 cells were seeded in 96-well flat bottom plates (Corning, Amsterdam, The Netherlands) and pulsed for 2 hours with 200 µl of the test compounds in medium at the indicated concentrations. After 2 hours, cells were washed once with 200 µl of fresh medium. For B3Z and OTIIZ assay, 50.000 B3Z or OTIIZ cells were added per well in 200 µl of medium and incubated with D1 cells overnight. The following day TCR activation was detected by measurement of absorbance at 595 nm upon color conversion of chlorophenol red-β-D-galactopyranoside (Calbiochem®, Merck, Bullington, MA, USA) by the beta-galactosidase enzyme. For OT-I and OT-II T cell stimulations, CD8 and CD4 T cells were isolated from the spleens and lymph nodes of naïve OT-I and OT-II transgenic mice, respectively, by using CD8 or CD4 negative selection kits (BD Biosciences, San Jose, CA, USA) according to manufacturer instructions. The cells were labelled with 5 µM CFSE (Invitrogen, Carlsbad, CA, USA) at 37°C for 10 minutes and 50.000 cells per well were added on top of D1 cells. After 36 hours, supernatant was collected for the detection of INFγ and IL-2 production (BioLegend, San Diego, CA, USA) and brefeldin A (Sigma-Aldrich, St. Louis, MO, USA) at 5 µg/ml was added for 6

hours. At the end of the incubation, the cells were stained for FACS analysis and acquired on BD FACS LSR II 4L Full (BD Biosciences, San Jose, CA, USA).

***In vivo* antigen presentation.** CD8 and CD4 T cells were isolated from the spleens and lymph nodes of naïve OT-I and OT-II transgenic mice, respectively, by using CD8 or CD4 negative selection kits (BD Biosciences, San Jose, CA, USA) according to manufacturer instructions. The cells were labelled with 5 μM CFSE (Invitrogen, Carlsbad, CA, USA) at 37°C for 10 minutes and 1.000.000 OT-I or OT-II cells were injected intravenously in naïve C57BL/6 mice. On the next day, mice received an intradermal injection of 2 nmol of either OVA CTL peptide + CRX-527 conjugated or mixed, OVA T-helper peptide + CRX-527 conjugated or mixed, or vehicle (saline solution). To prepare the vaccine. the different compounds were dissolved in DMSO at a concentration of 500 μM and sonicated in water bath for 15 minutes. The required amounts for vaccination were mixed to saline solution and 30 μl per mouse were injected. After 48 hours, the inguinal lymph nodes were harvested and single cells suspension were obtained. A portion of these cells was used for direct staining for either DC or T cell analysis, while a portion was incubated with 5 μg/ml of Brefeldin A (Sigma-Aldrich, St. Louis, MO, USA) for 6 hours and was subsequently stained for cytokines. Precision count beads (Biolegend, San Diego, CA, USA) were added in some samples to allow cell quantification. Samples were acquired on BD FACS LSR II 4L Full (BD Biosciences, San Jose, CA, USA).

Prophylactic vaccination and B16-OVA tumor challenge. Naïve 6-8 weeks old C57BL/6 female mice were injected intradermally at the tail base with 2 nmol of the indicated conjugates or an equimolar mix of CRX-527 and peptide. To prepare the vaccine, the different compounds were dissolved in DMSO at a concentration of 500 μM and sonicated in water bath for 15 minutes. The required amounts for vaccination were added to saline solution and 30 μl per mouse were injected. Fourteen days later, the animals were boosted with the same vaccine formulations. After 28 days, 50.000 B16-OVA cells were injected subcutaneously in the flank and tumor growth was monitored. At different time points during the experiments, 20 μl of blood were collected from the tail vein for detection of SIINFEKL-specific T cell responses via SIINFEKL-H2-K^b tetramer staining. Mice were sacrificed when the tumor volume surpassed 1.500 mm^3.

Therapeutic vaccination against B16-OVA tumors. Naïve C57BL/6 female mice were injected subcutaneously in the flank with 50.000 B16OVA cells and tumor growth was monitored. When tumors reached a palpable size with an estimated volume of around 1 mm^3 (day 10), mice were vaccinated with 2 nmol of CRX-527, conjugated OVA peptides, or a mix of CRX-527 and OVA peptides.

Eight days later, 20 µl of blood were collected from the tail vein for the detection of SIINFEKL-specific T cell responses via SIINFEKL-H2-K^b tetramer staining. Tumor growth was monitored over time and mice were sacrificed when the tumor volume surpassed 1.000 mm^3 in conformance to ethical regulations for animal welfare.

TC-1 tumor challenge. Mice were subcutaneously injected in the flank with 100.000 TC-1 cells. For prophylactic vaccination, mice were vaccinated with 2 nmol of E7 peptide conjugated to CRX-527, or an equimolar mixture of the two, 17 and 7 days before tumor challenge. For therapeutic vaccination, mice were vaccinated with 2 nmol of compounds 6 and 13 days after tumor challenge. Tumor growth was monitored over time and mice were sacrificed when the tumor volume surpassed 1.000 mm^3 in conformance to ethical regulations for animal welfare.

Flow cytometry staining and antibodies. For flow cytometry staining, cells were washed and stained in PBA buffer (0.5% BSA, 0.02% Natriumazide in PBS) for 30 min on ice. For intracellular cytokine staining, cells were fixed and permeabilised with Intracellular Staining Permeabilization Wash Buffer (Biolegend, San Diego, CA, USA). Antibodies used were: PE-Cy7 anti-CD86, PE-Cy7 anti-IFNγ, Alexa Fluor 700 anti-CD45.1 (BD Pharmigen, San Diego, CA, USA), APC-R700 anti-CD8, V500 anti- I-A/I-E (BD Horizon, Franklin Lakes, NJ, USA), Alexa Fluor anti-CD4 (Invitrogen, Carlsbad, CA, USA), PE-Dazzle anti-TNFα, PerCP-Cy5.5 anti-CD8a, PerCP-Cy5.5 anti-CD172a, BV711 ant-CD25, BV605 anti-Ly6C, BV786 anti-XCR1, BV711 anti-CD64, BV650 anti-CD19 (Biolegend, San Diego, CA, USA), eF450 anti-CD45.1, PE anti-CD103, Fixable Viability Dye eFluor780 (eBioscience, San Diego, CA, USA). APC or PE labelled H2-K^b-SIINFEKL tetramers were made in-house.

Statistical analysis. Results are expressed as mean ± SD. Statistical significance among groups was determined by multiple comparison using the GraphPad software after ANOVA and multiple comparison test. Details of the used tests are described in the legends. Cumulative survival time was calculated by the Kaplan-Meier method, and the log-rank test was applied to compare survival between 2 groups. P-values of ≤0.05 were considered statistically significant.

REFERENCES

1. Morse MA, Gwin WR, 3rd, Mitchell DA. Vaccine Therapies for Cancer: Then and Now. Target Oncol. 2021;16(2):121-52.

2. Bodey B, Bodey B, Jr., Siegel SE, Kaiser HE. Failure of cancer vaccines: the significant limitations of this approach to immunotherapy. Anticancer Res. 2000;20(4):2665-76.

3. Spranger S. Mechanisms of tumor escape in the context of the T-cell-inflamed and the non-T-cell-inflamed tumor microenvironment. Int Immunol. 2016;28(8):383-91.

4. Heuts J, Jiskoot W, Ossendorp F, van der Maaden K. Cationic Nanoparticle-Based Cancer Vaccines. Pharmaceutics. 2021;13(5).

5. Wen R, Umeano AC, Kou Y, Xu J, Farooqi AA. Nanoparticle systems for cancer vaccine. Nanomedicine (Lond). 2019;14(5):627-48.

6. Hossain MK, Wall KA. Use of Dendritic Cell Receptors as Targets for Enhancing Anti-Cancer Immune Responses. Cancers (Basel). 2019;11(3).

7. Zom GG, Filippov DV, van der Marel GA, Overkleeft HS, Melief CJ, Ossendorp F. Two in one: improving synthetic long peptide vaccines by combining antigen and adjuvant in one molecule. Oncoimmunology. 2014;3(7):e947892.

8. Du JJ, Wang CW, Xu WB, Zhang L, Tang YK, Zhou SH, et al. Multifunctional Protein Conjugates with Built-in Adjuvant (Adjuvant-Protein-Antigen) as Cancer Vaccines Boost Potent Immune Responses. iScience. 2020;23(3):100935.

9. Belnoue E, Mayol JF, Carboni S, Di Berardino Besson W, Dupuychaffray E, Nelde A, et al. Targeting self and neo-epitopes with a modular self-adjuvanting cancer vaccine. JCI Insight. 2019;5.

10. Desch AN, Gibbings SL, Clambey ET, Janssen WJ, Slansky JE, Kedl RM, et al. Dendritic cell subsets require cis-activation for cytotoxic CD8 T-cell induction. Nat Commun. 2014;5:4674.

11. Zom GG, Khan S, Britten CM, Sommandas V, Camps MG, Loof NM, et al. Efficient induction of antitumor immunity by synthetic toll-like receptor ligand-peptide conjugates. Cancer Immunol Res. 2014;2(8):756-64.

12. Zom GG, Willems M, Khan S, van der Sluis TC, Kleinovink JW, Camps MGM, et al. Novel TLR2-binding adjuvant induces enhanced T cell responses and tumor eradication. J Immunother Cancer. 2018;6(1):146.

13. Slingerland M, Speetjens F, Welters M, Gelderblom H, Roozen I, van der Velden LA, et al. A phase I study in patients with a human papillomavirus type 16 positive oropharyngeal tumor treated with second generation synthetic long peptide vaccine conjugated to a defined adjuvant. J Clin Oncol. 2016;34(15).

14. Gential GPP, Hogervorst TP, Tondini E, van de Graaff MJ, Overkleeft HS, Codee JD, et al. Peptides conjugated to 2-alkoxy-8-oxo-adenine as potential synthetic vaccines triggering TLR7. Bioorg Med Chem Lett. 2019;29(11):1340-4.

15. Khan S, Bijker MS, Weterings JJ, Tanke HJ, Adema GJ, van Hall T, et al. Distinct uptake mechanisms but similar intracellular processing of two different Toll-like receptor ligand-peptide conjugates in dendritic cells. J Biol Chem. 2007;282(29):21145-59.

16. Willems MMJHP, Zom GG, Meeuwenoord N, Khan S, Ossendorp F, Overkleeft HS, et al. Lipophilic Muramyl Dipeptide-Antigen Conjugates as Immunostimulating Agents. Chemmedchem. 2016;11(2):190-8.

17. Zom GG, Willems MMJHP, Meeuwenoord NJ, Reintjens NRM, Tondini E, Khan S, et al. Dual Synthetic Peptide Conjugate Vaccine Simultaneously Triggers TLR2 and NOD2

and Activates Human Dendritic Cells. Bioconjugate Chem. 2019;30(4):1150-61.

18. Reintjens NRM, Tondini E, de Jong AR, Meeuwenoord NJ, Chiodo F, Peterse E, et al. Self-Adjuvanting Cancer Vaccines from Conjugation-Ready Lipid A Analogues and Synthetic Long Peptides. J Med Chem. 2020;63(20):11691-706.

19. Stover AG, Da Silva Correia J, Evans JT, Cluff CW, Elliott MW, Jeffery EW, et al. Structure-activity relationship of synthetic toll-like receptor 4 agonists. J Biol Chem. 2004;279(6):4440-9.

20. Cheong C, Matos I, Choi JH, Dandamudi DB, Shrestha E, Longhi MP, et al. Microbial stimulation fully differentiates monocytes to DC-SIGN/CD209(+) dendritic cells for immune T cell areas. Cell. 2010;143(3):416-29.

21. Bedoui S, Whitney PG, Waithman J, Eidsmo L, Wakim L, Caminschi I, et al. Cross-presentation of viral and self antigens by skin-derived CD103+ dendritic cells. Nat Immunol. 2009;10(5):488-95.

22. Tighe H, Takabayashi K, Schwartz D, Marsden R, Beck L, Corbeil J, et al. Conjugation of protein to immunostimulatory DNA results in a rapid, long-lasting and potent induction of cell-mediated and humoral immunity. Eur J Immunol. 2000;30(7):1939-47.

23. Kastenmuller K, Wille-Reece U, Lindsay RW, Trager LR, Darrah PA, Flynn BJ, et al. Protective T cell immunity in mice following protein-TLR7/8 agonist-conjugate immunization requires aggregation, type I IFN, and multiple DC subsets. J Clin Invest. 2011;121(5):1782-96.

24. Wang D, Sun B, Feng M, Feng H, Gong W, Liu Q, et al. Role of scavenger receptors in dendritic cell function. Hum Immunol. 2015;76(6):442-6.

25. Alloatti A, Kotsias F, Pauwels AM, Carpier JM, Jouve M, Timmerman E, et al. Toll-like Receptor 4 Engagement on Dendritic Cells Restrains Phago-Lysosome Fusion and Promotes Cross-Presentation of Antigens. Immunity. 2015;43(6):1087-100.

26. Horrevorts SK, Duinkerken S, Bloem K, Secades P, Kalay H, Musters RJ, et al. Toll-Like Receptor 4 Triggering Promotes Cytosolic Routing of DC-SIGN-Targeted Antigens for Presentation on MHC Class I. Front Immunol. 2018;9:1231.

27. Burgdorf S, Scholz C, Kautz A, Tampe R, Kurts C. Spatial and mechanistic separation of cross-presentation and endogenous antigen presentation. Nat Immunol. 2008;9(5):558-66.

28.Mantegazza AR, Zajac AL, Twelvetrees A, Holzbaur EL, Amigorena S, Marks MS. TLR-dependent phagosome tubulation in dendritic cells promotes phagosome cross-talk to optimize MHC-II antigen presentation. Proc Natl Acad Sci U S A. 2014;111(43):15508-13.

29. Lopez-Haber C, Levin-Konigsberg R, Zhu Y, Bi-Karchin J, Balla T, Grinstein S, et al. Phosphatidylinositol-4-kinase IIalpha licenses phagosomes for TLR4 signaling and MHC-II presentation in dendritic cells. Proc Natl Acad Sci U S A. 2020;117(45):28251-62.

30. Allan RS, Waithman J, Bedoui S, Jones CM, Villadangos JA, Zhan Y, et al. Migratory dendritic cells transfer antigen to a lymph node-resident dendritic cell population for efficient CTL priming. Immunity. 2006;25(1):153-62.

31.Salmon H, Idoyaga J, Rahman A, Leboeuf M, Remark R, Jordan S, et al. Expansion and Activation of CD103(+) Dendritic Cell Progenitors at the Tumor Site Enhances Tumor Responses to Therapeutic PD-L1 and BRAF Inhibition. Immunity. 2016;44(4):924-38.

32. Roberts EW, Broz ML, Binnewies M, Headley MB, Nelson AE, Wolf DM, et al. Critical Role for CD103(+)/CD141(+) Dendritic Cells Bearing CCR7 for Tumor Antigen Trafficking and Priming of T Cell Immunity in

Melanoma. Cancer Cell. 2016;30(2):324-36.

33. Williford JM, Ishihara J, Ishihara A, Mansurov A, Hosseinchi P, Marchell TM, et al. Recruitment of CD103(+) dendritic cells via tumor-targeted chemokine delivery enhances efficacy of checkpoint inhibitor immunotherapy. Sci Adv. 2019;5(12):eaay1357.

34. Langlet C, Tamoutounour S, Henri S, Luche H, Ardouin L, Gregoire C, et al. CD64 expression distinguishes monocyte-derived and conventional dendritic cells and reveals their distinct role during intramuscular immunization. J Immunol. 2012;188(4):1751-60.

35. Min J, Yang D, Kim M, Haam K, Yoo A, Choi JH, et al. Inflammation induces two types of inflammatory dendritic cells in inflamed lymph nodes. Exp Mol Med. 2018;50(3):e458.

36. Sheng J, Chen Q, Soncin I, Ng SL, Karjalainen K, Ruedl C. A Discrete Subset of Monocyte-Derived Cells among Typical Conventional Type 2 Dendritic Cells Can Efficiently Cross-Present. Cell Rep. 2017;21(5):1203-14.

37. Didierlaurent AM, Morel S, Lockman L, Giannini SL, Bisteau M, Carlsen H, et al. AS04, an aluminum salt- and TLR4 agonist-based adjuvant system, induces a transient localized innate immune response leading to enhanced adaptive immunity. J Immunol. 2009;183(10):6186-97.

38. Pillet S, Aubin E, Trepanier S, Poulin JF, Yassine-Diab B, Ter Meulen J, et al. Humoral and cell-mediated immune responses to H5N1 plant-made virus-like particle vaccine are differentially impacted by alum and GLA-SE adjuvants in a Phase 2 clinical trial. NPJ Vaccines. 2018;3:3.

39. Coler RN, Day TA, Ellis R, Piazza FM, Beckmann AM, Vergara J, et al. The TLR-4 agonist adjuvant, GLA-SE, improves magnitude and quality of immune responses elicited by the ID93 tuberculosis vaccine: first-in-human trial. NPJ Vaccines. 2018;3:34.

40. Albershardt TC, Leleux J, Parsons AJ, Krull JE, Berglund P, Ter Meulen J. Intratumoral immune activation with TLR4 agonist synergizes with effector T cells to eradicate established murine tumors. NPJ Vaccines. 2020;5(1):50.

41. Somaiah N, Chawla SP, Block MS, Morris JC, Do K, Kim JW, et al. A Phase 1b Study Evaluating the Safety, Tolerability, and Immunogenicity of CMB305, a Lentiviral-Based Prime-Boost Vaccine Regimen, in Patients with Locally Advanced, Relapsed, or Metastatic Cancer Expressing NY-ESO-1. Oncoimmunology. 2020;9(1):1847846.

42. Grewal EP, Erskine CL, Nevala WK, Allred JB, Strand CA, Kottschade LA, et al. Peptide vaccine with glucopyranosyl lipid A-stable oil-in-water emulsion for patients with resected melanoma. Immunotherapy. 2020;12(13):983-95.

43. Bhatia S, Miller NJ, Lu H, Longino NV, Ibrani D, Shinohara MM, et al. Intratumoral G100, a TLR4 Agonist, Induces Antitumor Immune Responses and Tumor Regression in Patients with Merkel Cell Carcinoma. Clin Cancer Res. 2019;25(4):1185-95.

44. Ahrends T, Spanjaard A, Pilzecker B, Babala N, Bovens A, Xiao Y, et al. CD4(+) T Cell Help Confers a Cytotoxic T Cell Effector Program Including Coinhibitory Receptor Downregulation and Increased Tissue Invasiveness. Immunity. 2017;47(5):848-61 e5.

45. Provine NM, Larocca RA, Aid M, Penaloza-MacMaster P, Badamchi-Zadeh A, Borducchi EN, et al. Immediate Dysfunction of Vaccine-Elicited CD8+ T Cells Primed in the Absence of CD4+ T Cells. J Immunol. 2016;197(5):1809-22.

46. Winzler C, Rovere P, Zimmermann VS, Davoust J, Rescigno M, Citterio S, et al. Checkpoints and functional stages in DC maturation. Adv Exp Med Biol. 1997;417:59-64.

SUPPLEMENTARY FIGURES

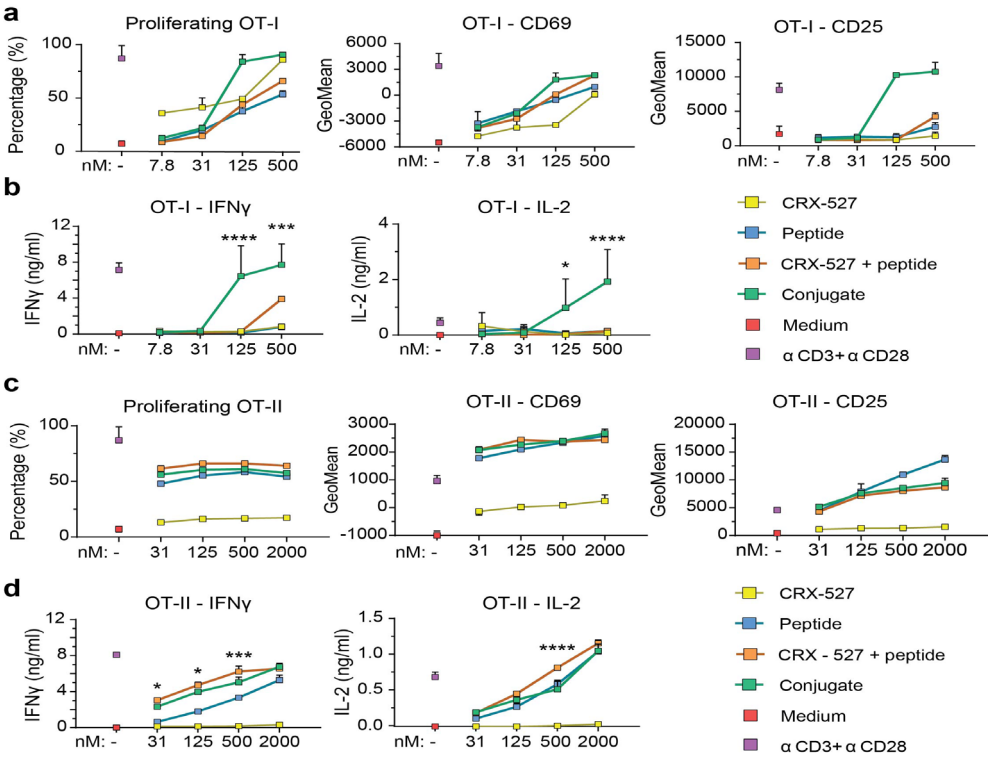

Figure S1: CRX-527-peptide conjugates induce OT-I and OT-II cell activation *in vitro*. D1 dendritic cells were pulsed for 2 hours with the indicated compounds at different concentrations and incubated for 48 hours with purified CFSE-labelled OT-I or OT-II T cells. In the last 5 hours, supernatant was collected for cytokine detection by ELISA and cells were incubated with Brefeldin A followed by staining for activation markers and cytokines. (**A**) Percentage of proliferating cells and expression of CD69 and CD25 activation markers on OT-I cells. Medium and stimulation with αCD3 + αCD28 antibodies were used as negative and positive controls. (**B**) Production of IFNγ and IL-2 cytokines by OT-I as detected in the supernatant by ELISA. (**C**) Percentage of proliferating cells and expression of CD69 and CD25 activation markers on OT-II cells. Medium and stimulation with αCD3 + αCD28 antibodies were used as negative and positive controls. (**D**) Production of IFNγ and IL-2 cytokines by OT-II as detected in the supernatant by ELISA.

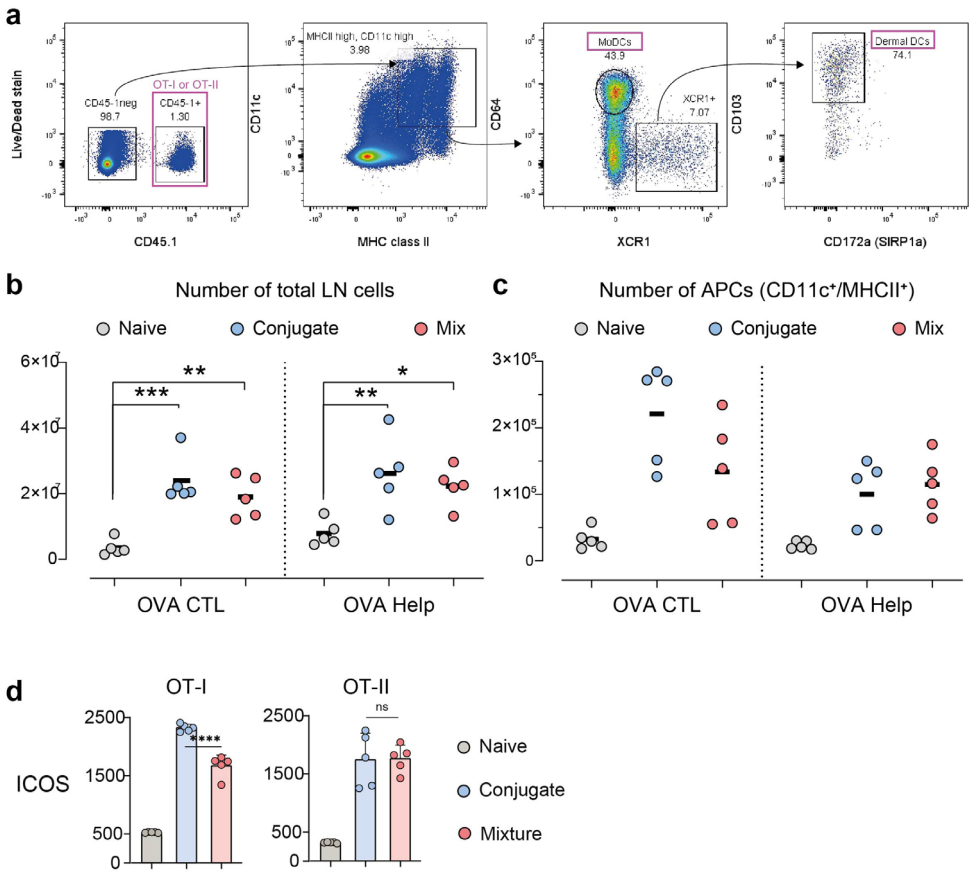

Figure S2: OVA CTL and Help CRX-527-peptide conjugates promote APCs influx in the draining lymph node upon *in vivo* injection. Mice (n=5 per group) were adoptively transferred with CFSE labelled OT-I or OT-II 24 hours before receiving 2 nmol of OVA CTL or Help CRX-527conjugates, or an equimolar mix of peptide and CRX-527. 48 hours later the inguinal lymph nodes were harvested for analysis of OT-I or OT-II T cell proliferation and activation. (**A**) Gating strategy for identification of OT-I or OT-II cells (expressing the congenic marker CD45.1) and CD11c+MHCII+ APCs, MoDCs (CD64+XCR1-) and dermal DCs (XCR1+CD103+CD172a-) (**B** and **C**). Absolute count of total cells in the two inguinal lymph nodes (**B**) and APCs (**C**) upon injection of OVA CTL or Help peptides mixed with Lipid A or in form of conjugates. (**D**) Fluorescence intensity of ICOS activation markers as detected by flow cytometry in OT-I or OT-II cells. Statistical significance of the conjugates compared to the mix was determined by one-way ANOVA followed by Sidak's multiple comparison test; ***** p< 0.0001.

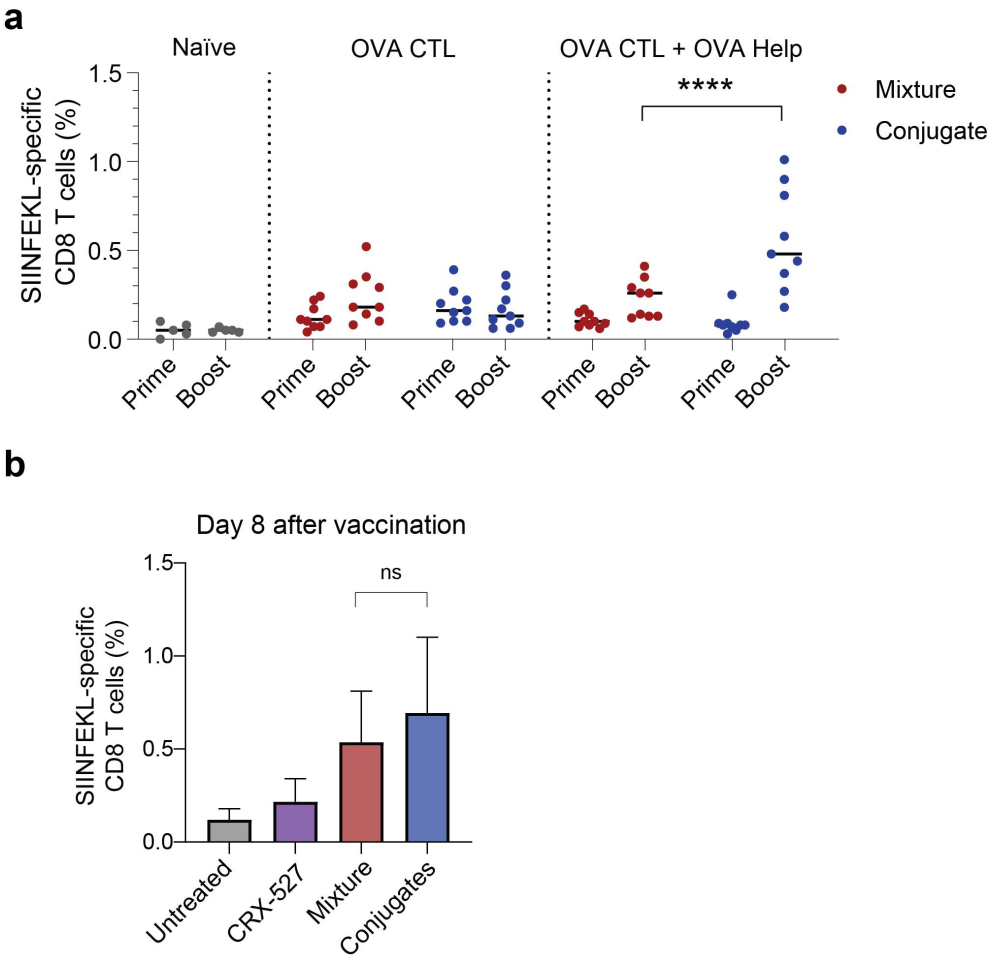

Figure S3: OVA CTL and Help CRX-527-peptide conjugates effectively induce SIINFEKL-specific T cell responses upon prophylactic or therapeutic vaccination (**A**) Frequency of SIINFEKL-specific T cells in blood of individual mice (n=5) one week after prime or booster injection with CRX-527 and OVA CTL and Help peptides in conjugated form or mixed before B16OVA tumor challenge. Statistical significance of the conjugates compared to the mix was determined by one-way ANOVA followed by Tukey's multiple comparison test; ***** $p < 0.0001$. (**B**) Levels of SIINFEKL-specific CD8 T cells detected after therapeutic vaccination in B16OVA tumor-bearing mice. Statistical significance of the conjugates compared to the mix was determined by one-way ANOVA followed by Tukey's multiple comparison test.

V

4

MULTIVALENT, STABILIZED MANNOSE-6-PHOSPHATES FOR THE TARGETED DELIVERY OF TOLL-LIKE RECEPTOR LIGANDS AND PEPTIDE ANTIGENS

Reintjens NRM, Tondini E, Vis C, McGlinn T, Meeuwenoord NJ, Hogervorst TP, Overkleeft HS, Filippov DV, van der Marel GA, Ossendorp F, Codée JDC

Chembiochem 2021 Jan 15;22(2):434-440

ABSTRACT

Mannose-6-phosphate (M6P) is recognized by the mannose-6-phosphate receptor and plays an important role in the transport of cargo to the endosomes, making it an attractive tool to improve endosomal trafficking of vaccines. We here describe the assembly of peptide antigen conjugates carrying clusters of mannose-6-*C*-phosphonates (M6Po). The M6Po's represent stable M6P mimics that are resistant to cleavage of the phosphate group by endogenous phosphatases. Two different strategies for the incorporation of the M6Po clusters in the conjugate have been developed: the first relying on a "post-assembly" click approach employing an M6Po bearing an alkyne functionality; the second hinges on an M6Po *C*-glycoside amino acid building block that can be used in solid-phase peptide synthesis. The generated conjugates were further equipped with a TLR7-ligand to stimulate dendritic cell (DC) maturation. While antigen presentation is hindered by the presence of the M6Po clusters, the incorporation of the M6Po clusters leads to increased activation of DCs, demonstrating their potential in improving vaccine adjuvanticity by intraendosomally active TLR-ligands.

INTRODUCTION

Carbohydrates play an important role in many biological processes, such as cell-cell communication, pathogen recognition and protein folding. Mannose-6-phosphate (M6P), a D-mannopyranose bearing a phosphate group at the *C*-6 position, serves as a signaling moiety on the termini of glycan branches mounted on newly synthesized proteins in the trans-Golgi network and is essential for the transportation of these proteins to the late endosomes and lysosomes. The mannose-6-phosphate receptor (MPR), a P-type lectin, plays an important role in this transportation through binding to M6P.[1,2] There are two members of this lectin family: the cation-dependent mannose-6-phosphate receptor (CD-MPR) and the cation-independent mannose-6-phosphate receptor (CI-MPR). The latter has a high affinity for ligands containing multiple M6Ps due to the presence of two M6P binding domains, which can simultaneously bind two M6Ps.[3–5]215 kDa A small fraction of MPRs can be found on the cell surface of which only CI-MPR binds and internalizes M6P-bound substrates.[6] Therefore, the CI-MPR is an efficient tool for targeted delivery to the endosomes, as was shown by the conjugation of M6P analogues to acid α-glucosidase leading to improved delivery of this enzyme in the treatment of the lysosomal myopathy Pompe disease.[7] The MPR has also been exploited as a drug delivery system for cancer therapy,[8,9]hen-egg white lysozyme (HEL for example, doxorubicin was delivered via mannose-6-phosphate-modified human serum albumin as carrier and *N*-hexanoyl-D-*erythro*-sphingosine with M6P-functionalized liposomes.[10,11] pharmacological intervention with antiproliferative drugs may result in antifibrotic effects. In this article, the antiproliferative effect of three cytostatic drugs was tested in cultured rat HSC. Subsequently, the antifibrotic potential of the most potent drug was evaluated in vivo. As a strategy to overcome drug-related toxicity, we additionally studied how to deliver this drug specifically to HSC by conjugating it to the HSC-selective drug carrier mannose-6-phosphate-modified human serum albumin (M6PHSA Our group has previously reported that a cathepsin inhibitor that is covalently attached to an M6P cluster could effectively be delivered into the endolysosomal pathway.[12]

The activity of peptide-based anti-cancer vaccines may be enhanced by the targeted delivery of these antigens to antigen presenting cells. In this context,

mannosylated antigens, destined for the mannose receptor or DC-SIGN present on dendritic cells (DCs), have been widely explored.[13–16] We, therefore, reasoned that conjugate vaccines in which an M6P moiety is covalently bound to an antigenic peptide might be targeted effectively to immune cells expressing the MPR, leading to improved uptake and more efficient delivery to the lysosomes where the cargo is processed for MHC loading, ultimately resulting in enhanced antigen presentation. Since dephosphorylation by endogenous phosphatases is one of the potential drawbacks of the use of M6P, several stable M6P analogues have previously been evaluated, such as a malonyl ether, a malonate or an isosteric *C*-phosphonate ester.[17,18] The *C*-phosphonate proved to be a stable and effective replacement for the phosphate monoester.[19]

We here describe the incorporation of a cluster of mannose-6-phosphonates (M6Po) in two types of peptide antigen-conjugates (**1**-**8**, Figure 1), wherein two different M6Po building blocks, **9** and **10**, respectively, are used to construct M6Po-clusters and conjugate them to either the *N*- or the *C*-terminus of a synthetic long peptide (SLP). In this study, two different ovalbumin derived SLPs are used: DEVA$_5$K (DEVSGLEQLESIINFEKLAAAAAK), which harbours the MHC-I presented epitope SIINFEKL, and HAAHA (ISQAVHAAHAEINEAGRK), which contains an MHC-II epitope. Our goal is to enhance the immune response by increasing endosomal trafficking of the peptide vaccine via the MPR which led to the design of bis-conjugates (**2**, **4**, **6,** and **8**) in which the Toll-like receptor 7 ligand (TLR7L) 2-alkoxy-8-oxo-adenine is added at either the *N*- or the *C*-terminus of the M6Po-SLP.[20,21] We coupled an α-configured spacer,[12,18,22] carrying an alkyne function to the *O*-M6Po building block **9** to allow for the copper mediated 1,3-dipolar cycloaddition to azide-functions incorporated in the SLP, while *C*-M6Po building block **10** was used to generate the HAAHA-conjugates via solid-phase peptide synthesis (SPPS). This building block is a *C*-analogue[23] of *O*-M6Po, in which the anomeric oxygen is replaced with a CH_2, preventing hydrolysis under the acidic conditions used in SPPS. An additional advantage of this SPPS-compatible building block is the possibility to prepare conjugates of peptides that are not suitable for copper mediated 1,3-dipolar cycloaddition. It also allows one to incorporate azide or alkyne click handles in conjugate vaccine constructs that can be exploited for labelling or visualization purposes. We here report the synthesis and immunological evaluation of these dual conjugated peptide vaccine constructs.

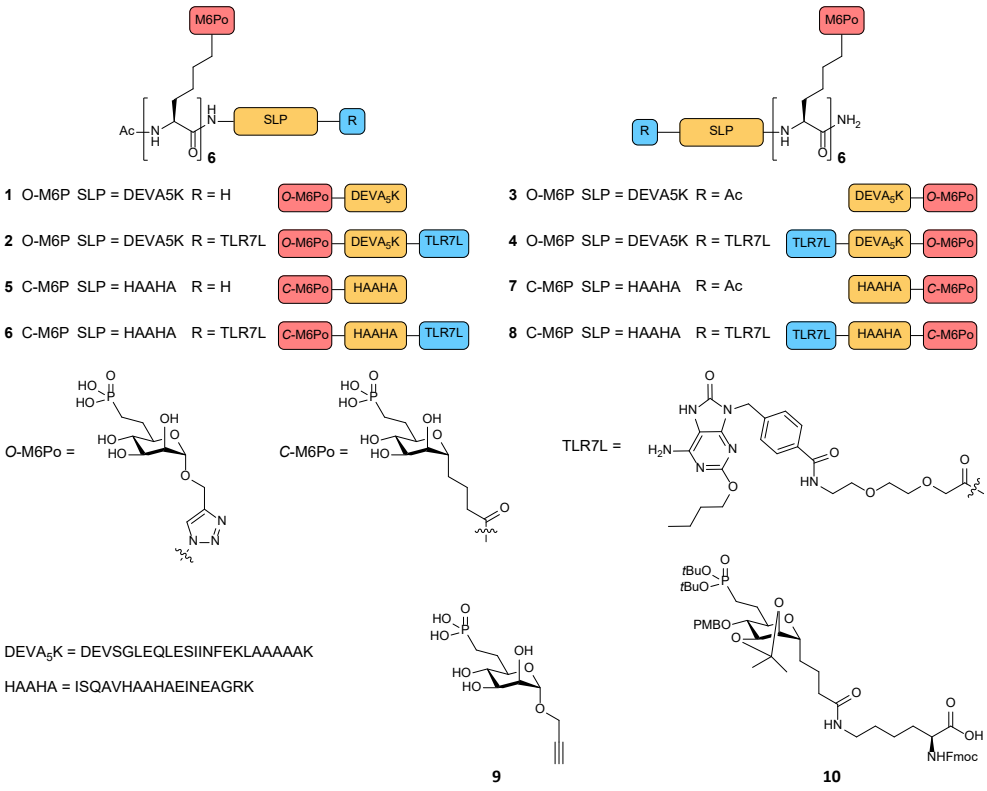

Figure 1. Structures of the *O*-M6Po conjugates **1**-**4**, *C*-M6Po conjugates **5**-**8**, and building blocks **9** and **10**.

RESULTS AND DISCUSSION

Synthesis of M6Po-conjugates

The first type of *O*-M6Po conjugates comprises the six-fold addition of α-propargyl mannose-6-phosphonate (*O*-M6Po) building block (**9**) to azide containing peptides. Synthesis of the required building block **9** started from propargyl-D-mannose **11** (Scheme 1A). As we found that the use of *para*-methoxybenzyl ethers for the protection of the secondary alcohols led to the formation of a 3,6-ether bridge when the C-6-hydroxyl was triflated, to enable the subsequent substitution by a phosphonate anion (See supporting information Scheme S1), we placed an isopropylidene group over the 2,3-*cis*-diol system to prevent this intramolecular side reaction.[24,25] Thus, tritylation of **11** and subsequent installation of the isopropylidene gave **13**, of which the remaining alcohol was masked as a *p*-methoxybenzyl ether to give the fully protected mannose **14**. The alkyne in **14** was protected with a TMS group using TMSCl and *n*-BuLi at -78°C. Removal

of the trityl in the thus obtained **15** with a catalytic amount of *p*-toluenesulfonic acid in DCM/MeOH was accompanied by partial removal of the isopropylidene ketal. Reinstallation of the isopropylidene and subsequent deprotection of the mixed ketal simultaneously formed on the primary alcohol gave **16** in 98% over three steps. Alcohol **16** was treated with Tf_2O and pyridine at -40°C[26] and the obtained crude triflate was added to a mixture of dimethyl methylphosphonate and *n*-BuLi in THF at -70°C, yielding compound **17** in 72% over two steps. Removal of the TMS protecting group gave **18**, which was transformed into key building block **9** by a two-step deprotection sequence. The deprotection of the phosphonate using TMSBr was followed by the removal of the *p*-methoxybenzyl and isopropylidene groups by treatment with AcOH/H_2O at 90°C to deliver key building block **9** in 27% yield over 15 steps starting from D-mannose.

En route to mannose-6-phosphonate SPPS building block **10** (Scheme 1B), the trityl group of known compound **19**[23] was removed as described above to give alcohol **20** in 72% over three steps. Conversion of **20** to the primary triflate, followed by nucleophilic substitution with the anion of di-*tert*-butyl methylphosphonate[27] gave phosphonate **21** in 72% over two steps on 3 mmol scale.[28] Cross metathesis with methyl acrylate, followed by the reduction of the double bond with $NaBH_4$ and ruthenium trichloride then resulted in compound **22**.[29,30] Hydrolysis of the obtained methyl ester, was followed by condensation with Fmoc-L-Lys-OMe and subsequent treatment of **24** with LiOH at 0°C, which left the Fmoc group unaffected, then delivered the key SPPS building block **10** in 80% yield.

Next, the assembly of the (*O*-M6Po)$_6$-SIINFEKL conjugates was undertaken. Immobilized peptides **25** and **28** were prepared through standard SPPS HCTU/Fmoc chemistry using Tentagel S Ram as solid support (Scheme 2A). The *C*-terminal lysine of **25** was protected with a MMT group since we aimed to make M6Po-peptide conjugates as well as conjugates containing both an M6Po-cluster and a TLR7-ligand. TFA/TIS/H_2O (95/2.5/2.5 v/v/v) treatment removed all protecting groups and cleaved the peptides from the resin to give peptides **26** and **29** in 1% and 6% yield respectively, after purification. Alternatively, the MMT protecting group at the *C*-terminal lysine of **25** was selectively deprotected using a cocktail of TFA/TIS/DCM (2/2/96 v/v/v). The released amine was subsequently coupled with the spacer **33** and the Boc-protected TLR7-ligand building block **34**.[21]

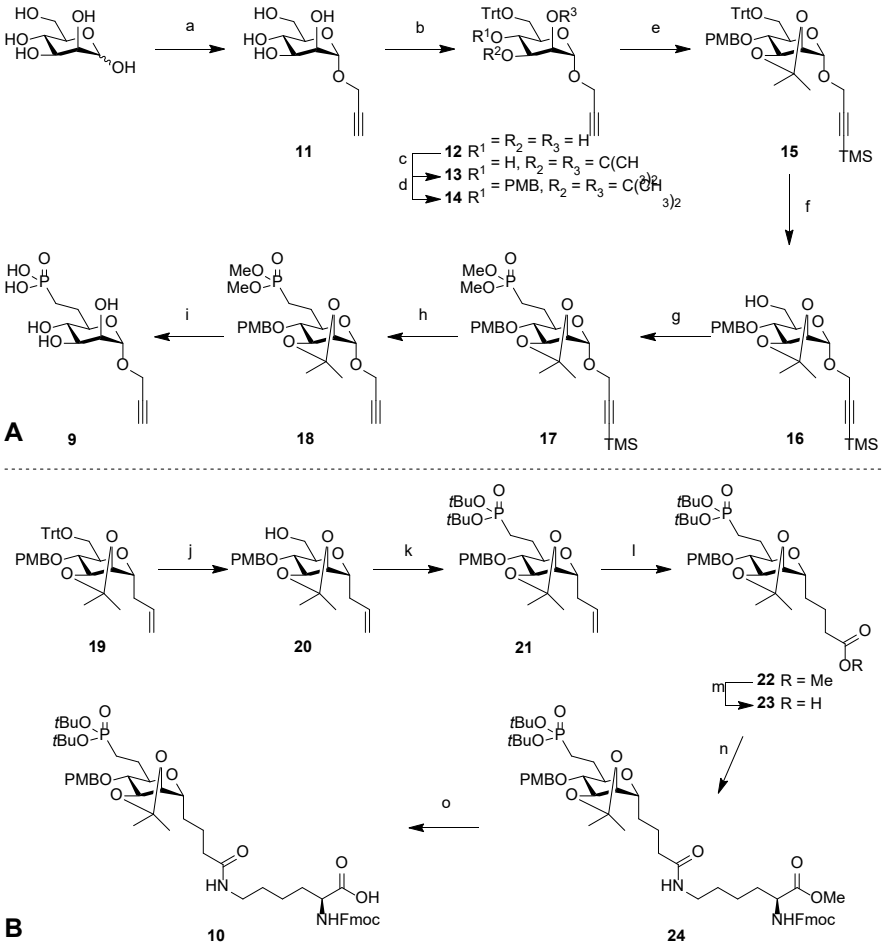

Scheme 1. Synthesis of alkyne building blocks **9** and **10**. *Reagents and conditions*: a) *i.* Ac_2O, pyridine; *ii.* propargyl alcohol, $BF_3{\cdot}OEt_2$, 50°C; *iii.* NaOMe, MeOH, 70% over three steps; b) TrtCl, Et_3N, DMF, 60°C, 83%; c) *p*-toluenesulfonic acid, 2,2-dimethoxypropane, 87%; d) *p*-methoxybenzyl chloride, NaH, DMF, 95%; e) TMSCl, *n*-BuLi, THF, -78°C, 97%; f) *i.* *p*-toluenesulfonic acid, DCM/MeOH; *ii.* *p*-toluenesulfonic acid, 2,2-dimethoxypropane; *iii.* 1 M HCl, EtOAc, 0°C, 98% over three steps: g) *i.* Tf_2O, pyridine, DCM, -40°C; *ii.* *n*-BuLi, dimethyl methylphosphonate, THF, -70**°C to -50°C,** 72% over two steps; h) TBAF, THF, quant.; i) *i.* TMSBr, pyridine, MeCN; *ii.* AcOH/H_2O, 90°C, 81% over two steps; j) *i.* *p*-toluenesulfonic acid, DCM/MeOH; *ii.* *p*-toluenesulfonic acid, 2,2-dimethoxypropane; *iii.* 1 M HCl, EtOAc, 0°C, 75% over three steps; k) *i.* Tf_2O, pyridine, DCM, -40°C; *ii.* *n*-BuLi, di-*tert*-butyl methylphosphonate, THF, -70**°C to -50°C,** 72% over two steps; l) *i.* methyl acrylate, CuI, Grubbs 2nd gen. catalyst, DCE, 60°C; *ii.* $NaBH_4$, $RuCl_3$, MeOH, DCE, 45°C, 72% over two steps; m) LiOH, THF/H_2O, quant; n) Fmoc-L-Lys-OMe, HCTU, DIPEA, DMF, 86%; o) LiOH, THF/H_2O, 0°C, 80%.

After deprotection, release from the resin and RP-HPLC purification peptides **27** and **30** were obtained in a 2% yield. Coupling of *O*-M6Po building block **9** to peptides **26**, **27**, **29** and **30** was performed using a cocktail of $CuSO_4$, sodium ascorbate and tris(benzyltriazolylmethyl)amine in DMSO/H_2O,[31] with the addition of a 20 mM Tris/150 mM NaCl buffer. After RP-HPLC, conjugates **1**-**4** were obtained in 5% (0.3 mg), 18% (0.9 mg), 18% (1.0 mg) and 31% (3.3 mg) yield respectively.

The HAAHA peptide contains two histidines, which can coordinate to copper and thereby inhibit the reduction of Cu(II) to Cu(I).[32] Therefore, conjugates **5**-**8** were generated by an online SPPS synthesis (Scheme 2B) using *C*-M6Po building block **10**, which is equipped with acid-labile protecting groups that can be removed at the end of the SPPS concomitantly with all other acid-labile peptide protecting groups and release of the peptide from the resin. Tentagel S Ram resin was elongated with ISQAVHAAHAEINEAGRK using automated SPPS, of which the lysine(MMT) at the *C*-terminus will be used for elongation at a later stage of the synthesis. Six consecutive coupling and Fmoc removal cycles with building block **10** gave immobilized peptide **31**. Peptide **32**, bearing the *C*-M6Po cluster at the *C*-terminal end, was generated by assembling the hexa-*C*-M6Po peptide through manual couplings of building block **10**, followed by automated SPPS to

Scheme 2. Synthesis of **A)** *O*-M6Po conjugates **1**-**4** and **B)** *C*-M6Po conjugates **5**-**8**. *Reagents and conditions*: a) *i.* 20% piperidine, DMF; *ii.* Fmoc SPPS cycle for K(N_3)-K(N_3)-K(N_3)-K(N_3)-K(N_3)-K(N_3)-DEVSGLEQLESIINFEKLAAAAAK; *iii.* 20% piperidine, DMF; *iv.* Ac_2O, DIPEA, DMF; b) TFA/TIS/H_2O (95/2.5/2.5 v/v/v), 3h; c) RP-HPLC; d) **9**, 20 mM Tris/150 mM NaCl buffer, $CuSO_4$/NaAsc/TBTA, H_2O/DMSO; e) TFA/TIS/DCM (2/2/96 v/v/v); f) *i.* {2-[2-(Fmoc-amino)ethoxy] ethoxy}acetic acid, HCTU, DIPEA, DMF; *ii.* 20% piperidine, DMF; *iii.* 4-((2-butoxy-6-((*tert*-butoxycarbonyl)amino)-8-oxo-7,8-dihydro-9H-purin-9-yl)methyl)benzoid acid, HCTU, DIPEA, DMF; g) *i.* 20% piperidine, DMF; *ii.* Fmoc SPPS cycle for DEVSGLEQLESIINFEKLAAAAAK-K(N_3)-K(N_3)-K(N_3)-K(N_3)-K(N_3)-K(N_3); *iii.* 20% piperidine, DMF; h) Ac_2O, DIPEA, DMF; i) *i.* 20% piperidine, DMF; *ii.* Fmoc SPPS cycle for ISQAVHAAHAEINEAGRK; *iii.* 20% piperidine, DMF; *iv.* **10**, HCTU, DIPEA, DMF; *v.* 5x repeat of *iii.* and *iv.*; *vi.* 20% piperidine, DMF; *vii.* Ac_2O, DIPEA, DMF; j) AcOH/TFE/DCM (1/2/7 v/v/v); k) *i.* 20% piperidine, DMF; *ii.* **10**, HCTU, DIPEA, DMF; *iii.* 5x repeat of *i.* and *ii.*; *iv.* 20% piperidine, DMF *v.* Fmoc SPPS cycle for ISQAVHAAHAEINEAGRK; *iii.* 20% piperidine, DMF; Yield peptides and conjugates: **26**) 4.6 mg, 1%; **27**) 4.0 mg, 2%; **29**) 17.4 mg, 6%; **30**) 8.2 mg, 2%; **1**) 0.3 mg, 5%; **2**) 1.0 mg, 18%; **3**) 0.9 mg, 18%; **4**) 3.3 mg, 31%; **5**) 13.3 mg, 10%; **6**) 11.0 mg, 8%; **7**) 3.1 mg, 2%; **8**) 17.0 mg, 11%.

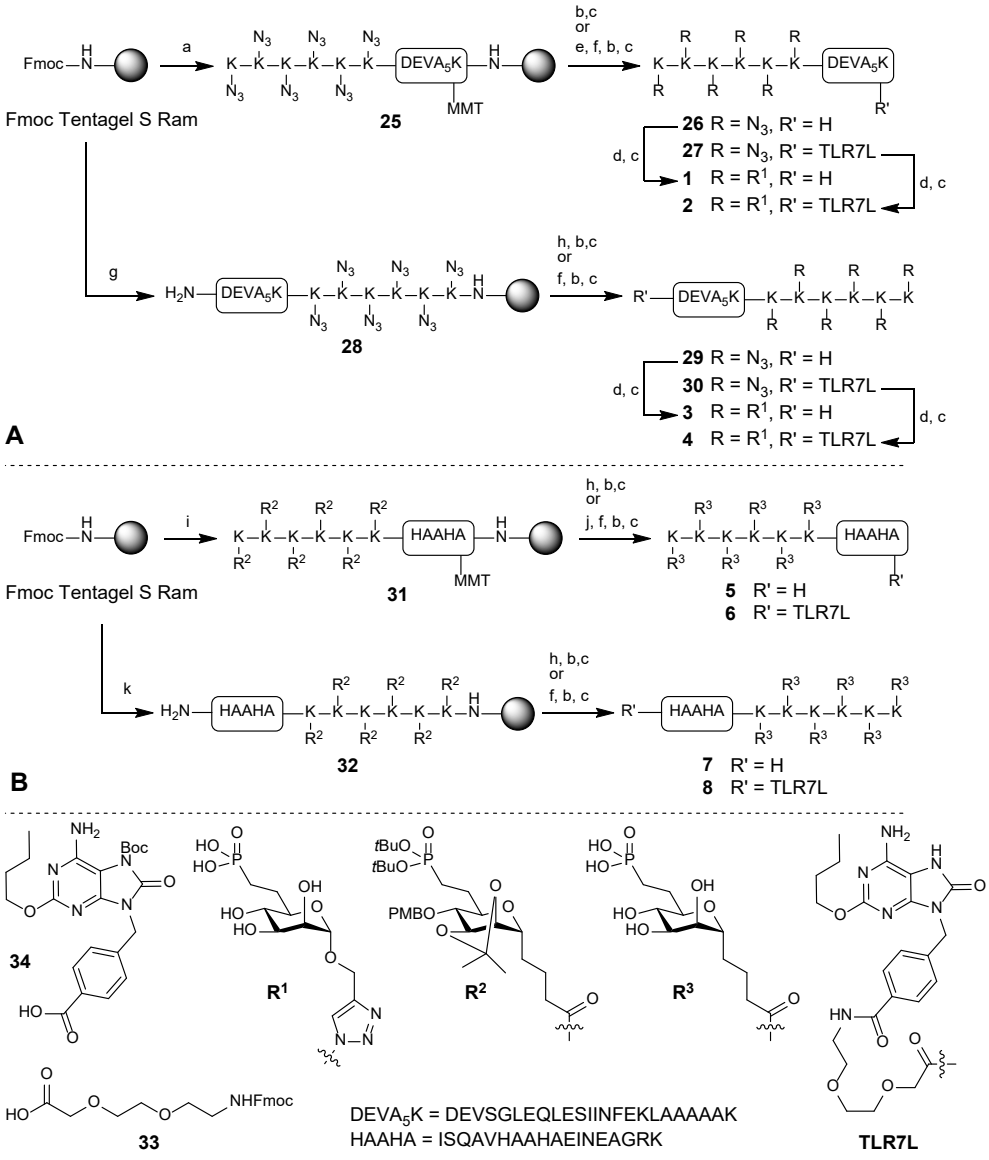

assemble the rest of the peptide. Immobilized and protected peptides **31** and **32** were deprotected and simultaneously cleaved from the resin with the TFA/TIS cocktail to provide conjugates **5** (13.3 mg) and **7** (3.1 mg) after purification by RP-HPLC in 10% and 8% yield respectively, demonstrating the suitability of **10** for SPPS. To obtain conjugate **6**, bearing the TLR7-ligand, the MMT-group in **31** was selectively removed with a cocktail of AcOH/TFE/DCM (1/2/7 v/v/v). The obtained free amine was elongated with spacer **33** and Boc-protected TLR7-ligand building block **34** to give conjugate **6** (11.0 mg) in 2% yield, after removal of all

the protecting groups, cleavage from the resin and RP-HPLC purification. The same sequence of events was applied to the *N*-terminal amine in immobilized peptide **32** to afford conjugate **8** (17.0 mg) in 8% yield.

Immunological evaluation

We assessed the capacity of the conjugates **1**-**8** to induce maturation of dendritic cells (DCs) and stimulate antigen presentation (Figure 2). In these assays reference compounds **35**-**40**, lacking the mannose-6-phosphonate clusters, were used as a control (See supporting information Scheme S2). The activation of DCs can be measured by the detection of the production of interleukin-12 (IL-12). First, the *O*-M6Po conjugates **1**-**4** were evaluated (Figure 2A). To this end, murine bone marrow/derived DCs were stimulated for 24 hours with the compounds and the amount of secreted IL-12 was measured in the supernatant. As expected, conjugation with solely a cluster of M6Po (as in conjugates **1** and **3**) does not induce DC maturation. In contrast, the TLR7-ligand SLP conjugates (**36** and **37**) induce IL12 production due to stimulation of the TLR7 receptor.

Interestingly, the conjugates carrying the M6Po-cluster and the TLR7-ligand (**2** and **4**) induced a stronger activation of the DCs than their counterparts solely bearing a TLR7-ligand (*i.e.,* SLP-conjugates **36** and **37**). The position of the M6Po-clusters and TLR7 ligand in these conjugates did not seem to influence the activity of the conjugates. Similar effects were observed for the conjugates **6** and **8** with the *C*-M6Po-clusters, indicating that the *C*-mannosyl-6-*C*-phosphonate is an adequate mimic of its *O*-mannosyl counterpart and that the enhanced stimulatory effect is independent of the peptide sequence (Figure 2B, see also supporting Figure S1). Overall this indicates that conjugation of the M6Po-cluster to a peptide antigen adjuvanted with a TLR7-ligand enhances DC maturation by improving uptake of the conjugate and/or trafficking of the conjugates to the endosomally located TLR7 receptor.

Processing of the two peptides was investigated by assessing presentation of the SIINFEKL epitope on MHC-I by the DCs to $CD8^+$ T cells and presentation of the helper epitope (HAAHA) to $CD4^+$ T cells. For the former assay, a hybridoma (B3Z) $CD8^+$ T cell line was used, while the latter employed an OTIIZ hybridoma $CD4^+$ T cell line. As can be seen in Figures 2C and 2D, attachment of the TLR7-ligand to the SLPs led to the enhanced presentation of the antigens (See for example **35** *vs.* **36**/**37** and **38** *vs.* **40**), however the inclusion of the M6Po-clusters hampered presentation through both the MHC class I and MHC class II pathways (See for example **36** *vs.* **4**, **37** *vs.* **2** and **40** *vs.* **6**). This indicates that the conjugation of M6Po-clusters affects intracellular trafficking or processing of the peptides.

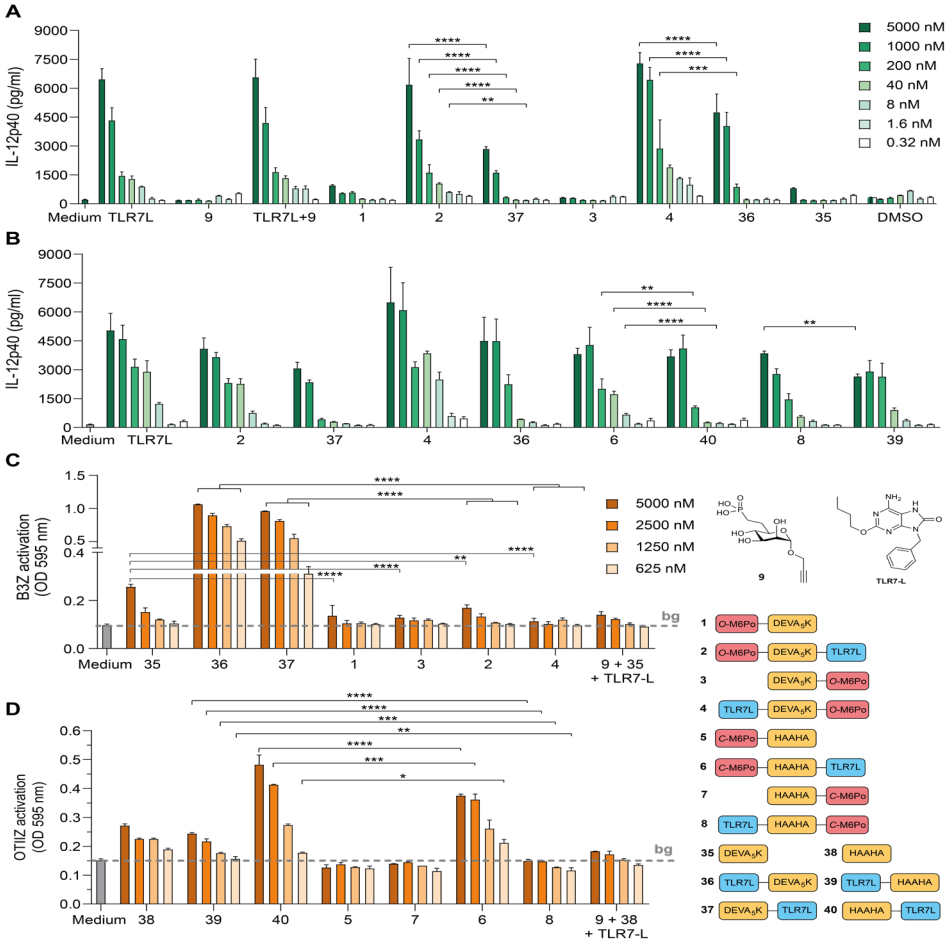

Figure 2. M6Po-conjugation enhances DC activation of theTLR7-ligand conjugates but inhibits antigen presentation. **A)** Murine bone marrow-derived dendritic cells were stimulated in triplicates for 24 hours with the indicated conjugates of the $DEVA_5K$ peptide. The induction of DC maturation was analyzed by measuring IL-12 production with sandwich ELISA specific for the IL-12p40 subunit. The bars represent the standard deviation of the mean of the triplicates. **B)** The induction of IL-12p40 of the $DEVA_5K$ and the HAAHA conjugates was compared by stimulating bone-marrow derived dendritic cells for 24 hours followed by sandwich ELISA. **C** and **D)** Antigen uptake and presentation to T cells was measured by incubating dendritic cells in duplicates with the indicated compounds for 3 hours, followed by incubation with the reporter hybridoma T cell lines. The SIINFEKL-specific hybridoma T cell line B3Z served as readout for the $DEVA_5K$ peptide, while the OTIIZ hybridoma cell line was used to detect presentation of the HAAHA epitope. B3Z or OTIIZ activation was determined by colorimetric reaction of the lacZ reporter enzyme. Results are representative of three independently performed experiments. The statistical differences between the compounds at the same concentrations were calculated by 2-way ANOVA followed by multiple comparison and Tukey corrections. * $p<0.05$, ** $p< 0.01$, *** $p<0.001$, **** $p<0.0001$.and Tukey corrections. * $p<0.05$, ** $p< 0.01$, *** $p<0.001$, **** $p<0.0001$.

CONCLUSION

In conclusion, we have described the development of two mannose-6-*C*-phosphonate (M6Po) building blocks which allow for stabilized M6P-analogues to be incorporated in peptide sequences to target the M6P receptor. To prevent dephosphorylation by endogenous phosphatases, the O-phosphate in the naturally occurring mannose-6-phosphate was replaced by a C-phosphonate moiety. The first building block carries an *O*-propargyl group at the anomeric center of the mannose-6-*C*-phosphonate, which allows for the incorporation of the M6Po in peptide sequences through an azide-alkyne click reaction. The second building block, a *C*-mannoside, was designed and synthesized for application in solid-phase peptide synthesis. The acid-stable anomeric linkage and protecting groups used enabled the streamlined in-line incorporation of the building block during SPPS. With the building blocks, various peptide conjugates were assembled, containing either an MHC-I or an MHC-II epitope, an M6Po-cluster presenting six mannose-6-phosphonates, and a TLR7-ligand. Although immunological evaluation has shown that conjugation of the M6Po-clusters inhibits antigen presentation, the ability of the TLR7-ligand conjugates to induce DC maturation was significantly improved. While the M6Po clusters effectively trafficked the conjugates to the endosome, where the conjugates interacted with TLR7 receptor, the processing of the conjugates was impeded by the M6Po-clusters. Future conjugates will be designed featuring cleavable linkers that allow for the release of the clusters during endolysosomal processing, effectively liberating the incorporated peptide antigens for presentation.

REFERENCES

[1] N. Dahms, Biochim. Biophys. Acta - Gen. Subj. 2002, 1572, 317–340.

[2] P. Ghosh, N. M. Dahms, S. Kornfeld, Nat. Rev. Mol. Cell Biol. 2003, 4, 202–213.

[3] J. J. Distler, J. F. Guo, G. W. Jourdian, O. P. Srivastava, O. Hindsgaul, J. Biol. Chem. 1991, 266, 21687–92.

[4] P. Y. Tong, W. Gregory, S. Kornfeld, J. Biol. Chem. 1989, 264, 7962–9.

[5] S. J. York, L. S. Arneson, W. T. Gregory, N. M. Dahms, S. Kornfeld, J. Biol. Chem. 1999, 274, 1164–71.

[6] K. Prydz, A. W. Brändli, M. Bomsel, K. Simons, J. Biol. Chem. 1990, 265, 12629–35.

[7] K. El Cheikh, I. Basile, A. Da Silva, C. Bernon, P. Cérutti, F. Salgues, M. Perez, M. Maynadier, M. Gary-Bobo, C. Caillaud, et al., Angew. Chemie Int. Ed. 2016, 55, 14774–14777.

[8] E. Dalle Vedove, G. Costabile, O. M. Merkel, Adv. Healthc. Mater. 2018, 7, 1701398.

[9] C. A. Parra-López, R. Lindner, I. Vidavsky, M. Gross, E. R. Unanue, J. Immunol. 1997, 158, 2670–9.

[10] R. Greupink, H. I. Bakker, W. Bouma, C. Reker-Smit, D. K. F. Meijer, L. Beljaars, K. Poelstra, J. Pharmacol. Exp. Ther. 2006, 317, 514–521.

[11] C. Minnelli, L. Cianfruglia, E. Laudadio, R. Galeazzi, M. Pisani, E. Crucianelli, D. Bizzaro, T. Armeni, G. Mobbili, J. Drug Target. 2018, 26, 242–251.

[12] S. Hoogendoorn, G. H. M. van Puijvelde, J. Kuiper, G. A. van der Marel, H. S. Overkleeft, Angew. Chemie Int. Ed. 2014, 53, 10975–10978.

[13] C. R. Becer, M. I. Gibson, J. Geng, R. Ilyas, R. Wallis, D. A. Mitchell, D. M. Haddleton, J. Am. Chem. Soc. 2010, 132, 15130–15132.

[14] E. A. B. Kantchev, C.-C. Chang, D.-K. Chang, Biopolymers 2006, 84, 232–240.

[15] R.-J. E. Li, T. P. Hogervorst, S. Achilli, S. C. Bruijns, T. Arnoldus, C. Vivès, C. C. Wong, M. Thépaut, N. J. Meeuwenoord, H. van den Elst, et al., Front. Chem. 2019, 7, 650.

[16] T. P. Hogervorst, R. J. J. E. Li, L. Marino, S. C. M. Bruijns, N. J. Meeuwenoord, D. V. Filippov, H. S. Overkleeft, G. A. Van Der Marel, S. J. Van Vliet, Y. Van Kooyk, et al., ACS Chem. Biol. 2020, 15, 728–739.

[17] V. Barragan-Montero, A. Awwad, S. Combemale, P. de Santa Barbara, B. Jover, J.-P. Molès, J.-L. Montero, ChemMedChem 2011, 6, 1771–1774.

[18] D. B. Berkowitz, G. Maiti, B. D. Charette, C. D. Dreis, R. G. MacDonald, Org. Lett. 2004, 6, 4921–4924.

[19] S. Banik, K. Pedram, S. Wisnovsky, N. Riley, C. Bertozzi, 2019. Preprint available at chemRxiv https://doi.org/10.26434/ chemrxiv.7927061.v2.

[20] J. J. Weterings, S. Khan, G. J. van der Heden, J. W. Drijfhout, C. J. M. Melief, H. S. Overkleeft, S. H. van der Burg, F. Ossendorp, G. A. van der Marel, D. V. Filippov, Bioorg. Med. Chem. Lett. 2006, 16, 3258–3261.

[21] G. P. P. Gential, T. P. Hogervorst, E. Tondini, M. J. van de Graaff, H. S. Overkleeft, J. D. C. Codée, G. A. van der Marel, F. Ossendorp, D. V. Filippov, Bioorg. Med. Chem. Lett. 2019, 29, 1340–1344.

[22] X. Fei, C. M. Connelly, R. G. MacDonald, D. B. Berkowitz, Bioorg. Med. Chem. Lett. 2008, 18, 3085–3089.

[23] N. Reintjens, T. Koemans, N. Zilverschoon, R. Castelli, R. Cordfunke, J.-W. Drijfhout, N. Meeuwenoord, H. Overkleeft, D. Filippov, G. Van der Marel, et al., European J. Org. Chem. 2020, DOI 10.1002/ejoc.202000587.

[24] L. M. Mikkelsen, S. L. Krintel, J. Jiménez-Barbero, T. Skrydstrup, J. Org. Chem. 2002, 67, 6297–6308.

[25] L. Liu, C.-Q. Wang, D. Liu, W.-G. He, J.-Y. Xu, A.-J. Lin, H.-Q. Yao, G. Tanabe, O. Muraoka, W.-J. Xie, et al., Org. Lett. 2014, 16, 5004–5007.

[26] A fast work-up was necessary due to the instability of the formed triflate as decomposition was observed when concentrating in vacuo at 40°C instead of 30°C..

[27] It was found to be important to co-evaporate the phosphonate reagents with toluene before treatment with n-BuLi.

[28] The yield dropped to 49% when increasing the scale to 30 mmol due to the instability of the primary triflate.

[29] P. K. Sharma, S. Kumar, P. Kumar, P. Nielsen, Tetrahedron Lett. 2007, 48, 8704–8708.

[30] K. Voigtritter, S. Ghorai, B. H. Lipshutz, J. Org. Chem. 2011, 76, 4697–4702.

[31] Q. Liu, H. A. V. Kistemaker, S. Bhogaraju, I. Dikic, H. S. Overkleeft, G. A. van der Marel, H. Ovaa, G. J. van der Heden van Noort, D. V. Filippov, Angew. Chemie Int. Ed. 2018, 57, 1659–1662.

[32] J. Zhou, K. Xu, P. Zhou, O. Zheng, Z. Lin, L. Guo, B. Qiu, G. Chen, Biosens. Bioelectron. 2014, 51, 386–390.

5

DUAL PEPTIDE CONJUGATES SIMULTANEOUSLY TRIGGERING TLR2 AND TLR7 FOR CANCER VACCINATION

Tondini E, van den Ende TC, Camps MGM, Arakelian T, Overkleeft HS, van der Marel GA, Filippov DV, Ossendorp F

Manuscript in preparation

ABSTRACT

Activation of Toll-like receptors (TLRs) can be exploited during vaccination to promote optimal T cell priming, and the stimulation of different TLRs can determine the outcome of the immune response induced. In this study, we investigate the possibility of simultaneously triggering TLR2 and TLR7 via a molecularly defined dual conjugate vaccine to induce antigen specific CD8 and CD4 T cell responses. We show that conjugation of a TLR2 or a TLR7 agonist to a peptide moiety enhances the efficacy of the vaccine compared to administration of unconjugated peptide and adjuvant. In addition, we report vaccine efficacy of dual conjugates bearing the two TLR agonists positioned on the N- and C-terminal ends of two synthetic long peptides. We show that these conjugates are immunologically active and can induce functional CD8 and CD4 responses, by analyzing cytokine profiles of specific T cells. These data show the potency of TLR2 and TLR7 dual conjugates and set the basis for their use for peptide-based T cell vaccination.

INTRODUCTION

Peptide-based vaccination necessitates of the combination of peptide antigen with strong adjuvants in order to activate the immune system and to generate an adequate antigen-specific response. The Toll-like receptor (TLR) family is a family of structurally related receptors that has evolved in vertebrate organisms to recognize different pathogen related-structures. Binding of a ligand to its TLR gives start to an inflammatory response and initiates the activation of innate and adaptive immune reactions. For this reason, TLR stimulation is also exploited for vaccination purposes.

While TLR agonists in vaccines are usually provided next to the antigen, we explored direct conjugation of defined TLR agonists to synthetic peptide antigens, to enhance vaccine efficacy via delivery of antigen and maturation signals to the same antigen-presenting cells (APCs). This was demonstrated for at least three different ligands: the TLR2 agonist Pam_3CysSK_4 [1, 2], the TLR4 agonist CRX-527 [3], and the TLR9 ligand CpG [1]. Conjugation of the TLR agonists to peptides resulted in enhanced uptake and antigen processing and presentation by DCs in vitro, and stronger induction of CD8 or CD4 T cell responses in vivo [1-3].

The TLR2 ligand Pam_3CysSK_4 has been successfully employed in cancer treatment. In pre-clinical studies, Pam conjugated vaccines demonstrated effective tumor eradication which was associated with the modulation of the tumor microenvironment towards a pro-inflammatory phenotype [4], as opposed to the suppressive micro-environment of untreated animals. The optimized version of this agonist UPam [5], also named Amplivant [4], has also been selected for the clinical testing of HPV-related malignancies as defined conjugates of six peptides derived from a E6 protein (Trial ID: NCT02821494). These conjugates demonstrated efficacy in activating human dendritic cells as well as enhanced ability to activate specific T cells derived from HPV16+ cervical cancer patients [6].

Recently, we synthetized and tested the conjugation of a TLR7 agonist derived from hydroxy-adenine which also demonstrated enhanced immunological activity in vitro compared to free peptide [7]. TLR7 and 8 represents an interesting TLR pathway for cancer immunotherapy. Both TLR7 and the structurally related TLR8 recognize viral ssRNA [8] and are strong type I interferon inducers, which promote Th1-skewed immunity aimed at clearing infected cells. Conjugation of a TLR7 agonist to protein antigen has been explored in HIV vaccines, where a broader Th1 and CTL response was observed both in mice and nonhuman primates [9]. TLR7 stimulation as local treatment has also been investigated for can-

cer immunotherapy. For example, treatment of tumors in mice with the synthetic agonist MEDI9197 was shown to induce pro-inflammatory cytokines such as IL-12, IFNα and IFNγ, and to activate local innate cells to promote Th1 polarization as well as activation of natural killer and CD8 T cells [10]. The same was reported for the hydroxy-adenine analogue R848 in pancreatic cancer [11].

During infections, pathogens cause the simultaneous triggering of multiple TLR receptors which results in the fine-tuning of the most appropriate immune response. Therefore, the combination of different TLR ligands in cancer vaccines could synergize and potentiate the T cell responses by skewing them towards the most fitting response for tumor clearance. The previous pre-clinical studies with Pam demonstrated enhanced efficacy of the vaccine conjugate compared to the simple mixture of ligand and peptide, however a portion of the animals still failed to clear tumor [2]. To improve this effect, we synthetized a new conjugate bearing both Pam_3CysSK_4 and the TLR7 agonist 2-butoxy-8-hydroxyadenine, with the hypothesis that integration of the signaling from the two TLRs could further skew the immune response induced towards a more efficient anti-tumor T cell immune response.

RESULTS

We previously described that conjugation of either a CD8 or CD4 T cell epitope to the TLR2 ligand Pam_3CysSK_4 led to enhanced priming of T cell responses. We first investigated how the conjugation of the TLR7 agonist to synthetic long peptides containing either the CD8 and CD4 epitopes of ovalbumin (**Fig 1A**) affects the induction of CD8 and CD4 responses *in vivo*, and how they compare to the Pam_3CysSK_4 conjugates. The two sets of conjugates, or their respective components mixed, were injected at equimolar doses in a prime and boost setting (**Fig.1B**). The induction of CD8 responses specific for the ovalbumin epitope SIINFEKL was monitored over time in blood. The Pam_3CysSK_4 conjugates induce significantly higher SIINFEKL-specific CD8 responses compared to an equimolar mixture of the components (**Fig 1C**, left panel), as previously described [2]. Conjugation of the TLR7 agonist 2-butoxy-8-hydroxyadenine (hydroxy-adenine) to the peptides also results in higher induction of specific CD8 responses compared to the mixture (**Fig 1C**, right panel), confirming a beneficial effect of conjugation *in vivo* also for this ligand. At equimolar doses, the Pam conjugates induce a higher frequency of SIINFEKL-specific CD8 responses (around 1% of total CD8 T cells) compared to hydroxy-adenine (0.5% of total CD8). These responses were

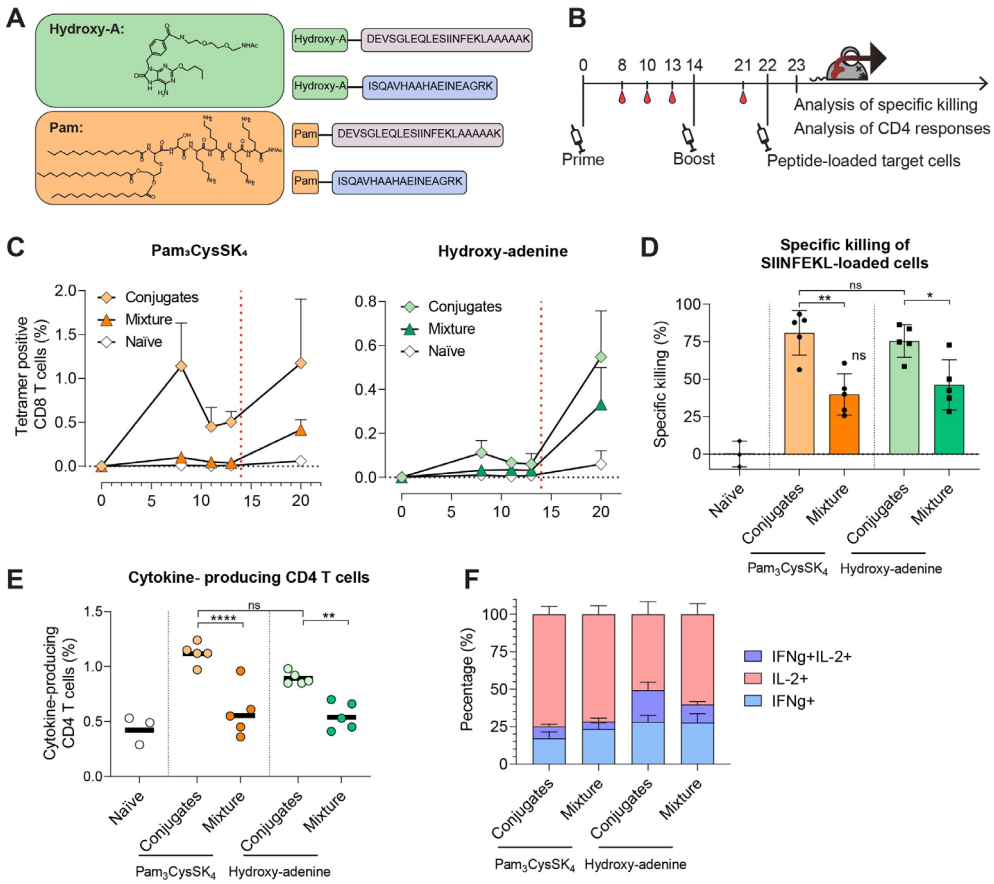

Figure 1: Enhanced CD8 and CD4 T cell priming by Pam_3CysSK_4 or hydroxy-adenine conjugated peptides A Schematic representation of the ligands and peptides used for conjugation and the four conjugates synthetized. **B** Schematic representation of the vaccination experiment. Mice (n=5) were injected with 5 nmol of each conjugates or an equimolar mixture of peptides and ligand at day 0 and 14. At different time points, blood was withdrawn for monitoring the induction of SIINFEKL-specific CD8 responses. At day 22, animals were injected with labelled cells loaded with either SIINFEKL or an irrelevant peptide. Next day mice were sacrificed for analysis of specific killing and CD4 responses via intracellular cytokine staining. **C** Frequency of SIINFEKL-specific cells as measured in blood by tetramer staining at the indicated days. The red line indicates the booster injection (day 14). **D** Calculated specific killing of SIINFEKL-loaded target cells. Statistical significance was determined by one-way ANOVA followed by multiple comparison and Tukey correction. * $p<0.05$, ** $p<0.01$. **E** Frequency of the CD4 responses induced upon vaccination as detected by cytokine staining. Represented are the fraction of total cells producing IL-2, IFNγ or both cytokines. **F** Production of IFNγ, IL-2 or both IFNγ and IL-2 by OVA Help-specific CD4 T cells.

tested for their functionality by analyzing specific killing in an *in vivo* cytotoxicity assay with SIINFEKL-loaded target cells. The groups that were vaccinated with the Pam or the hydroxy-adenine conjugates displayed strong killing capacity (**Fig 1D**). Even though the levels of SIINFEKL-specific cells measured one day before the essay was half compared to the Pam conjugates group (**Fig 1C**), the hydroxy-adenine conjugate performed as effectively as the Pam conjugates in killing capacity. Notably, for both ligands, mice vaccinated with the mixture of the components display significantly lower killing capacity compared to their respective conjugates (**Fig 1D**).

The induction of CD4 OVA-specific Helper responses was analyzed by intracellular cytokine staining. Both conjugates with Pam_3CysSK_4 or hydroxy-adenine ligands induced significantly higher frequency of specific CD4 T cells compared to their respective mixtures (**Fig 1E**). The two adjuvants displayed differences in cytokine production. Pam-adjuvanted vaccines induced a majority (75%) of IL-2 producing cells, and only 25% of these responses were positive for IFNγ. In contrast, cells primed with the TLR7 agonist hydroxy-adenine display a higher production of IFNγ. In particular, in the conjugated group, the cells that produced IFNγ reached 50% of the total response. In summary, conjugation of a TLR7 agonist to a peptide results in enhanced priming of both CD8 and CD4 responses, similarly to what previously reported with other conjugated vaccines. Moreover, stimulation of TLR2 or TLR7 during priming results in differential cytokine production by CD4 T cells.

To explore how dual TLR triggering could affect T cell priming and functionality, we designed dual Pam_3CysSK_4-hydroxy-adenine conjugates and investigated whether the two TLR2 and TLR7 agonists synergize on a single peptide. Two conjugates were synthetized bearing the TLR7 ligand at the N-terminus and Pam_3CysSK_4 at the C-terminus of two synthetic long peptides containing either the CD8 or the CD4 epitope of ovalbumin (**Fig 2A**). First, the effect of the dual conjugation on ligand activity was tested *in vitro*. Dendritic cells were incubated with the compounds and analyzed for IL-12 production. As can be seen in **Fig 2B**, the dual conjugates induce increased production of IL-12 compared to the single Pam or hydroxy-adenine conjugates. The dual conjugates were subsequently compared to the mixture of the free ligands in their ability to induce DC maturation. Conjugation of the two TLR2 and TLR7 agonists to the same peptide is necessary to induce enhanced IL-12 production (**Fig 2C**). In fact, the mixture of the two ligands was not as efficient in inducing IL-12.

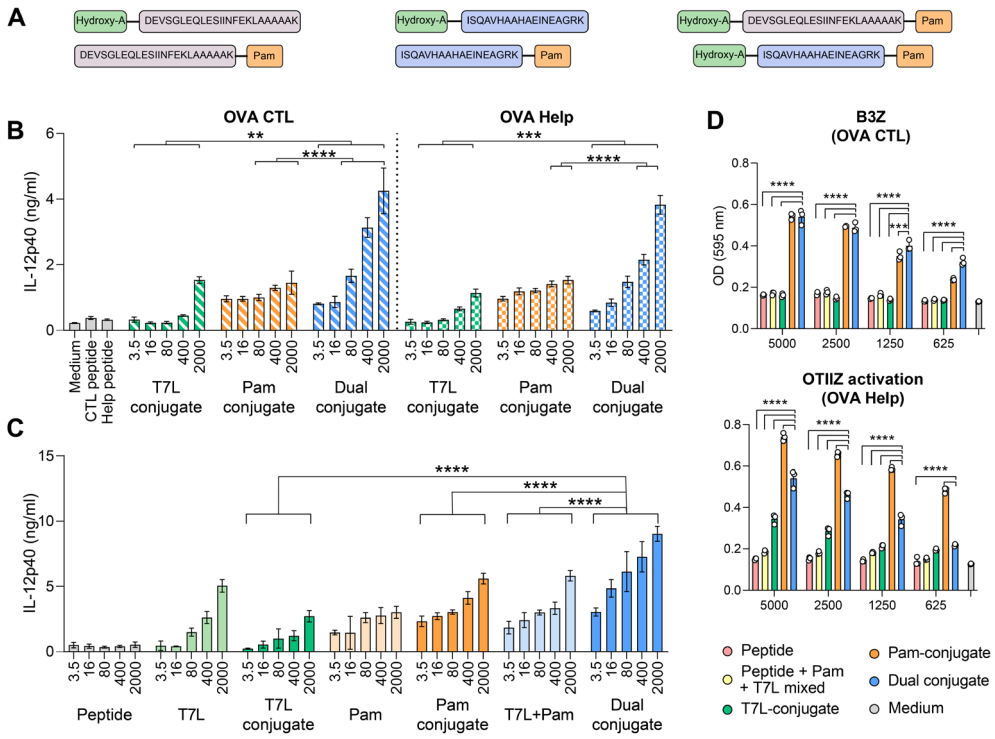

Figure 2: Immunological activity dual peptide conjugates bearing hydroxy-adenine and Pam3CysSk4 A Schematic representation of the conjugates synthetized. **B** IL-12 production upon overnight incubation of bone marrow-derived dendritic cells (BMDCs) with the indicated conjugates at varying concentrations. **C** Induction of IL-12 in BMDCs by the free TLR ligands or by ligands conjugated to the OVA CTL peptide. **D** Antigen presentation in MHC class I or class II of the conjugates to B3Z and OTIIZ hybridoma T cells, respectively. Activation of the two reported cell lines was detected by colorimetric reaction of CPRG by beta-galactosidase and measurement of absorbance at 595nm. Statistical significance was determined by two-way ANOVA followed by multiple comparison and Dunnet correction. *** $p<0.001$, **** $p<0.0001$

Secondly, MHC class I and II antigen presentation by the two dual conjugates were evaluated with the two reporter hybridoma T cell lines B3Z and OTIIZ, which are respectively specific for the CD8 and the CD4 epitopes of ovalbumin. Analysis of B3Z activation revealed that presentation of the CD8 epitope SIINFEKL was enhanced by the dual conjugate compared to free peptide and the hydroxy-adenine conjugate, in a similar fashion to the Pam_3CysSK_4 mono conjugate (**Fig 2D**).

MHC class II presentation of the Helper epitope and consequent OTIIZ activation were instead slightly lower in the dual conjugate compared to the Pam conjugate, while the hydroxy-adenine mono conjugate was not as efficient. Nevertheless, the Helper epitope in the dual conjugate was still presented more

efficiently compared to free peptide. Overall, these data indicate that the dual Pam_3CysSK_4-hydroxy-adenine conjugates exhibit robust immunological activity *in vitro*. In particular, the dual conjugates induce increased IL-12p40 cytokine production by DCs, as well as increased uptake and presentation of the epitopes compared to unconjugated peptide.

Next, the ability of the dual conjugates to prime CD8 or CD4 T cells *in vivo* was evaluated. The dual conjugates, or the corresponding mono conjugates, were injected in mice intradermally at the tail base. The lymph nodes were collected 7 days later for *ex vivo* expansion followed by analysis of the primed CD8 and CD4 responses by intracellular cytokine staining (**Fig 3A**). As previously observed, the conjugate bearing the TLR7 agonist hydroxy-adenine was less strong than the Pam3CysSk4 conjugate at inducing antigen-specific CTL responses (**Fig 3A**). The dual CTL conjugate induced high levels of CD8 specific T cell responses (**Fig. 3B**), which was higher than the hydroxy-adenine mono conjugate, and comparable to the Pam_3CysSK_4 mono conjugate. In addition, the mixture of the two ligands and the peptide also displayed high levels of specific CD8 responses. When looking at the polyfunctionality of these responses, all groups display a majority of IFNγ/TNFα double producing CD8 T cells (**Fig. 3C**). Of notice, compared to both mono conjugates and the mixture, the dual conjugate displays the highest proportion of double positive cells. As for the CD4 responses, the Pam_3CysSK_4 mono conjugate induces the highest amounts of CD4 T cell responses (**Fig. 3D**), followed by the dual conjugate, the hydroxy-adenine conjugate and the mixture. When characterizing the different cytokines produced by these responses, the hydroxy-adenine conjugate promotes, as a classical Th1 inducer, a majority of $CD40L^+/IFN\gamma^+$ and $CD40L^+/IFN\gamma^+/IL\text{-}2^+$ cells, while production of IFNγ was lower in cells primed by the Pam conjugate. Overall, the dual conjugate induces a higher portion of $CD40L^+/IL\text{-}2^+$ CD4 T cells compared to the two mono conjugates. Moreover, a significant portion of cells in the different vaccination groups is $CD40L^+$ but does not produce any of the cytokines analyzed.

To summarize, these results indicate that the dual conjugates synthetized are immunologically active and capable of inducing T cell responses *in vivo*. We re port optimal CD8 T cell induction by the dual conjugates, with enhanced IFNγ/TNFα double production by the dual conjugate compared to the two mono conjugates. As for CD4 induction, we report a differential cytokine profile based on the presence of the TLR7 or TLR2 agonists.

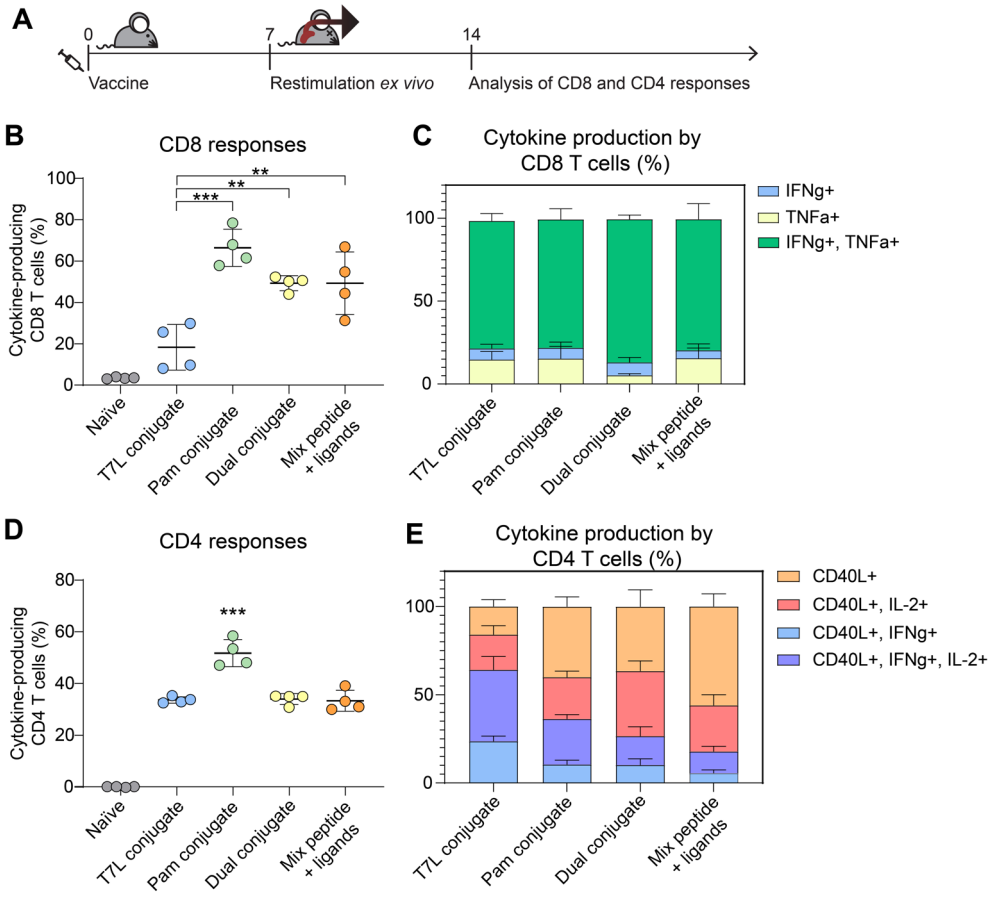

Figure 3: Effective priming of antigen-specific CD8 and CD4 T cells by the dual conjugates A Schematic representation of the experiment. Mice (n=4) were injected with 5 nmol of either the mono conjugates, the dual conjugates or a mix of peptide and ligands bearing either the OVA CTL or OVA Help peptide. One week later, splenocytes were isolated and expanded *ex vivo* with peptide-loaded dendritic cells (with no adjuvant included). After one week, CD8 and CD4 responses specific for the OVA peptides were analyzed via intracellular cytokine staining. **B** Frequency of CD8 T cell vaccine-specific responses represented as the total of cytokine producing cells in response to OVA CTL peptide. **C** Fraction of CD8 T cells producing IL-2, IFNγ, or both cytokines within the cytokine-producing CD8 T cells. **D** Frequency of CD4 T cell vaccine-specific responses represented as the total of cytokine producing cells in response to OVA Help peptide. **E** Fraction of CD4 T cells producing CD40L, IL-2, IFNγ, or more than one of these cytokines within the cytokine-producing CD4 T cells. Statistical significance was determined by two-way ANOVA followed by multiple comparison and Dunnet correction. *** $p<0.001$, **** $p<0.0001$

DISCUSSION

In this work, we explore the design of a peptide conjugate that combines two distinct TLR agonists in a single vaccine molecule. Differential TLR signaling can influence both the innate and the adaptive system towards the most optimal type of response to clear a given pathogen. The analysis of the mono conjugates shows that the two ligands have different effects. On one side, the amplitude of the CD8 responses is larger for the TLR2 ligand, (**Fig 1**) suggesting that Pam_3CysSK_4 is more potent than hydroxy-adenine. On the other side, despite the lower frequency of CD8 responses induced by hydroxy-adenine, both conjugates achieve high killing of antigen-specific cells, showing the strength of the TLR7 pathway. As for CD4 responses, both conjugates enhance the amount of specific T cells induced, but the two ligands induce a differential cytokine skewing. IFNγ induction by the TLR7 agonist is in line with the anti-viral role that this receptor has, while Pam_3CysSK_4 promotes higher IL-2 production. Besides the different cytokine skewing, these data evidence how conjugation represents a superior vaccine formulation compared to the classical delivery of adjuvant next to the antigen. The mechanism by which this happens may vary based on the adjuvant. For example, conjugation of Pam was described to enhance *in vitro* and *in vivo* uptake by DCs [1]. This effect was not dependent on TLR2 but on unidentified endocytosis pathways, most likely mediated by a scavenger receptor present on DCs. The same was observed for a TLR9 ligand. Instead, conjugation of a TLR7/8 agonist to protein antigen did not mediate increased uptake, however the conjugated vaccine was shown to activate and enter the cross-presentation pathway within DCs [12]. As reported by Oh and colleagues, unconjugated antigen was endocytosed but was unable of being presented. Antigen presentation could be induced by the TLR7/8 conjugate in multiple DC subsets and was directly dependent on type I interferons, which also promoted DC recruitment and accumulation in the lymph nodes [13, 14]. IL-12 was also found to be indispensable for T cell priming for this conjugate, however this cytokine acted on T cells and did not regulate any DC function [13].

Combination of the two ligands onto a single molecule enhances the maturating properties of the vaccine while not hampering the processing and presentation properties of the conjugated peptides (**Fig.2**). Vaccination with the dual conjugate *in vivo* induces effective priming of CD8 and CD4 T cell responses (**Fig. 3**). Given the limited number of cytokines analyzed, it was not possible to in detail characterize the functional phenotype of the CD8 and CD4 T cells induced by the dual conjugate versus the mono conjugates, however inclusion of more

cytokines could further elucidate the type of response promoted. In a study using human monocyte-derived DCs, TLR2 signaling was combined with TLR7/8 agonists [15]. Interestingly, it was reported that TLR2 interfered with the type I interferon amplification loop initiated by TLR7/8 stimulation, which resulted in the inhibition of the production of the Th1-promoting cytokine IL-12p70, formed by the heterodimer of the p40 and p35 subunits. The result was the skewing towards a Th2 and Th17 phenotype. We detected increased production of IL-12p40, which is a subunit of both IL-12p70 and IL-23. The latter one is involved in Th17 skewing; therefore, it should be determined whether in our setting the synergy between TLR2 and TLR7 also results in Th17 promotion. In contrast, an adjuvant incorporating covalently linked TLR2 and TLR7 agonists have been reported to synergize in promoting poly-functional CTL responses and balanced Th1/Th2 responses [16].

TLR synergism may be influenced by the type of cells targeted and their activation status. For example, it was reported that TLR2 stimulation induced both pro-inflammatory cytokines and type I interferons in monocytes, however the production of type I interferons was abolished upon differentiation into macrophages [17]. This underlines that responsiveness to the ligands themselves may vary from cell type and differentiation status. Therefore, it will be useful to determine in our immune system which cells are the recipients of the conjugates and how the two pathways interact within these cells. Finally, it is yet to be established how these responses will deal with different type of pathogens or malignancies.

In conclusion, we have developed a novel dual TLR ligand-peptide conjugate that simultaneously triggers TLR2 and TLR7. The dual conjugates display immunological activity and proper CD8 and CD4 T cell priming. Further characterization of the conjugates and their performance in immune control will determine whether this approach will potentiate peptide-based vaccines.

MATERIAL AND METHODS

Peptide synthesis. Ovalbumin-derived antigenic peptides DEVSGLEQLESIINFEKLAAAAAK and ISQAVHAAHAEINEAGRK were assembled using solid-phase peptide synthesis that was performed on a TRIBUTE® Peptide Synthesiser (Gyros Protein Technologies AB, Arizona, USA) starting with Tentagel S-RAM resin (0.22-0.25 mmol/g) on a 100 µmol scale using established Fmoc protocols [7]. The C-terminal lysine residue of the peptides was side-chain protected with a very TFA-sensitive 4-monomethoxytrityl (MMT) protective group to enable the selective installation of a second ligand. Using established protocols1-2, the first

TLR-ligand, either TLR-2 or TLR-7, was attached to the N-terminus of the peptides via an amide bond. Subsequently, the MMT protecting group was selectively removed by exposing the resin to a solution of 1% TFA in DCM 10 times for 30 seconds and 2 times for 5 minutes. The resin was six times washed with DCM, dried under a N2 flow, and the second TLR-ligand (either for TLR-7 or TLR-2) was coupled to the thus liberated amine of the lysine side chain using an amide bond forming reaction. Conjugates and peptides were deprotected and cleaved by shaking the resin with a mixture of 95:2.5:2.5 TFA:H2O:TIS for 105 minutes in a plastic syringe fitted with a filter and purified with RP HPLC.

Cell culture. Bone marrow-derived dendritic cells were differentiated from bone marrow stem cells that were harvested from the femurus and tibia of C57BL/6 mice and cultured in IMDM (Lonza) supplemented with FCS (Greiner) , Glutamax (Gibco), penicillin (Gibco), β-mercaptoethanol (Merck) and R1 supernatant. R1 supernatant was obtained by culturing NIH3T3 fibroblasts transfected with GM-CSF. The B3Z and OTIIZ cell lines were cultured in IMDM medium (Lonza supplemented with 8% FCS (Greiner), penicillin and streptomycin, glutamine (Gibco) β-mercaptoethanol (Merck), and hygromycin B (AG Scientific Inc, San Diego, CA, USA) to maintain expression of the beta-galactosidase reporter gene.

In vitro DC maturation assay. The test compounds were dissolved in DMSO at a concentration of 1 mM and sonicated in water bath for 15 minutes. Murine bone marrow-derived dendritic cells were seeded in 96-well plates at a density of 50.000 cells/well and incubated with titrated amounts of compounds. After 3 hours of incubation, the cells were washed once and incubated with fresh medium. After 16 hours, supernatant was harvested for ELISA analysis (Biolegend) to measure the amount of produced IL-12p40.

In vitro antigen presentation assay. The test compounds were dissolved in DMSO at a concentration of 1 mM and sonicated in water bath for 15 minutes. 50.000 D1 cells were seeded in 96-well flat bottom plates and incubated with the indicated test compounds. After 2 hours 50.000 B3Z or OTIIZ were added per well and incubated with the D1 cells overnight. The following day, B3Z or OTIIZ activation was detected by measurement of absorbance at 595 nm upon color conversion of chlorophenol red-β-D-galactopyranoside (Calbiochem) the reporter enzyme.

Mice. Female C57BL/6 mice were purchased from Charles River Laboratories. Congenic CD45.1^{+} C57BL/6 mice were bred at the Leiden University medical Centre animal facility. All animal experiments were in accordance with the Dutch

national regulations and received ethical and technical approval by the local Animal Welfare Body.

Immunization of mice and in vivo specific killing. 6-8 weeks old C57BL/6 female mice were injected intradermally at the tail base with 5 nmol of Pam_3CysSK_4 or hydroxy-adenine conjugates or an equimolar mix of peptides and ligands. Fourteen days later, the animals were boosted with the same vaccine formulations. At different time points during the experiments, 20 µl of blood were collected from the tail vein for detection of SIINFEKL-specific T cell responses via SIINFEKL-H2-Kb tetramer staining. At the end of the experiments, spleens were removed and processed in single cell suspensions for *ex vivo* analysis. Splenocytes were incubated for 5 hours with peptide-loaded DCs in the presence of Brefeldin A, to block cytokine exocytosis. Afterwards, samples cells were stained for surface markers and intracellularly for IL-2, IFNγ and TNFα. For analysis of *in vivo* cytotoxicity, splenocytes were harvested from $CD45.1^+$ C57BL/6 naïve mice, processed into single cell suspension and labelled with either 5 or 0.005 µM CFSE for 10 min at 37°C. Cells that were labelled with 0.005 µM CFSE (CFSE low) were loaded for 1 hour at 37°C with 1µM SIINFEKL peptide, while cells that were labelled with 5 µM CFSE (CFSE high) were loaded in the same conditions with an irrelevant epitope derived from the E6 protein of Human Papilloma Virus (sequence: RAHYNIVTF). 1'000'000 splenocytes per peptide-loaded group were injected intravenously in vaccinated or naïve mice. One day after transfer, mice were sacrificed and the spleens were harvested and processed into single cell suspensions. Splenocytes were subsequently stained with eFluor®450 anti-CD45.1 antibody (eBioscience, San Diego, USA) and analyzed by flow cytometry to detect $CD45.1^+/CFSE^+$ target cells. Specific killing was calculated according to the following equation: Specific killing = 100 - [100*((CFSE target peptide)/(CFSE irrelevant) immunized mice)/((CFSE target peptide)/(CFSE irrelevant) naïve mice)]

Immunization of mice and ex vivo expansion. 6-8 weeks old C57BL/6 female mice were injected intradermally at the tail base with 5 nmol of Pam_3CysSK_4 or hydroxy-adenine conjugates or the dual conjugates, or an equimolar mixture of peptide and ligand. Seven days later, lymph nodes were removed and processed in single cell suspensions and incubated with peptide-loaded BMDCs for 7 days. After 7 days, cells were incubated for 5 hours with peptide-loaded DCs in the presence of Brefeldin A, to block cytokine exocytosis. Afterwards, samples cells were stained for surface markers and intracellularly for IL-2, IFNγ and CD40L or TNFα.

REFERENCES

1. Khan, S., et al., Distinct uptake mechanisms but similar intracellular processing of two different toll-like receptor ligand-peptide conjugates in dendritic cells. J Biol Chem, 2007. 282(29): p. 21145-59.

2. Zom, G.G., et al., Efficient induction of antitumor immunity by synthetic toll-like receptor ligand-peptide conjugates. Cancer Immunol Res, 2014. 2(8): p. 756-64.

3. Reintjens, N.R.M., et al., Self-Adjuvanting Cancer Vaccines from Conjugation-Ready Lipid A Analogues and Synthetic Long Peptides. J Med Chem, 2020. 63(20): p. 11691-11706.

4. Zom, G.G., et al., Novel TLR2-binding adjuvant induces enhanced T cell responses and tumor eradication. J Immunother Cancer, 2018. 6(1): p. 146.

5. Willems, M.M., et al., N-tetradecylcarbamyl lipopeptides as novel agonists for Toll-like receptor 2. J Med Chem, 2014. 57(15): p. 6873-8.

6. Zom, G.G., et al., TLR2 ligand-synthetic long peptide conjugates effectively stimulate tumor-draining lymph node T cells of cervical cancer patients. Oncotarget, 2016. 7(41): p. 67087-67100.

7. Gential, G.P.P., et al., Peptides conjugated to 2-alkoxy-8-oxo-adenine as potential synthetic vaccines triggering TLR7. Bioorg Med Chem Lett, 2019. 29(11): p. 1340-1344.

8. Zhang, Z., et al., Structural Analysis Reveals that Toll-like Receptor 7 Is a Dual Receptor for Guanosine and Single-Stranded RNA. Immunity, 2016. 45(4): p. 737-748.

9. Wille-Reece, U., et al., Immunization with HIV-1 Gag protein conjugated to a TLR7/8 agonist results in the generation of HIV-1 Gag-specific Th1 and CD8+ T cell responses. J Immunol, 2005. 174(12): p. 7676-83.

10. Mullins, S.R., et al., Intratumoral immunotherapy with TLR7/8 agonist MEDI9197 modulates the tumor microenvironment leading to enhanced activity when combined with other immunotherapies. J Immunother Cancer, 2019. 7(1): p. 244.

11. Michaelis, K.A., et al., The TLR7/8 agonist R848 remodels tumor and host responses to promote survival in pancreatic cancer. Nat Commun, 2019. 10(1): p. 4682.

12. Oh, J.Z. and R.M. Kedl, The capacity to induce cross-presentation dictates the success of a TLR7 agonist-conjugate vaccine for eliciting cellular immunity. J Immunol, 2010. 185(8): p. 4602-8.

13. Oh, J.Z., et al., TLR7 enables cross-presentation by multiple dendritic cell subsets through a type I IFN-dependent pathway. Blood, 2011. 118(11): p. 3028-38.

14. Kastenmuller, K., et al., Protective T cell immunity in mice following protein-TLR7/8 agonist-conjugate immunization requires aggregation, type I IFN, and multiple DC subsets. J Clin Invest, 2011. 121(5): p. 1782-96.

15. Wenink, M.H., et al., TLR2 promotes Th2/Th17 responses via TLR4 and TLR7/8 by abrogating the type I IFN amplification loop. J Immunol, 2009. 183(11): p. 6960-70.

16. Gutjahr, A., et al., Cutting Edge: A Dual TLR2 and TLR7 Ligand Induces Highly Potent Humoral and Cell-Mediated Immune Responses. J Immunol, 2017. 198(11): p. 4205-4209.

17. Oosenbrug, T., et al., An alternative model for type I interferon induction downstream of human TLR2. J Biol Chem, 2020. 295(42): p. 14325-14342.

6

CATIONIC SYNTHETIC LONG PEPTIDES-LOADED NANOGELS: AN EFFICIENT THERAPEUTIC VACCINE FORMULATION FOR INDUCTION OF T-CELL RESPONSES

Kordalivand N*, Tondini E*, Lau CYJ, Vermonden T, Mastrobattista E, Hennink WE, Ossendorp F, Nostrum CFV

J Control Release. 2019; 315:114-125

*equal contribution

ABSTRACT

Recent studies have shown a high potency of protein-based vaccines for cell-mediated cancer immunotherapy. However, due to their poor cellular uptake, efficient immune responses with soluble protein antigens are often not observed. As a result of superior cellular uptake, nanogels loaded with antigenic peptides were investigated in this study as carrier systems for cancer immunotherapy. Different synthetic long peptides (SLPs) containing the CTL and $CD4^+$ T-helper (Help) epitopes were synthesized and covalently conjugated via disulfide bonds to the polymeric network of cationic dextran nanogels. Cationic nanogels with a size of 210 nm, positive zeta potential (+24 mV) and high peptide loading content (15%) showed triggered release of the loaded peptides under reducing conditions. An *in vitro* study demonstrated the capability of cationic nanogels to maturate dendritic cells (DCs). Importantly, covalently SLP-loaded nanogels adjuvanted with poly(I:C) showed superior $CD8^+$ T cell responses compared to soluble peptides and nanogel formulations with physically loaded peptides both *in vitro* and *in vivo*. In conclusion, covalently SLPs-loaded cationic nanogels are a promising system to provoke immune responses for therapeutic cancer vaccination.

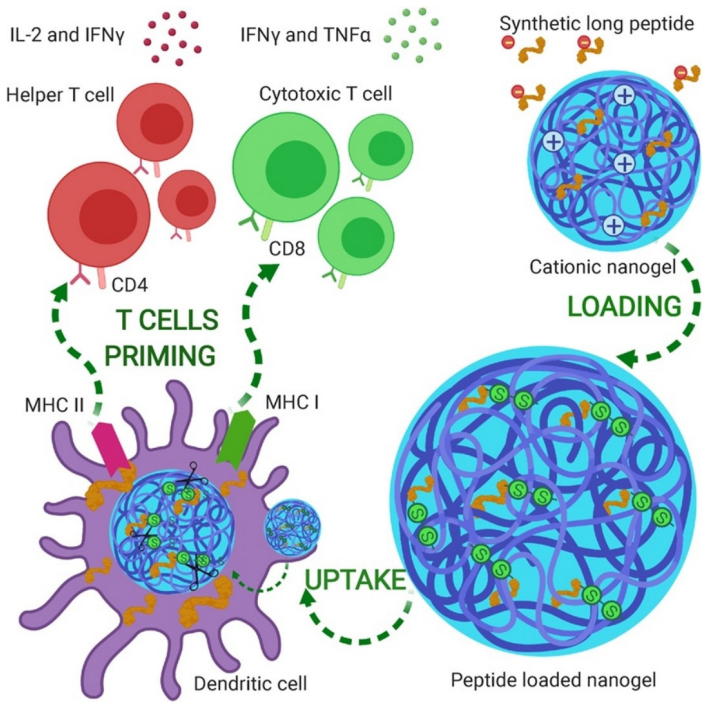

INTRODUCTION

Therapeutic vaccination has attracted much attention in recent years as a promising strategy for the treatment of different types of cancers. Stimulation of $CD8^+$ cytotoxic T lymphocytes (CTLs) and $CD4^+$ T- helper (Th) cells through MHC class I and class II pathways, respectively, is fundamental to induce effective antitumor responses [1-3]. Dendritic cells (DCs) as the most specialized antigen-presenting cells (APCs) play a crucial role in the activation of T-cell immune responses and subsequent tumor eradication [4-8]. Synthetic long peptides (SLPs) including CTL and Th epitopes were successful in clinical trials against several tumor types due to their remarkable ability to elicit a cellular immune response [9-11]. Despite superior characteristics compared to protein-based vaccines [12-13], SLPs have also important drawbacks including their susceptibility for enzymatic degradation, rapid clearance from the injection site and poor cellular uptake that limit their therapeutic efficacy [9-10, 14-15].

Different vehicles have been developed to formulate SLPs as well as other soluble antigens with the aim to improve their therapeutic effects [16-22]. Montanide, a water-in-oil emulsion-based vaccine formulation has been extensively used in clinical trials to deliver SLPs into DCs [23-25]. In 2011, a phase III clinical trial was conducted in patients with advanced melanoma. Three subcutaneous injections at 3 week intervals of Montanide-based vaccine (gp100209-217) showed significant improvement in response rates and progression-free survival compared to interleukin-2 treatment alone [26]. Oka et al. showed strong induction of antigen-specific $CD8^+$ CTL responses in patients immunized with WT-1-derived peptide vaccine in Montanide [27]. However, it was shown that due to T cell dysfunction and deletion resulting from the depot at the injection site, complete tumor eradication did not occur[28]. Therefore, due to the drawbacks of these emulsion formulations such as local adverse side effects at the site of injection, poor stability and non-controlled release kinetics, alternative delivery methods like particulate delivery systems have recently gained growing interest [29-31]. Self-assembling peptide-based systems are an alternative approach to enhance the cellular uptake of peptides and raise immunogenicity against peptide epitope vaccines [32]. Black et al. showed that self-assembled diC16-OVA provide effective *in vivo* protection from tumors by stimulating OVA-specific T-cells. By anchoring the hydrophobic tail into cell membranes, these nano-sized micelles improve the DCs uptake without TLR stimulation [33].

Moreover, it has been demonstrated that poly(lactic-*co*-glycolic acid) (PLGA)

nanoparticles can be used to encapsulate SLPs and provoke T-cell responses. By optimizing these nanoparticles regarding loading and release as well as size, Silva *et al.* showed an enhanced CD8+ T cell activation in vitro when compared to soluble peptides [34]. Hamdy et al. showed effective activation of T cells and induction of therapeutic antitumor effects in B16 melanoma tumors by co-encapsulating of $TRP2_{180-188}$ along with TLR ligand A into PLGA nanoparticles [35]. L-BLP25, a liposome-based vaccine showed strong survival rates in phase I and II trials in non-small cell lung cancer patients [36]. In a recent *in vivo* study, Varypataki *et al.* showed a remarkable capacity of cationic liposome formulation as an antigen delivery system [31] indicating that particulate systems are attractive candidates as SLP delivery platforms with clinical translation potential.

Among various nanoparticulate systems, nanogels have shown excellent properties as systems for the intracellular delivery of biopharmaceuticals including therapeutic antigens [38-42]. These nano-sized crosslinked networks are able to load biopharmaceuticals such as proteins and peptides and to protect them against undesirable (enzymatic) degradation [43-45]. Their properties can be tailored by varying the particle size, cross-link density and surface chemistry (PEGylation and targeting ligand decorations) [46-48]. The particle size and surface chemistry of nanogels largely influence their internalization by different cells. It has been shown that the uptake of relatively large particle (>1 µm) occurs by phagocytosis, whereas particles with a size between 500 nm - 1 µm are taken up via micropinocytosis [49]. Smaller particles (<100 nm) are internalized via clathrin-mediated or cavelae-mediated endocytosis. Further, positively charged nanogels are less cytocompatible than neutral or negatively charged particles [50]. Furthermore, the loaded biotherapeutics can be released from nanogels in a sustainable and controllable manner due to hydrolytic degradation of the network which in turn is dependent on the selected building blocks [51-52]. Importantly, triggered release of biotherapeutics from responsive nanogels can be acquired in response to biological stimuli (e.g. pH, enzymes and reducing agents) [42, 53-57]. Zhong et al. showed that 95% of cytochrome C loaded in reduction sensitive nanogels was released under reductive conditions. These nanogels loaded with this protein showed more cytotoxic effects against tumor cells compared to free cytochrome C [58]. Tang et al. developed enzyme responsive nanogels in which a polymeric shell composed of peptide crosslinker was formed by free radical polymerization on the surface of the protein. The entrapped protein can be released upon recognition and cleavage of the peptide crosslinker by furin, a peptidase present

in the Golgi apparat [59]. These features make nanogels attractive systems for antigen/vaccine delivery. In a recent study, Li *et al.* showed strong *in vivo* antitumor responses elicited by ovalbumin protein-loaded in nanogels. The strong features in that study were that the ovalbumin as a model antigen was very conveniently loaded into the pre-fabricated nanogels by electrostatic interactions, that the ovalbumin could subsequently be fixed into the nanogel by formation of a covalent disulfide bond between the protein and the nanogel network, and the protein was released by disulfide reduction in the lysosomes after internalization of the nanogels by dendritic cells. It was shown that these ovalbumin loaded cationic nanogels provoked robust antigen specific T-cell responses resulting in high percentage (40%) of regression of established tumor and substantial delay in tumor progression *in vivo* [60]. Therefore, these cationic nanogels are a potentially interesting delivery system for SLPs for cancer immunotherapy. Moreover, these nanogels have attractive advantages compared to other particulate systems in terms of loading of sensitive peptides during the manufacturing process. The peptides are loaded into the nanogels after particle formations (post-loading) which avoids possible unwanted modifications and aggregation of the peptides under harsh process conditions, e.g. the use of organic solvents and high shear forces, applied for the preparation of polymeric nanoparticles based on aliphatic polyesters of the PLGA/PLLA family of polymers.

In the present study, we explored the potency of SLP-loaded nanogels for the induction of T-cell responses. For that purpose, four SLPs covering $CD8^+$ and $CD4^+$ epitopes were synthesized and loaded both physically and chemically in cationic dextran-based nanogels. The formulated nanogels were characterized for size, zeta-potential and release profile *in vitro*. The capability of SLP loaded nanogels in priming antigen-specific T-cells was assessed *in vitro*. Finally, an *in vivo* study in mice was conducted to evaluate the antitumor immune response of these antigen-loaded nanogels.

RESULTS AND DISCUSSION

Peptide synthesis and characterization

Four peptides (CTL, Help, Cys-CTL and Cys-Help) were synthesized by solid-phase peptide synthesis (**Table 1**). The synthesized peptides were purified by Prep-HPLC to at least 90% purity and the obtained yields for the different peptides were approx. 40%. The UPLC chromatograms of the synthesized and purified peptides are shown in **Figure 1**. Mass spectroscopic analysis (**Figure 2**) showed that the main peaks eluting at approximately 5 min (**Figure 1A**), 9 min (Figure

1B), 13 min (**Figure 1C**) and 10 min (**Figure 1D**) correspond to CTL SLP, Cys-CTL SLP, Help SLP and Cys-Help SLP, respectively. To explain, MS analysis showed the $[M+2H]^{2+}$ of the main peaks at m/z 1317.7, 1369.3, 1232.1 and 1283.6 which are attributed to the masses of CTL SLP, Cys-CTL SLP, Help SLP and Cys-Help, respectively. In the MS experiment, DTT was added to the samples before analysis. Therefore no peaks attributed to the dimeric structures were observed, whereas when the samples were not treated with DDT, extra peaks were present in the chromatograms of Cys-CTL and Cys-Help (**Figure 1**) that according to MS correspond with the dimeric peptides formed due to the disulfide formation between the cysteine moieties. As listed in Table 1, the molecular masses of the different synthesized peptides measured by MS are similar to the theoretical values demonstrating that the aimed peptides were indeed obtained.

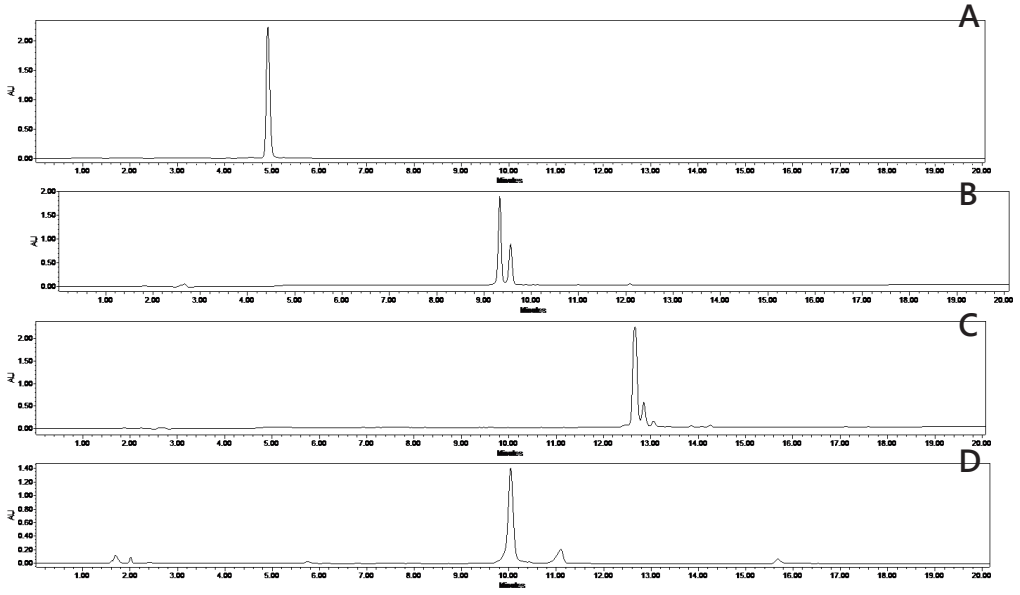

Figure 1. UPLC chromatograms of SLPs. A) Help, B) Cys-Help, C) CTL, D) Cys-CTL

Preparation and characterization of nanogel formulations

It has been shown that small nanoparticles (~200 nm) can be internalized by antigen presenting cells (APCs) and have a better ability to promote CD8+ T-cell immunity, which is crucial for immunotherapy of cancer [49-50]. Moreover, positively charged nanoparticles show the highest uptake by DCs. Therefore, in the present study, we were aiming to have a high loading and preferable particles that after loading still have a positive zeta-potential to allow uptake by DCs [71].

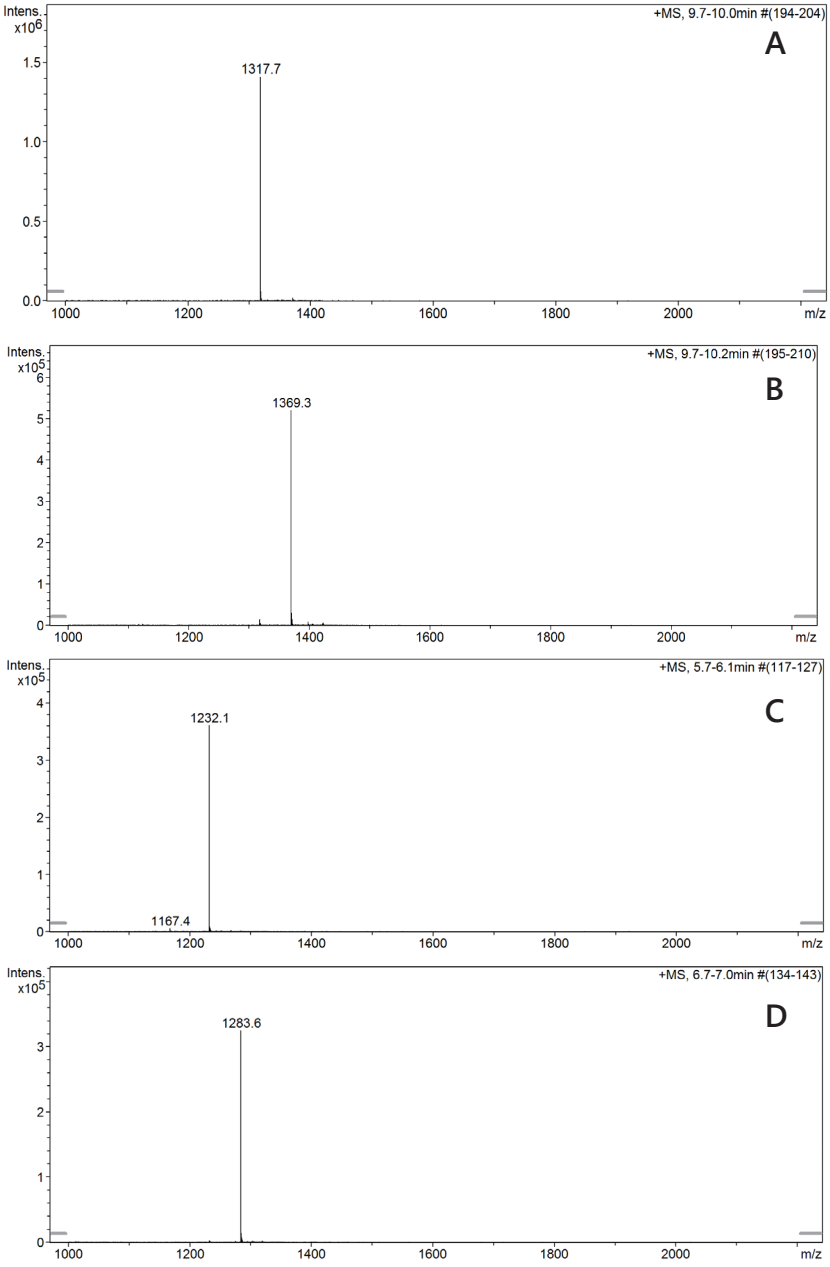

Figure 2. MS spectra of SLPs obtained via Fmoc solid phase peptide synthesis. A) CTL, B) Help, C) Cys-CTL, D) Cys-Help

Table 1. Characteristics of the synthesized peptides used in this study.

Peptide name	Peptide Sequence	Calculated molecular mass (g/mol)	Observed $[M+2H]^{2+}$ (g/mol)	Molecular mass (g/mol)*	Isoelectric point (PI) ***
CTL	NH_2-DEWSGLEQLESIIN-FEKLAAAAAK-COOH	2633.9	1317.7	2633.4	3.9
** Cys-CTL	NH_2-CDEWSGLEQLESI-INFEKLAAAAAK-COOH	2737.1	1369.3	2736.6	3.9
Help	NH_2-DEWEISQAVHAA-HAEINEAGRE-COOH	2462.6	1232.1	2462.2	4.1
** Cys-Help	NH_2-CDEWEISQAVHAA-HAEINEAGRE-COOH	2565.7	1283.6	2565.2	4.1

*Determined by mass spectroscopy (ESI)

** Cysteine residue is located at the N-terminus of the peptide

*** Determined theoretically using an Innovagen peptide calculator program[70]

Following the inverse mini-emulsion technique [44, 57,] cationic dextran nanogels were obtained by exposing an emulsion of a dispersed water phase containing soluble polymer (dextran methacrylate) and monomers (TMAEMA, linker) in a continuous oil phase to UV irradiation, which resulted in photopolymerization of the methacrylate units. The average size of obtained empty nanogels was 207 nm and the nanogels showed positive zeta potential (+24.7 mV) which can be explained by copolymerization of TMAEMA monomers in the dextran network. After washing and freeze-drying, the photo-crosslinked nanogels were loaded both physically and covalently with the SLPs (CTL and Help) and Cys-SLPs (CTL and Help), respectively. The negatively charged peptides (pI values ~4, table 1) were absorbed into the cationic particles via electrostatic interactions, while the peptides containing a cysteine amino acid residue were additionally linked to the methacrylamide-disulfide linker that was present in the nanogels (Scheme 1). As shown in Table 2, the nanogels were physically loaded with a high efficiency with both peptides (CTL and Help) in a buffer of HEPES with low ionic strength (20 mm, pH 7.4). This demonstrates the capability of cationic nanogels for absorbing oppositely charged peptides exploiting electrostatic interactions as a driving force for the loading process. The obtained peptide-loaded nanogels were positively charged (zeta potential: +21-24 mV) and had an average size of about 210 nm and narrow size distribution (PDI <0.03).

The zeta potential of the nanogels slightly dropped from +24.7 to +22.6 mV and +24.6 mV for covalent CTL and Help, respectively, which is in agreement with a previous study where OVA was loaded into cationic nanogels[57]. This also

excludes that the peptides are adsorbed on the surface of the particles since then a negative zeta potential will be measured. Thus, the loading of the peptides had not affected the characteristics (size, charge) of the nanogels.

Table 3 shows that the CTL SLP was released from the nanogels in buffer of pH 7.4 containing 150 mM NaCl, indicating that under these high ionic strength conditions the electrostatic interactions between the polymer matrix and the absorbed peptides were broken. In contrast to CTL SLP, the Help SLP was not released in buffer of neutral pH and 150 mM NaCl. However, in a buffer of lower pH (150 mM NaCL, pH 4) the loaded peptide was quantitatively released in 2 hours demonstrating the pH-dependent release property of this peptide (Table 3). Importantly, nanogels loaded with both Cys-CTL and Cys-Help showed high loading even after two washings using the high ionic strength buffer (150 mM, pH 7 and 150 mM, pH 4 for CTL and Help, respectively, Table 2) demonstrating that these peptides were indeed immobilized/covalently linked to the nanogel network by thiol-disulfide exchange reaction as observed previously for thiolated ovalbumin and thiolated RNase [42, 57].

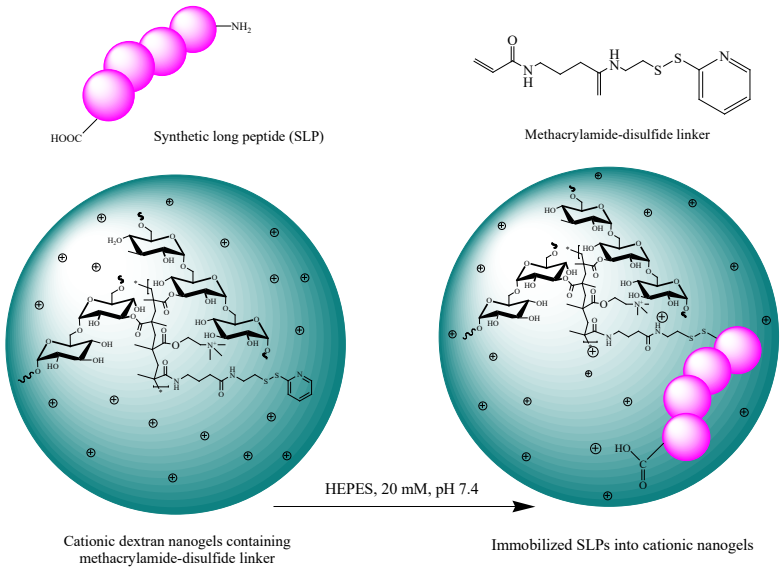

Scheme 1. Schematic representation of the cationic dextran nanogels containing *N*-(4-(2-(pyridine-2-yldisulfanyl)ethyl)-amidobutyl) methacrylamide as linker (left), and SLP loaded nanogels (right).

Table 2. Characteristics of SLP-loaded dex-MA-*co*-TMAEMA nanogels. Mean values with corresponding standard deviations of three independently prepared batches are shown.

Dex-MA-co-TMAEMA nanogels	Z_{ave} (nm)	ζ-potential (mV)	Loading efficiency [a] (%)	Loading content [b] (%)
Empty nanogels	207±3	+24.7±0.8	NA	NA
Non-covalent CTL-loaded nanogels	210±6	+23.0±0.9	100	15.0±0.0
Non-covalent Help-loaded nanogels	212±3	+24.3±1.0	100	15.0±0.0
Covalent CTL-loaded nanogels [c]	206±5	+22.6±0.3	86.7±0.5	13.7±0.1
Covalent Help-loaded nanogels [d]	215±2	+24.6±0.7	95.8±0.5	14.5±0.1

[a] Loaded peptide in nanogels/feed peptide weight x 100%

[b] Loaded peptide/dry peptide-loaded nanogels weight x 100%

[c] After washing with high ionic strength buffer of pH 7.4

[d] After washing with high ionic strength buffer of pH 4.0

Table 3. Percentage of released non-covalently bound peptides from nanogels in low and high ionic strength buffer of different pH. Mean values with corresponding standard deviations of three independently prepared batches are shown.

Samples	Released in HEPES 20 mM pH 7.4 (%)	Released in PBS 150 mM pH 7.4 (%)	Released in PBS 150 mM pH 4.0 (%)
Non-covalent CTL-loaded nanogels	0.0	98.7±7.7	NA
Non-covalent Help-loaded nanogels	0.0	0.0	95.5±3.9

To prove the triggered release of covalently linked peptides from cationic nanogels in reducing condition, CTL peptide and HELP peptide formulations were incubated in buffer containing glutathione as reducing agent. Figure 3 shows that upon addition of glutathione, triggered-release of peptides was observed (80% for Help SLP loaded nanogels and 100% for CTL SLP loaded nanogels) within 1 hour, revealing that the formed disulfide bonds between the linker present in the nanogels and cysteine groups of the N-terminus of the peptide were cleaved un-

der these reducing conditions which lead to release of peptides from the nanogels. This rapid triggered release from reduction-sensitive dextran nanogels is in line with our previous studies where proteins (ovalbumin or RNase A) were reversibly immobilized into cationic and anionic nanogels, respectively, via the same reducible linker [42, 57]. This release pattern results attractive for vaccination as the loaded peptides can be kept protected extracellularly and only released upon internalization due to the exposure to the endosomal reductive environment.

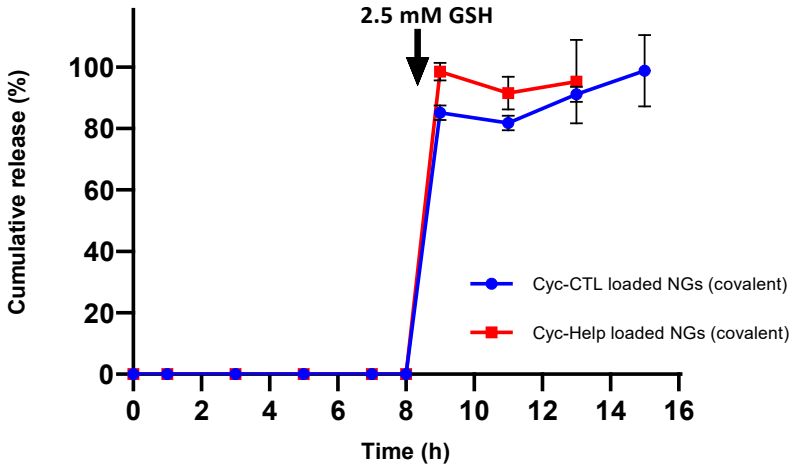

Figure 3. Release of Cys-Help and Cys-CTL from dex-MA-co-TMAEMA nanogels in PBS pH 4.0 and pH 7.4 at 37 C respectively; glutathione was added (2.5 mM final concentration) at 8 h. Data are shown as mean ± SD (n = 3).

Cytotoxicity and DC maturation

To determine the cytotoxicity of the different nanogel formulations, D1 dendritic cells were stimulated for 24 h at different concentrations of the free peptides as well as formulated in nanogels and cell viability and dendritic cell maturation were evaluated. Figure 4 shows that both peptides in their free form at the highest concentration tested (25 g/mL) exhibited excellent cytocompatibility for D1 cells (viability > 95%). The nanogels (concentrations ranging from 2.7 to 175 g/mL were well-tolerated by DCs, which is in agreement with our previous studies 50. However, at increasing concentrations (25 g/mL of peptide, 175 g/mL of nanogels) some toxicity was observed for covalent HELP peptide loaded nanogels (viability 80%) and both CTL peptide formulations (viability 80%).

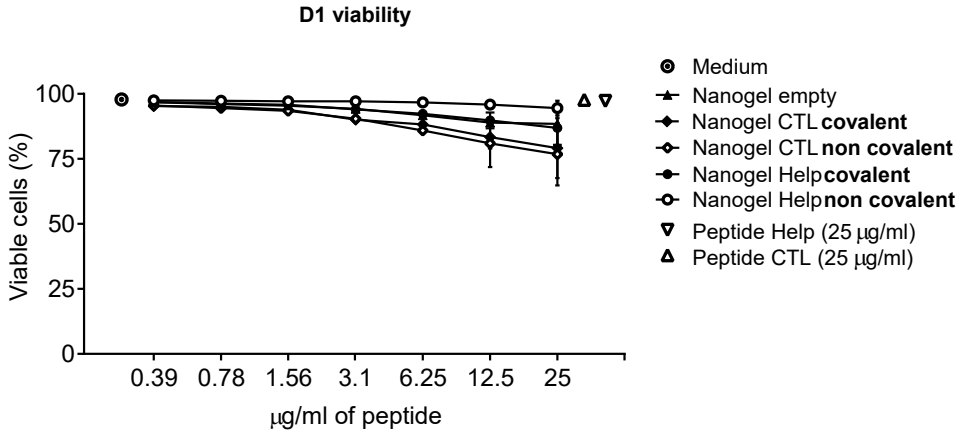

Figure 4. The viability of D1 cells, incubated for 24 h with free peptides (CTL and Help), non-covalent and covalent CTL peptide-loaded nanogels, non-covalent and covalent Help peptide-loaded nanogels. The colorimetric reading at 490 nm of nontreated cells were set at 100%; the data are shown as mean ± SD (n = 3).

Dendritic cells are susceptible to exogenous stimuli and can undergo maturation upon the encounter of foreign substances. This process leads to the upregulation of costimulatory molecules that in turn will enhance T cell activation. The ability of the nanogels to induce DC maturation was assessed by measuring the expression of the two costimulatory molecules, $CD40^+$ and $CD86^+$ (Figure 5)[72]. As expected, incubation of immature cells with LPS, as a positive control, resulted in increased $CD40^+$ and $CD86^+$ expression. There were no marked effects on DCs maturation in the presence of the free peptides (CTL and Help) while all nanogel formulations caused the up-regulation of co-stimulatory molecules ($CD40^+$ and $CD86^+$) in a concentration dependent manner. These data are in line with previous studies in which it was reported that positively charged particles are able to induce the maturation of DCs [73]. Maturation of DCs has a vital role in efficient DC-T cell interaction and of antigen-specific immune response initiation [20, 74].

In vitro antigen presentation

An essential step in the induction of a T cell response is the presentation of the epitopes on MHC I or MHC II molecules. The ability of dendritic cells to process and present the peptide upon nanogel-mediated uptake was investigated *in vitro* with the B3Z and OTIIZ T cell hybridoma reporter cell lines, which are specific respectively for the CTL and helper epitopes of OVA. Immature dendritic cells were pulsed for two hours with the free peptide or the different nanogels formulations and subsequently incubated with B3Z or OT IIZ cells for 24h.

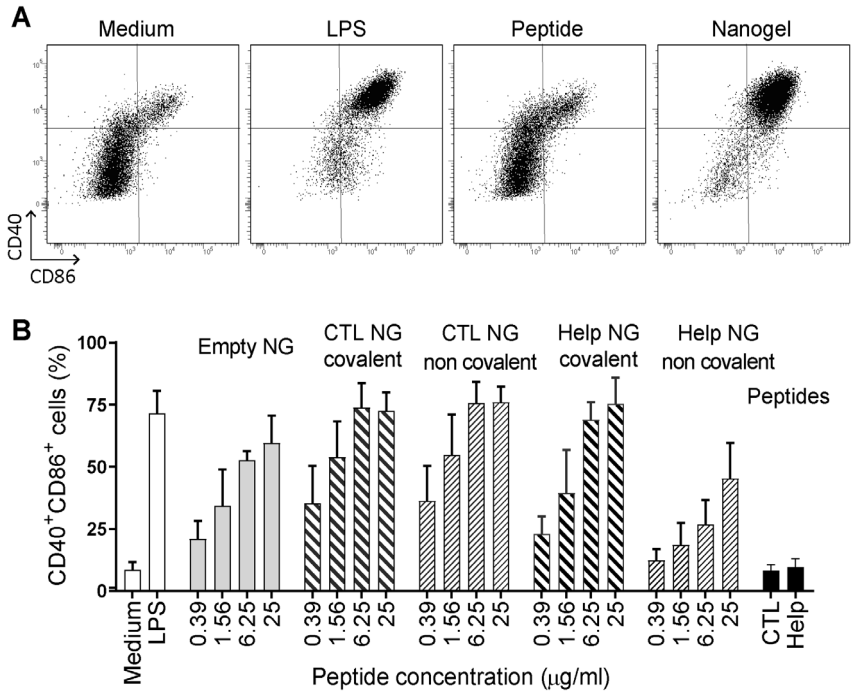

Figure 5. Nanogels induce maturation in DCs and upregulation of CD86⁺ and CD40⁺ co-stimulatory molecules. A. Representative dot plots for the expression of the costimulatory molecules CD40⁺ and CD86⁺ displayed for the highest concentration tested (25 μg/mL) after overnight incubation of D1 DCs . LPS (1 μg/mL) is used as positive control for DC maturation. **B.** Percentages of cells that upregulated CD40⁺ and CD86 after overnight incubation with titrated amounts of the indicated formulations. LPS (1 μg/mL) was used as positive control and soluble CTL and Help peptides (25 μg/mL) were used as controls. The data are shown as mean ± SD (n=3).

Antigen-dependent T cell activation was measured via a colorimetric assay. As shown in Figure 6A, the soluble peptides (CTL and Cys-CTL) display limited T cell activation, attributable to the poor cellular uptake of soluble peptide by DCs. In contrast, incubation of DCs with covalently conjugated CTL-loaded nanogels led to significantly enhanced activation of CD8⁺ T cells in a concentration-dependent manner. Moreover, this effect was dependent on the covalent attachment of the peptide to the nanogels, as the non-covalent CTL-loaded nanogels and physical mixtures of nanogels and soluble peptides did not result in an increase of T cell activation compared to free peptide. This could indicate that the non-covalent nanogels were not able to retain the peptide efficiently before uptake by the cells, whereas the nanogels with covalently immobilized peptide promote enhanced uptake of the peptide which is released only under the reducing condi-

tions of the endosomes. These data are also in line with previous publications on OVA-conjugated nanogels in which it was shown that OVA can be delivered into DCs via the nanogel carrier and subsequently released intracellularly leading to antigen presentation and activation of $CD8^+$ T cells [57, 60].

MHC class II presentation was also analyzed by detecting activation of OTIIZ. As shown in Figure 6B, all nanogel formulations display enhanced MHC II antigen presentation compared to free soluble peptide, differently from what observed with class I presentation. This effect is at least partially independent from the disulfide bond as both the non-covalently loaded nanogels as well as the mixture of helper peptide and empty nanogels already display increased OTIIZ activation. This could be explained by an overall increased uptake of the peptide that is still retained in the nanogels. However, the covalently loaded nanogels still yield the highest activation, indicating that peptide protection by nanogels before uptake is indeed occurring and that intracellular release allows efficient MHC II presentation.

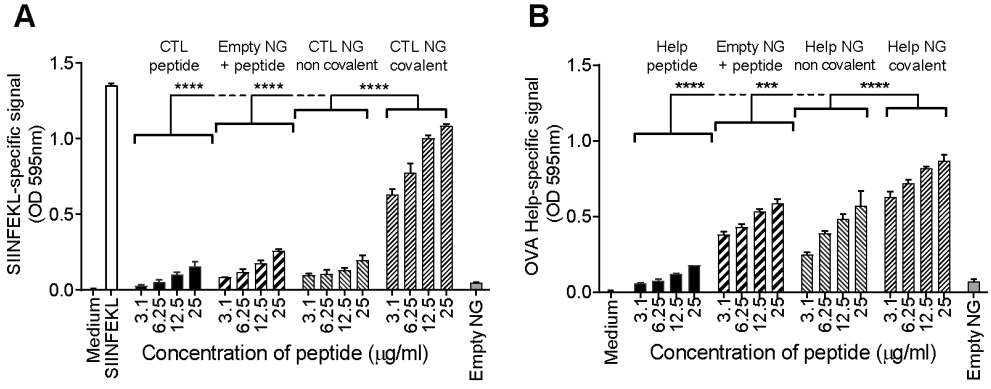

Figure 6. Enhanced MHC class I and class II presentation upon nanogel-mediated uptake of peptide A. MHC class I presentation of nanogel-formulated CTL peptide by DCs was analyzed by measuring the activation of B3Z hybridoma $CD8^+$ T cell line upon overnight incubation with DCs pulsed for 2 hours with titrated amounts of the indicated formulations. SIINFEKL peptide (100 ng/mL) was used as positive control. **B.** MHC class II presentation of nanogel-formulated Help peptide was analyzed by measuring the activation of the OTIIZ hybridoma $CD4^+$ T cell line upon overnight incubation with DCs pulsed for 2 hours with titrated amounts of the indicated formulations. For both A and B, each bar represents the average of triplicates with SD. Statistical significance of the differences between the different formulations at every concentration was determined by 2-way ANOVA followed by multiple comparison and Dunnet correction. The experiment was repeated three times with similar outcomes.

In conclusion, *in vitro* evaluation of nanogels as peptide carriers on DCs exhibit low toxicity and maturating properties. Moreover, the covalent attachment of the peptide to the nanogel via a disulfide link results functional for peptide retention into the nanogels until arrival to the endosomes, where peptide can be released to enter both the class I and class II presentation pathways.

In vivo induction of $CD8^+$ T cells

We observed that covalently loaded nanogels promote uptake of peptide by DCs and increased antigen presentation, the potency of peptide-loaded nanogels to induce *de novo* T cell-mediated immunity was investigated *in vivo*. Mice were injected intradermally with different nanogel formulations containing SLPs and poly(I:C) as adjuvant[20]. As nanogels were able to induce *in vitro* DC maturation, the potential of covalently loaded nanogels as a self-adjuvating vaccine was also investigated. Mice received a prime and booster immunization on day 0 and 14 respectively. The SIINFEKL-specific $CD8^+$ T cell responses could be monitored in blood via SIINFEKL/H2-Kb tetramer staining. As presented in Figure 7A, at day 9 after the prime immunization, vaccination with only the CTL SLPs raises little $CD8^+$ responses. However, covalent loading of the same peptide into nanogels significantly enhance T cell induction. The addition of a helper epitope and therefore a $CD4^+$ T cell helper response greatly enhances the induction of specific $CD8^+$ T cells, as observed in mice vaccinated with combination of CTL and Help peptide. The combination of adjuvanted covalent CTL and Helper nanogels induces the highest responses for SIINFEKL. Furthermore, the addition of an adjuvant is important for optimal induction, as the nonadjuvanted group displays no induction. Importantly, the nanogels with covalently immobilized peptides adjuvanted with poly (I:C) showed superior $CD8^+$ T cell responses activation as compared to nanogels physically loaded with the peptides (both adjuvanted with poly (I:C)), again indicating the key role of covalent conjugation of peptides to the nanogels.

One week after the booster injection (on day 22), the $CD8^+$ T cell responses in blood samples were analyzed again quantitatively. Booster injection induced an overall increase of the magnitude of SIINFEKL-specific $CD8^+$ responses in all groups, except the one vaccinated with CTL peptide only, underlining the importance of $CD4^+$ T cell help for optimal $CD8^+$ induction. Notably, nanogel-formulated CTL peptide display responses comparable to the peptide group that contains both the CTL and the Helper epitopes, highlighting the importance of the method of peptide delivery for optima T cell induction. This is especially evident in the

combination group of CTL and Help covalent loaded nanogels. Non covalently loaded nanogel do not achieve the same effect and it can be concluded that, although the peptide-loaded nanogels showed effective DC maturing properties *in vitro* (Figure 5), a strong TLR ligand adjuvant (poly(I:C)) was needed to achieve a strong DC activation *in vivo*.

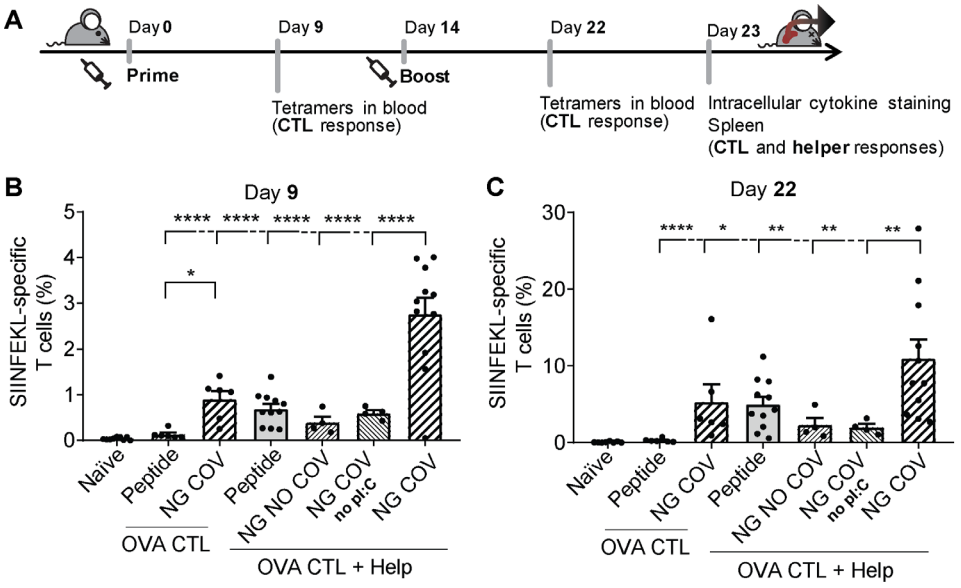

Figure 7. Peptide vaccination with covalently loaded nanogels enhances induction of CTL responses A. Schematic overview of the vaccination experiment. All groups were vaccinated intradermally twice at interval of two weeks with 10 µg of the indicated peptide (CTL or Help) or a mixture of both and adjuvanted with 20 µg of poly(I:C), except for the nonadjuvanted group (NG COV no poly(I:C)). The induction of CTL responses was monitored in blood by SIINFEKL-Kb tetramer staining at day 9 and day 22. At day 23 spleens were harvested to analyze both CTL and helper responses via intracellular cytokine staining. **B** and **C.** Levels of SIINFEKL-specific $CD8^+$ T cells as percentages of total $CD8^+$ T cells upon tetramer staining in blood after prime (day 9, panel B) and booster (day 22, panel C) vaccine injections. Statistical significance was determined by one-way ANOVA followed by multiple comparison and Bonferroni correction. *: $p<0.05$, **: $p<0.01$, ***: $p<0.001$, ****: $p<0.0001$

Upon antigen recognition, CTL T cells produce different cytokines that are important for their functions, the most important being IFNγ and TNFα. Therefore, mice were sacrificed at day 23, and OVA-specific $CD8^+$ and $CD4^+$ T cells responses were both analyzed in cells harvested from spleens upon intracellular cytokine staining (ICS).The number of $CD8^+$ T cells in the spleen producing these two cytokines in response to SIINFEKL displays a similar response among groups

as observed in blood via tetramer staining (Figure 8A). Double TNFα and IFNγ producers are indicators of the quality of the response, as the ability of producing both cytokines is associated with improved differentiation and effector functions. Notably, we observe that the highest percentage of double producers is observed in the adjuvanted covalent-loaded nanogels group when CTL and helper peptides are combined (Figure 8B).

Cytokine staining also allows quantification of CD4⁺ T cell helper responses, by staining of IFNγ and IL-2 producing cells. All groups exhibit similar amount of OVA-specific CD4⁺ T cell responses (Figure 8C), and the nanogel seem to only partially increase the overall amount of Help responses. However, when looking at the quality of T cells in terms of single or double producer, the covalently loaded nanogel exhibit the most efficient T cell responses with the highest percentage of total double producers (Figure 8D).

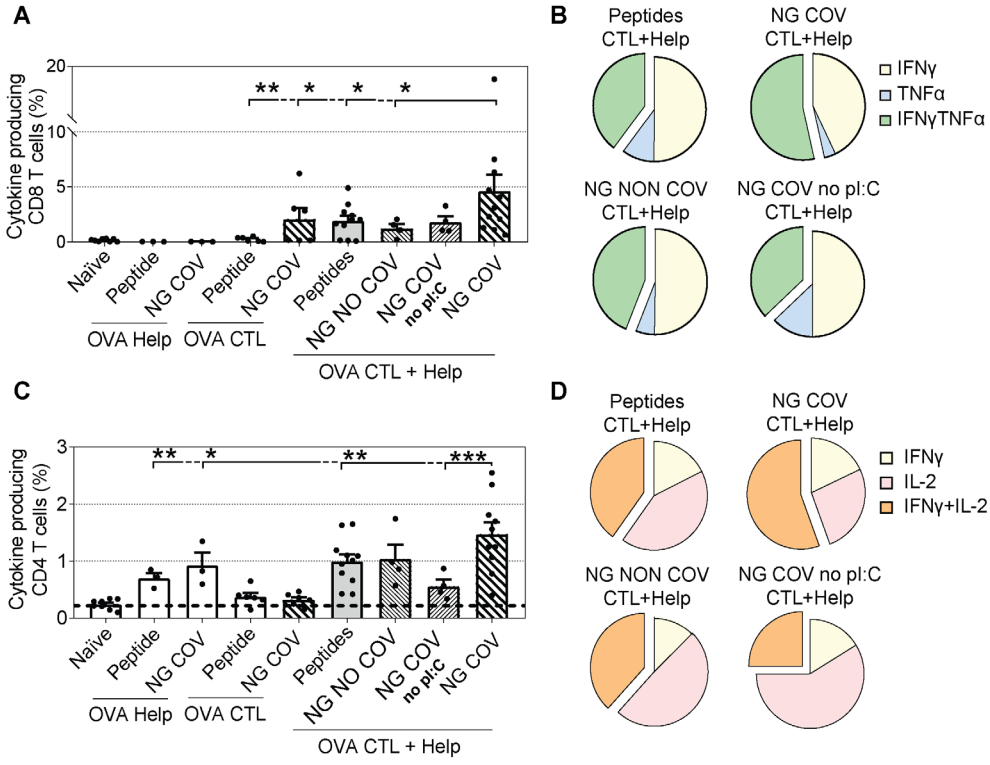

Figure 8. Vaccination with nanogel-formulated peptides induces higher quality CD8⁺ and CD4⁺ T cell responses. A-D Splenocytes from vaccinated mice were incubated ex vivo with CTL and Help peptide-loaded DCs and cytokine producing CD8⁺ (**A**) and CD4⁺ (**C**) were detected via intracellular cytokine staining. The average percentage of single or double cytokine producers among cytokine producing CD8⁺ (**B**) and CD4⁺ (**D**) T cells is represented.

CONCLUSIONS

In this study, we demonstrated the potential of cationic dextran nanogels to induce antigen-specific immune responses. SLP conjugated nanogels were internalized by DCs and activated these immature cells and subsequently boost the antigen presentation *in vitro*. An *In vivo* study showed that the covalently conjugated peptide nanogels in the presence of poly I:C can effectively stimulate strong functional $CD8^+$ and $CD4^+$ responses in comparison to naked SLP and non-conjugated formulations, indicating the key role of reducible covalent bond for intracellular delivery of vaccine peptides. Therefore, cationic dextran nanogels are promising carriers as vaccine formulations for cancer immune therapy.

MATERIAL AND METHODS

Materials. Dextran (from Leuconostoc ssp) Mw=40,000 Da, glycidyl methacrylate (GMA) and hydroxyethyl methacrylate (HEMA) were obtained from Sigma Chemical Co. (St. Louis, MO, USA). Methacrylate-derivatized dextran (dex-MA) with a degree of substitution of 8 (DS, i.e. a number of MA groups per 100 glucopyranose units as analyzed by ^{1}H-nuclear magnetic resonance (NMR) spectroscopy) was synthesized as described by van Dijk-Wolthuis *et al.* [61-62]. [2-(Methacryloyloxy)-ethyl] trimethylammonium chloride (TMAEMA, 80 wt % solution in water) and light mineral oil (M8410) were purchased from Sigma (St. Louis, MO, USA). ABIL EM 90 and Irgacure 2959 were purchased from Goldschmidt (Essen, Germany) and Ciba Specialty Chemicals (Hercules, USA), respectively. Fmoc-amino acids were obtained from Iris Biotech GmbH (Germany). Acetone, acetonitrile, dimethyl sulfoxide, n-hexane and trifluoroacetic acid (TFA), HBTU/HOBt and *N,N*-diisopropylethylamine were products of Biosolve (Valkenswaard, the Netherlands). Glutathione, thioanisole, 1,4-Dithiothreitol (DTT), ethanedithiol (EDT) and anisole were obtained from Sigma-Aldrich (Zwijndrecht, the Netherlands). *N*-2-hydroxyethylpiperazine-*N*'-2-ethanesulfonic acid (HEPES) was purchased from Acros Chimica (Geel, Belgium). Phosphate buffer saline (Na+ 163.9 mM, Cl- 140.3 mM, HPO42- 8.7 mM, H2PO4- 1.8 mM, pH 7.4) was purchased from Braun (Germany). Chlorophenol red-β-D-galactopyranoside was acquired from Sigma (St. Louis, MO, USA). Chlorophenol red-β-d-galactopyranoside (CPRG) was provided by Merck (Darmstadt, Germany). All other chemicals used were obtained from commercial suppliers and were of analytical grade. *N*-(4-(2-(pyridine-2-yldisulfanyl)ethyl)-amidobutyl) methacrylamide was synthesized as described previously [57].

Cell lines. D1 cells, a long-term growth factor-dependent immature myeloid dendritic cell line of splenic origin derived from a female C57BL/6 mouse was cultured at 37°C with 5% CO_2 in IMDM (Iscove's Modified Dulbecco's Medium, Lonza) [63]. B3Z, a $CD8^+$ T cell hybridoma specific for the SIINFEKL epitope of OVA [64] was maintained in IMDM (Iscove's Modified Dulbecco's Medium, Lonza) supplemented with 100 IU/mL penicillin/streptomycin (Gibco™, Bleiswijk, the Netherlands), 2 mM glutamine (Gibco, Bleiswijk, the Netherlands), 25 µM 2-mercaptoethanol and 500 µg/mL Hygromycin B (AG Scientific, San Diego, USA).

Mice. Female C57BL/6 (H-2b) mice were obtained from Charles River Laboratories (L'Arbresle, France) and kept under standardized conditions in the Leiden University Medical Centre animal facility. The *in vivo* experiment as described in section 2.8 was carried out according to the Dutch Experiments on Animal Act, which serves the implementation of "Guidelines on the protection of experimental animals" by the Council of Europe.

Synthesis of SLPs. The peptide epitopes (Table 1) were synthesized by standard Fmoc solid phase peptide synthesis using a Symphony peptide synthesizer (Symphony; Protein Technologies, Tucson, AZ, United States) using protocols as described by Coin *et al.* [65]. In brief, *N*-methyl-2-pyrrolidone (NMP) was used as a coupling and washing solvent during the synthesis process. For each coupling step, Fmoc-amino acids were activated by 4 eq HBTU/HOBt and 8 eq *N,N*-diisopropylethylamine to react with the free N-terminal amino acids present on the resin (Sigma-Aldrich, the Netherlands) for one hour. After each coupling step, the Fmoc groups were removed by four times treatment of 20% piperidine in NMP for ten minutes. Reagent R TFA/thioanisole/EDT/anisole (90/5/3/2) was used to simultaneously cleave the peptide off from the resin and remove the side chain protecting groups. The synthesized peptides were purified by Prep-HPLC using Reprosil-Pur C18 column (10 µm, 250 × 22 mm) eluted with water-acetonitrile gradient from 5 to 80% acetonitrile (10 mM ammonium bicarbonate, pH 8.3) in 40 minutes at a flow-rate of 15 mL/min with UV detection at 220 nm. Fractions of 30 mL were collected, and the purity was confirmed by analytical UPLC using Waters XBridge C18 column eluted with water-acetonitrile gradient 5 to 80% ACN (10 mM ammonium bicarbonate, pH 8.3) in 8 minutes at flow rate 1 m/min and UV detection at 280 and 220 nm.

LC–MS analysis was carried out using an Acquity UPLC system, (Waters Corporation, Milford, USA) combined with an Agilent Technologies 6300 Series LC/MSD ion-trap mass spectrometer (Santa Clara, CA, USA) in the positive ion mode.

A gradient was used with a mobile phase A (95% H_2O, 5% ACN plus 0.1% formic acid) and a mobile phase B (100% ACN plus 0.1% formic acid). Elution was done at room temperature using a BEH300 C18 1.7 µm column. The eluent linearly changed from 100% A to 100% B in 20 min with a flow rate of 1 mL/min. The MS settings were: capillary voltage, 2 kV; nebulizer pressure, 60 psi; dry gas flow, 11 L/min; dry gas temperature, 350 ℃; scan range, m/z 50–2000. To prevent disulfide bond formation between the two cysteine residues in peptides (Cys-CTL and Cys-Help), dithiothreitol (10 mg/mL) was added to the peptides before MS analysis.

Preparation and characterization of peptide-loaded nanogels. Cationic nanogels were prepared by inverse mini-emulsion technique as previously described [44, 57]. In brief, an emulsion with aqueous droplets containing 120 mg of methacrylated dextran (DS 8), trimethyl aminoethyl methacrylate (160 µL) and the pyridyldisulfide-containing methacrylamide monomer, *N*-(4-(2-(pyridine-2-yldisulfanyl)ethyl)-amidobutyl)methacrylamide synthesized as described previously [57], (27 mg) was photo-polymerized (Bluepoint UV source, 60% amplitude, 940 mW/cm^2 , Hönle UV technology, Germany) for 15 min. Particles were washed with acetone and four times with acetone/hexane (1:1, v/v) to remove the used mineral oil and surfactant. Finally, nanoparticles were collected by redispersion in water and freeze drying. To covalently conjugate Cys-peptides to the nanogel network (covalent NGs), 4.25 mL of a suspension of cationic nanogels (4 mg/mL) in HEPES buffer (20 mM, pH 7.4) was mixed with 750 l peptide solutions (4 mg/mL) and incubated overnight at room temperature. To remove non-reacted peptides, the particles were washed twice with high ionic strength buffer (PBS 150 mM,pH 7.4) and the final pellets obtained after centrifugation (15,000 rpm, 1h) were washed with water and subsequently lyophilized. The physically loaded nanogels (non-covalent NGs) were prepared by adding the peptides lacking cysteine residues (Table 1, CTL and Help) to the particle dispersions in a HEPES buffer solution (20 mM, pH 7.4). After overnight incubation at room temperature, the particles were recovered by centrifugation (15,000 rpm, 1h), subsequently washed with water and lyophilized. The particle size and zeta potential of the obtained particles were measured in HEPES (10 mM, pH 7.4) using DLS (Malvern ALV/CGS-3 Goniometer, Malvern Instruments, Malvern, UK) and Zetasizer (Zetasizer Nano, Malvern Instruments, USA), respectively.

In vitro release. To study the release of SLP from the nanogels, freeze-dried CTL SLP-loaded and Help SLP-loaded nanogels (5 mg/mL) were suspended in

PBS (Na^+ 163.9 mM, Cl^- 140.3 mM, HPO_4^{2-} 8.7 mM, H_2PO4^- 1.8 mM) at pH 7.4 or pH 4.0, and incubated at 37 °C. At different time points, 3 samples were taken and centrifuged (15,000 rpm, 1 h) and the collected supernatants were subsequently analyzed by reversed-phase ultrahigh-performance liquid chromatography (RP_UPLC) for peptide quantification. To trigger release of the immobilized peptides, glutathione at a final concentration of 2.5 mM was added to the nanogel dispersion and the obtained supernatants after centrifugation (15,000 rpm, 1 h) were analyzed for concentration of peptides using UPLC (Acquity UPLC, Waters Corporation, Milford, USA) equipped with a BEH300 C18 1.7 µm column. Solvent mixtures consisting of 100% H_2O/0.05% TFA and 100% ACN/0.04% TFA were used as eluent A and B, respectively. A gradient was run from 5 to 70% B at a flow rate of 1 mL/min. The injection volume was 7.5 µl and the detection wavelength was 280 nm. The calibration curve was linear between 10 to 1000 µg/mL CTL and Help SLP peptides.

Cell viability and DC maturation. D1 cells (100,000 cells/well) were seeded in 96-well round-bottomed plates and incubated with empty nanogels, non-covalent NGs (loaded with CTL and Help peptides), covalent NGs (loaded with CTL and Help peptides) and soluble peptides (CTL and Help) at indicated concentrations (range 0.39-25 µg mL^{-1}) in culture medium. After 24 h of incubation, the relative cell viability and dendritic cell maturation were assessed by 7-aminoactinomycin D exclusion and staining with fluorescent antibodies directed against $CD86^+$ and $CD40^+$ (eBioscience, Landsmeer, the Netherlands) followed by acquisition by BD™ LSR II flow cytometer.

In vitro antigen presentation. The immunogenicity of the peptide-loaded nanogels was evaluated by an *in vitro* T hybridoma assay [64]. In detail, immature D1 cells (50,000 cells/well) were incubated in 96-well flat-bottomed plates in supplemented IMDM with peptide-loaded nanogels (non-covalent and covalent) or soluble peptides (CTL and Help) in PBS (composition given in section 2.1) at 37 °C and at different concentrations (0.39-25 g/mL of peptide). After 2 h, the cells were washed with supplemented IMDM culture medium in order to remove excess antigen. Subsequently, 50,000/well B3Z T, a $CD8^+$ T cell hybridoma cell or OTIIZ, a $CD4^+$ T-cell hybridoma cell line both producing a β-galactosidase construct upon TCR triggering, were added followed by overnight incubation at 37 °C. MHC class I and II antigen presentation was measured indirectly by a colorimetric assay using chlorophenol red-β-d-galactopyranoside (CPRG) and the color conversion was detected by measuring absorbance at 595 nm [66-67].

Immunization of mice. Mice were immunized by intradermal injections of the formulations in the tail base area. All formulations were prepared at the day of injections and consisted of 10 µg of the different peptides (CTL, Help or both combined) in a total volume of 30 µl PBS (composition given in section 2.1). The nanogel vaccines were adjuvanted with 20 µg of poly(I:C) (InvivoGen, Toulouse, France). Immunization was performed at day 0 (prime injection) and at day 14 (booster injection). During the study, blood samples were collected from the tail vein at day 8 and 22 to monitor T cell responses. At day 23, spleens were harvested for *ex vivo* analysis of $CD8^+$ and $CD4^+$ T cell responses[68].

Analysis of antigen-specific CD8 and CD4 T cell responses. For detection of SIINFEKL-specific $CD8^+$ T cells, surface staining was performed on blood samples after red blood cell lysis. Cells were washed using staining buffer and incubated for 15 minutes at room temperature with labelled SIINFEKL-tetramers. After 15 minutes, cells were incubated on ice and a mix containing 7-aminoactinomycin D (Life Technologies, for viability staining) and fluorescently labelled antibodies against $CD8^+$ (BioLegend, San Diego, USA) and $CD3^+$ (eBioscience, Landsmeer, the Netherlands) was added[69]. Intracellular cytokine analysis of splenocytes was performed after incubating the cells for 5-6 hours with previously loaded nanogels (with 2 µg/mL of CTL and Help peptide), in presence of the protein transport inhibitor Brefeldin A (10 µg/mL, BD Biosciences, Breda, the Netherlands). After incubation, the cells were stained for surface markers $CD3^+$, $CD8^+$ and $CD4^+$ and fixed overnight in 0.1% paraformaldehyde. Next day, permeabilization and intracellular staining of IFNγ, TNFα and IL-2 was performed and the samples were subsequently analyzed on BD™ LSR II flow cytometer as described previously[69].

Statistical analysis. Graph Pad Prism software version 7 was used for statistical analysis. Two-way analysis of variance (ANOVA) tests was used to evaluate the induced $CD8^+$ and $CD4^+$ T-cell responses and cytokine production *in vivo*. Statistical significance is considered when $p < 0.05$.

REFERENCES

[1] Shanker, A.; Marincola, F. M., Cooperativity of adaptive and innate immunity: implications for cancer therapy. Cancer Immunology, Immunotherapy : CII, 60 (8): 1061-74, 2011.

[2] Bos, R.; Sherman, L. A., CD4+ T-cell help in the tumor milieu is required for recruitment and cytolytic function of CD8+ T lymphocytes. Cancer Research, 70 (21): 8368-77, 2010.

[3] Koury, J.; Lucero, M.; Cato, C.; Chang, L.; Geiger, J.; Henry, D.; Hernandez, J.; Hung, F.; Kaur, P.; Teskey, G.; Tran, A., Immunotherapies: Exploiting the immune system for cancer treatment. J Immunol Res. (4):9585614, 2018.

[4] Palucka, K.; Ueno, H.; Fay, J.; Banchereau, J., Dendritic cells and immunity against cancer. Journal of Internal Medicine, 269 (1): 64-73, 2011.

[5] Palucka, K.; Banchereau, J., Dendritic-cell-based therapeutic cancer vaccines. Immunity, 39 (1): 38-48, 2013.

[6] Mantia-Smaldone, G. M.; Chu, C. S., A review of dendritic cell therapy for cancer: progress and challenges. BioDrugs, 27 (5): 453-68, 2013.

[7] Hu, Z.; Ott, P. A.; Wu, C. J., Towards personalized, tumour-specific, therapeutic vaccines for cancer. Nature Reviews Immunology, 18, 168-182, 2017.

[8] Banchereau, J.; Palucka, K., Cancer vaccines on the move. Nature Reviews Clinical Oncology,15, 9-10, 2017.

[9] Bijker, M. S.; Melief, C. J.; Offringa, R.; van der Burg, S. H., Design and development of synthetic peptide vaccines: past, present and future. Expert Review of Vaccines, 6 (4): 591-603, 2007.

[10] Melief, C. J.; van der Burg, S. H., Immunotherapy of established (pre)malignant disease by synthetic long peptide vaccines. Nature Reviews. Cancer, 8 (5): 351-360, 2008.

[11] Sabbatini, P.; Tsuji, T.; Ferran, L.; Ritter, E.; Sedrak, C.; Tuballes, K.; Jungbluth, A. A.; Ritter, G.;

Aghajanian, C.; Bell-McGuinn, K.; Hensley, M. L.; Konner, J.; Tew, W.; Spriggs, D. R.; Hoffman, E. W.; Venhaus, R.; Pan, L.; Salazar, A. M.; Diefenbach, C. M.; Old, L. J.; Gnjatic, S., Phase I trial of overlapping long peptides from a tumor self-antigen and poly-ICLC shows rapid induction of integrated immune response in ovarian cancer patients. Clinical Cancer Research, 18 (23): 6497-508, 2012.

[12] Rosalia, R. A.; Quakkelaar, E. D.; Redeker, A.; Khan, S.; Camps, M.; Drijfhout, J. W.; Silva, A. L.; Jiskoot, W.; van Hall, T.; van Veelen, P. A.; Janssen, G.; Franken, K.; Cruz, L. J.; Tromp, A.; Oostendorp, J.; van der Burg, S. H.; Ossendorp, F.; Melief, C. J., Dendritic cells process synthetic long peptides better than whole protein, improving antigen presentation and T-cell activation. European Journal of Immunology, 43 (10): 2554-65, 2013.

[13] Black, M.; Trent, A.; Tirrell, M.; Olive, C., Advances in the design and delivery of peptide subunit vaccines with a focus on toll-like receptor agonists. Expert Review of Vaccines, 9 (2): 157-73, 2010.

[14] Skwarczynski, M.; Toth, I., Peptide-based synthetic vaccines. Chemical Science, 7 (2): 842-854, 2016.

[15] Li, W.; Joshi, M. D.; Singhania, S.; Ramsey, K. H.; Murthy, A. K., Peptide vaccine: progress and challenges. Vaccines, 2 (3): 515, 2014.

[16] Irvine, D. J.; Hanson, M. C.; Rakhra, K.; Tokatlian, T., Synthetic nanoparticles for vaccines and immunotherapy. Chemical Reviews, 115 (19): 11109-11146, 2015.

[17] De Geest, B. G.; Willart, M. A.; Hammad,

H.; Lambrecht, B. N.; Pollard, C.; Bogaert, P.; De Filette, M.; Saelens, X.; Vervaet, C.; Remon, J. P.; Grooten, J.; De Koker, S., Polymeric multilayer capsule-mediated vaccination induces protective immunity against cancer and viral infection. ACS Nano, 6 (3): 2136-49, 2012.

[18] Chen, W.; Huang, L., Induction of cytotoxic T-lymphocytes and antitumor activity by a liposomal lipopeptide vaccine. Molecular Pharmaceutics, 5 (3): 464-71, 2008.

[19] Dimier-Poisson, I.; Carpentier, R.; N'Guyen, T. T.; Dahmani, F.; Ducournau, C.; Betbeder, D., Porous nanoparticles as delivery system of complex antigens for an effective vaccine against acute and chronic Toxoplasma gondii infection. Biomaterials, 50: 164-175, 2015.

[20] Varypataki, E. M.; van der Maaden, K.; Bouwstra, J.; Ossendorp, F.; Jiskoot, W., Cationic liposomes loaded with a synthetic long peptide and poly(I:C): a defined adjuvanted vaccine for induction of antigen-specific T cell cytotoxicity. The AAPS Journal, 17 (1): 216-226, 2015.

[21] Rosalia, R. A.; Cruz, L. J.; van Duikeren, S.; Tromp, A. T.; Silva, A. L.; Jiskoot, W.; de Gruijl, T.; Lowik, C.; Oostendorp, J.; van der Burg, S. H.; Ossendorp, F., CD40-targeted dendritic cell delivery of PLGA-nanoparticle vaccines induce potent anti-tumor responses. Biomaterials, 40: 88-97, 2015.

[22] Sun, Q.; Barz, M.; De Geest, B. G.; Diken, M.; Hennink, W. E.; Kiessling, F.; Lammers, T.; Shi, Y., Nanomedicine and macroscale materials in immuno-oncology. Chemical Society Reviews, 48 (1): 351-381, 2019.

[23] Aucouturier, J.; Ascarateil, S.; Dupuis, L., The use of oil adjuvants in therapeutic vaccines. Vaccine, 24 Suppl 2, S2-44-5, 2006.

[24] Aucouturier, J.; Dupuis, L.; Deville, S.; Ascarateil, S.; Ganne, V., Montanide ISA 720 and 51: a new generation of water in oil emulsions as adjuvants for human vaccines. Expert review of vaccines, 1 (1): 111-118, 2002.

[25] Kenter, G. G.; Welters, M. J.; Valentijn, A. R.; Lowik, M. J.; Berends-van der Meer, D. M.; Vloon, A. P.; Drijfhout, J. W.; Wafelman, A. R.; Oostendorp, J.; Fleuren, G. J.; Offringa, R.; van der Burg, S. H.; Melief, C. J., Phase I immunotherapeutic trial with long peptides spanning the E6 and E7 sequences of high-risk human papillomavirus 16 in end-stage cervical cancer patients shows low toxicity and robust immunogenicity. Clinical Cancer Research, 14 (1): 169-77, 2008.

[26] Schwartzentruber, D.J.; Lawson, D.H.; Richards, J.M. ; Conry, R.M.; Miller, D.M.; Treisman, J.; Gailani, F.; Riley, L.; Conlon, K.; Pockaj, B.; Kendra, K.L.; White, R.L.; Gonzalez, R.; Kuzel, T.M.; Curti, B.; Leming, P.D.; Whitman, E.D.; Balkissoon, J.; Reintgen, D.S.; Kaufman, H.; Marincola, F.M.; Merino, M.J.; Rosenberg, S.A.; Choyke, P.; Vena, D.; Hwu, P., gp100 peptide vaccine and interleukin-2 in patients with advanced melanoma. The New England Journal of Medicine, 364 (22): 2119-2127, 2011.

[27] Oka, A. Tsuboi, T. Taguchi, T. Osaki, T. Kyo, H. Nakajima, O.A. Elisseeva, Y. Oji, M. Kawakami, K. Ikegame, N. Hosen, S. Yoshihara, F. Wu, F. Fujiki, M. Murakami, T. Masuda, S. Nishida, T. Shirakata, S. Nakatsuka, A. Sasaki, K. Udaka, H. Dohy, K. Aozasa, S. Noguchi, I. Kawase, H. Sugiyama, Induction of WT1 (Wilms' tumor gene)-specific cytotoxic T lymphocytes by WT1 peptide vaccine and the resultant cancer regression. Proceedings of the National Academy of Sciences of the United States of America, 101 (38): 13885-13890, 2004.

[28] Hailemichael, Y.; Dai, Z.; Jaffarzad, N.; Ye, Y.; Medina, M.A.; Huang, X.F.; Dorta-Estremera, S.M.; Greeley, N.R.; Nitti, G.; Peng, W.; Liu, C.; Lou, Y.; Wang, Z.; Ma, W.; Rabinovich, B.; Sowell, R.T; Schluns, K.S.; R.E. Davis, R.E.; Hwu, P.; Overwijk, W.W.; Persistent antigen at vaccination sites induces tumor-specific CD8(+) T cell sequestration, dysfunction and deletion. Nature Medicine, 19 (4): 465-472, 2013.

[29] Cruz, L. J.; Tacken, P. J.; Fokkink, R.; Joost-

en, B.; Stuart, M. C.; Albericio, F.; Torensma, R.; Figdor, C. G., Targeted PLGA nano- but not microparticles specifically deliver antigen to human dendritic cells via DC-SIGN in vitro. Journal of Controlled Release, 144 (2): 118-26, 2010.

[30] Fischer, S.; Schlosser, E.; Mueller, M.; Csaba, N.; Merkle, H. P.; Groettrup, M.; Gander, B., Concomitant delivery of a CTL-restricted peptide antigen and CpG ODN by PLGA microparticles induces cellular immune response. Journal of Drug Targeting, 17 (8): 652-61, 2009.

[31] Rahimian, S.; Fransen, M. F.; Kleinovink, J. W.; Amidi, M.; Ossendorp, F.; Hennink, W. E., Particulate systems based on poly(lactic-co-glycolic)acid (pLGA) for immunotherapy of cancer. Current Pharmaceutical Design, 21 (29): 4201-4216, 2015.

[32] Rad-Malekshahi, M.; Fransen, M. F.; Krawczyk, M.; Mansourian, M.; Bourajjaj, M.; Chen, J.; Ossendorp, F.; Hennink, W. E.; Mastrobattista, E.; Amidi, M., Self-assembling peptide epitopes as novel platform for anticancer vaccination. Molecular Pharmaceutics, 14 (5): 1482-1493, 2017.

[33] Black, M.; Trent, A.; Kostenko, Y.; Lee, J.S.; Olive, C.; Tirrell, M.; Self-assembled peptide amphiphile micelles containing a cytotoxic T-cell epitope promote a protective immune response in vivo. Advanced Materials, 24(28):3845-3849, 2012.

[34] Silva, A. L.; Rosalia, R. A.; Sazak, A.; Carstens, M. G.; Ossendorp, F.; Oostendorp, J.; Jiskoot, W., Optimization of encapsulation of a synthetic long peptide in PLGA nanoparticles: low-burst release is crucial for efficient CD8(+) T cell activation. European Journal of Pharmaceutics and Biopharmaceutics, 83 (3): 338-345, 2013.

[35] Hamdy, S.; Molavi, O.; Ma, Z.; Haddadi, A.;, Alshamsan A.; Gobti, Z.; Elhasi, S.; Samuel, J.; Lavasanifar, A.; Co-delivery of cancer-associated antigen and Toll-like receptor 4 ligand in PLGA nanoparticles induces potent CD8+ T cell-mediated anti-tumor immunity. Vaccine, 26(39):5046-57, 2008.

[36] Butts, C.; Maksymiuk, A; Goss,; Soulieres, D.; Marshall, E.; Cormier, Y.; Ellis, P.M.; Price, A.; Sawhney, R.; Beier, F.; Falk, M.; Murray, N., Updated survival analysis in patients with stage IIIB or IV non-small-cell lung cancer receiving BLP25 liposome vaccine (L-BLP25): phase IIB randomized, multicenter, open-label trial. Journal of Cancer Research and Clinical Oncology, 137 (9): 1337-1342, 2011.

[37] Varypataki, E. M.; Silva, A. L.; Barnier-Quer, C.; Collin, N.; Ossendorp, F.; Jiskoot, W., Synthetic long peptide-based vaccine formulations for induction of cell mediated immunity: A comparative study of cationic liposomes and PLGA nanoparticles. Journal of controlled release, 226: 98-106, 2016.

[38] Li, D.; van Nostrum, C. F.; Mastrobattista, E.; Vermonden, T.; Hennink, W. E., Nanogels for intracellular delivery of biotherapeutics. Journal of Controlled Release, 259: 16-28, 2017.

[39] Jiang, Y.; Chen, J.; Deng, C.; Suuronen, E. J.; Zhong, Z., Click hydrogels, microgels and nanogels: Emerging platforms for drug delivery and tissue engineering. Biomaterials, 35 (18): 4969-4985, 2014.

[40] Zhang, H.; Zhai, Y.; Wang, J.; Zhai, G., New progress and prospects: The application of nanogel in drug delivery. Materials Science & Engineering. C, Materials for Biological Applications, 60, 560-568, 2016.

[41] Dragan, E. S., Design and applications of interpenetrating polymer network hydrogels. A review. Chemical Engineering Journal, 243: 572-590, 2014.

[42] Kordalivand, N.; Li, D.; Beztsinna, N.; Sastre Torano, J.; Mastrobattista, E.; van Nostrum, C. F.; Hennink, W. E.; Vermonden, T., Polyethyleneimine coated nanogels for the intracel-

lular delivery of RNase A for cancer therapy. Chemical Engineering Journal, 340, 32-41, 2018.

[43] Hamidi, M.; Azadi, A.; Rafiei, P., Hydrogel nanoparticles in drug delivery. Advanced Drug Delivery Reviews, 60 (15): 1638-1649:2008.

[44] Raemdonck, K.; Naeye, B.; Buyens, K.; Vandenbroucke, R. E.; Høgset, A.; Demeester, J.; De Smedt, S. C., Biodegradable dextran nanogels for RNA interference: focusing on endosomal escape and intracellular siRNA delivery. Advanced Functional Materials, 19 (9): 1406-1415, 2009.

[45] Vermonden, T.; Censi, R.; Hennink, W. E., Hydrogels for Protein Delivery. Chemical Reviews, 112 (5): 2853-2888, 2012.

[46] Mauri, E.; Cappella, F.; Masi, M.; Rossi, F., PEGylation influences drug delivery from nanogels. Journal of Drug Delivery Science and Technology, 46: 87-92, 2018.

[47] Naeye, B.; Raemdonck, K.; Remaut, K.; Sproat, B.; Demeester, J.; De Smedt, S. C., PEGylation of biodegradable dextran nanogels for siRNA delivery. European Journal of Pharmaceutical Sciences, 2010, 40 (4): 342-351, 2010.

[48] Murphy, E. A.; Majeti, B. K.; Mukthavaram, R.; Acevedo, L. M.; Barnes, L. A.; Cheresh, D. A., Targeted nanogels: a versatile platform for drug delivery to tumors. Molecular Cancer Therapeutics, 10 (6): 972-982, 2011.

[49] Akinc, A.; Battaglia, G., Exploiting endocytosis for nanomedicines, Cold Spring Harbor Perspectives in Biology, 5(11): a016980, 2013.

[50] Sahay, G.; Alakhova, D.Y.; Kabanov, A.V., Endocytosis of nanomedicines, Journal of Controlled Release, 145(3):182-195, 2010.

[51] Li, Y.; Maciel, D.; Rodrigues, J.; Shi, X.; Tomás, H., Biodegradable polymer nanogels for drug/nucleic acid delivery. Chemical Reviews, 115 (16): 8564-8608, 2015.

[52] Wu, H.-Q.; Wang, C.-C., Biodegradable smart nanogels: a new platform for targeting drug delivery and biomedical diagnostics. Langmuir, 32 (25): 6211-6225, 2016.

[53] Molla, M. R.; Marcinko, T.; Prasad, P.; Deming, D.; Garman, S. C.; Thayumanavan, S., Unlocking a caged lysosomal protein from a polymeric nanogel with a pH trigger. Biomacromolecules, 15 (11): 4046-4053, 2014.

[54] Wen, J.; Anderson, S. M.; Du, J.; Yan, M.; Wang, J.; Shen, M.; Lu, Y.; Segura, T., Controlled protein delivery based on enzyme-responsive nanocapsules. Advanced Materials, 23 (39): 4549-4553, 2011.

[55] Meng, F.; Hennink, W. E.; Zhong, Z., Reduction-sensitive polymers and bioconjugates for biomedical applications. Biomaterials, 30 (12): 2180-2198, 2009.

[56] Brulisauer, L.; Gauthier, M. A.; Leroux, J. C., Disulfide-containing parenteral delivery systems and their redox-biological fate. Journal of Controlled Release, 195: 147-154, 2014.

[57] Li, D.; Kordalivand, N.; Fransen, M. F.; Ossendorp, F.; Raemdonck, K.; Vermonden, T.; Hennink, W. E.; van Nostrum, C. F., Cationic nanogels: reduction-sensitive dextran nanogels aimed for intracellular delivery of antigens, Advanced Functional Materials, 25 (20): 2992, 2015.

[58] Jiang, X1.; Wang, X., Cytochrome C-mediated apoptosis, Annual Review of Biochemistry, 73:87-106, 2004.

[59] Biswas, A1.; Joo, KI.; Liu, J.; Zhao, M.; Fan, G.; Wang, P.; Gu, Z.; Tang, Y., Endoprotease-mediated intracellular protein delivery using nanocapsules. ACS Nano, 5(2):1385-1394, 2011.

[60] Li, D.; Sun, F.; Bourajjaj, M.; Chen, Y.; Pieters, E. H.; Chen, J.; van den Dikkenberg, J. B.; Lou, B.; Camps, M. G.; Ossendorp, F.; Hennink, W. E.; Vermonden, T.; van Nostrum, C. F., Strong in vivo antitumor responses induced by an antigen immobilized in nanogels via

reducible bonds. Nanoscale, 8 (47): 19592-19604, 2016.

[61] van Dijk-Wolthuis, W. N. E.; Franssen, O.; Talsma, H.; van Steenbergen, M. J.; Kettenes-van den Bosch, J. J.; Hennink, W. E., Synthesis, characterization, and polymerization of glycidyl methacrylate derivatized dextran. Macromolecules, 28 (18), 6317-6322, 1995.

[62] van Dijk-Wolthuis, W. N. E.; Kettenes-van den Bosch, J. J.; van der Kerk-van Hoof, A.; Hennink, W. E., Reaction of dextran with glycidyl methacrylate: an unexpected transesterification. Macromolecules, 30 (11): 3411-3413, 1997.

[63] Winzler, C.; Rovere, P.; Rescigno, M.; Granucci, F.; Penna, G.; Adorini, L.; Zimmermann, V. S.; Davoust, J.; Ricciardi-Castagnoli, P., Maturation stages of mouse dendritic cells in growth factor-dependent long-term cultures. The Journal of Experimental Medicine, 185 (2):317-328, 1997.

[64] Sanderson, S.; Shastri, N., LacZ inducible, antigen/MHC-specific T cell hybrids. International Immunology, 6 (3): 369-376, 1994.

[65] Coin, I.; Beyermann, M.; Bienert, M., Solid-phase peptide synthesis: from standard procedures to the synthesis of difficult sequences. Nature Protocols, 2: 3247-3256, 2007.

[66] Cory, A. H.; Owen, T. C.; Barltrop, J. A.; Cory, J. G., Use of an aqueous soluble tetrazolium/formazan assay for cell growth assays in culture. Cancer Communications, 3 (7): 207-212, 1991.

[67] Sanderson, S.; Shastri, N., LacZ inducible, antigen/MHC-specific T cell hybrids. International Immunology, 6 (3), 369-376, 1994.

[68] Zom, G. G.; Khan, S.; Britten, C. M.; Sommandas, V.; Camps, M. G.; Loof, N. M.; Budden, C. F.; Meeuwenoord, N. J.; Filippov, D. V.; van der Marel, G. A.; Overkleeft, H. S.; Melief, C. J.; Ossendorp, F., Efficient induction of antitumor immunity by synthetic toll-like receptor ligand-peptide conjugates. Cancer Immunology Research, 2 (8): 756-764, 2014.

[69] Komanduri, K. V.; Viswanathan, M. N.; Wieder, E. D.; Schmidt, D. K.; Bredt, B. M.; Jacobson, M. A.; McCune, J. M., Restoration of cytomegalovirus-specific CD4+ T-lymphocyte responses after ganciclovir and highly active antiretroviral therapy in individuals infected with HIV-1. Nature Medicine, 4 (8): 953-956, 1998.

[70] Yadav, M.; Jhunjhunwala, S.; Phung, Q. T.; Lupardus, P.; Tanguay, J.; Bumbaca, S.; Franci, C.; Cheung, T. K.; Fritsche, J.; Weinschenk, T.; Modrusan, Z.; Mellman, I.; Lill, J. R.; Delamarre, L., Predicting immunogenic tumour mutations by combining mass spectrometry and exome sequencing. Nature, 515 (7528): 572-576, 2014.

[71] Foged, C.; Brodin, B.; Frokjaer, S.; Sundblad, A., Particle size and surface charge affect particle uptake by human dendritic cells in an in vitro model. International Journal of Pharmaceutics, 298(2):315-322, 2005.

[72] Slawek, A.; Maj, T.; Chelmonska-Soyta, A., CD40, CD80, and CD86 costimulatory molecules are differentially expressed on murine splenic antigen-presenting cells during the pre-implantation period of pregnancy, and they modulate regulatory T-cell abundance, peripheral cytokine response, and pregnancy outcome. American Journal of Reproductive Immunology, 70 (2): 116-126, 2013.

[73] Bancos, S.; Tyner, K. M.; Weaver, J. L., Immunotoxicity testing for drug–nanoparticle conjugates: regulatory considerations. In Handbook of Immunological Properties of Engineered Nanomaterials, McNeil, S. E., Ed. World Scientific Publishing Ltd.: Singapore, pp 671-685.

[74] Sakaguchi, S.; Yamaguchi, T.; Nomura, T.; Ono, M., Regulatory T cells and immune tolerance. Cell, 133 (5): 775-787, 2008.

7

A POLY-NEOANTIGEN DNA VACCINE SYNERGIZES WITH PD-1 BLOCKADE TO INDUCE T CELL-MEDIATED TUMOR CONTROL

Tondini E, Arakelian T, Oosterhuis K, Camps M, van Duikeren S, Han W, Arens R, Zondag G, van Bergen J, Ossendorp F

Oncoimmunology. 2019;8(11):1652539

ABSTRACT

The combination of immune stimulating strategies has the potency to improve immunotherapy of cancer. Vaccination against neoepitopes derived from patient tumor material can generate tumor-specific T cell immunity, which could reinforce the efficacy of checkpoint inhibitor therapies such as anti-PD-1 treatment. DNA vaccination is a versatile platform that allows inclusion of multiple neoantigen-coding sequences in a single formulation and therefore represents an ideal platform for neoantigen vaccination. We developed an anti-tumor vaccine based on a synthetic DNA vector designed to contain multiple cancer-specific epitopes in tandem. The DNA vector encoded a fusion gene consisting of three neoepitopes derived from the mouse colorectal tumor MC38 and their natural flanking sequences as 40 amino acid stretches. In addition, we incorporated as reporter epitopes the helper and CTL epitope sequences of ovalbumin. The poly-neoantigen DNA vaccine elicited T cell responses to all three neoantigens and induced functional CD8 and CD4 T cell responses to the reporter antigen ovalbumin after intradermal injection in mice. The DNA vaccine was effective in preventing outgrowth of B16 melanoma expressing ovalbumin in a prophylactic setting. Moreover, the combination of therapeutic DNA vaccination and anti-PD-1 treatment was synergistic in controlling MC38 tumor growth whereas individual treatments did not succeed. These data demonstrate the potential of DNA vaccination to target multiple neoepitopes in a single formulation and highlight the cooperation between vaccine-based and checkpoint blockade immunotherapies for successful eradication of established tumors.

INTRODUCTION

Tumor cells accumulate somatic point mutations that can alter wild-type protein sequences making them immunologically different from healthy cells. T cells can detect these alterations by virtue of recognition of processed and presented peptides up to single amino acid alterations, named antigenic neoepitopes (1). However, the initiation of spontaneous tumor-specific T cell responses is limited by the lack of proper immune stimulation and is often dampened by the immune suppressive activity exerted by the tumor (2). Checkpoint inhibitor therapies unleash these T cells and result in long-term survival of patients with previously untreatable cancers (3). Still, only a minority of patients benefits from checkpoint inhibitor therapies, leaving room for complementary strategies (4). These may include vaccination against neoantigens, which can not only boost pre-existing responses, but also induce *de novo* priming of tumor-specific T cells.

The design of personalized cancer vaccines harboring tumor mutations is still in early stage and needs to meet several requirements (5). Exact prediction of the neoantigens likely to generate a peptide epitope that will bind to the relevant MHC alleles and induce functional T cell responses is still not fully achievable by the current *in silico* systems used for epitope prediction. Therefore, it is required to include a sufficient number of candidate sequences to increase chances of including actual T cell epitopes in the vaccine. Furthermore, the inclusion of multiple antigens could promote the generation of a broad immune response, which may enhance vaccine efficacy and contribute to counteract immune suppression. Another requisite for patient-tailored cancer vaccines is versatility in synthesis and production of several different sequences, as the heterogeneous array of antigen sequences varies across individual patients. This aspect is not trivial in classical peptide-based systems, as amino acid sequence dictates the physicochemical properties of the vaccine, adding complications to the manufacturing process and formulation (6). In short, an ideal neoantigen vaccine platform should be flexible enough to be able to incorporate a multitude of epitopes and allow fast and reliable production independently of the exact amino acid sequences of the selected epitopes.

In the last few years efforts in refining neoantigen identification and formulation of cancer vaccines for therapeutic treatment have demonstrated the potential of this approach in preclinical models for synthetic peptide- and RNA-based vaccines (7-10). These studies have led the way for the first in-human application in two independent pioneering trials in melanoma patients (11, 12). Vaccination

with neoepitopes derived from single amino acid mutations selected upon sequencing of patients' material elicited tumor-specific T cell responses with clinical benefits both with peptide- and RNA-based vaccines.

Up until recently, DNA-based vaccines targeting neoantigen have been scarcely explored. DNA represents a versatile platform that can accommodate any sequence without affecting its stability or solubility. In addition, DNA is easily synthesized and production costs are relatively low. DNA vaccines were first shown to be immunogenic nearly 30 years ago (13-15). Since then, numerous studies have explored the potential of gene immunization. Methods for optimizing administration routes, delivery and plasmid design have been central in a variety of preclinical and clinical studies (16). Several studies demonstrated that immune responses can be induced by intramuscular, intradermal or intravenous administration of DNA (14, 17, 18) and original administration devices such as gene gun (19), electroporation (20) and tattooing (21) have been employed to improve transfection efficiency and induction of both humoral and cellular immune responses. A recent study using electroporation-mediated DNA delivery of multiple neoantigen constructs showed effective induction of anti-tumor CD8 T cell responses in mice (22).

In this study we show efficacy of DNA vectors as a vaccine carrier for multiple neoantigens based on a string-of-bead design. Using regular intradermal injection without the need of specialized equipment or an adjuvant, the DNA vaccine induced multiple CD8 and CD4 T cell responses against both reporter epitopes and neoantigens. We demonstrate that vaccination enables T cell mediated anti-tumor control in a prophylactic as well as in a therapeutic setting. Furthermore, we show that DNA vaccination can synergize with and improve the efficacy of checkpoint inhibitor therapy.

RESULTS

Development of a poly-neoantigen DNA vaccine for in vitro and in vivo antigen presentation to T cells.

We aimed to include multiple antigenic sequences in a single DNA vaccine construct, and therefore we designed a plasmid encoding five epitopes in tandem in a single open reading frame (**Fig. 1A**). Three epitopes (Dpagt, Reps1, Adpgk) are described neoantigens containing specific point-mutated MHC class I binding sequences present in the mouse colon carcinoma cell line MC38 (7). The other two epitopes are respectively the helper (Help) and the cytotoxic T lymphocyte

(CTL) epitopes from the model antigen chicken ovalbumin (OVA), and were included as control reporter epitopes for CD4 and CD8 T cell responses, respectively. Every epitope is flanked by its natural amino acid sequence for a total length of approximately 40 amino acids, and is linked to the next epitope by a linker encoding four alanines. Transcription is driven by the strong viral promoter of the immediate early gene 1 (IE1) of human cytomegalovirus (HCMV).

We first analyzed whether these five artificially connected sequences lead to the generation of the expected peptide epitopes and their presentation on MHC molecules. Upon transfection of the designed DNA construct, the translated protein product needs to be processed in such a way that the T cell epitopes are generated and presented by MHC molecules. MC38 cells, which do not express the ovalbumin gene, were transfected with the neoantigen construct and the presentation of the ovalbumin CTL epitope SIINFEKL was detected by staining the SIINFEKL/H2-K^b complex with the 25-D1.16 antibody (**Fig. 1B,** upper panel). Transfection with the poly-neoantigen construct, but not with a control GFP-encoding construct, displayed positive staining for SIINFEKL/H2-K^b complexes. Moreover, after transfection with the neoantigen construct, cells were recognized by the hybridoma T cell line B3Z, which express a TCR specific for SIINFEKL/H2-K^b (**Fig. 1B**, lower panel).

Next, we tested the ability of the neoantigen DNA construct to transfect cells and present the expected reporter ovalbumin epitopes *in vivo*. The plasmid was injected intradermally in mice 7, 4, 2, or 0 days prior transfer of CFSE-labelled OT-I and OT-II T cells, which possess transgenic TCRs specific respectively for the CTL and the helper epitopes of ovalbumin. Antigen induced proliferation of these cells was analyzed 3 days after transfer in draining lymph nodes and spleen (**Fig. 1C and D, Fig. S1 A and B**). Injection of the construct was able to induce both OT-I and, to a lesser extent, OT-II proliferation, confirming successful transfection and presentation of the epitopes also *in vivo*. OT-I and OT-II proliferation upon DNA vaccine injection exhibited different kinetics compared to traditional synthetic peptide vaccine (**Fig. 1D**). DNA vaccination presents a slower onset of T cell proliferation compared to peptide vaccination, with optimal induction between 5 and 7 days after DNA vaccination (**Fig. 1D**, *left panel*), as opposed to 3 days for peptide vaccination (**Fig. 1D**, *right panel*).

Finally, we evaluated whether the position of the epitopes or the artificial linker sequence between them could influence the efficiency of antigen presentation *in vivo*. To test this, we created a variant of the original neoantigen DNA construct

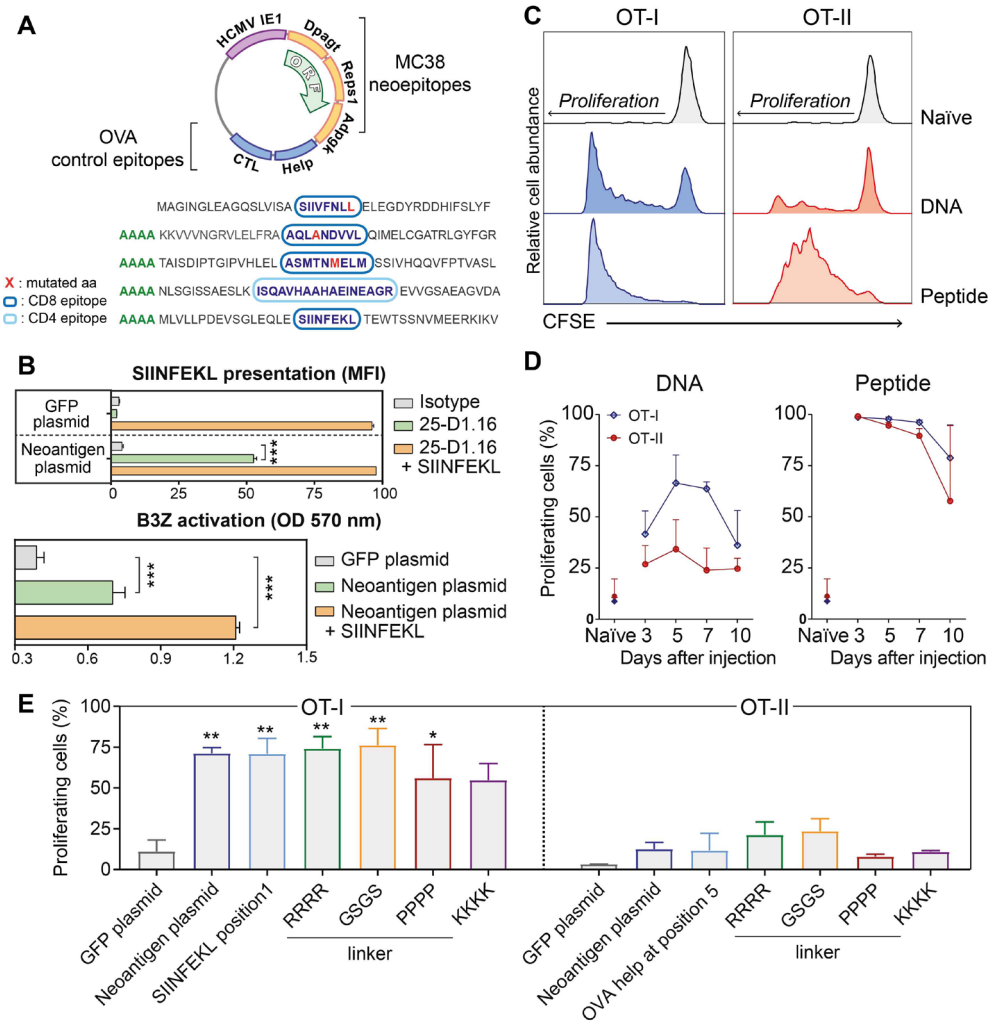

in which the reporter SIINFEKL epitope was positioned as the first epitope at the N-terminal end of the polypeptide and additional variants in which the epitopes were connected via different amino acid linkers. We evaluated OT-I and OT-II proliferation upon vaccination *in vivo* (**Fig. 1E**). Overall, we observed no significant differences in OT-I or OT-II proliferation between the variants tested. Altogether these results demonstrate efficient MHC surface presentation of the CD8 and CD4 reporter epitopes of ovalbumin, irrespective of the position and linker sequence in the poly-antigen encoding DNA construct. This shows the feasibility of the string-of-bead design as a method to target multiple antigens in a single vaccine construct.

Figure 1: The poly-antigen DNA vaccine activates antigen-specific CD8 and CD4 T cells *in vivo*. A) Schematic representation of the neoantigen DNA vaccine and the resulting poly-epitope peptide sequence. Direction of the open reading frame (ORF) is indicated. The individual CD8 and CD4 epitopes in the peptide are encircled in dark or light blue, respectively. For each of the three neoepitopes, the amino acid (aa) change resulting from somatic mutation is highlighted in red. **B)** *Upper panel*: Quantification of the mean fluorescence intensity (MFI) using 25-D1.16 antibody of the SIINFEKL peptide presentation on MHC I molecule after transfecting MC38 cells *in vitro* with either the GFP plasmid (negative control) or the neoantigen plasmid. *Lower panel:* Activation of SIINFEKL-specific T cell hybridoma B3Z cells by MC38 cells transfected with the neoantigen DNA vaccine. The SIINFEKL synthetic peptide (1 µM) was added as a positive control (orange bars), and a plasmid coding for GFP was used as a negative control. Statistical significance was determined by t test, ***p<0.0001 **C)** Proliferation of adoptively transferred OT-I and OT-II cells, 3 days after intradermal injection of 10 µg of the neoantigen DNA vaccine. **D)** Kinetics of *in vivo* antigen presentation to OT-I or OT-II cells after injection of the DNA construct. Proliferation of the OT-I (blue lines) and OT-II cells (red lines) measured by CFSE dilution in the inguinal lymph nodes of C57BL/6 mice immunized with either neoantigen DNA vaccine (*left panel*) or 50 µg of OVA CTL and helper peptides (*right panel*), used as positive controls for OT-I and OT-II cells proliferation, respectively. Error bars indicate mean ± SEM, N=2. **E)** Proliferation of adoptively transferred OT-I and OT-II cells, 3 days after intradermal injection of 10 µg of different variants of neoantigen DNA vaccine. Error bars indicate mean ± SEM, N=2. Significance in relation to the GFP plasmid negative control was determined by t-test.

The DNA vaccine primes neoantigen-specific T cell responses in vivo

Next, we evaluated the ability of our DNA vaccine to generate all five encoded epitopes *in vivo* and its ability to induce *de novo* priming of antigen-specific T cells in wild-type C57BL/6 mice. Previous studies have highlighted an influence on vaccine efficacy depending on its formulation, methods and routes of administration (14, 17, 18, 28). To determine the optimal delivery route of our designed DNA vaccine, the construct was administered to mice via different routes (intradermal, subcutaneous, intramuscular, intraperitoneal and intravenous) and the immune response was boosted twice in intervals of two weeks (**Fig. S2A**). Tetramer staining in blood at several time points revealed effective priming of SIINFEKL-specific CD8 T cells for the groups that intradermally and intravenously received the DNA vaccines (**Fig. S2B** and **S2C**). In addition, splenocytes of vaccinated mice restimulated *ex vivo* with peptide-loaded dendritic cells displayed responses for all five epitopes encoded by the DNA vaccine (**Fig. S2D** and **S2E**). We concluded that intradermal injection of the neoantigen DNA vaccine was able to induce *de novo* priming of T cells upon classical needle-mediated administration *in vivo*.

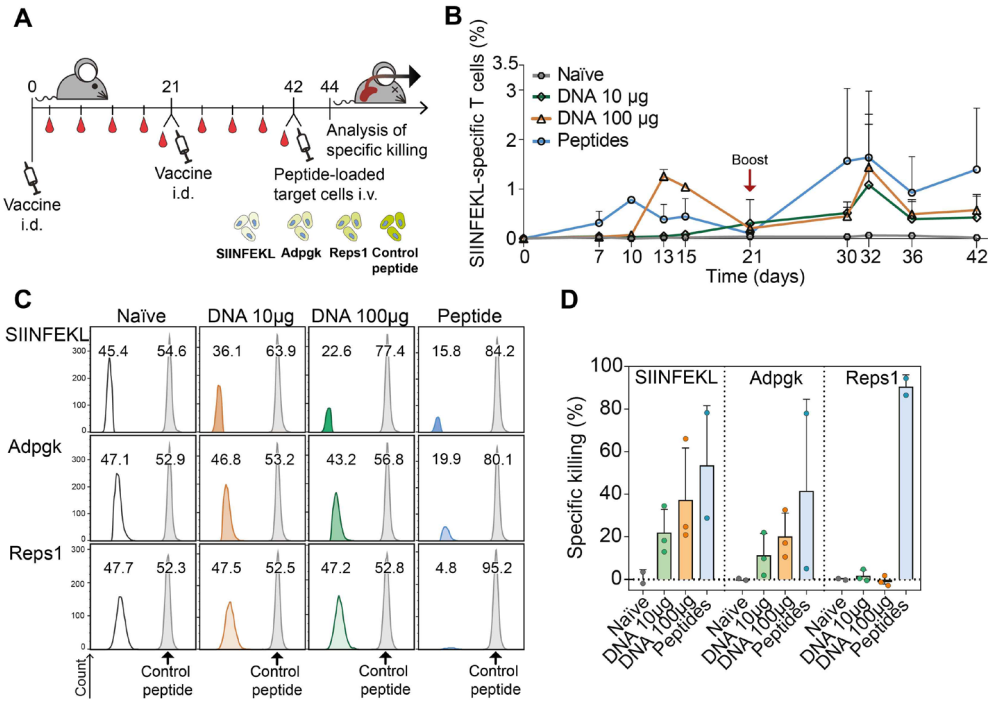

Figure 2: DNA vaccine primed T cells are functional. A) Schematic representation of the vaccine administration, tetramer staining, target cells injection and specific killing analysis schedule in C57BL/6 mice. Mice were vaccinated intradermally with 10 or 100 µg of DNA (or a mix of peptides as positive control). SIINFEKL-specific responses were monitored in blood at different time points. To evaluate killing capacity of the responses induced after vaccination, mice were injected with CFSE-labelled splenocytes loaded with minimal peptides and specific killing was analyzed two days later. **B)** Kinetics of the SIINFEKL-specific $CD8^+$ T cells responses induced by the vaccines measured by SIINFEKL-H2-K^b tetramers, reported as percentage of total $CD8^+$ T cells. **C)** Representative flow cytometry histograms of CFSE-labelled antigen- or control peptide-loaded splenocytes detected in naïve and vaccinated mice. Two days after transfer, these target cells were detected in the spleen and specific killing was calculated. Percentages represent the relative proportions between cells loaded with irrelevant peptide (in grey) and target cells (white, orange, green or blue). **D)** Specific killing by T cells in naïve mice versus mice vaccinated with DNA (10 or 100 µg) or peptide after transfer of antigen-loaded splenocytes. Error bars indicate mean ± SEM.

To evaluate the cytotoxic function of the DNA vaccine-induced CD8 T cells, we analyzed the kinetics of the SIINFEKL-specific CD8 T cells and their capacity to specifically kill target cells presenting the epitopes. We also explored the dosing of plasmid administration to optimize the T cell response. C57BL/6 mice were vaccinated and boosted with two different doses of DNA vector or with peptides, and the ability to kill splenocytes loaded with either SIINFEKL, Adpgk or Reps1

peptide was determined (**Fig. 2A**). The kinetics of DNA vaccination was slower compared to the synthetic peptide vaccination, as the peak of the priming response appeared 3 days later (**Fig. 2B**). After the boost, T cell responses to DNA and peptide vaccination were similar. Considering the dose, 100 µg of DNA appeared to be more effective mostly in the priming phase.

CD8 T cells primed by DNA were effective in killing SIINFEKL and Adpgk peptide-loaded T cells at day 44. Cytotoxicity against the Reps1 epitope was not detected upon DNA vaccination (**Fig. 2C and 2D**). Vaccination with a higher dose of DNA marginally improved the killing capacity of the SIINFEKL-specific CD8 T cells and correlated with the levels of tetramer-specific cells present in blood two days before injecting target cells (see **Fig. 2B,** day 42). Based on these results we concluded that the poly-neoantigen DNA vaccine is able to induce functional CD8 T cells against multiple epitopes and we proceeded to evaluate its efficacy in immune control of cancer.

Prophylactic and therapeutic DNA vaccination elicits tumor control

We next investigated whether the T cell responses induced by DNA vaccination were able to provide immune control of tumors *in vivo* for both the OVA reporter epitopes and the neoantigens.

First, we evaluated anti-tumor efficacy for the reporter ovalbumin epitopes. Mice were prophylactically vaccinated with DNA or peptides before being challenged with the OVA-expressing melanoma cell line B16-OVA (**Fig. 3A**). To explore the impact of DNA dosing on the induction of T cell responses, two different amounts of DNA were tested and the induction of ovalbumin-specific CD8 responses was monitored by tetramer staining in blood samples (**Fig. S3**). Unvaccinated control mice developed tumors within 20 days from challenge. Mice vaccinated with DNA developed tumors later than unvaccinated controls, and a significant number of mice were fully protected from this aggressive tumor. A lower dose of vaccine corresponded to a lower protection but was still effective to prevent tumor growth in ~40% of the animals (**Fig. 3B** and **3C**). Vaccination with a higher dose of DNA resulted in full protection of 60% of the mice (**Fig. 3B** and **3C**). Hence, DNA vaccines were effective in inducing protective antitumor T cell responses, comparable or better than the mice that received synthetic peptide vaccination. Moreover, a higher dose of vaccine corresponded to stronger protection, and this dose was used for further studies in a therapeutic setting.

After demonstrating the potential for antitumor activity of the DNA vaccine in the B16 melanoma model, which expresses the ovalbumin antigen but not

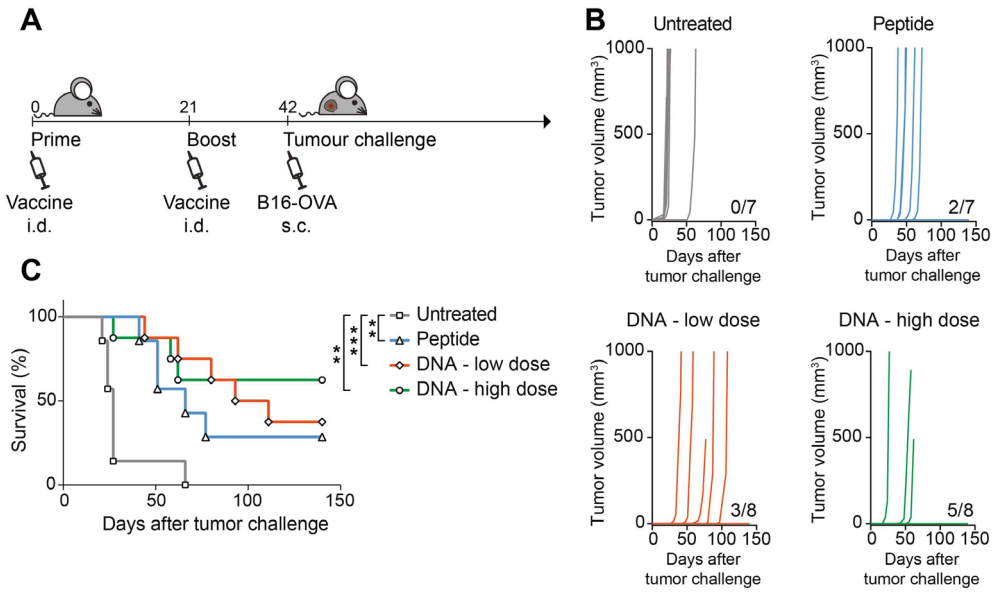

Figure 3: DNA vaccination protects from challenge with B16-OVA. A) Schematic representation of the schedule followed for vaccine administration and tumor challenge in C57BL/6 mice. Mice were vaccinated with a low (10 µg) or a high (90 µg) dose of DNA or with peptide and subsequently challenged with B16-OVA melanoma cells. Tumor growth was monitored for 150 days after challenge. **B)** Tumor growth curves (represented in mm^3) of individual mice in non-vaccinated versus vaccinated groups. The number of tumor-free mice for each vaccination group is indicated. Shown is one of two independently performed experiments which resulted in similar outcomes. **C)** Overall survival of mice either untreated or vaccinated with peptide or DNA vaccines. Statistical significance was determined via Log-rank Mantel-Cox test. $^{**}p<0.01$, $^{***}p<0.0001$.

the MC38-specific neoantigens, we evaluated the therapeutic efficacy of the same DNA vaccine in the MC38 tumor model. Mice were first inoculated with the MC38 colon carcinoma cell line, expressing the three neoantigens Dpagt1, Reps1 and Adpgk but not the ovalbumin epitopes. Mice with established tumors were vaccinated therapeutically on day 5 followed by a booster vaccination at day 26. As MC38 is known to exert a strong immunosuppressive effect (29), we combined the vaccine with the immunomodulatory anti-PD-1 antibody treatment on day 8,12, 22 and 29 (**Fig. 4A**). Without any treatment, tumors progressed rapidly and all mice succumbed within 21 days from tumor inoculation. Vaccination with DNA or peptides gave little or no delay and eventually all mice showed rapid tumor outgrowth, except for one mouse in the DNA vaccinated group. Anti-PD-1 treatment induced some delay in tumor growth, but was not sufficient to prevent tumor outgrowth. Remarkably, when anti-PD-1 treatment was combined with

DNA vaccination, tumor growth was significantly delayed and 25% of mice were able to clear the tumor and survive long term (**Fig. 4B** and **4C**). Notably, this effect was only observed with DNA vaccination but could not be achieved with the synthetic peptide vaccine.

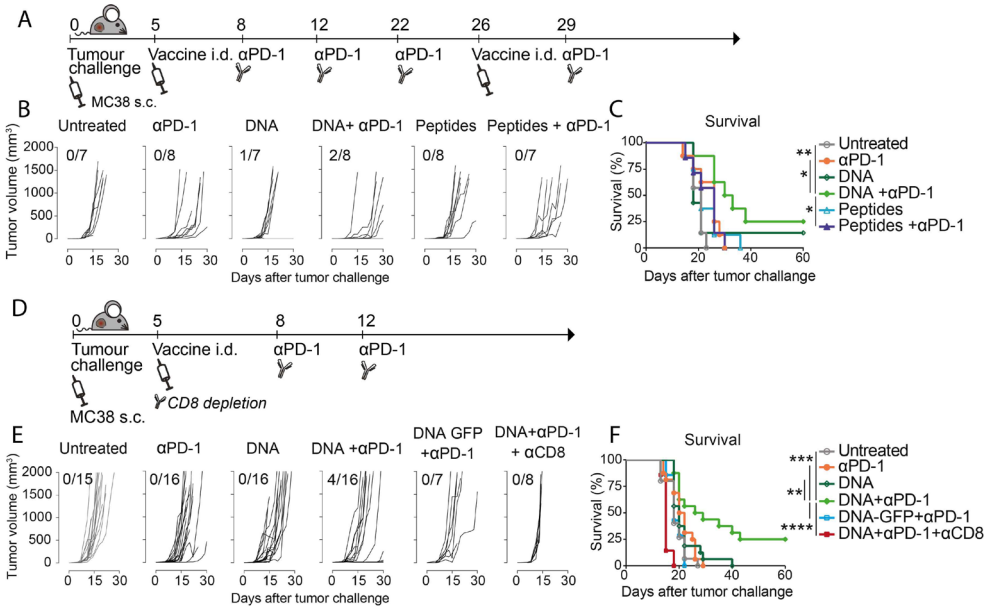

Figure 4: Therapeutic DNA vaccination combined with anti-PD-1 treatment promotes tumor eradication in CD8 T cell-dependent manner. A) Schematic representation of the MC38 tumor challenge experiment in C57BL/6 mice in therapeutic setting. Mice were injected subcutaneously with MC38 cells at day 0, vaccinated with DNA construct at days 5 and 26. Vaccination was combined with anti-PD-1 treatment at days 8, 12, 22 and 29. Tumor growth was monitored for 60 days after challenge. **B)** Tumor growth curves (measured in mm^3) of individual mice in untreated or treated with single or combined anti-PD-1, DNA vaccine and peptide mix. The number of tumor-free mice for each group is indicated. **C)** Overall survival of mice represented in **B**. **D)** Schematic representation of the MC38 tumor challenge experiment in C57BL/6 mice and depletion of CD8 cells during vaccine and anti-PD-1 combination treatment. Mice were injected subcutaneously with MC38 cells at day 0, injected with anti-CD8 antibody at day 5, vaccinated with DNA construct and injected with anti-PD-1 antibody at days 5, 8 and 12. **E)** Tumor growth curves (measured in mm^3) of individual mice untreated or treated with single or combined anti-PD-1, DNA vaccine and anti-CD8. The number of tumor-free mice for each group is indicated. Vaccination with a control DNA construct (DNA-GFP) that does not contain the three MC38-specific neoantigens is used as a negative control. **F.** Overall survival of mice represented in **E.** Statistical significance was determined via Log-rank Mantel-Cox test. * $p<0.05$, **$p<0.01$, *** $p< 0.001$, **** $p<0.0001$

In addition, a single dose of the DNA vaccine combined with anti-PD-1 treatment (**Fig. 4D**) also resulted in substantial delay of tumor outgrowth and complete tumor clearance was observed in some mice, resulting in a 25% cure rate. (**Fig. 4E** and **4F**). Importantly, this effect was not observed when vaccination was performed with a GFP-coding plasmid and was abolished when CD8 T cells were depleted right after vaccination, indicating the implication of neoantigen-specific CD8 T cell responses in tumor growth control. Altogether these data demonstrate that the designed poly-neoantigen DNA construct is an effective vaccine vector and that this design holds potential for neoantigen vaccination for specific immunotherapy of cancer.

DISCUSSION

In this study we demonstrate that a poly-neoantigen DNA vaccine not only provides prophylactic protection against tumor challenge but also synergizes with PD-1 blockade for tumor control in a therapeutic setting. The versatile DNA platform presented here allows the inclusion of multiple epitopes in tandem derived from multiple antigenic sequences, increasing the chances of triggering relevant T cell responses to improve the overall effectiveness of neoantigen-specific immunotherapy.

Our vaccine vector was able to induce functional responses without any additional adjuvant. DNA vectors may act as self-adjuvating vaccines as the innate immune system possesses various means to sense foreign or cytoplasmic DNA and activates an inflammatory response. Low unmethylated CpG rich regions linked to bacterial production of the DNA vaccine may contribute to immunogenicity via TLR9 signaling (30, 31). Furthermore, cytoplasmic sensors in the STING axis were also reported to play a role in DNA-mediated immunization (32). Nevertheless, efforts in optimizing the immunogenicity of DNA vaccines demonstrated that the inclusion in the sequence of pro-inflammatory cytokines such as IL-12 (33) and GM-CSF (34-36) and costimulatory-molecules such as B7-1, B7-2 (37, 38) or CD40L (39) have a beneficial effect in generating effective immune responses. As we report significant but partial tumor control, it will be of interest to improve the cure rate by including such genetic adjuvants, which can readily be incorporated in the vaccine sequence.

The induction of CD8 as well as CD4 T cell responses is critical for cancer immunotherapy, as the ability of cytotoxic CD8 T cells to effectively attack and kill tumor cells depends on the presence of concomitant help provided by CD4 T

cells (40, 41). This is especially important given the high frequency of CD4 neo-epitopes in tumor cells (9, 11, 12), and given recent observations that CD4 T cells can control tumors independently of CD8 T cells (42, 43). In a recent report, applying neoantigen DNA vaccination with electroporation resulted preferentially in the induction of CD8 responses (22). In contrast, our intradermal DNA vaccination approach efficiently induced both CD8 and CD4 responses. Our data indicate that both MHC I and MHC II presentations occur; however induction of CD8 T cell responses appears more pronounced than induction of CD4 responses. This may suggest that antigen presentation is performed mainly by directly transfected cells and consequently cytosolic antigen is more efficiently presented. MHC II presentation occurs mainly on exogenously acquired antigen by specialized antigen presenting cells (APCs). Previous reports investigating the working mechanism of intradermal DNA vaccination have highlighted that transfection takes place both in epidermal cells and, to a lesser extent, directly in professional APCs (44, 45). It is still controversial whether antigen presentation upon DNA vaccination occurs by directly transfected cells or antigen is indirectly acquired from transfected cells by APCs (46).We believe that it will be important to elucidate the mechanism in the context of intradermal DNA vaccination in order to control and elicit optimal MHC II presentation.

The chosen colon cancer cell line MC38 tumor model represents a clinically relevant tumor both in light of neoantigen vaccination studies as well as immunomodulatory treatments. MC38 is known to induce spontaneous CD8-mediated immune responses in mice with growing tumors but due to its highly immunosuppressive microenvironment, these T cells are apparently inactive and not able to eradicate tumor cells (29). Treatment of MC38 tumor-bearing mice at early stages with immunomodulating antibodies against PD-1 or PD-L1, elicit effector T cell responses which can mediate tumor regression (27). Here we show that vaccination against the selected neoantigens (7) in combination with anti-PD-1 can mediate tumor regression in a CD8 T cells-dependent fashion, while anti-PD-1 antibody by itself could not effectuate tumor clearance. Physiologically, the PD-1 axis contributes to negatively regulate peripheral activated CD8 T cells but malignant cells exploit this mechanism to shutdown spontaneous tumor-specific T cells responses. Indeed, a recent report by Xiong and colleagues showed that neo-epitope specific CD8 T cells express high level of co-inhibitory molecules, including PD-1 (47). When CD8 T cells are properly activated, by means of vaccination for example, they also upregulate PD-1 and are

therefore more susceptible to immune suppression. Accordingly, integration of anti-PD-1 blockade therapy resulted in complete response in both RNA- and peptide-based vaccination clinical studies for respectively one (11) and two (12) patients that experienced recurrence after vaccination. Altogether these observations show that specific immunotherapy can synergize with PD-1 checkpoint therapy most likely by supporting adequate effector functions of the increased frequencies of tumor-specific T cells.

Immunization with multiple epitopes in one formulation may result in reduced responses to individual epitopes. The occurrence of immune-dominant neoantigens has been reported in several studies (48-50). Nevertheless, a study identifying neoepitopes in patients with chronic leukemia reports how immune-dominance plays a role primarily in the induction of spontaneous responses, while vaccination against multiple epitopes diversifies the tumor-specific T cell repertoire and amplifies the heterogeneity of tumor-specific T cell responses (50). In addition, tumor immunoediting could lead to antigen loss and the outgrowth of resistant tumor variants that do not possess one or more of the targeted neoantigens. The inclusion of multiple epitopes in a vaccine may be important to avoid the outgrowth of such resistant clones. Therefore, the beneficial effects of a more diversified T cell response are likely to outweigh a potential reduction of individual T cell specificities due to immuno-dominance.

Interestingly, we observed that primarily the Adpgk neoepitope appears to induce effector T cells which are able to recognize and eliminate antigen-loaded cells (see **Fig.2D**). In contrast, DNA-induced Reps1 specific T cells were not able to kill target cells as opposed to the responses induced by peptide vaccination. Differences in induction of T cell responses depending on the method of immunization have also been reported in RNA vaccination studies (9). Why these differences between peptide and gene immunization occur is as yet not clear; however, considering the notion that some responses to tumor neoantigens can still be irrelevant for tumor eradication (51), these observations support the rationale of including multiple potential neoantigens in therapeutic cancer vaccines.

Personalized therapy against tumor neoantigens represents an exciting prospect for clinical translation. A personalized therapeutic cancer vaccine requires a flexible, cost-effective vaccine platform. Here, we show a proof of concept of a DNA vector as a versatile vaccine platform for inclusion of multiple tumor neoantigens. Moreover, we show that this DNA vaccine synergizes with anti-PD-1 treatment in tumor control. Our data report the potency of stimulating tumor-specific

responses via DNA vaccination in a string-of-bead design to achieve effective immunotherapy and underline the importance of combining different immunotherapy strategies in order to achieve effective clinical responses.

METHODS

Animals. For vaccination and tumor experiments, 6-8 weeks old female C57BL/6 were purchased from Charles River Laboratories. The TCR transgenic OT-I and OT-II mouse strains were obtained from Jackson Laboratory and maintained on CD45.1^{+} C57BL/6 background. Mice were housed in specific pathogen-free (SPF) conditions at the LUMC animal facility. All animal experimentations were approved by and according to guidelines of the Dutch Animal Ethical Committee.

Cell lines. The B3Z hybridoma cell line was cultured in IMDM medium (Lonza) supplemented with 8% FCS (Greiner), penicillin and streptomycin, glutamine (Gibco), β-mercaptoethanol (Merck), hygromycin B (AG Scientific Inc) to maintain expression of the beta-galactosidase reporter gene. B16-OVA and MC38 tumor cell lines were cultured in IMDM medium supplemented with penicillin/streptomycin, glutamine and 8% FCS. B16-OVA were cultured in the presence of G418 (Life Technologies) for maintenance of OVA expression (23). For ex vivo stimulation of lymphocytes, the dendritic cell line D1 was used and cultured as previously described (24).

DNA construct and peptides. Codon-optimized antigen sequences, fused by alanine linkers were synthesized and cloned into a CMV-driven expression vector containing a rabbit beta-globin poly-A signal and kanamycin resistance marker (ATUM). As control, DasherGFP was cloned in the same plasmid vector. Plasmids were propagated in *E. coli* cultures and purified using Nucleobond Xtra maxi EF columns (Macherey-Nagel) according to manufacturer's instructions. For vaccination, plasmids were column-purified twice, each time using a fresh column, and dissolved at 3 mg/ml in TrisEDTA buffer (1:0.1 mM). Synthetic long peptides for the five **epitopes** were synthetized by LUMC peptide facility **SIIVFNLL**ELEGDYR (Dpagt), LFRA**AQLANDVVL**QIM (Reps1), EL**ASMTNMELM**SSIV (Adpgk), ISQAVHAAHAEINEAGR (OVA CD4), DEVSGLEQLE**SIINFEKL**AAAAAK (OVA CD8) and used as peptide controls for all experiments.

***In vitro* transfection and antigen recognition assay.** 3'000 MC38 cells were seeded overnight in 96-well flat bottom plates. Next day, cells were transfected using the SAINT-DNA transfection kit (SD-2001, kindly provided by Synvolux). In brief, a solution of plasmids and cationic lipids was mixed in a ratio 1:20 (µg

DNA: µl Saint-DNA) in titrating quantities. SIINFEKL presentation by H2-K^b was detected with 25-D1.16 antibody (25) in-house conjugated to Alexa 647. After 48 hours, 50'000 B3Z cells per well were added and incubated with transfected cells overnight. The following day, TCR activation triggered by recognition of the SIINFEKL epitope was detected by measurement of absorbance at 570 nm upon colour conversion of chlorophenol red-β-D-galactopyranoside (Calbiochem®, Merck).

***In vivo* proliferation of adoptively transferred OT-I and OT-II cells.** Naïve C57BL/6 mice received an intradermal injection of lipoplexes comprising vaccine or control plasmids complexed to cationic lipid SAINT18 (kindly provided by Synvolux) (26) 7, 4, 2 or 0 days prior transfer of ovalbumin specific OT-I and OT-II cells. $CD8^+$ cells or $CD4^+$ cells were isolated from spleens and lymph nodes of $CD45.1^+$ OT-I or OT-II mice with enrichments sets (BD Biosciences), labelled with 5 µM CFSE (Invitrogen) and intravenously injected in vaccinated mice. Three days after transfer, proliferation of OT-I and OT-II cells was measured in lymph nodes and spleens by CFSE detection in $CD45.1^+/CD8^+$ or $CD45.1^+/CD4^+$ T cells.

Vaccination with peptide mix. Peptide vaccination was used as positive control for priming and tumor experiments *in vivo*. It consisted of a mix of 50 µg of the five long peptides containing the five epitopes encoded in the DNA vaccine. The formulation was adjuvanted with 20 µg of poly(I:C) (Invivogen)

Priming of endogenous T cells. Naïve C57BL/6 mice were injected with plasmid-SAINT18 complexes in a 1:0.75 ratio (µg DNA : nmole SAINT18) in 0.9% NaCl (26) either intradermally (30 µl), subcutaneously (30 µl), intramuscularly (30 µl), intraperitoneally (100 µl) or intravenously (100 µl) and boosted after 14 and 28 days. The level of SIINFEKL-specific CD8 T cells was monitored in blood with labelled tetramers. Twelve days after second booster injection, splenocytes were harvested and expanded for one week with D1 dendritic cells loaded with long peptide pools. Intracellular staining was performed upon stimulation with individual long peptides overnight in presence of 2 µg/ml Brefeldin A (Sigma Aldrich). T cells and cytokines were detected by antibody staining and analyzed with FlowJo software. The following antibody mix was used: eFluor450 anti-CD3, PE-Cy7 anti-CD4 (eBioscience), BV605 anti-mouse CD8α, APC anti-IFNγ (Biolegend), FITC anti-TNFα (eBioscience), PE IL-2 (eBioscience).

***In vivo* specific killing**. Naïve C57BL/6 were primed and boosted after 21 days with 10 or 100ug of plasmid-SAINT18 complexes. 21 days after boost, vaccinated mice received peptide-loaded splenocytes to measure cytotoxic activity of en-

dogenously primed T cells. To this end, splenocytes were harvested from CD45.1$^+$ or WT C57BL/6 naïve mice, labelled with 5, 0.25 or 0.0025 µM CFSE and differentially loaded for 1 hour at 37ºC with 1µM SIINFEKL, Adpgk or Reps1 epitopes or an irrelevant peptide epitope derived from the E6 protein of Human Papilloma Virus (sequence: RAHYNIVTF). 4'000'000 splenocytes per peptide-loaded group were injected intravenously in vaccinated mice. One day after transfer, mice were sacrificed and single cell suspension were analyzed by flow cytometry. Specific killing was calculated according to the following equation: Specific killing = 100 - [100***(**(CFSE target peptide)/(CFSE irrelevant) immunized mice**)**/**(**(CFSE target peptide)/(CFSE irrelevant) naïve mice**)**]

Prophylactic vaccination and B16-OVA tumor challenge. Naïve C57BL/6 female mice were vaccinated intradermally with 10 or 90 µg of plasmid-SAINT18 complexes. At day 42 (21 days after booster injection) 50'000 B16-OVA cells were injected subcutaneously in the flank and tumor growth was monitored. Mice were sacrificed when the tumor volume surpassed 1000 mm^3.

MC38 tumor challenge and therapeutic vaccination. Naïve C57BL/6 female mice were injected subcutaneously in the flank with 350'000 MC38 cells and tumor growth was monitored. When tumors reached a palpable size with an estimated volume of 1 to 2 mm^3 (day 5), mice were vaccinated with 10ug of plasmid-SAINT18 complexes. Three and 7 days after vaccination, 50 µg of anti-PD-1 (Clone RMP1-14, InvivoPlus, BioXCell) antibody was injected subcutaneously next to the tumor mass (27). Mice were sacrificed when the tumor volume surpassed 1'000 mm^3.

Statistical analysis. Results are expressed as mean ± SD. Statistical significance among groups was determined by multiple comparison using the Graphpad software after ANOVA or non-parametric Kruskal-Wallis test. Cumulative survival time was calculated by the Kaplan-Meier method, and the log-rank test was applied to compare survival between 2 groups. P-values of ≤0.05 were considered statistically significant.

REFERENCES

1. Lurquin C, Van Pel A, Mariame B, De Plaen E, Szikora JP, Janssens C, et al. Structure of the gene of tum- transplantation antigen P91A: the mutated exon encodes a peptide recognized with Ld by cytolytic T cells. Cell. 1989;58(2):293-303.

2. Swann JB, Smyth MJ. Immune surveillance of tumors. J Clin Invest. 2007;117(5):1137-46.

3. Sharma P, Allison JP. Immune checkpoint targeting in cancer therapy: toward combination strategies with curative potential. Cell. 2015;161(2):205-14.

4. Seidel JA, Otsuka A, Kabashima K. Anti-PD-1 and Anti-CTLA-4 Therapies in Cancer: Mechanisms of Action, Efficacy, and Limitations. Front Oncol. 2018;8:86.

5. Aldous AR, Dong JZ. Personalized neoantigen vaccines: A new approach to cancer immunotherapy. Bioorg Med Chem. 2018;26(10):2842-9.

6. Heuts J, Varypataki EM, van der Maaden K, Romeijn S, Drijfhout JW, van Scheltinga AT, et al. Cationic Liposomes: A Flexible Vaccine Delivery System for Physicochemically Diverse Antigenic Peptides. Pharm Res. 2018;35(11):207.

7. Yadav M, Jhunjhunwala S, Phung QT, Lupardus P, Tanguay J, Bumbaca S, et al. Predicting immunogenic tumour mutations by combining mass spectrometry and exome sequencing. Nature. 2014;515(7528):572-6.

8. Bekri S, Uduman M, Gruenstein D, Mei AHC, Tung K, Rodney-Sandy R, et al. Neoantigen Synthetic Peptide Vaccine for Multiple Myeloma Elicits T Cell Immunity in a Pre-Clinical Model. Blood. 2017;130.

9. Kreiter S, Vormehr M, van de Roemer N, Diken M, Lower M, Diekmann J, et al. Mutant MHC class II epitopes drive therapeutic immune responses to cancer. Nature. 2015;520(7549):692-6.

10. Kranz LM, Diken M, Haas H, Kreiter S, Loquai C, Reuter KC, et al. Systemic RNA delivery to dendritic cells exploits antiviral defence for cancer immunotherapy. Nature. 2016;534(7607):396-401.

11. Sahin U, Derhovanessian E, Miller M, Kloke BP, Simon P, Lower M, et al. Personalized RNA mutanome vaccines mobilize poly-specific therapeutic immunity against cancer. Nature. 2017;547(7662):222-6.

12. Ott PA, Hu Z, Keskin DB, Shukla SA, Sun J, Bozym DJ, et al. An immunogenic personal neoantigen vaccine for patients with melanoma. Nature. 2017;547(7662):217-21.

13. Tang DC, DeVit M, Johnston SA. Genetic immunization is a simple method for eliciting an immune response. Nature. 1992;356(6365):152-4.

14. Ulmer JB, Donnelly JJ, Parker SE, Rhodes GH, Felgner PL, Dwarki VJ, et al. Heterologous protection against influenza by injection of DNA encoding a viral protein. Science. 1993;259(5102):1745-9.

15. Wang B, Ugen KE, Srikantan V, Agadjanyan MG, Dang K, Refaeli Y, et al. Gene inoculation generates immune responses against human immunodeficiency virus type 1. Proc Natl Acad Sci U S A. 1993;90(9):4156-60.

16. Fioretti D, Iurescia S, Fazio VM, Rinaldi M. DNA vaccines: developing new strategies against cancer. J Biomed Biotechnol. 2010;2010:174378.

17. Raz E, Carson DA, Parker SE, Parr TB, Abai AM, Aichinger G, et al. Intradermal gene immunization: the possible role of DNA uptake in the induction of cellular immunity to viruses. Proc Natl Acad Sci U S A. 1994;91(20):9519-23.

18. Williams BB, Wall M, Miao RY, Williams B, Bertoncello I, Kershaw MH, et al. Induction of T cell-mediated immunity using a

c-Myb DNA vaccine in a mouse model of colon cancer. Cancer Immunol Immunother. 2008;57(11):1635-45.

19. Porgador A, Irvine KR, Iwasaki A, Barber BH, Restifo NP, Germain RN. Predominant role for directly transfected dendritic cells in antigen presentation to CD8+ T cells after gene gun immunization. J Exp Med. 1998;188(6):1075-82.

20. Luxembourg A, Hannaman D, Ellefsen B, Nakamura G, Bernard R. Enhancement of immune responses to an HBV DNA vaccine by electroporation. Vaccine. 2006;24(21):4490-3.

21. Bins AD, Jorritsma A, Wolkers MC, Hung CF, Wu TC, Schumacher TN, et al. A rapid and potent DNA vaccination strategy defined by in vivo monitoring of antigen expression. Nat Med. 2005;11(8):899-904.

22. Duperret EK, Perales-Puchalt A, Stoltz R, G HH, Mandloi N, Barlow J, et al. A Synthetic DNA, Multi-Neoantigen Vaccine Drives Predominately MHC Class I CD8(+) T-cell Responses, Impacting Tumor Challenge. Cancer Immunol Res. 2019;7(2):174-82.

23. Falo LD, Jr., Kovacsovics-Bankowski M, Thompson K, Rock KL. Targeting antigen into the phagocytic pathway in vivo induces protective tumour immunity. Nat Med. 1995;1(7):649-53.

24. Winzler C, Rovere P, Rescigno M, Granucci F, Penna G, Adorini L, et al. Maturation stages of mouse dendritic cells in growth factor-dependent long-term cultures. J Exp Med. 1997;185(2):317-28.

25. Porgador A, Yewdell JW, Deng Y, Bennink JR, Germain RN. Localization, quantitation, and in situ detection of specific peptide-MHC class I complexes using a monoclonal antibody. Immunity. 1997;6(6):715-26.

26. Endmann A, Baden M, Weisermann E, Kapp K, Schroff M, Kleuss C, et al. Immune response induced by a linear DNA vector: influence of dose, formulation and route of injection. Vaccine. 2010;28(21):3642-9.

27. Fransen MF, Schoonderwoerd M, Knopf P, Camps MG, Hawinkels LJ, Kneilling M, et al. Tumor-draining lymph nodes are pivotal in PD-1/PD-L1 checkpoint therapy. JCI Insight. 2018;3(23).

28. McCluskie MJ, Brazolot Millan CL, Gramzinski RA, Robinson HL, Santoro JC, Fuller JT, et al. Route and method of delivery of DNA vaccine influence immune responses in mice and non-human primates. Mol Med. 1999;5(5):287-300.

29. Kleinovink JW, Marijt KA, Schoonderwoerd MJA, van Hall T, Ossendorp F, Fransen MF. PD-L1 expression on malignant cells is no prerequisite for checkpoint therapy. Oncoimmunology. 2017;6(4):e1294299.

30. Sato Y, Roman M, Tighe H, Lee D, Corr M, Nguyen MD, et al. Immunostimulatory DNA sequences necessary for effective intradermal gene immunization. Science. 1996;273(5273):352-4.

31. Klinman DM, Yamshchikov G, Ishigatsubo Y. Contribution of CpG motifs to the immunogenicity of DNA vaccines. J Immunol. 1997;158(8):3635-9.

32. Suschak JJ, Wang S, Fitzgerald KA, Lu S. A cGAS-Independent STING/IRF7 Pathway Mediates the Immunogenicity of DNA Vaccines. J Immunol. 2016;196(1):310-6.

33. Jalah R, Patel V, Kulkarni V, Rosati M, Alicea C, Ganneru B, et al. IL-12 DNA as molecular vaccine adjuvant increases the cytotoxic T cell responses and breadth of humoral immune responses in SIV DNA vaccinated macaques. Hum Vaccin Immunother. 2012;8(11):1620-9.

34. Leachman SA, Tigelaar RE, Shlyankevich M, Slade MD, Irwin M, Chang E, et al. Granulocyte-macrophage colony-stimulating factor priming plus papillomavirus E6 DNA vaccination: effects on papilloma formation and regression in the cottontail rabbit papillomavirus--rabbit model. J Virol. 2000;74(18):8700-8.

35. Qing Y, Chen M, Zhao J, Hu H, Xu H, Ling N, et al. Construction of an HBV DNA vaccine by fusion of the GM-CSF gene to the HBV-S gene and examination of its immune effects in normal and HBV-transgenic mice. Vaccine. 2010;28(26):4301-7.

36. Lindencrona JA, Preiss S, Kammertoens T, Schuler T, Piechocki M, Wei WZ, et al. CD4+ T cell-mediated HER-2/neu-specific tumor rejection in the absence of B cells. Int J Cancer. 2004;109(2):259-64.

37. Kim JJ, Bagarazzi ML, Trivedi N, Hu Y, Kazahaya K, Wilson DM, et al. Engineering of in vivo immune responses to DNA immunization via codelivery of costimulatory molecule genes. Nat Biotechnol. 1997;15(7):641-6.

38. Agadjanyan MG, Kim JJ, Trivedi N, Wilson DM, Monzavi-Karbassi B, Morrison LD, et al. CD86 (B7-2) can function to drive MHC-restricted antigen-specific CTL responses in vivo. J Immunol. 1999;162(6):3417-27.

39. Mendoza RB, Cantwell MJ, Kipps TJ. Immunostimulatory effects of a plasmid expressing CD40 ligand (CD154) on gene immunization. J Immunol. 1997;159(12):5777-81.

40. Ossendorp F, Mengede E, Camps M, Filius R, Melief CJ. Specific T helper cell requirement for optimal induction of cytotoxic T lymphocytes against major histocompatibility complex class II negative tumors. J Exp Med. 1998;187(5):693-702.

41. Borst J, Ahrends T, Babala N, Melief CJM, Kastenmuller W. CD4(+) T cell help in cancer immunology and immunotherapy. Nat Rev Immunol. 2018;18(10):635-47.

42. Perez-Diez A, Joncker NT, Choi K, Chan WF, Anderson CC, Lantz O, et al. CD4 cells can be more efficient at tumor rejection than CD8 cells. Blood. 2007;109(12):5346-54.

43. Xie Y, Akpinarli A, Maris C, Hipkiss EL, Lane M, Kwon EK, et al. Naive tumor-specific CD4(+) T cells differentiated in vivo eradicate established melanoma. J Exp Med. 2010;207(3):651-67.

44. Elnekave M, Furmanov K, Nudel I, Arizon M, Clausen BE, Hovav AH. Directly transfected langerin+ dermal dendritic cells potentiate CD8+ T cell responses following intradermal plasmid DNA immunization. J Immunol. 2010;185(6):3463-71.

45. Bedoui S, Davey GM, Lew AM, Heath WR. Equivalent stimulation of naive and memory CD8 T cells by DNA vaccination: a dendritic cell-dependent process. Immunol Cell Biol. 2009;87(3):255-9.

46. Gurunathan S, Klinman DM, Seder RA. DNA vaccines: immunology, application, and optimization*. Annu Rev Immunol. 2000;18:927-74.

47. Xiong H, Mittman S, Rodriguez R, Pacheco-Sanchez P, Moskalenko M, Yang Y, et al. Coexpression of Inhibitory Receptors Enriches for Activated and Functional CD8(+) T Cells in Murine Syngeneic Tumor Models. Cancer Immunol Res. 2019;7(6):963-76.

48. Castle JC, Kreiter S, Diekmann J, Lower M, van de Roemer N, de Graaf J, et al. Exploiting the mutanome for tumor vaccination. Cancer Res. 2012;72(5):1081-91.

49. Carreno BM, Magrini V, Becker-Hapak M, Kaabinejadian S, Hundal J, Petti AA, et al. Cancer immunotherapy. A dendritic cell vaccine increases the breadth and diversity of melanoma neoantigen-specific T cells. Science. 2015;348(6236):803-8.

50. Rajasagi M, Shukla SA, Fritsch EF, Keskin DB, DeLuca D, Carmona E, et al. Systematic identification of personal tumor-specific neoantigens in chronic lymphocytic leukemia. Blood. 2014;124(3):453-62.

51. Vormehr M, Reinhard K, Blatnik R, Josef K, Beck JD, Salomon N, et al. A non-functional neoepitope specific CD8(+) T-cell response induced by tumor derived antigen exposure in vivo. Oncoimmunology. 2019;8(3):1553478.

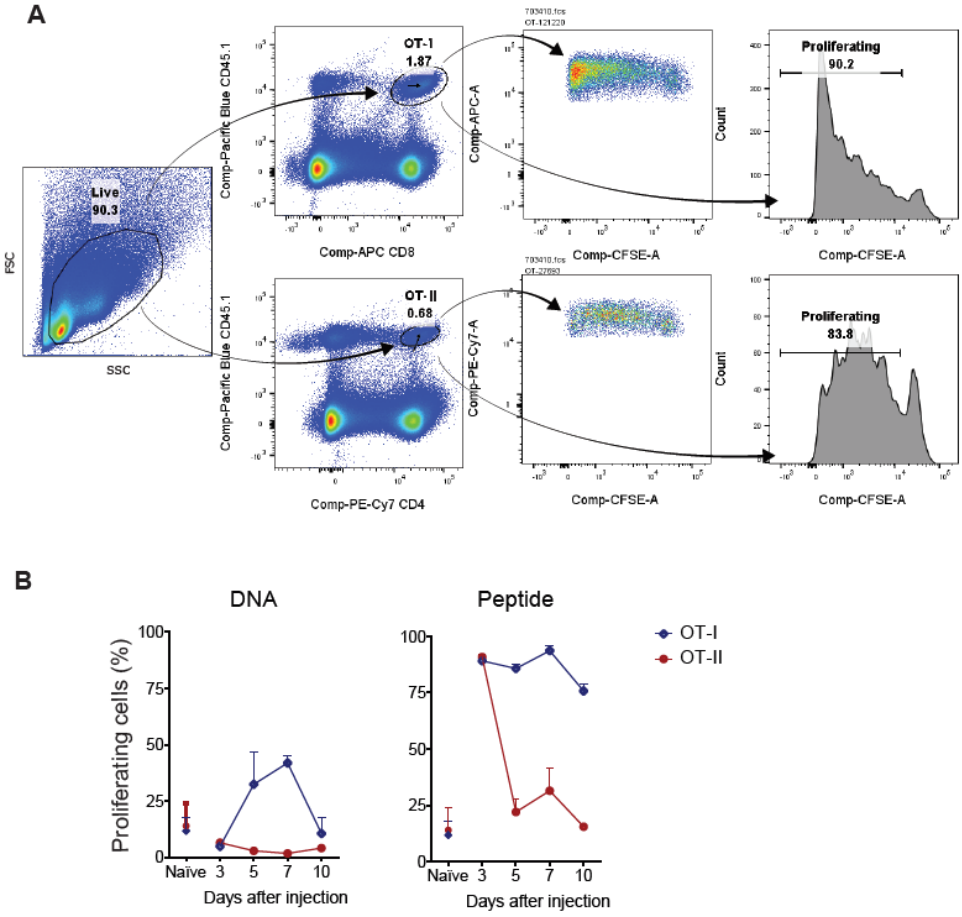

Figure S1: The poly-antigen DNA vaccine activates antigen-specific CD8 and CD4 T cells *in vivo*. A) Representative gating strategy for the detection of OT-I and OT-II cells. **B)** Kinetics of *in vivo* antigen presentation to OT-I or OT-II cells after injection of the DNA construct. Proliferation of the OT-I (blue lines) and OT-II cells (red lines) measured by CFSE dilution in the spleens of C57BL/6 mice immunized with either neoantigen DNA vaccine (*left panel*) or 50 µg of OVA CTL and helper peptides (*right panel*), used as positive controls for OT-I and OT-II cells proliferation, respectively. Error bars indicate mean ± SEM.

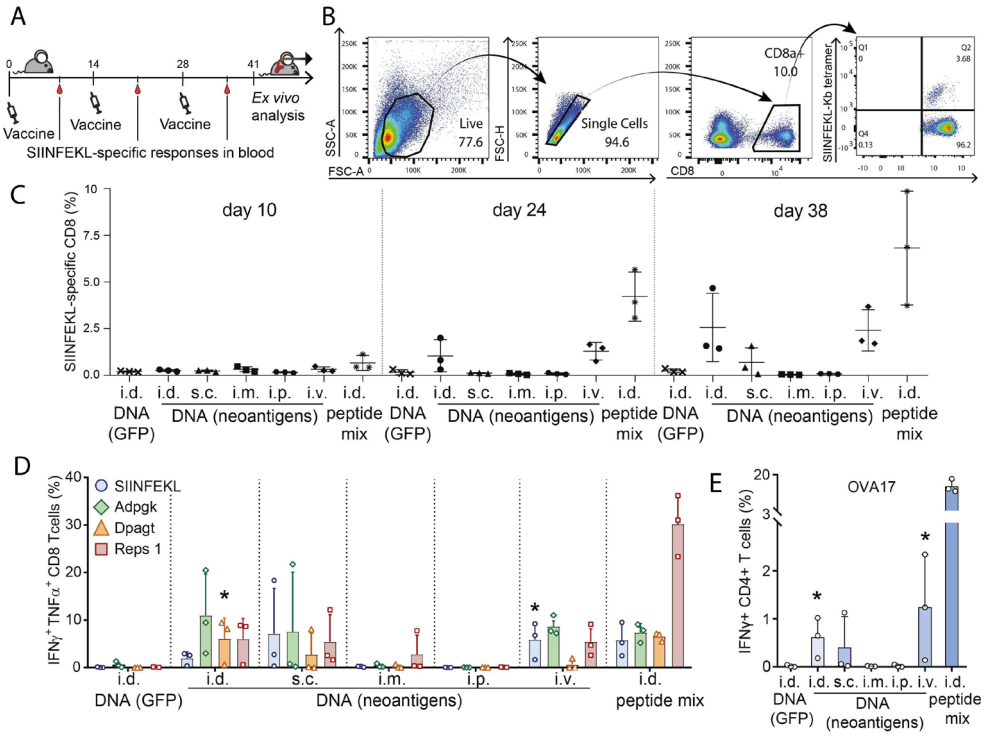

Figure S2: The DNA construct induces T cell priming for all epitopes after intradermal or intravenous injection. A) Schematic representation of the vaccine administration and tetramer staining schedule in C57BL/6 mice. Mice were injected via different routes with 10 µg of the neoantigen DNA construct at days 0, 14 and 28. A peptide mix of the same antigens was taken along as a control. Blood was taken at 3 different time points for antigen-specific T cells staining. At day 41, mice were sacrificed and spleens were removed for T cell cytokine production analysis. **B)** Representative flow cytometry dot plots showing the gating strategy for analysis of SIINFEKL-specific CD8 T cell in blood of vaccinated mice. **C)** Percentage of *de novo* induced SIINFEKL-specific responses in blood after administration of the neoantigen DNA vaccine via distinct injection routes analyzed in the blood with SIINFEKL-H2-K^b specific tetramers. i.d.: intradermal; s.c.: subcutaneous; i.m.: intramuscular; i.p.: intraperitoneal; i.v.: intravenous.. **D)** Percentage of the CD8$^+$ IFNγ$^+$ TNFα$^+$ double producing cells in the spleens after *ex vivo* restimulation of the splenocytes with the respective peptides for the CTL SIINFEKL epitope as well as all the neoepitopes encoded in the DNA vaccine. **E)** Percentage of the CD4$^+$ IFNγ$^+$ cells in the spleens after *ex vivo* restimulation of the splenocytes with OVA17 peptide, the 17-mer helper peptide of ovalbumin. The GFP construct and the long synthetic peptides of the individual epitopes served respectively as negative and positive controls. Error bars indicate mean ± SEM. Statistical significance between DNA (neoantigens) or peptide and control DNA (GFP) was determined by t test, * $p<0.05$, ** $p<0.01$, *** $p< 0.001$.

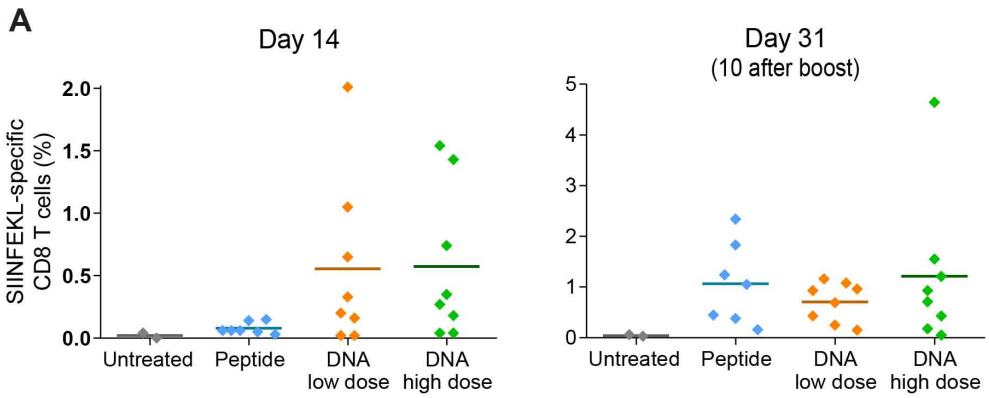

Figure S3: DNA vaccination protects from challenge with B16-OVA. A) Frequency of SIINFEKL-specific CD8 T cells responses in blood after prime and boost vaccination with low (10 µg) or a high (90 µg) dose of DNA or peptide. Vaccination was followed by tumor challenge.

GENERAL DISCUSSION

8

Therapeutic vaccination against cancer is supported by a strong immunologic rational and by encouraging preclinical data, however the clinical translation of this tumor-specific therapy has been challenging. To date, only two therapeutic cancer vaccines have been approved in the clinic [1]: Sipuleucel-T, a dendritic cell-based vaccine against the prostatic acid phosphatase antigen for the treatment of prostate cancer, and T-VEC, a modified herpes virus that expresses GM-CSF and acts as *in situ* vaccine for melanoma. Apart from Sipuleucel-T and T-VEC, most cancer vaccines tested in the clinic in the last decades have been discontinued before or during phase 3 trials, failing to produce a significant benefit for patients. Concomitantly, immunotherapies using immune checkpoint blocking antibodies, such as anti PD-1/PD-L1 or anti-CTLA4 antibodies, have demonstrated promising outcomes in clinical trials, underlining the role of the immune system, including T cell immunity, in tumor regression [2]. The apparent discordance between the failed attempts of cancer vaccines and the success of immunotherapy can be harmonized by the knowledge gained during these studies: T cells can in fact recognize tumor cells and mediate tumor eradication, but they do so within a much more hostile environment than previously understood. Contemporarily, the vaccination field has also undergone a process of optimization in relation to vaccine formulation and delivery methods. The correlation between successful priming and the equipment of T cells with strong effector and memory functions was established, as well as their relationship with anti-tumor efficacy.

Compared to the initial attempts, there are now many lessons that have been learnt about the induction of effective anti-tumor T cell immunity and that can be applied to the current development of cancer vaccines. Optimal cancer vaccines should be targeted to DCs, should comprise a potent adjuvant that can skew towards Th1 response and should generate a response against a broad range of antigens, possibly inducing both cytotoxic CD8 T cells (CTLs) and CD4 helper T cells [3].

These features are key throughout different stages of the T cell responses:

- during **priming**, where antigen presentation by professional DCs together with potent co-stimulation by adjuvant and CD4 helper T cells will induce differentiation of robust effector and memory functions, maximizing T cell fitness;

- during the **effector phase**, where T cell responses will have to deal with tumor resistance mechanisms and the collaboration between CTLs and helper T cells is fundamental for an optimal anti-tumor response. In addition, the inclusion of multiple epitopes maximizes the chances to target relevant antigens as well to diversify the response in case of antigen loss by the tumor cells.

In this thesis, several of these concepts were explored and implemented for the design and formulation of novel well-defined cancer vaccines.

DC targeting and formulation

The physiological role of DCs is to integrate innate signals for the generation of an adaptive response. It is crucial for a vaccine to reach and activate DCs, and the formulation of vaccines plays a key role in DC targeting. In **Chapter 2** and **3**, conjugation of the TLR4 ligand CRX-527 to an antigenic peptide demonstrates

an enhancement of vaccine-induced T cell responses. The reasons may be multiple. On one hand, the uptake of the peptide and the presentation of both CD8 and CD4 epitopes appear to be increased upon conjugation to the TLR4 ligand. This could be due to interaction of CRX-527 with the co-receptor CD14. Interaction of the natural ligand LPS with this co-receptor facilitates binding with the TLR4 signaling complex at the cell surface [4]. Besides its chaperoning role, CD14 has been directly implicated in internalization of the TLR4-ligand complex by triggering a signaling cascade that activates endocytic pathways [5]. CRX-527 agonism was shown to be independent from the co-receptor CD14 [6], however the presence of CD14 at the cell surface was reported to potentiate downstream signaling, possibly indicating interaction of CRX-527 with the co-receptor, which could also stimulate internalization. In general, resemblance of the agonist to a PAMP, may implicate affinity for one or more scavenger receptor that are expressed by DCs [7, 8]. In fact, the facilitated uptake of antigen conjugated to PAMPS has been reported for other receptors: TLR2 in [9, 10] and **chapter 5**, TLR7 in **chapter 4,** TLR9 [8, 9], and various C-type lectin receptors [11, 12]. The scavenger receptor CD36 has affinity for diacylglycerides such as zymosan, which is also a TLR2/6 agonist [13].

In addition, several lines of evidence underline how, the presence of antigen and signaling of TLR ligands in the same endosomes promote processing and presentation of the endosomal cargo rather than degradation [14, 15]. Furthermore, especially upon injection *in vivo*, it is likely that antigen-adjuvant conjugates enable antigen presentation and co-stimulation to be delivered to T cells by the same DCs, resulting in improved T cell priming as demonstrated in **chapter 2** by the increased differentiation of T cells into effector memory T cells, by the enhanced anti-tumor efficacy reported in **chapter 3**, and by the higher numbers of specific T cells induced reported in **chapter 5**.

Encapsulation of antigen into biodegradable nanoparticles is a promising strategy employed to improve vaccine targeting and efficacy. In fact, **chapter 6** shows that loading of peptide antigens into cationic dextran nanogel improves uptake and antigen presentation of the epitopes by DCs, *in vitro*. *In vivo*, this translates into enhanced induction of antigen-specific CD8 and CD4 T cells. The quality of these responses is also improved as indicated by the increased poly-functional cytokine profile observed. Cationic nanoparticles have gained growing interest in recent years, as evidence accumulates on their natural affinity towards DCs and their maturing properties [16-18], as well as their ability to allow antigen depot formation upon subcutaneous or intradermal injection and prolonged antigen presentation [18-20], which results in an overall improvement of the T cell responses. These properties are connected to the cationic nature of the molecules. Vaccinations with peptide encapsulated into cationic liposomes, for example, results in a similar improvement of T cell induction and translates into superior preclinical anti-tumor efficacy [19]. The reduction-sensitivity of the nanogels described in this thesis, which allows peptide release only in reducing

conditions, seems to be intimately linked to the observed improvement. Antigen covalently bound to self-assembling nanoparticles have been developed and successfully employed in recent studies. For examples, peptide antigens and adjuvant coupled with lipoprotein-mimicking molecules that assemble in nanosized discs could improve antigen delivery to lymphoid organs and sustain presentation by dendritic cells [21]. Similarly to what was observed in **chapter 6**, this resulted in up to 45-fold increase of antigen specific T cells. Another self-assembling nanoparticle system containing covalently bound peptide and TLR7 agonist was applied to putative neoantigens and was shown to expand the breadth of CD4 and CD8 responses in mice and primates [22].

While *in vitro* studies allow characterization of the vaccine in a controlled setting, it is evident that the success of cancer vaccination is also influenced by the route of administration. While most vaccinations are typically injected intramuscularly, the vaccinations reported in this thesis are performed intradermally. Compared to the intramuscular route, which is relatively inefficient and require high doses to achieve immunogenicity, intradermal vaccination represents a safe and accessible route, that could improve vaccine immunogenicity for T cells and lower the required dose per injection. This is based on the notion that the dermis is patrolled by many DC subsets, which are involved in antigen uptake and transport to the draining lymph nodes. In particular, CD103+ migratory DCs have sparked the interest of tumor immunologist for their increasingly evident role in anti-tumor T cell immunity [23]. CD103+ DCs are found intratumorally and mediate attraction and stimulation of CTLs [24-26], playing a role also in immune checkpoint therapies. Therefore, the involvement of these DC subset for the stimulation of an anti-tumoral immune response is auspicated. In **chapter 3**, the mobilization of this subset was described upon vaccination with CRX-527-peptide conjugates.

Adjuvants

Proper polarization of the immune response is determined by the instructions given by DCs, which in turn integrate environmental cues to distinguish between different types of threats. The same concept can be exploited during vaccination through the choice of adjuvants.

In **chapter 3**, the TLR4 agonist CRX-527 was successfully employed for the first time to generate anti-tumor immunity. TLR4 represents an interesting target for stimulation during vaccination as it has a wide expression pattern and a broad immunological effect. The signaling complex TLR4 is well studied and it triggers two independent signaling cascades. Upon ligand binding, TLR4 requires heterodimerization with the co-receptor MD-2, which mediates activation of the MyD88-TRAF6 pathway at the cell surfaces and consequent NF-kB-mediated transcription of pro-inflammatory cytokines [4]. Internalization of the TLR4 complex initiates signaling via the TRIF pathway, which activates IRF3-mediated transcription of type I interferons [27]. Exploitation of these potent pathways for

vaccination purposes has always been cautious, because the native ligand LPS is associated with toxicity and sepsis [28]. However, the molecularly defined agonist employed in this thesis allows controlled used of this adjuvant as well as strong immunological activity (as low as 1 nmol per mouse) showing no side-effects. Moreover, it could generate a Th1 skewed response which efficiently mediated protection from tumor challenge upon prophylactic vaccination. Therapeutically, the vaccine could significantly control tumor growth, however vaccination may be combined with another therapy to reach full effectiveness. Recently, a similar synthetic TLR4 agonist has also been described. Glucopyranosil lipid A (G100) also shows Th1 skewing and effective adjuvanticity in cancer vaccines [29], where combination with PD-1/PD-L1 blockade demonstrates synergism in pre-clinical setting. In addition, this adjuvant showed excellent activity as intra-tumoral monotherapy [30], and this therapy is currently under clinical investigation for the treatment of Merkel cell skin carcinoma [31]. TLR4 expression in DCs has also been implicated in recognition of DAMPS in anti-tumor immunity [32]. Altogether, these reports support the rational for triggering TLR4 during cancer vaccination.

Stimulation of other TLRs can also be exploited during cancer vaccinations. For example, the triggering of TLR7 is attractive in the context of anti-tumoral immunity because it drives production of type I interferons and the induction of an anti-viral response, which, among all types, most resembles the response required for the elimination of tumor cells. In **chapter 4**, it was explored whether the dual conjugation of a TLR7 agonist and the ligand for an intracellular trafficking receptor to antigenic peptides could improve vaccine efficacy. The M6P receptor mediates physiological trafficking of lysosomal enzymes [33] between Golgi and pre-lysosomes. Even though it was reported an enhancement of DC maturation, the antigen presentation was hampered by the addition of Mannose-6 phosphate (M6P). While it may not represent a strategy to improve vaccine efficacy, these observations underline the complexity of routing that exogenous antigen undergoes, from initial uptake to processing and MHC presentation rather than degradation. In this case, conjugation of the TLR7 ligand potentiated antigen presentation which was abolished by the addition of the M6P.

In **chapter 5**, the same TLR7 agonist was tested in combination with the TLR2 ligand Pam_3CysSK_4. Dual conjugation preserved the immunological activity of the ligands and the antigen, and represents a promising strategy to further investigate, especially regarding the type of immunity raised by dual TLR stimulation. This approach has potentially endless possibilities of combination, for example with other TLR ligands or other PAMP receptors ligands such as NOD-like receptors, CLRs, STING agonists or ligands for uptake and trafficking receptors. The system that vaccination tries to artificially replicate, is governed by the triggering of different receptors by the various PAMPS present on pathogens, therefore a vaccine may be potentiated by the integration of different signaling pathways. For example, dual conjugation of Pam3CysSK4 and NOD2 agonist to antigenic peptides, synergizes in the induction of DC maturation as well as Th1 cytokine production by T cells [34].

Antigen selection

The vaccination efficacy of a determined tumor antigen is defined by a number of immunological and tumor-related factors. The immunogenicity of an antigen may vary based on a) the processing pattern regulated by the proteasome or other proteolytic enzymes, b) the binding affinity of the epitope for the MHC molecules, which can influence the strength of the immune response, c) the nature of the affinity for MHC class II or I, which determines CD4 versus CD8 T cell induction, and d) the T cell receptor repertoire i.e. the presence and frequency of specific precursor T cells. On the tumor side, the immunological efficacy of an antigen will vary depending on the antigen and MHC expression levels within single tumor cells but also on clonal distribution in the primary tumor and metastasis. All these factors are difficult to predict and the potency of most antigens can thus far only be determined empirically. Therefore, selection of the right antigen for cancer vaccines is an open challenge.

An optimal cancer vaccine should be able to evoke both CTL and T helper responses. This is important during priming of vaccine-induced T cells, as T helper cells actively support CTL differentiation [35] as well as on tumor site, where CTLs mediate direct recognition and killing of tumor cells while specific helper T cells modulate the tumor microenvironment and support CTLs activity.

In **chapter 3** it was clearly depicted with two antigen models how the two responses complement each other for full anti-tumor efficacy. The inclusion of a helper epitope plays a crucial role during CTL priming. In fact, help presence impacts the development of CTL effector functions, the breadth of the response and the formation of memory precursors [35, 36]. This is believed to happen in a two-step priming process. This model postulates that CD8 and CD4 are independently primed by migratory conventional (c) DC1 and cDC2, respectively [37]. After this initial activation, primed CD8 and CD4 T cells produce chemokines that attracts plasmacytoid (p) DCs accumulation, via CCL3, and cDC1, via XCL1 [38]. In this second step, pDCs promote further stimulation via type I interferons, while CD4 T cells interact with cDC1 via CD40L, which amplifies upregulation of CD80/CD86 and CD70 co-stimulatory molecules and IL-12 and IL-15 production by DCs [39]. This in turn potentiates CD8 T cell expansion and differentiation of memory and effector functions upon antigen-specific interaction with cDC1 [35, 40]. Lack of help-induced signals during priming impairs CTL differentiation and coveys them to predysfunction, which can still be rescued, and eventually terminal exhaustion [41]. This argues that inclusion of help, even tumor non-specific, is advisable in the design of a cancer vaccine to potentiate T cell priming. During anti-tumor activity, tumor-specific help can exert additional functions through recognition of MHC class II positive tumors or by locally presented antigen by dendritic cells in tumor or draining LN, or by activation of tumor-specific macrophages [42], production of cytokines that recruit and support CTL proliferation and effector functions [43, 44], or even direct cytotoxicity activity [45].

The latest technological advances in high throughput techniques have played an important role in substantiating molecular and biological details in cancer

vaccination. Sequencing techniques allow mutational profiling of individual tumors, uncovering all putative mutation-derived antigens [46]. RNA sequencing and proteomic analysis enable the verification of antigen expression while immune-peptidome techniques can detect epitope presentation [47, 48]. These innovations have further broadened antigen repertoire for cancer vaccines and directed research towards personalized vaccines.

In **chapter 7**, a possible approach to meet this new challenge was explored. Nucleotide-based vaccines have gained wide interest since the emergence of personalized vaccines because they can more easily accommodate diverse sequences and include multiple antigens. This is advantageous not only in the light of personalized therapy but also for broadening the immune response induced. A DNA plasmid containing multiple epitopes in a similar design to the one reported in this thesis has also been developed in pre-clinical setting with epitopes targeting three different tumor models and was shown to also generate T cell immunity successfully and to mediate tumor control [49]. RNA-based and adenoviral vectors with mini-genes are also under investigations for these purposes [50, 51]. Nucleotide-based vaccines are easy to manufacture and their physicochemical properties are not altered by the sequence encoded. In contrast, the production and the solubilization of peptide-based vaccines under GMP conditions is challenging due to the unique properties of every amino acid sequence, creating extra barriers for optimal antigen selection. An exemplification of the swiftness of genetic vaccines was the quick development of RNA- and adenoviral-based vaccines containing the Spike protein of the SARS2-coronavirus during the COVID19 pandemic [52-55]. These vaccines were able to awake both B-cell mediated antibody responses as well as CD4 and CD8 T cell responses with a Th1 profile [54, 56].

Nevertheless, peptide-based systems have also been successfully applied to personalized vaccines in pre-clinical and early clinical settings [21, 47, 57] and advancement in peptide synthesis methods are also under development [58]. Promising results were obtained in a recent Phase I clinical study named HESPECTA, using the optimized TLR2 ligand Amplivant conjugated to two HPV16 E6 long synthetic peptides. This study showed safety and robust immunogenicity in HPV16+ cancer patients which were intradermally vaccinated in four doses groups (unpublished, manuscript in preparation).

All platforms represent valid alternatives to investigate for the potency of cancer vaccines. In addition, the existence of these different platforms allows for testing heterologous prime/boost protocols to further potentiate vaccine efficacy [59, 60].

Combination therapies

Several lines of evidence suggest that the limited success of cancer vaccines may be due to its use as monotherapy. In **chapter 7**, the combination of vaccination and anti-PD1 blockade resulted in most optimal therapeutic effect, while separately both therapies had limited effect. A growing number of reports successful-

ly combines immunotherapeutic treatments to improve T cell-mediated tumor control. In particular, combinations with immune checkpoint inhibitors (ICI), such as anti-PD1/PD-L1, seem to be complementary to vaccination: on one side vaccination increases the pool of tumor-specific T cells on which ICI can act, and on the other side ICI helps preventing the inhibition of effector functions of vaccine-induced T cells in the tumor microenvironment [29, 51, 61]. Also in the clinic, the synergism between ICI and vaccination is becoming evident as reports show how PD-1 treatment could rescue vaccinated cancer patients with progressing tumors in melanoma [50, 62, 63] and HPV-16 malignancies [64], and vice versa, how vaccination before anti-PD1 treatment could double the response rate and survival to treatment in patients bearing HPV16-related malignancies [65]. Moreover, key activating or inhibitory receptors involved in cancer immunity are being identified. For example, the expression of the CD8 T cell inhibitor NKG2A was found to correlate with unresponsiveness to anti-PD1 treatment in patients with HPV16 malignancies [65, 66], while the activator ICOS was found to be positively expressed by tumor-specific T cells in mice responding to PD-L1 treatment. Based on this analysis, the targeting ICOS with activating antibodies was able to double the survival rate in tumor models by synergizing with PD-L1 therapy [67]. These observations set the basis for the rational combination of ICIs and vaccination.

Next to immunotherapies, vaccination can synergize with other therapies. Chemotherapy for example, can cause immunogenic cell death of tumor cells causing the induction of tumor-specific T cells [68]. Vaccination can boost these responses and increase therapeutic efficacy of the treatments as shown for the combination of cisplatin and peptide vaccination in mouse models and patients for HPV16+ tumors [69, 70]. Ablative therapies such as radiotherapy and photodynamic therapy were also reported to synergize with vaccines [71, 72]. Combination of cancer vaccine with these therapies have the added value of partially debulking the tumor mass, creating a damaged environment that is easy to infiltrate and control by T cells, which could eliminate residual cancer cells and establish immunological memory to prevent recurrences and metastases. Abscopal effects on distant secondary tumors have been described in pre-clinical models for combination of photodynamic therapy or radiotherapy with vaccination [73, 74].

Concluding remarks

After more than twenty years of break-in, we just started to disclose the real potential of cancer vaccination. New challenges and possibilities are awaiting to be tackled. In this thesis, different strategies were explored to refine the formulation of cancer vaccines, to maximize vaccine performance and to address current demands. This constitutes only one building block of a much wider task, which is the rational integration of cancer therapies for the successful treatment of cancer.

REFERENCES

1. Morse, M.A., W.R. Gwin, 3rd, and D.A. Mitchell, *Vaccine Therapies for Cancer: Then and Now.* Target Oncol, 2021. **16**(2): p. 121-152.

2. Galluzzi, L., et al., *The hallmarks of successful anticancer immunotherapy.* Sci Transl Med, 2018. **10**(459).

3. Melief, C.J., et al., *Therapeutic cancer vaccines.* J Clin Invest, 2015. **125**(9): p. 3401-12.

4. Fitzgerald, K.A., D.C. Rowe, and D.T. Golenbock, *Endotoxin recognition and signal transduction by the TLR4/MD2-complex.* Microbes Infect, 2004. **6**(15): p. 1361-7.

5. Zanoni, I., et al., *CD14 controls the LPS-induced endocytosis of Toll-like receptor 4.* Cell, 2011. **147**(4): p. 868-80.

6. Legat, A., et al., *CD14-independent responses induced by a synthetic lipid A mimetic.* Eur J Immunol, 2010. **40**(3): p. 797-802.

7. Wang, D., et al., *Role of scavenger receptors in dendritic cell function.* Hum Immunol, 2015. **76**(6): p. 442-6.

8. Lahoud, M.H., et al., *DEC-205 is a cell surface receptor for CpG oligonucleotides.* Proc Natl Acad Sci U S A, 2012. **109**(40): p. 16270-5.

9. Khan, S., et al., *Distinct uptake mechanisms but similar intracellular processing of two different toll-like receptor ligand-peptide conjugates in dendritic cells.* J Biol Chem, 2007. **282**(29): p. 21145-59.

10. Zom, G.G., et al., *Efficient induction of antitumor immunity by synthetic toll-like receptor ligand-peptide conjugates.* Cancer Immunol Res, 2014. **2**(8): p. 756-64.

11. Burgdorf, S., et al., *Spatial and mechanistic separation of cross-presentation and endogenous antigen presentation.* Nat Immunol, 2008. **9**(5): p. 558-66.

12. Wamhoff, E.C., et al., *A Specific, Glycomimetic Langerin Ligand for Human Langerhans Cell Targeting.* ACS Cent Sci, 2019. **5**(5): p. 808-820.

13. Hoebe, K., et al., *CD36 is a sensor of diacylglycerides.* Nature, 2005. **433**(7025): p. 523-7.

14. Lopez-Haber, C., et al., *Phosphatidylinositol-4-kinase IIalpha licenses phagosomes for TLR4 signaling and MHC-II presentation in dendritic cells.* Proc Natl Acad Sci U S A, 2020. **117**(45): p. 28251-28262.

15. Mantegazza, A.R., et al., *TLR-dependent phagosome tubulation in dendritic cells promotes phagosome cross-talk to optimize MHC-II antigen presentation.* Proc Natl Acad Sci U S A, 2014. **111**(43): p. 15508-13.

16. Vangasseri, D.P., et al., *Immunostimulation of dendritic cells by cationic liposomes.* Mol Membr Biol, 2006. **23**(5): p. 385-95.

17. Li, D., et al., *Strong in vivo antitumor responses induced by an antigen immobilized in nanogels via reducible bonds.* Nanoscale, 2016. **8**(47): p. 19592-19604.

18. Heuts, J., et al., *Cationic Nanoparticle-Based Cancer Vaccines.* Pharmaceutics, 2021. **13**(5).

19. Varypataki, E.M., et al., *Efficient Eradication of Established Tumors in Mice with Cationic Liposome-Based Synthetic Long-Peptide Vaccines.* Cancer Immunol Res, 2017. **5**(3): p. 222-233.

20. Schmidt, S.T., et al., *Comparison of two different PEGylation strategies for the liposomal adjuvant CAF09: Towards induction of CTL responses upon subcutaneous vaccine administration.* Eur J Pharm Biopharm, 2019. **140**: p. 29-39.

21. Kuai, R., et al., *Designer vaccine nanodiscs for personalized cancer immunotherapy.* Nat Mater, 2017. **16**(4): p. 489-496.

22. Lynn, G.M., et al., *Peptide-TLR-7/8a conjugate vaccines chemically programmed for nanoparticle self-assembly enhance CD8 T-cell immunity to tumor antigens.* Nat Biotechnol, 2020. **38**(3): p. 320-332.

23. Wculek, S.K., et al., *Dendritic cells in cancer immunology and immunotherapy.* Nat Rev Immunol, 2020. **20**(1): p. 7-24.

24. Roberts, E.W., et al., *Critical Role for CD103(+)/CD141(+) Dendritic Cells Bearing CCR7 for Tumor Antigen Trafficking and Priming of T Cell Immunity in Melanoma.* Cancer Cell, 2016. **30**(2): p. 324-336.

25. Salmon, H., et al., *Expansion and Activation of CD103(+) Dendritic Cell Progenitors at the Tumor Site Enhances Tumor Responses to Therapeutic PD-L1 and BRAF Inhibition.* Immunity, 2016. **44**(4): p. 924-38.

26. Williford, J.M., et al., *Recruitment of CD103(+) dendritic cells via tumor-targeted chemokine delivery enhances efficacy of*

checkpoint inhibitor immunotherapy. Sci Adv, 2019. **5**(12): p. eaay1357.

27. Gandhapudi, S.K., P.M. Chilton, and T.C. Mitchell, *TRIF is required for TLR4 mediated adjuvant effects on T cell clonal expansion*. PLoS One, 2013. **8**(2): p. e56855.

28. Bazin, H.G., et al., *The 'Ethereal' nature of TLR4 agonism and antagonism in the AGP class of lipid A mimetics*. Bioorg Med Chem Lett, 2008. **18**(20): p. 5350-4.

29. Albershardt, T.C., et al., *Therapeutic efficacy of PD1/PDL1 blockade in B16 melanoma is greatly enhanced by immunization with dendritic cell-targeting lentiviral vector and protein vaccine*. Vaccine, 2020. **38**(17): p. 3369-3377.

30. Albershardt, T.C., et al., *Intratumoral immune activation with TLR4 agonist synergizes with effector T cells to eradicate established murine tumors*. NPJ Vaccines, 2020. **5**(1): p. 50.

31. Bhatia, S., et al., *Intratumoral G100, a TLR4 Agonist, Induces Antitumor Immune Responses and Tumor Regression in Patients with Merkel Cell Carcinoma*. Clin Cancer Res, 2019. **25**(4): p. 1185-1195.

32. Fang, X., et al., *Breed-linked polymorphisms of porcine toll-like receptor 2 (TLR2) and TLR4 and the primary investigation on their relationship with prevention against Mycoplasma pneumoniae and bacterial LPS challenge*. Immunogenetics, 2013. **65**(11): p. 829-34.

33. Ghosh, P., N.M. Dahms, and S. Kornfeld, *Mannose 6-phosphate receptors: new twists in the tale*. Nat Rev Mol Cell Biol, 2003. **4**(3): p. 202-12.

34. Zom, G.G., et al., *Dual Synthetic Peptide Conjugate Vaccine Simultaneously Triggers TLR2 and NOD2 and Activates Human Dendritic Cells*. Bioconjug Chem, 2019. **30**(4): p. 1150-1161.

35. Ahrends, T., et al., *CD4(+) T Cell Help Confers a Cytotoxic T Cell Effector Program Including Coinhibitory Receptor Downregulation and Increased Tissue Invasiveness*. Immunity, 2017. **47**(5): p. 848-861 e5.

36. Ahrends, T., et al., *CD4(+) T cell help creates memory CD8(+) T cells with innate and help-independent recall capacities*. Nat Commun, 2019. **10**(1): p. 5531.

37. Hor, J.L., et al., *Spatiotemporally Distinct Interactions with Dendritic Cell Subsets Facilitates CD4+ and CD8+ T Cell Activation to Localized Viral Infection*. Immunity, 2015. **43**(3): p. 554-65.

38. Brewitz, A., et al., *CD8(+) T Cells Orchestrate pDC-XCR1(+) Dendritic Cell Spatial and Functional Cooperativity to Optimize Priming*. Immunity, 2017. **46**(2): p. 205-219.

39. Greyer, M., et al., *T Cell Help Amplifies Innate Signals in CD8(+) DCs for Optimal CD8(+) T Cell Priming*. Cell Rep, 2016. **14**(3): p. 586-597.

40. Agarwal, P., et al., *Gene regulation and chromatin remodeling by IL-12 and type I IFN in programming for CD8 T cell effector function and memory*. J Immunol, 2009. **183**(3): p. 1695-704.

41. Busselaar, J., et al., *Helpless Priming Sends CD8(+) T Cells on the Road to Exhaustion*. Front Immunol, 2020. **11**: p. 592569.

42. Bogen, B., et al., *CD4(+) T cells indirectly kill tumor cells via induction of cytotoxic macrophages in mouse models*. Cancer Immunol Immunother, 2019. **68**(11): p. 1865-1873.

43. Sledzinska, A., et al., *Regulatory T Cells Restrain Interleukin-2- and Blimp-1-Dependent Acquisition of Cytotoxic Function by CD4(+) T Cells*. Immunity, 2020. **52**(1): p. 151-166 e6.

44. Bos, R. and L.A. Sherman, *CD4+ T-cell help in the tumor milieu is required for recruitment and cytolytic function of CD8+ T lymphocytes*. Cancer Res, 2010. **70**(21): p. 8368-77.

45. Quezada, S.A., et al., *Tumor-reactive CD4(+) T cells develop cytotoxic activity and eradicate large established melanoma after transfer into lymphopenic hosts*. J Exp Med, 2010. **207**(3): p. 637-50.

46. Castle, J.C., et al., *Exploiting the mutanome for tumor vaccination*. Cancer Res, 2012. **72**(5): p. 1081-91.

47. Yadav, M., et al., *Predicting immunogenic tumour mutations by combining mass spectrometry and exome sequencing*. Nature, 2014. **515**(7528): p. 572-6.

48. Zhang, X., et al., *Application of mass spectrometry-based MHC immunopeptidome profiling in neoantigen identification for tumor immunotherapy*. Biomed Pharmacother, 2019. **120**: p. 109542.

49. Duperret, E.K., et al., *A Synthetic DNA, Multi-Neoantigen Vaccine Drives Predominately MHC Class I CD8(+) T-cell Responses, Impacting Tumor Challenge*. Cancer Immunol Res, 2019. **7**(2): p. 174-182.

50. Sahin, U., et al., *Personalized RNA mutanome vaccines mobilize poly-specific therapeutic immunity against cancer.* Nature, 2017. **547**(7662): p. 222-226.

51. D'Alise, A.M., et al., *Adenoviral vaccine targeting multiple neoantigens as strategy to eradicate large tumors combined with checkpoint blockade.* Nat Commun, 2019. **10**(1): p. 2688.

52. Polack, F.P., et al., *Safety and Efficacy of the BNT162b2 mRNA Covid-19 Vaccine.* N Engl J Med, 2020. **383**(27): p. 2603-2615.

53. Baden, L.R., et al., *Efficacy and Safety of the mRNA-1273 SARS-CoV-2 Vaccine.* N Engl J Med, 2021. **384**(5): p. 403-416.

54. Ewer, K.J., et al., *T cell and antibody responses induced by a single dose of ChAdOx1 nCoV-19 (AZD1222) vaccine in a phase 1/2 clinical trial.* Nat Med, 2021. **27**(2): p. 270-278.

55. Bos, R., et al., *Ad26 vector-based COVID-19 vaccine encoding a prefusion-stabilized SARS-CoV-2 Spike immunogen induces potent humoral and cellular immune responses.* NPJ Vaccines, 2020. **5**: p. 91.

56. Sahin, U., et al., *COVID-19 vaccine BNT162b1 elicits human antibody and TH1 T cell responses.* Nature, 2020. **586**(7830): p. 594-599.

57. Ott, P.A., et al., *An immunogenic personal neoantigen vaccine for patients with melanoma.* Nature, 2017. **547**(7662): p. 217-221.

58. Yeo, J., et al., *Liquid Phase Peptide Synthesis via One-Pot Nanostar Sieving (PEPSTAR).* Angew Chem Int Ed Engl, 2021. **60**(14): p. 7786-7795.

59. Ring, S.S., et al., *Heterologous Prime Boost Vaccination Induces Protective Melanoma-Specific CD8(+) T Cell Responses.* Mol Ther Oncolytics, 2020. **19**: p. 179-187.

60. Guo, Q., et al., *Heterologous prime-boost immunization co-targeting dual antigens inhibit tumor growth and relapse.* Oncoimmunology, 2020. **9**(1): p. 1841392.

61. Hesse, C., et al., *A Tumor-Peptide-Based Nanoparticle Vaccine Elicits Efficient Tumor Growth Control in Antitumor Immunotherapy.* Mol Cancer Ther, 2019. **18**(6): p. 1069-1080.

62. Ott, P.A., et al., *A Phase Ib Trial of Personalized Neoantigen Therapy Plus Anti-PD-1 in Patients with Advanced Melanoma, Non-small Cell Lung Cancer, or Bladder Cancer.* Cell, 2020. **183**(2): p. 347-362 e24.

63. Sahin, U., et al., *An RNA vaccine drives immunity in checkpoint-inhibitor-treated melanoma.* Nature, 2020. **585**(7823): p. 107-112.

64. Aggarwal, C., et al., *Immunotherapy Targeting HPV16/18 Generates Potent Immune Responses in HPV-Associated Head and Neck Cancer.* Clin Cancer Res, 2019. **25**(1): p. 110-124.

65. Massarelli, E., et al., *Combining Immune Checkpoint Blockade and Tumor-Specific Vaccine for Patients With Incurable Human Papillomavirus 16-Related Cancer: A Phase 2 Clinical Trial.* JAMA Oncol, 2019. **5**(1): p. 67-73.

66. van Montfoort, N., et al., *NKG2A Blockade Potentiates CD8 T Cell Immunity Induced by Cancer Vaccines.* Cell, 2018. **175**(7): p. 1744-1755 e15.

67. Beyrend, G., et al., *PD-L1 blockade engages tumor-infiltrating lymphocytes to co-express targetable activating and inhibitory receptors.* J Immunother Cancer, 2019. **7**(1): p. 217.

68. Beyranvand Nejad, E., et al., *Tumor Eradication by Cisplatin Is Sustained by CD80/86-Mediated Costimulation of CD8+ T Cells.* Cancer Res, 2016. **76**(20): p. 6017-6029.

69. van der Sluis, T.C., et al., *Vaccine-induced tumor necrosis factor-producing T cells synergize with cisplatin to promote tumor cell death.* Clin Cancer Res, 2015. **21**(4): p. 781-94.

70. Welters, M.J., et al., *Vaccination during myeloid cell depletion by cancer chemotherapy fosters robust T cell responses.* Sci Transl Med, 2016. **8**(334): p. 334ra52.

71. Zom, G.G., et al., *Novel TLR2-binding adjuvant induces enhanced T cell responses and tumor eradication.* J Immunother Cancer, 2018. **6**(1): p. 146.

72. Zhang, F., et al., *Optimal combination treatment regimens of vaccine and radiotherapy augment tumor-bearing host immunity.* Commun Biol, 2021. **4**(1): p. 78.

73. Kleinovink, J.W., et al., *Combination of Photodynamic Therapy and Specific Immunotherapy Efficiently Eradicates Established Tumors.* Clin Cancer Res, 2016. **22**(6): p. 1459-68.

74. Ruckert, M., et al., *Combinations of Radiotherapy with Vaccination and Immune Checkpoint Inhibition Differently Affect Primary and Abscopal Tumor Growth and the Tumor Microenvironment.* Cancers (Basel), 2021. **13**(4).

APPENDICES &

NEDERLANDSE SAMENVATTING

Het immuunsysteem heeft zich ontwikkeld om ons lichaam te beschermen door gevaren voor onze gezondheid te herkennen en verwijderen. Dit kan gaan om ziekteverwekkers die infecties veroorzaken, maar ook om tumorcellen. Een immuunrespons wordt georkestreerd door een verfijnd netwerk van immuuncellen en moleculen die gezamenlijk de immuunrespons opstarten en uitvoeren.

Een immuunrespons ontwikkelt zich in een aantal gecontroleerde stappen. Het opstarten van het immuunsysteem vereist een combinatie van meerdere signalen die de immuuncellen stimuleren. Zodra de immuunrespons is voltooid, wat enkele dagen tot weken kan duren, wordt deze weer stopgezet door verschillende mechanismes die de immuuncellen afremmen. Deze downregulatie is essentieel omdat een continue ongeremde activatie van het immuunsysteem kan leiden tot immuungerelateerde aandoeningen.

Men heeft recent ontdekt dat deze mechanismes die het immuunsysteem in toom houden ook een rol kunnen spelen in de vorming van kanker, door de tumorcellen te helpen ontsnappen aan het immuunsysteem. Het immuunsysteem kan tumorcellen herkennen en aanvallen, maar de meeste kankers hebben een manier gevonden om dit te onderdrukken.

Immuuntherapie voor kanker is een onderdeel van de medische wetenschap dat erop gericht is om anti-tumor immuniteit te versterken en de immuunremming te onderdrukken. Voor een aantal soorten tumoren is immuuntherapie met immuun-checkpointremmers inmiddels zelfs al standaardbehandeling geworden, maar ook verscheidene andere mogelijke behandelingen worden onderzocht, waaronder de therapeutische kankervaccins die in dit proefschrift worden beschreven.

Therapeutische kankervaccinatie heeft als doel om een immuunrespons te starten tegen tumor-specifieke eiwitten. Deze immuunrespons wordt uitgevoerd door T-lymfocyten (ook T-cellen genoemd), die geïnstrueerd worden om de tumorcellen te herkennen op basis van het tumor-specifieke eiwit waarvoor het vaccin de instructie bevat. Deze behandeling heeft de potentie om specifiek tumorcellen aan te vallen zonder de overige gezonde cellen te beschadigen. Helaas is de toepassing van kankervaccins tot nog toe beperkt gebleven vanwege een gebrekkige effectiviteit, die kan worden toegeschreven aan suboptimale vaccinformuleringen en aan immuunsuppressie in de tumor.

In dit proefschrift worden verscheidene pre-klinische benaderingen onderzocht om de potentie van kankervaccins te verhogen door betere manieren van formulering en toediening van het vaccin. In **hoofdstuk 2** en **3** wordt het ontwerp, de synthese en de in vitro en in vivo evaluatie van een nieuw conjugaat-vaccin gepresenteerd. Covalente binding van peptide-antigeen aan het

sterke adjuvans CRX-527, een chemisch gedefinieerde Toll-like receptor (TLR) 4 ligand, vergrootte de vaccinpotentie ten opzichte van de klassieke aanpak waarbij ongeconjugeerd antigeen gemengd met dit adjuvans wordt toegediend. Dit vertaalde zich in betere T-celgemedieerde bescherming van gevaccineerde muizen tegen een agressieve melanoomtumor. Hetzelfde concept is toegepast voor een peptidevaccin met als adjuvans de TLR7 ligand hydroxyadenine. Dit adjuvans is minder potent dan CRX-527, maar kan de anti-tumorfuncties verbeteren van de T-celrespons die door het vaccin wordt opgewekt. In twee verschillende studies werd het effect van dubbele conjugatie onderzocht waarbij peptide-antigenen werden gekoppeld aan hydroxyadenine en aan een tweede ligand. In **hoofdstuk 4** werd dubbele conjugatie van hydroxyadenine en het ligand mannose-6-fosfaat (M6P) aan peptide-antigeen bestudeerd. Intracellulaire targeting van de M6P-receptor resulteerde uiteindelijk in een lagere activatie van T-cellen, hetgeen aantoont hoe de formulering van het vaccin diens effectiviteit kan beïnvloeden door de intracellulaire routing te veranderen. **Hoofdstuk 5** beschrijft het ontwerp van een peptide-vaccin geconjugeerd aan twee verschillende adjuvantia: hydroxyadenine en Pam3CysSK4. Laatstgenoemde wordt op dit moment klinisch onderzocht voor de behandeling van HPV16-gerelateerde tumoren. In dit hoofdstuk wordt dit nieuw ontworpen dubbel-geconjugeerde vaccin gevalideerd, als uitgangspunt voor verdere pre-klinische evaluatie van de anti-tumor effectiviteit.

Een andere strategie die momenteel onderzocht wordt ter verbetering van de vaccineffectiviteit is encapsulatie van het vaccin in nanoparticles. In **hoofdstuk 6** worden dextran nanogels onderzocht als dragers van peptide-vaccins. Hierbij werden peptides covalent gebonden aan de nanoparticles om het antigeen na injectie te beschermen tegen verspreiding en degradatie voordat het de immuuncellen bereikt. Deze strategie resulteerde in hogere aantallen specifieke T-cellen in gevaccineerde muizen, welke bovendien een sterker polyfunctioneel profiel hadden, wat de gedachte ondersteunt dat nanogels een geschikte drager zijn om peptide-vaccins toe te dienen.

Dankzij de snelle ontwikkeling van sequencing en high-throughput technologie in de laatste decennia kunnen potentiële tumor-antigenen worden geïdentificeerd op basis van tumorcellen van één patiënt. Het onderzoek naar kankervaccins richt zich daarom ook steeds meer op gepersonaliseerde kankervaccins, en dit concept is ook onderzocht in muizen. **Hoofdstuk 7** beschrijft een nieuw ontwerp van een DNA-kankervaccin. DNA-vaccins zijn flexibel, kosteneffectief en eenvoudig te produceren, hetgeen voldoet aan de eisen van gepersonaliseerde kankervaccins. Bovendien toont dit hoofdstuk hoe afzonderlijke immuuntherapieën zoals kankervaccins en immuun-checkpointremmers in vivo kunnen samenwerken bij het onder controle brengen van de tumor.

RIASSUNTO IN ITALIANO

Il sistema immunitario si è evoluto per sorvegliare il nostro corpo, attivandosi per rimuovere qualsiasi cosa rappresenti una minaccia alla nostra salute come patogeni, che causano infezioni o malattie, o cellule tumorali. La risposta immunitaria è orchestrata da una sofisticata rete di molecole e cellule del sistema immunitario che interagiscono tra loro.

Una sequenza controllata e finemente regolata di eventi dà il via alla risposta immunitaria. Innanzitutto, l'attivazione del sistema immunitario richiede l'integrazione di segnali distinti per poter stimolare efficacemente le cellule effettrici. Successivamente alla risposta immunitaria, la cui durata può variare da pochi giorni a diverse settimane, svariati meccanismi vengono attivati per sopprimere le cellule del sistema immunitario. Questa inibizione è essenziale poiché l'attivazione eccessiva o prolungata del sistema immunitario può portare a conseguenze patologiche.

Le ultime ricerche hanno portato alla luce che le cellule tumorali sono in grado di adottare le medesime strategie del sistema immunitario per evadere i meccanismi che il corpo utilizza per riconoscerle e ucciderle. Infatti, il sistema immunitario possiede, tra le altre cose, l'abilità intrinseca di riconoscere ed attaccare le cellule tumorali, ma la maggior parte delle cellule cancerose evolve in modo da sopprimere questi attacchi e potersi espandere.

L'immunoterapia del cancro è un ramo nascente della ricerca biomedica, il cui obiettivo è quello di potenziare l'immunità antitumorale e di sovvertire la soppressione del sistema immunitario esercitata dalle cellule cancerose. Questa ricerca ha portato allo sviluppo di terapie che sono già diventate parte dei trattamenti standard per alcuni tipi di cancro (come gli inibitori dei checkpoint immunitari), ma molte altre potenziali terapie sono in fase di ricerca, quali i vaccini terapeutici discussi in questa tesi.

Lo scopo dei vaccini terapeutici è quello di stimolare una risposta immunitaria contro specifiche proteine tumorali. Questa risposta viene mediata dai linfociti T, o cellule T, che possono essere istruiti a riconoscere ed attaccare le cellule tumorali in base alla proteina (anche detta antigene) contenuta nel vaccino. Questa terapia ha il potenziale di uccidere specificamente le cellule cancerogene lasciando illese le cellule sane. Ad oggi, l'utilizzo dei vaccini terapeutici è limitato dalla mancanza di efficacia terapeutica. Ciò può essere attribuito alla mancanza di una formulazione ottimale del vaccino o alla soppressione del sistema immunitario esercitata dal tumore.

In questa tesi sono stati esplorati diversi approcci a livello preclinico per aumentare l'efficacia dei vaccini contro il cancro, modificando la loro formulazione e somministrazione. Nei **capitoli 2** e **3** viene presentato un nuovo vaccino

coniugato, dalla sua progettazione e sintesi, alla valutazione in vitro ed in vivo. Viene dimostrato come il legame covalente tra l'antigene e il potente adiuvante CRX-527 potenzi il vaccino rispetto alla classica somministrazione di antigene misto ad adiuvante. Questo si traduce in una maggiore protezione indotta dal vaccino contro un aggressivo modello sperimentale di melanoma nei topi. Lo stesso concetto è stato applicato ad un vaccino adiuvato dall'idrossiadenina. Questo adiuvante è meno potente rispetto a CRX-527 ma ha il vantaggio di indurre specifiche funzioni antitumorali nelle cellule T indotte dal vaccino. L'adiuvante è stato coniugato all'antigene e ad una seconda molecola per esplorare l'effetto di una doppia coniugazione sul vaccino. Nel **capitolo 4**, l'idrossiadenina è stata coniugata all'antigene assieme al mannosio-6-fosfato. L'aggiunta del mannosio altera il traffico intracellulare dell'antigene, risultando in una minore attivazione delle cellule T da parte delle cellule dendritiche. Questo dimostra come la formulazione possa influenzare sia positivamente che negativamente l'efficacia di un dato vaccino. Nel **capitolo 5** viene studiata la formulazione dell'antigene coniugato all'idrossiadenina e all'adiuvante Pam, quest'ultimo già in fase di sperimentazione clinica per il trattamento di tumori legati al papilloma virus. Questo capitolo riporta la sintesi e validazione di questo nuovo vaccino coniugato, aprendo la strada per ulteriori studi preclinici per valutarne l'efficacia antitumorale.

L'incapsulazione dei vaccini all'interno di nano-particelle è un'altra strategia sotto studio per migliorare l'efficacia dei vaccini. Nel **capitolo 6**, nano-gel di destrano vengono testati come potenziali trasportatori dell'antigene contenuto nel vaccino. L'antigene è stato covalentemente legato ai nano-gel per protezione e per evitarne la dispersione e degradazione prematura dopo l'iniezione, prima di poter raggiungere le cellule del sistema immunitario. Ciò risulta in una maggiore induzione di cellule T nei topi vaccinati, aventi un maggiore profilo poli-funzionale. Questo risultato supporta l'ipotesi che i nano-gel rappresentino un veicolo potenzialmente interessante per la somministrazione di vaccini terapeutici.

Il rapido sviluppo di tecnologie per il sequenziamento degli ultimi decenni ha permesso di identificare potenziali antigeni tumorali alla risoluzione di un singolo individuo dalle cellule tumorali raccolte dal paziente stesso. I vaccini personalizzati sono la nuova frontiera dei vaccini per il cancro, e questo concetto è stato esplorato nei topi nel **capitolo 7**, dove viene presentato il design di un nuovo vaccino a DNA. I vaccini a DNA rappresentano una piattaforma flessibile, economica e di facile produzione adatta a soddisfare i requisiti dei vaccini personalizzati. Inoltre, questo capitolo mostra come immunoterapie diverse come i vaccini per il cancro e gli inibitori dei checkpoint immunitari possano collaborare e potenziare il controllo delle cellule tumorali da parte del sistema immunitario.

ENGLISH SUMMARY

The immune system has evolved to guard our body and to remove anything that represents a threat to our health, such as pathogens that cause infections or diseases, or tumor cells. The immune response is orchestrated by a sophisticated network of immune cells and molecules which interact with each other to initiate and execute an immune reaction.

An immune response develops over several controlled steps. Activation of the immune system requires a combination of multiple distinct signals to properly stimulate effector cells. After execution of the immune reaction, which may take from several days up to several weeks, several mechanisms are activated to dampen and inhibit the immune cells. This down-regulation is essential because the ongoing activation of the immune system may have pathological consequences if left uncontrolled.

It was recently realized that during cancer pathogenesis these regulatory mechanisms also represent escape strategies adopted by tumor cells. In fact, the immune system has the intrinsic potential to recognize and attack tumor cells, however most cancers evolve ways to suppress this.

Cancer immunotherapy is a blooming branch of medical sciences aimed at potentiating anti-tumor immunity and reverse immune suppression. It led to the development of novel treatments that have already become part of standard care for different cancers (such as immune checkpoint inhibitors) but many additional potential treatments are under investigation, such as therapeutic cancer vaccines discussed in this thesis.

Therapeutic cancer vaccination is aimed at raising an immune response against tumor-specific proteins. This response is mediated by T lymphocytes, or T cells, which can be instructed to recognize and kill tumor cells based on the cancer-specific protein antigen provided by the vaccine. This therapy holds the potential to specifically attack tumor cells leaving healthy cells unharmed. However, the employment of cancer vaccines has been so far limited by lack of therapeutic efficacy. This can be attributed to suboptimal vaccine formulations and to immune suppression at the tumor site.

In this thesis, different approaches were explored in pre-clinical setting to increase the potency of cancer vaccines by improving the way the vaccine is formulated and delivered. In **chapters 2** and **3** a novel conjugate vaccine was presented, from its design to its synthesis and evaluation in vitro and in vivo. It was shown that the covalent linkage of peptide antigen to the potent adjuvant CRX-527, a chemically defined Toll like receptor (TLR) 4 ligand, enhanced vaccine potency compared to the classical administration of antigen mixed with this ad-

juvant. This translated into improved T cell-mediated protection in mice induced by the vaccine against an aggressive melanoma tumor .

The same concept was applied to a peptide vaccine adjuvanted by the TLR7 ligand hydroxyadenine. This adjuvant is less potent than CRX-527 but can improve the anti-tumor functions of the T cell response induced by the vaccine. An antigenic peptide was coupled to the adjuvant and a second ligand to explore the effect of dual conjugation in two different studies. In **chapter 4,** dual conjugation of hydroxyadenine and the ligand mannose 6-phosphate to antigenic peptide was explored. Intracellular targeting to the M6P receptor eventually resulted in lower activation of T cells. This demonstrated how vaccine formulation may impact vaccine efficacy by modifying intracellular routing. In **chapter 5,** it was explored the design of a peptide vaccine conjugated to two distinct adjuvants: hydroxyadenine and Pam3CysSK4, the latter being currently evaluated in the clinic for the treatment of HPV16-related malignancies. This chapter reports the validation of this newly designed and potent dual conjugated vaccine and opens the way for further pre-clinical evaluation for its anti-tumor efficacy.

Encapsulation of the vaccine in nano-sized particles is another strategy currently explored for improving vaccine potency. In **chapter 6**, dextran nanogels were evaluated as carriers of peptide vaccines. Peptides were covalently linked to these nanoparticles to protect the antigen after injection in vivo from dispersal and degradation before reaching immune cells. This resulted in the induction of higher numbers of specific T cell responses in vaccinated mice, that displayed a higher poly-functional profile, supporting the idea that nanogels represent a suitable carrier to potentiate the delivery of peptide-based vaccines.

The rapid development of sequencing and high throughput technologies of the last decades has allowed the identification of potential tumor antigens at high resolution of cancer cells collected from a single patient. Personalized cancer vaccines are the new frontier of cancer vaccine research, and this concept was explored in mice. In **chapter 7**, a new design for a DNA cancer vaccine was presented. DNA vaccines represent a flexible, cost effective and easily manufactured platform suitable to meet the demands of personalized cancer vaccines. Moreover, this chapter shows how separate immunotherapies such as cancer vaccines

ACKNOWLEDGMENTS

Many people participated to the realization of my PhD, and I am grateful to all of them. I had the luck to meet and work with talented people and to be accompanied along the way by many caring friends that deserve a mention. Thank you all for being part in one or the other way to this accomplishment.

Ferry, you guided me with patience and experience, and I am thankful for this opportunity, as well as for supporting me throughout these years. You were always able to see the positive side of things and you always encouraged me to keep trying when I wanted to give up.

My PhD work could not have been possible without my many talented collaborators. Thank you to "the chemists": *Dima, Jeroen, Gijs, Niels* and *Thomas*! Combining our two worlds is not always easy but it certainly leads to great ideas and results. My thanks also go to *Rene* and *Neda* for developing and testing with us the nanogels. To all ImmuneTune people: thank you, it was a pleasure to start with you my PhD project and to participate to the start of your own ambitious project. *Jereon***,** you were fundamental in learning how to plan and execute my first experiments. *Gerben, Wanda, Koen* and *Bram*, it was a pleasure to work with you.

My office, and the E3 section, is where most action took place and where I spent most of my time in these years. Luckily, it was populated by my great colleagues from Tumor Immunology & TI-adopted friends. It was a pleasure to have you around and I want to thank you all for any answered question, any offered help, any scientific and technical discussion I had with you. Thank you to *Jeroen* Mattarello, my PhD companion *Brett*, It'sElectricBoogieBoogie *Guillaume*, my concert pal *Esme*, my office neighbor *Iris*, YouShutUpWithTheShutUp *Ruben*, and super *Candido*. I enjoyed our trip in the same PhD boat. A special thanks to *Marcel*, you were always there to help me, especially in the beginning, and taught me most of what I know in the lab. And, of course, to *Tsolere*: your brightness, smartness, kindness and patience were exactly what I needed for my last stretch.

The colleagues that left: *Jan Willem*, you were the first to welcome me and you literally gave me shelter in the most turbulent times, thank you! *Nataschja*, my super supervisor; *Heng Sheng* and *Hreinn*, friends of many LUMC dinners; *Ayshe*, *Marieke, Anke, Jana* and *Elham*.

The colleagues that are still there: *Tetje*, with whom I can always share a laugh about how forgetful and clumpsy we are; *Suzanne*, always smiling and ready to

help; *Ramon*, always available for any question; *Mariska*, you joined only at the end but provided me with precious help and delightful company; *Reza* kind and smart office pal; *Giulia, Felicia, Tamara, Christine, Koen, Felix, Jasper, David, Dena, Dominique*: it was nice to cross your paths and I wish you all good luck for your future!

In the last part of my PhD and afterwards, I had the luck to meet and collaborate with Frame, full of kind, hardworking, and motivated people that could teach me a lot in little time. *Ronald* and *Wigard*, it was a pleasure to work under your guidance. *Katka*, you inspired me with your kindness, wisdom and humour. *Salvador, Michael, Maja, Eva* and *Mark*: you were super colleagues! I wish you all the best.

My master in Leiden was my way into my PhD, and during that time I made precious friends that stayed with me and supported me throughout the following years. *Harry, Nina*, and *Miguel*, you were always there whenever I needed you the most: thank you for all the good memories we made together. Leiden was also the home of my Italian extended family. Ovviamente first and foremost *Luana*. Grazie amica per tutto, sei stata preziosa in questi anni. La tua allegria e voglia di ridere sono qualita' uniche in te e spero che rimarranno sempre tue. *Luis* e piccola *Zazi*, vi voglio un mondo di bene e vi ringrazio per essere stati la mia famiglia adottiva. *Elena*, grazie per aver sempre fatto il tifo per me e per essere un'ispirazione di volonta' e impegno. *Simone, Ale* e *Rita* siete stati una compagnia speciale in questi anni e sono grata per tutte le mangiate, risate e bevute insieme. Thanks to the many inspiring brilliant women I had the pleasure to confront with during these years: sweet *Mahrokh*, le mie bio-orsette *Anna* e *Giuly*, le mie amiche di sempre *Mari* e *Fabi*. Thanks to my omnipresent Leiden friends: *Michiel, Nick* and *Marian***.** I will always cherish our beer sessions and chats together.

My family was also crucial during my PhD. Grazie a mami *Anna* e papi *Diego* per la vostra presenza anche da lontano, grazie per le vostre visite di supporto e per la vostra calda accoglienza ogni volta che ritorno a casa. E' confortante sapere di avere sempre un nido a cui tornare. Grazie ai miei fratelli *Ale* e *Max* e la mia sorella acquisita *Martina*, mi avete viziata con il vostro aiuto e la vostra disponibilita' durante tutti questi anni. Mi avete tutti (e cinque) dato tantissimo e vi voglio tanto bene! E grazie al mio *Mimmo*, che non mi lascia mai riposare e che mi sprona sempre a dare di piu'.

CURRICULUM VITAE

Elena was born in Trento, Italy, in 1990. She started her Bachelor studies at the University of Trento in 2009, where she obtained her BSc degree in Molecular Science and Biotechnology. In 2013 she moved to Leiden, the Netherlands, to pursue her Master degree in Animal Biology and Disease Models. During her MSc studies she learnt and became passionate about the field of immunology, and she developed particular interest in the subject of tumor immunology. After obtaining her master degree, Elena started her PhD project in 2015 in the Tumor Immunology group under the supervision of Ferry Ossendorp. During her PhD, she investigated various formulations to increase the efficacy of peptide- and DNA-based cancer vaccines in pre-clinical mouse models. In 2021, she started working as an Immunology Scientist at Frame Therapeutics B.V., Amsterdam, where she is conducting pre-clinical research on frameshift mutations for cancer vaccination. In Autumn 2021, she is going to start a post Doc fellowship at the National Instutite of Health in Bethesda, Maryland (USA) investigating the mechanisms of antigen presentation.

LIST OF PUBLICATIONS

Multivalent, Stabilized Mannose-6-Phosphates for the Targeted Delivery of Toll-Like Receptor Ligands and Peptide Antigens

Reintjens NRM*, **Tondini E***, Vis C, McGlinn T, Meeuwenoord NJ, Hogervorst TP, Overkleeft HS, Filippov DV, van der Marel GA, Ossendorp F, Codée JDC

Chembiochem 2021 Jan 15;22(2):434-440

Self-adjuvanting cancer vaccines from conjugation-ready lipid A analogues and synthetic long peptides

Reintjens NRM*, **Tondini E***, de Jong AR, Meeuwenoord NJ, Chiodo F, Peterse E, Overkleeft HS, Filippov DV, van der Marel GA, Ossendorp F, Codée JDC

J Med Chem 2020; 63(20):11691-11706

Identification of a neo-epitope dominating endogenous CD8 T cell responses to MC-38 colorectal cancer

Hos BJ, Camps MGM, Bulk J, **Tondini E**, van den Ende TC, Ruano D, Franken K, Janssen GMC, Ru A, Filippov DV, Arens R, van Veelen PA, Miranda N, Ossendorp F

Oncoimmunology 2019;1673125.

Cationic synthetic long peptides-loaded nanogels: An efficient therapeutic vaccine formulation for induction of T-cell responses

Kordalivand N*, **Tondini E***, Lau CYJ, Vermonden T, Mastrobattista E, Hennink WE, Ossendorp F, Nostrum CFV

J Control Release 2019; 315:114-125

A poly-neoantigen DNA vaccine synergizes with PD-1 blockade to induce T cell-mediated tumor control

Tondini E, Arakelian T, Oosterhuis K, Camps M, van Duikeren S, Han W, Arens R, Zondag G, van Bergen J, Ossendorp F

Oncoimmunology 2019; 8(11):1652539

Peptides conjugated to 2-alkoxy-8-oxo-adenine as potential synthetic vaccines triggering TLR7

Gential GPP, Hogervorst TP, **Tondini E**, van de Graaff MJ, Overkleeft HS, Codée JDC, van der Marel GA, Ossendorp F, Filippov DV

Bioorg Med Chem Lett 2019; 29 (11), 1340-1344

Dual synthetic peptide conjugate vaccine simultaneously triggers TLR2 and NOD2 and activates human dendritic cells

Zom GG, Willems MM, Meeuwenoord NJ, Reintjens NRM, **Tondini E**, Khan S, Overkleeft HS, van der Marel GA, Codée JDC, Ossendorp F, Filippov DV

Bioconjugate chem 2019; 30 (4), 1150-1161

Approaches to improve chemically defined synthetic peptide vaccines

Hos BJ*, **Tondini E***, van Kasteren SI, Ossendorp F

Frontiers in Immunology 2018; 9(884)